



Vanderbilt University

2016-2017 NASA Student Launch

Flight Readiness Review

March 6, 2017

Contents

1	Summary	11
1.1	Team Summary	11
1.1.1	Project Title and School Name	11
1.1.2	Team Members	11
1.1.3	NAR Association	13
1.1.4	Vanderbilt Aerospace Design Laboratory	13
1.1.4.1	Preamble	13
1.1.4.2	Vanderbilt AIAA Student Chapter	14
1.1.4.3	Constitutional Articles Vanderbilt AIAA	14
1.2	Launch Vehicle Summary	15
1.3	Recovery System Summary	15
1.3.1	Milestone Review Flysheet	18
1.4	Payload Summary	20
1.4.1	Cold Gas Thruster System	20
1.4.2	Control System	20
2	Changes Made Since CDR	21
2.1	Changes to Vehicle Criteria	21
2.2	Changes to Payload Criteria	21
2.2.1	Changes to Payload Thruster System	21
2.2.2	Changes to Payload Electronics	21
2.3	Changes to Project Plan	22
2.3.1	Changes to Testing	22
2.3.2	Changes to Requirements	22
2.3.3	Changes to Budget	22
2.3.4	Changes to Timeline	23
3	Vehicle Criteria	24
3.1	Fullscale Launch Vehicle Overview	24
3.2	Detailed Changes Since CDR	25
3.3	Design & Construction of Launch Vehicle	27
3.3.1	Nosecone	27
3.3.2	Airframe Fabrication	29
3.3.3	Payload & Avionics Section	32
3.3.3.1	Payload Section	32
3.3.3.2	Avionics Section	33
3.3.4	Aluminum Bulkheads	36
3.3.5	Tail Section	38
3.3.6	Tailcone	43
3.3.7	Final Assembly	45
3.4	Critical Design Features	45
3.4.1	Structural Elements	45

3.4.2	Vehicle Electrical Elements	48
3.5	Flight Reliability Confidence	49
3.5.1	Mission Statement	49
3.5.2	General Mission Success Criteria	49
3.5.3	Launch Vehicle Mission Success Criteria	50
3.5.4	Recovery System Mission Success Criteria	50
3.6	Recovery Subsystem	50
3.6.1	Structural Elements	50
3.6.2	Recovery System Electrical Elements	54
3.6.3	Redundancy Features	55
3.6.4	Parachute Sizes and Descent Rates	58
3.6.5	Drawings and Schematics	61
3.6.6	Rocket-Locating Transmitters	64
3.7	Mission Performance Predictions	65
3.7.1	Mission Performance Criteria	65
3.7.2	MATLAB Flight Simulation	66
3.7.2.1	Trajectory Equations	66
3.7.2.2	Drag	67
3.7.2.3	Side Wind	68
3.7.2.4	Standard Atmosphere Model	69
3.7.2.5	Compressibility	69
3.7.2.6	Motor Burn Profiles	70
3.7.2.7	Parachute Deployment	70
3.7.3	MATLAB Payload Experiment Simulation	71
3.7.3.1	Rotation Equations	71
3.7.3.2	Thrust	72
3.7.3.3	Resistive Torque	72
3.7.3.4	Computational Modeling	75
3.7.3.5	Solenoid Actuation Properties	76
3.7.4	Flight Test Validation	77
3.7.4.1	Initial Subscale Flight	77
3.7.4.2	FULLSCALE Flight	78
3.7.4.3	Second Subscale Flight	78
3.7.5	Example Simulation	80
3.7.6	FULLSCALE Flight Predictions and Sensitivity Analysis	85
3.7.6.1	Launch Stability	85
3.7.6.2	Landing Kinetic Energy	87
3.7.6.3	Side Wind	89
3.7.6.4	Motor Thrust Variability	90
3.7.6.5	Launch Mass Variability	90
3.8	FULLSCALE Flight Results	91
3.8.1	Introduction	91
3.8.2	Comparison of Flight Data and Simulations	93
3.8.3	Motor Thrust Analysis and Associated Altitude Loss	93
3.8.4	Effective Drag Coefficient and Associated Altitude Loss	95

3.8.5	Flight Altitude Conclusions	96
3.8.6	Fulldscale Roll Analysis	96
3.8.7	Subscale Relaunch	98
3.8.8	Conclusions and Moving Forward	101
4	Payload Criteria	102
4.1	Design and Construction	102
4.1.1	Design Selection	102
4.1.2	Payload Mission Requirements Overview	103
4.1.3	Cold Gas Thruster Nozzle Design	104
4.1.4	Cold Gas Thruster Nozzle Construction	105
4.1.4.1	Nozzle Fabrication Safety Measures	105
4.1.4.2	Nozzle Fabrication Machines Utilized	106
4.1.4.3	Nozzle Fabrication Required Equipment	106
4.1.4.4	Nozzle Fabrication Steps	106
4.1.5	Payload Assembly and Rocket Integration	108
4.1.5.1	Risk Mitigation	112
4.2	Precision Measurement	114
4.2.1	Measurement Devices and Propagation of Uncertainty	114
4.2.2	Sampling Frequency	116
4.3	Payload Electronics	117
4.3.1	System Level Design	117
4.3.2	Electronics - Component Detail	118
4.3.2.1	Solenoid Valves	118
4.3.2.2	Microprocessor	119
4.3.2.3	Auxiliary Circuit Board	119
4.3.2.4	Inertial Measurement Unit	123
4.3.2.5	Power Supply	123
4.3.2.6	Mounting Sled	124
4.4	Control Schemes	125
4.4.1	Fulldscale Control System	125
4.4.2	Future Control System Improvements	126
4.5	Payload Software	128
5	Safety	132
5.1	Team Safety Structure	132
5.2	Student Safety Officer	133
5.3	Written Safety Statement	134
5.4	Safety Officer/LEUP Holder	134
5.5	Facilities	135
5.6	Safety Equipment	135
5.7	Injury/Emergency Situations	135
5.8	Purchase, Storage, Transport, and Use of Rocket Motors	135
5.9	Transportation of Other Hazardous Materials	135
5.10	NAR High Power Rocket Safety Code	136

5.11	Cognizance of Federal, State, and Local Laws and Regulations	136
5.12	Safety Data Sheets	136
5.13	Final Assembly and Launch Procedures	136
5.13.1	Launch Pad, Launch Rail, and Ignition System	137
5.14	Launch Operations Procedures	138
5.15	Hazard Analysis	138
5.15.1	Risk Assessment Matrix	138
5.15.2	Personnel Hazard Analysis	140
5.15.3	Propulsion Failure Modes	147
5.15.4	Payload/Control Failure Modes	150
5.15.5	Recovery System Failure Modes	155
5.15.6	Miscellaneous Failure Modes	159
5.15.7	Environmental Effects Analysis	162
5.15.8	Project Management	168
6	Launch Operations Procedures	171
6.1	Launch Field General Setup	172
6.2	Launch Pad and Launch Rail	173
6.3	Software and Controls	174
6.4	Payload Skeleton and Electronics	175
6.5	Tail Section	177
6.6	Avionics Section	178
6.7	Drogue Parachute Assembly and Integration	180
6.8	Main Parachute	181
6.9	Launch Vehicle Final Integration	182
6.10	Motor Installation and CG Operations	183
6.11	Launch Pad Operations	184
6.12	Igniter Installation	186
6.13	Post-Flight Inspection	187
6.14	Troubleshooting in the Field	188
6.15	Pack List: Full List of Necessary Hardware	188
7	Project Plan	190
7.1	Testing	190
7.1.1	Thruster Testing	190
7.1.2	Electronics Testing	200
7.1.2.1	Avionics Testing	200
7.1.2.2	Payload Electronics Testing	203
7.1.3	Software Testing	205
7.1.3.1	IMU	205
7.1.3.2	Solenoid Actuator	205
7.1.3.3	High Level and Bang-Bang Controllers	206
7.1.4	The FRAME	207
7.1.4.1	Introduction	207
7.1.4.2	Purpose	207

7.1.4.3	Advantages	208
7.1.4.4	General Criteria For Success	209
7.1.4.5	Design Choices	209
7.1.4.6	Motor Characterization	211
7.1.4.7	Torque Transmission	217
7.1.4.8	Testing	221
7.1.4.9	Conclusions	231
7.1.5	Recovery System Testing	231
7.1.5.1	Altimeter Testing	231
7.1.6	Carbon Fiber Reinforced Blue Tube testing	233
7.2	Requirements Compliance	235
7.2.1	NASA Handbook Requirements	235
7.2.2	Team Derived Requirements	253
7.3	Budgeting and Timeline	263
7.3.1	Budget	263
7.3.2	Timeline of Operations	283
Appendix		289

A Air Delivery System Safety	290	
A.1	System Overview	290
A.2	Solenoid Valve Selection	291
A.3	External Effects of the System	292

List of Figures

1	Recovery System Flowchart	16
2	CAD Model of Full Scale Launch Vehicle	24
3	Fullscale Launch Vehicle in VADL Shop	24
4	Experimental Flight Overview	25
5	Payload Section CAD at CDR	26
6	Payload Section CAD at FRR	26
7	Fullscale Launch Vehicle Payload Section	26
8	Fullscale Launch Vehicle on Launch Rail	27
9	Fullscale Nosecone CAD Schematic	27
10	Purchased Nosecone - Photo from ApogeeRockets.com	28
11	Nosecone Fabrication	29
12	Completed Nosecone	29
13	Sections of the Fullscale Launch Vehicle	30
14	Rolling the Carbon Fiber Tubes	30
15	Hotbox with Airframe Curing Inside	31
16	Airframe Directly after Exiting Hotbox	32
17	Completed Airframe Section	32
18	Diagram of Nosecone & Payload Sections	33

19	Fabricated Nosecone & Payload Section	33
20	Diagram of Avionics Sections	34
21	Coupler Tube with Weld Nuts Installed	35
22	Finished Avionics Section	35
23	Fullscale CAD with Aluminum Bulkheads	36
24	Aluminum Bulkhead Fabrication	37
25	Completed Avionics Bay	37
26	Checking the Fit of the Motor Tube	38
27	Parachute/Centering Bulkhead (Subscale)	38
28	CAD Diagram of Tail Section	39
29	The Construction of the Motor Tube Assembly	40
30	Applying Carbon Fiber Fillets to the Motor Tube Assembly	41
31	The Laser Cut Fin Slotting Jig	41
32	Paul Slots the Tail Airframe	42
33	Nina applies Loctite Epoxy to Secure the Motor Tube Assembly	42
34	Securing the Motor Tube Assembly to the Airframe	43
35	Closeup of The Carbon Fiber Fillets	43
36	The Tailcone Mold and ABS Model	44
37	The Finished Carbon Fiber Boattail	44
38	The Finished Carbon Fiber Boattail Integrated Onto the Tail Section	45
39	The Completed Assembly of the Fullscale Launch Vehicle	45
40	Block Diagram of Thrust Transfer	46
41	Stress-Strain Diagram for Solid Body Tube	46
42	Failure Points for Bodytube with Stress Concentrations	47
43	Stress-Strain Diagram for Bodytube with Holes	47
44	XT60 Connector for Wire-to-wire Connections	48
45	Technical Drawings of the Molex 4 Pin Locking Connector for Wire-to-board Connections	49
46	Manufacturer's Mechanical Test Requirements for Molex Right Angle Connector .	49
47	Screw Switch for Electrical System Arming	49
48	Wooden Bulkhead Test Set-up	51
49	Plywood Bulkhead Failure Testing	52
50	Equivalent Stresses Due to Black Powder Ignition	53
51	Bulkhead Deformation Due to Black Powder Ignition	53
52	Avionics Bulkhead Safety Factor Graphic	54
53	Recovery Electronics Schematic	55
54	Systematic Redundancies Flowchart	56
55	Recovery System Flowchart	57
58	Avionics Full Assembly	60
59	Successful Full-Scale Recovery	60
60	Subscale Parachute Deployment	61
61	Recovery System Vehicle	62
62	Recovery Electronics Schematic	62
63	Physical and CAD Assemblies of Recovery Bay	63
64	CAD Renderings of 3D Printed Recovery System Sled	63

65	Recovery System Airframe, Fabricated in House	64
66	Recovery System CAD Rendering	64
67	Big Red Bee BeeLine Transmitter	65
68	Instantaneous Flight Velocity Component Diagram	69
69	Loki Research L1400 Motor Data Profiles	70
70	Roll, Pitch, and Yaw of a Rocket	72
71	Trapezoidal Fin Schematic	73
72	Jet-Fin Interaction Countertorque Coefficient	75
73	Pressure Distribution at Fins for Various Angular Velocities	75
74	Damping Coefficient at an Axial Speed of 100 m/s	76
75	Subscale Altitude Drag Coefficient	77
76	Improvement to Resistive Torque Model	78
77	Second Subscale Flight Altitude Analysis	79
78	Second Subscale Flight Thrust Analysis	79
79	MATLAB Simulation Output	82
80	Example Simulation - Rocket Flight	84
81	Example Simulation - Payload Experiment	85
82	Location of CP and CG	86
83	Variation in Static Stability Margin	86
84	Kinetic Energy Management	88
85	Effect of Side Wind on Drift	89
86	Effect of Side Wind on Apogee	90
87	Variation in Apogee due to Variability in Thrust	91
88	Variation in Apogee due to Changes in Launch Mass	91
89	Full Scale Recovery	92
90	Fulyscale Launch Altimeter Data vs Projected Altitude	93
91	Thrust Profile Comparison	94
92	Altitude Comparison Based on Thrust Profiles	94
93	Fulyscale Motor Slow Ignition	95
94	Effect of Drag Coefficient on Altitude	96
95	Combination of Factors Leading to Reduced Altitude	97
96	Fulyscale Flight: Roll Data	97
97	Fulyscale Flight: Annotated Roll	98
98	Subscale Relaunch: Z Axis Characteristics vs Time	99
99	Subscale Relaunch: Z Axis Characteristics vs Time, Zoom	99
100	Subscale Relaunch: Roll Direction Analysis	100
101	Weighted Evaluation of Attitude Control Alternatives	103
102	Nozzle Technical Drawing	105
103	Payload Rocket Integration	108
104	Payload Assembly	109
105	Payload Component Flowchart	110
106	Bulkhead Redesign	112
107	Ninja Air Tank and Regulator	113
108	Nyquist Frequency: Phase Ambiguity	116
109	Payload Electronics Schematic	118

110	Physical and CAD Assemblies of Payload Electronics Bay	118
111	BeagleBone Black Wireless Single Board Computer	119
112	Auxiliary Circuit Board Layout	120
113	Auxiliary Board Main Power Circuitry	121
114	Auxiliary Board Solenoid Control	121
115	Auxiliary Board LED Indicators	122
116	Auxiliary Circuit Board Bill of Materials	122
117	Dimensions of VN-100 IMU	123
118	Tenergy Rechargeable Li-Ion Battery (11.1V, 2200 mAh)	124
119	Payload Electronics Mounting Sled	125
120	Simulated Bang-Bang Control With Oscillation	126
121	Comparison of Various Control Schemes	127
122	High Level Diagram of Flight Software	129
123	High Level Controller Flow Chart	130
124	Vanderbilt Aerospace Design Laboratory Safety Protocol	133
125	Risk Assessment Matrix	139
126	Signed Launch Checklist	171
127	Test Stand Schematic	190
128	Test Stand Nozzle and Solenoid Mounting	191
129	Test Stand Overview	191
130	Test Stand Load Cell Calibration	192
131	Load Cell Calibration Curve	192
132	Thruster and Pressure vs Time, Continuous Run	193
133	Thruster and Pressure vs Time, 1 Second Pulses	194
134	Thruster and Pressure vs Time, 0.5 Second Pulses	194
135	Thruster and Pressure vs Time, 0.25 Second Pulses	195
136	Thrust and Pressure vs Time, 1 Second Pulses, High Flow Regulator	196
137	Dual Thruster Arrangement, On and Off Test Stand	197
138	Thrust vs Time, 2000 psi	197
139	Thrust vs Time for Dual Nozzle Setup and Increased Tank Pressure	198
140	Regulator Outlet Orifice Comparison: 2nd vs Final Regulator	199
141	Thrust vs Time for Dual Nozzle, 2nd vs Final Regulator	199
142	Avionics Bay	201
143	Stratologger CF Altimeter	201
144	Payload Electronics at Fullscale Launch Test, Labeled	203
145	Solenoid Pin Value vs. Time	207
146	CAD and Picture of the FRAME	208
147	Cross Section View of Bearing System Enabling Frictionless Rotation	210
148	Top and Bottom Supports Enabling Vertical Orientation	211
149	High-Level Overview of Motor Control System	212
150	Operational-Amplifier Circuit for Motor Control	213
151	4020 Linear Servo Motor Controller	214
152	Low-Pass Filter Circuit	215
153	Microcontroller shield for FRAME motor control	215
154	Motor Controller Containment	216

155	Motor Control Containment	216
156	Picture of DC Motor Used to Simulate Aerodynamic Damping via Torque Inputs .	217
157	Picture of Pulley and Timing Belt Linkage Used to Transmit Torque from the DC Motor to the Shaft of the Bottom Support	217
158	Fin Gripper Used to Transmit Torque to the Flight Vehicle	218
159	Comparison of High Level Software Diagrams between Testing and Flight	219
160	Information Flow Between FRAME, ROSMOD, and KSP during Ground-based Testing	220
161	Dynamic Model and IMU Data Comparison	223
162	Subscale Flight and FRAME Angular Position Comparison	225
163	Fullscale Integration FRAME Test	226
164	Fullscale Angular Position vs Time for Various Axial Velocities	228
165	Fullscale Angular Position vs Time for Various Air Tank Pressures	230
167	Deployment Testing	232
168	Stress-Strain Diagram for Solid Bodytube	233
169	Failure Points for Bodytube with Stress Concentrations	234
170	Stress-Strain Diagram for Bodytube with Holes	234
171	Budget by Category	281
172	Budget and Present Expenditures	282

List of Tables

1	Testing Changes Summary	22
2	Parachute Parameters	58
3	Rocket Equations Symbol Definitions	66
4	Rotational Equations Symbol Definitions	72
5	Example Simulation Input Parameters	81
6	Landing Kinetic Energy of Components	87
7	Drift for Various Wind Conditions	89
8	Mission Requirements Evaluation Overview	103
9	Nozzle Overview	104
10	Payload Components and Pressure Ratings	113
11	VADL Precision Measurement and Uncertainty Documentation	114
12	Simplified Error Propagation Formulas	115
13	VADL Data Rate Documentation	117
14	Comparison of Control Schemes	127
15	Personnel Hazard Risk Assessment	140
16	Propulsion Failure Modes	147
17	Payload and Related Control Failure Modes	150
18	Recovery System Failure Modes	155
19	Miscellaneous Failure Modes and Hazard Analysis	159
20	Environmental Impact on Rocket	162
21	Rocket Impact on Environment	165
22	Project Management Risk and Mitigation	168

23	Single Nozzle Thrust Comparison for Two Regulators	196
24	Varying Pressure Thruster Test Summary	198
25	Total Thruster Test Summary	200
26	Testing Procedure and Results for Avionics	202
27	Testing Procedure and Results for Payload Electronics	204
28	Brushed DC Motor Specifications	213
29	Damping Torque Equations Symbol Definitions	220
30	NASA Handbook Requirements	236
31	Team Derived Requirements	254
32	Funding Source	263
33	2016-2017 Categorized Purchases	263

1 Summary

1.1 Team Summary

1.1.1 Project Title and School Name

Post-Boost Roll Control Using Cold Gas Thrusters

Vanderbilt University, Nashville, TN

Mailing Address:

Amrutar Anilkumar

Professor of the Practice of Aerospace and Mechanical Engineering

Director: Vanderbilt Aerospace Design Laboratory

Department of Mechanical Engineering

VU Station B # 351592

2301 Vanderbilt Place

Nashville, TN 37235-1592

1.1.2 Team Members

a. Team Advisor

Dr. Amrutar Anilkumar

Professor of the Practice of Aerospace and Mechanical Engineering

Department of Mechanical Engineering

Amrutar.V.Anilkumar@Vanderbilt.edu

b. Faculty Advisor for Control Systems

Dr. William Emfinger

Adjunct Assistant Professor of Mechanical Engineering

Department of Mechanical Engineering

c. Rocketry Mentor

Robin Midgett

Safety Officer and Rocketry Mentor

Senior Electronics Technician

NAR Level II Certified

Department of Mechanical Engineering

Robin.Midgett@Vanderbilt.edu

d. Graduate Student Mentors

(i) Dynamics Mentor

Brian

Postdoctoral Associate

Department of Mechanical Engineering

Brian.E.Lawson@Vanderbilt.edu

(ii) Instrumentation and Controls Mentor

Dexter

Graduate Student

Department of Mechanical Engineering

Dexter.A.Watkins@Vanderbilt.edu

(iii) Structures and Systems Integration Mentor

Ben

Graduate Student

Department of Mechanical Engineering

Benjamin.W.Gasser@Vanderbilt.edu

(iv) Fluids and Payload Mentor

Chris

Graduate Student

Department of Mechanical Engineering

Christopher.T.Lyne@Vanderbilt.edu

e. Senior Design Team

(i) Derek

Student Launch President, Fabrication Lead

Senior, Mechanical Engineering

Derek.J.Phillips@Vanderbilt.edu

(ii) Dustin

Student Launch Vice President, Payload Lead

Senior, Mechanical Engineering

Dustin.C.Howser@Vanderbilt.edu

(iii) Jimmy

Student Launch Treasurer, Payload Specialist and Systems Integrator

Senior, Mechanical Engineering

Jimmy.Pan@Vanderbilt.edu

(iv) Paul

Student Safety Officer, Simulation Lead

Senior, Chemical Engineering and Physics

Paul.J.Register@Vanderbilt.edu

(v) Arthur

Design Engineer, Software and Controls Lead

Senior, Mechanical Engineering

Arthur.T.Binstein@Vanderbilt.edu

(vi) Michael

Design Engineer, Data Acquisition Lead

Senior, Mechanical Engineering

Michael.G.Gilliland@Vanderbilt.edu

- (vii) Brian
Design Engineer, Computer-Aided Design Lead
Senior, Mechanical Engineering
Brian.J.Ramsey@Vanderbilt.edu
- (viii) Nina
Design Engineer, Structural Analysis Lead
Senior, Mechanical Engineering
Nina.A.Campano@Vanderbilt.edu
- (ix) Bradley
Design Engineer, Electrical Systems Lead
Senior, Electrical Engineering
Bradley.N.Bark@Vanderbilt.edu
- (x) Grady
Design Engineer, Ground-Based Testing Lead
Senior, Mechanical Engineering
Grady.T.Lynch@Vanderbilt.edu
- (xi) Paul
Design Engineer, Recovery System Lead
Senior, Mechanical Engineering
Paul.R.Moore@Vanderbilt.edu
- (xii) Ross
Design Engineer, Hardware-in-the-Loop Lead
Senior, Mechanical Engineering
Ross.M.Weber@Vanderbilt.edu

1.1.3 NAR Association

Music City Missile Club, NAR #589

Officers:

Chris Dondanville, President
Brian Godfrey, Vice President
Robin Midgett, Treasurer, treasurer@mc2rocketry.com
Chris Gill, NAR Advisor
Fred Kepner, Secretary

1.1.4 Vanderbilt Aerospace Design Laboratory

1.1.4.1 Preamble

The Vanderbilt Aerospace Design Laboratory www.vanderbilt.edu/usli was started as the Vanderbilt Aerospace Club in 2007 to meet the emerging needs of Vanderbilt engineering students aspiring to pursue careers and advanced studies in aerospace engineering. Its membership consists of engineering seniors who utilize this project to fulfill their senior design project

requirements, engineering graduate students whose research is allied to aerospace engineering, and engineering underclassmen with a demonstrated interest in aerospace engineering. Its agenda is to design and analyze unique rocket-flyable payload systems that highlight major challenges in space exploration and energy conversion. It also has a robust outreach program that works to build STEM enthusiasm in aerospace engineering among primary and secondary school students in Tennessee. The Vanderbilt Aerospace Design Laboratory (VADL) traditionally competes in the NASA Student Launch Competition, and project results are presented at AIAA Conferences and in select AIAA Journals. VADL also hosts the AIAA student chapter at Vanderbilt University.

1.1.4.2 Vanderbilt AIAA Student Chapter

The Vanderbilt AIAA student chapter, sponsored by the Vanderbilt Aerospace Design Laboratory, is a volunteer student organization that promotes aerospace engineering activities at Vanderbilt. It also conducts aerospace educational outreach at Middle Tennessee elementary, middle, and high schools. The aerospace activities apply directly to the profession of Aerospace Engineering (AE) and its practice. Implementation of the outreach program is most relevant to undergraduate upperclassmen and graduate students studying engineering with an aptitude for AE and to undergraduate upperclassmen in the School of Arts & Sciences or the School of Education who may be interested in school science teaching. AIAA members actively participate in the NASA Student Launch Competition through the School of Engineering's capstone senior design project.

1.1.4.3 Constitutional Articles Vanderbilt AIAA

- a. The AIAA must have a mechanical engineering professor who serves as the faculty advisor. In addition, the club must also have a financial advisor pursuant to Vanderbilt policy.
- b. AIAA members must actively seek to promote aerospace and STEM education and outreach in the Nashville area.
- c. The largest AIAA membership that can compete and be active in the NASA SL competition is 15 members. Preference for Student Launch Competition participation is given to Vanderbilt University School of Engineering (VUSE) seniors and graduate students with specific skill sets.
- d. Students who are selected to compete in the NASA SL competition must demonstrate qualities that will contribute to the club's mission and success at the competition. Such qualities may include prior rocketry experience, interest in aerospace engineering or science teaching as a career, a good academic standing, and a very strong work ethic in a field that is of use to the team (particularly educational outreach or engineering).
- e. The NASA SL Competition also serves as the senior design project for the VUSE Curriculum.
- f. Any amendments to this Constitution can be made by a vote of the members and approved by the faculty advisor.

1.2 Launch Vehicle Summary

Vanderbilt's full scale launch vehicle will have a body diameter of 5.52", an overall length of 99", and an overall weight of 34.0 lbs (30.9 lbs w/o motor fuel). The selected motor is a Loki Research L1400, which is an off-the-shelf re-loadable 54 mm motor. This specific motor has been chosen for its short burn time of 2.0 seconds allowing for higher initial vehicle velocity as the rocket departs the launch rail causing straighter flight while remaining subsonic throughout ascent. The predicted and targeted altitude of the rocket is 5280 ft AGL. The recovery system for this rocket is a dual deployment system comprised of a 18" drogue parachute deployed at apogee, followed by an 8' main parachute deployed at 750 ft AGL for a safe recovery of the rocket and payload. The recovery system is controlled by a redundant pair of barometric pressure based altimeters.

1.3 Recovery System Summary

The function of the Recovery System is to ensure a safe landing of the launch vehicle and payload. The experimental flight is not considered successful if we cannot recover the vehicle and any data gleaned during flight. While the paragraphs below summarize the recovery system, a more detailed analysis can be found in Sections 3.6.1 - 3.6.6. Figure 1 below shows a flow diagram of the planned events of the recovery system.

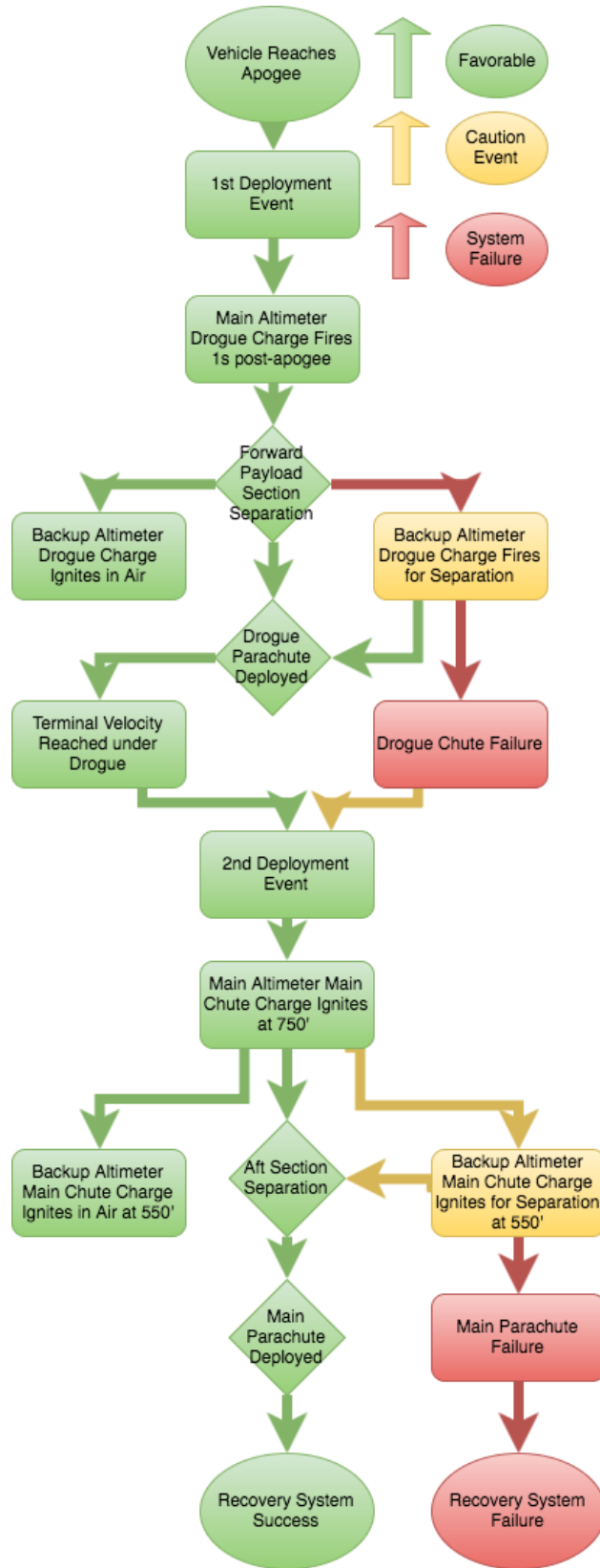


Figure 1: Recovery System Flowchart

Recovery of the launch vehicle is accomplished by a drogue parachute deploying one second after apogee and a main parachute deploying at 750 feet AGL. Two redundant PerfectFlite StratoLoggerCF altimeters initiate separation events, parachute deployment, and collect altitude data. Each altimeter is tested for successful charge ignition using Vanderbilt University's shock tube. Blast charges are tested for successful deployment of each parachute bay. Throughout this report, respective altimeters are referred to by "primary" or "main" altimeter, and "secondary" or "backup", indicating the order in which charges will fire. Primary and secondary charges do not ignite simultaneously, but are isolated events based on time-after-apogee and AGL altitude delays.

The dual-deployment recovery system has been designed based on calculations and past team's successes for simplicity, reliability, and testability. Each parachute is stored in its own compartment optimized for short opening time upon charge ignition. The first deployment event ejects the drogue parachute, which will slow the vehicle to velocity safe for deployment of the main parachute while also minimizing drift. The main parachute then opens at a lower altitude to reduce the landing energy of the rocket to a safe level. A radio transmitter will be attached to the main parachute in order to track the launch vehicle during descent while the rocket is unable to be visually located. Upon successful recovery and retrieval of the rocket, each altimeter will report the apogee of the previous flight using a series of audible tones.

1.3.1 Milestone Review Flysheet

Milestone Review Flysheet

Institution Vanderbilt University

Milestone Flight Readiness Review

Vehicle Properties	
Total Length (in)	99.0
Diameter (in)	5.5
Gross Lift Off Weight (lb)	34.0
Airframe Material	Carbon Fiber reinforced Blue Tube
Fin Material	Carbon Fiber
Drag	0.27

Motor Properties	
Motor Manufacturer	Loki Research
Motor Designation	L1400
Max/Average Thrust (lb)	428.6/319.5
Total Impulse (lbf-s)	2842.88
Mass Before/After Burn (lb)	5.59/3.08
Liftoff Thrust (lb)	428.6

Stability Analysis	
Center of Pressure (in from nose)	65.6
Center of Gravity (in from nose)	52.2
Static Stability Margin	2.43
Static Stability Margin (off launch rail)	2.94
Thrust-to-Weight Ratio	12.6
Rail Size and Length (in)	144
Rail Exit Velocity (ft/s)	84.7

Ascent Analysis	
Maximum Velocity (ft/s)	553
Maximum Mach Number	0.49
Maximum Acceleration (ft/s^2)	369
Target Apogee (From Simulations)(Ft)	4400
Stable Velocity (ft/s)	45
Distance to Stable Velocity (ft)	3

Recovery System Properties	
Drogue Parachute	
Manufacturer/Model	Fruity Chutes
Size	18"
Altitude at Deployment (ft)	apogee
Velocity at Deployment (ft/s)	31.4
Terminal Velocity (ft/s)	75.1
Recovery Harness Material	Kevlar
Harness Size/Thickness (in)	0.5 in (6000 lb)
Recovery Harness Length (ft)	25(11/16 W; 3000lb)
Harness/Airframe Interfaces	U-bolt and Quick Link
Kinetic Energy of Each Section (Ft-lbs)	Section 1 1227 Section 2 1416 Section 3 Section 4

Recovery System Properties	
Main Parachute	
Manufacturer/Model	Fruity Chutes
Size	96"
Altitude at Deployment (ft)	750
Velocity at Deployment (ft/s)	75.1
Terminal Velocity (ft/s)	15.1
Recovery Harness Material	Kevlar
Harness Size/Thickness (in)	0.5 in (6000 lb)
Recovery Harness Length (ft)	36
Harness/Airframe Interfaces	U-bolt, Eye-bolts, and Quick Link
Kinetic Energy of Each Section (Ft-lbs)	Section 1 49.6 Section 2 24.8 Section 3 32.5 Section 4

Recovery Electronics	
Altimeter(s)/Timer(s) (Make/Model)	StratologgerCF
Redundancy Plan	Two altimeters will be used for both main and drogue deployments
Pad Stay Time (Launch Configuration)	>>2 hrs

Recovery Electronics	
Rocket Locators (Make/Model)	Big Red Bee/ BeeLine Transmitter
Transmitting Frequencies	433.92 MHz
Black Powder Mass Drogue Chute (grams)	1.5 g (2.0 g)
Black Powder Mass Main Chute (grams)	4.5 g (5.0 g)

Milestone Review Flysheet

Institution	Vanderbilt University	Milestone	Flight Readiness Review
-------------	-----------------------	-----------	-------------------------

Autonomous Ground Support Equipment (MAV Teams Only)	
Capture Mechanism	Overview
Container Mechanism	Overview
Launch Rail Mechanism	Overview
	*** Include Description of rail locking mechanism***
Igniter Installation Mechanism	Overview

Payload	
Payload 1	Overview
	The payload for the 2016-2017 VADL launch vehicle is the integration of a dual thruster couple system in order to generate a torque around the rocket's main axis post-MECO. One couple is used to induce two full rotations about the roll axis, and the second couple is used to produce a countertorque to halt all rolling motion of the vehicle. The resulting angular position will be maintained by a robust control system that can actuate either thruster couple as needed.
Payload 2	Overview

Test Plans, Status, and Results	
Ejection Charge Tests	Ground deployment tests were conducted prior to the fullscale launch. In these tests, black powder charges are manually ignited to test shear pin breakage and parachute deployment. There were two charges placed in the fullscale rocket: one which functioned as the main charge and the second which functioned as the backup charge. Each charge was rated with a minimal safety factor of 2. Each charge successfully separated the rocket. The altimeters were tested in a shocktube to confirm their proper functionality.
Subscale Test Flights	A subscale test flight took place on December 14, 2016. The launch was a complete success, and the rocket was successfully recovered. The subscale launch tested a single thruster couple via two methods: continuous and pulsed. In order to supplement the data gathered during the fullscale launch, the subscale flight vehicle was launched for a second time on Sunday, February 26th. The goal of this launch was to verify payload actuation during flight and to develop an improved understanding of how the natural roll of the flight vehicle affects the cold gas thruster system's ability to induce two full rotations in a limited timeframe.
Fullscale Test Flights	In order to demonstrate the functionality of our fullscale flight vehicle, a launch was performed on Sunday, February 19th. The fullscale launch was also a complete success, with ideal execution of the dual deployment system, safe recovery of all onboard systems, and limited drift. Furthermore, the launch validated the payload's logic, as evidenced through IMU data gathered during the flight.

1.4 Payload Summary

1.4.1 Cold Gas Thruster System

VADL's chosen payload this year for the NASA USLI consists of roll control during post-MECO and pre-apogee flight. After analyzing various possible design solutions, VADL has chosen to perform this payload experiment through the use of tangential cold gas thrusters. Two pairs of thrusters will be used, mounted to the rocket orthogonal to the main axis and as close to the center of gravity as possible. Each pair consists of two thrusters that are 180 degrees apart and facing the same angular direction with one pair aligned for counter-clockwise rotation and the other pair aligned for clockwise rotation. The system will actuate each pair independently, first inducing two full rotations about the rocket main axis then alternating the thruster couple actuation to maintain a fixed angular position.

1.4.2 Control System

On a high level, VADL's payload objective is simple: creation of a system that can control the roll axis angular position of a launch vehicle. VADL's design for this system consists of four main components - the plant (launch vehicle), the actuator (cold gas thrusters), the sensor (inertial measurement unit) and the controller (microprocessor). A microprocessor running custom control software receives data from an IMU (Inertial Measurement Unit), and actuates the cold gas thrusters according to this data by utilizing a custom circuit board. As VADL seeks to couple IMU data with the aforementioned cold gas thrusters, transfer functions were characterized, control theories tested, and the best performing design ultimately chosen. This process was aided by the development of a ground-based test facility that allows for hardware-in-the-loop testing of several control schemes along with iterative testing of varied parameters within each scheme. Physically, this test facility consists of a vertical test stand isolating the full body of a launch vehicle in the primary rotation axis, with primary input from the internal thrusters as well as a disturbance input from an external motor for simulation of structurally induced rotation, side winds, jet-fin interaction, or other system disturbances. All of these components are tied together through the ROSMOD distributed system software package developed at the Vanderbilt Institute for Software Integrated Systems (ISIS), which allows for experiment development and data visualization.

2 Changes Made Since CDR

2.1 Changes to Vehicle Criteria

- (i) Rocket length has changed to 99" from 94.75" to accommodate payload assembly.
- (ii) Estimated mass has increased to 34.0 lbs from 30.3 lbs with the addition of mass in the payload section.
- (iii) Static Stability Margin has increased to 2.43 from 2.16 as payload mass increased.
- (iv) Additional general safety information, environmental precautions, launch operation procedures, and checklists have been added to augment the established safety protocol.

2.2 Changes to Payload Criteria

2.2.1 Changes to Payload Thruster System

- (i) Desired nozzle thrust has increased due to dampening effects of fins under high axial velocities through increased tank pressure in order to successfully complete flight experiment. The tank pressure has therefore increased to 4000 psi as a combination of compressed air topped off with compressed nitrogen. The composite air tank is rated to 4500 psi with a minimum burst pressure of 13500 psi.
- (ii) The fully specified payload experimental objective has been defined as achieving two rotations post-MECO, then maintaining a fixed angular position for the remainder of the experimental window by using bidirectional thrusters.
- (iii) Weight has been eliminated from the payload skeleton in order to approach simulation weight. This was done by:
 - (a) redesigning and cutting non-load-bearing bulkheads to eliminate unnecessary material,
 - (b) replacing two steel threaded rods with aluminum threaded rods,
 - (c) and replacing steel nuts with aluminum nuts.

2.2.2 Changes to Payload Electronics

- (i) The payload electronics assembly has been modified to include fewer interconnects which present failure modes when exposed to mechanical shock and vibration.
- (ii) The design of the payload's integrated arming switches has been modified for greater reliability.
- (iii) Signal presence must be monitored and logged by the payload computer for failure diagnosis and proof of actuation.
- (iv) The payload electronics assembly has been optimized for low mass while retaining structural strength and functionality.

2.3 Changes to Project Plan

2.3.1 Changes to Testing

Since CDR, VADL has been busy not only construction our full scale vehicle and payload, but also running various tests to analyze and verify the payload's performance. These include thruster performance analysis, vehicle integration tests on the ground-based test facility (the FRAME), and full flight tests. These testing updates can be seen summarized in Table 1 below.

Test Category	Test Description	Reasons for Tests
Thruster Performance Tests	Tests at both higher tank pressure and with a newly purchased regulator were performed	These tests were performed to characterize the thruster system's ability to offset regulator droop to increase output thrust for roll induction
FRAME Tests	Ground-based tests of the roll control payload system were performed with varying tank pressure, motor-induced axial flow damping, and control scheme type	These tests were performed to refine the control system to complete our in-flight experiment in the presence of axial flow damping
Flight Tests	A full scale vehicle launch and subscale relaunch took place in Manchester, TN and Lebanon, TN respectively	These flights took place to verify the robustness of our recovery system, the performance of the payload control system, the thruster actuation of our payload by on-board electronics, and attitude data storage of our on-board computer for incorporation into the ground-based testing damping model

Table 1: Testing Changes Summary

2.3.2 Changes to Requirements

The NASA Handbook Requirements (7.2.1) and Team Derived Requirements (7.2.2) have had status updates to show the team's progress in fulfilling them. The "document section" columns of these tables have been updated to correctly link to the relevant portion of the FRR. In addition, "Vehicle Requirements" has been updated to include Recovery, and requirements 5.9-5.16 have been added. A few thruster system requirements have been modified as the definition of the experiment has developed. Any changed requirements have been denoted with an asterisk.

2.3.3 Changes to Budget

The budget was reassessed after the fullscale launch and slightly reallocated. The changes included decreasing the FRAME budget from \$2,500 to \$2,300, the electronics budget from

\$2,500 to \$2,200, the tools budget from \$1,000 to \$800, and the miscellaneous budget from \$4,000 to \$3,800. These funds were reallocated to rocket fabrication, which increased from \$4,500 to \$5,400. VADL is on track to be under budget; the current spending is further explained in Section 7.3.1.

2.3.4 Changes to Timeline

The Gantt chart (7.3.2) has been converted from GanttProject.biz to Microsoft Project, allowing better formatting and visualization of critical paths and free slack. In addition, various dates have been refined throughout the fullscale fabrication process.

3 Vehicle Criteria

3.1 Fullscale Launch Vehicle Overview



Figure 2: CAD Model of Full Scale Launch Vehicle



Figure 3: Fullscale Launch Vehicle in VADL Shop

The Vanderbilt Aerospace Design Laboratory '16-'17 Student Launch vehicle has been built to provide a testing environment for this years attitude control payload experiment and be recovered afterwards for additional launches. Our launch vehicle has a body diameter of 5.52", an assembled height of 99", and an assembled mass of 34.0 lbs. The assembled fullscale launch vehicle center of gravity is 52.2" and the center of pressure is 65.6". The static stability margin at rail exit is calculated to be 2.94.

All vehicle primary structures have been fabricated using a reinforced carbon fiber-blue tube composite to combine robust strength and stiffness at a lower cost than pure carbon fiber. All internal bulkheads have been cut in-house using either high strength plywood, aluminum, or 1018 steel. A custom carbon fiber tail cone has been designed to accommodate the motor, and has been manufactured in-house using aerospace standard carbon fiber wet lay-up techniques. Vehicle components are each verified to the launch environment using finite element analysis in correspondence with the structural analysis payload, which translates to exceptional design confidence. The concept of flight operations has remained unchanged since the CDR, and is shown in Figure 4.

Each launch vehicle system will be described in detail along with its specific construction and fabrication process and a CAD schematic to explain assembly.

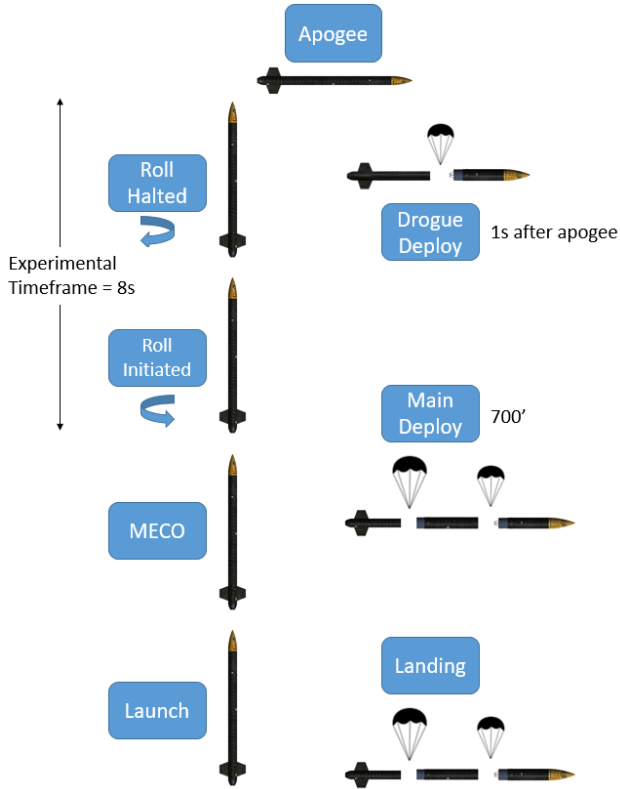


Figure 4: Experimental Flight Overview

3.2 Detailed Changes Since CDR

As mentioned in section 2.1, there are three changes to the fullscale launch vehicle that have occurred since the CDR. These are:

- (i) Rocket length changed to 99" from 94.75" to accommodate payload assembly.
- (ii) Estimated mass increased to 34.0 lbs from 30.3 lbs with the addition of mass in the payload section.
- (iii) Static Stability Margin increased to 2.43 from 2.16 as payload mass increased.
- (iv) Additional general safety information, environmental precautions, launch operation procedures, and checklists have been added to augment the established safety protocol.

Each of these changes is a resultant from the same design adjustment in the payload section. To complete the attitude control experiment set out by VADL in the '16-'17 student launch, two sets of cold gas thrusters need to be actuated and supplied with compressed air a compressed air tank in the nosecone. Flexible rubber hosing completes this task, running from the the output of the compressed air tank to each set of thrusters. For more information on the payload experiment, see section 4.

Essentially, the payload section of the launch vehicle increased by 4.25" due to the geometry constraints of the available hosing from the air tank regulator to the solenoids.

Given our needed hose specifications (a hose inner diameter greater than or equal to 1/8", operating pressure \geq 3000 psi, high flexibility), our local hosing supplier only had sufficient hosing in discrete length sections with 12" being the closest available to our CDR length estimate. Furthermore, the 0.75" minimum bend radius of this hose led to a small increase in air frame length to make sure this bend radius was not approached during assembly. Figures 5, 6, and 7 further illustrate this payload section lengthening.

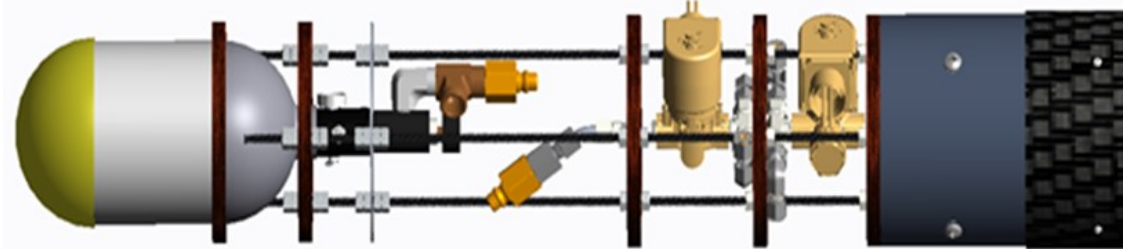


Figure 5: Payload Section CAD at CDR

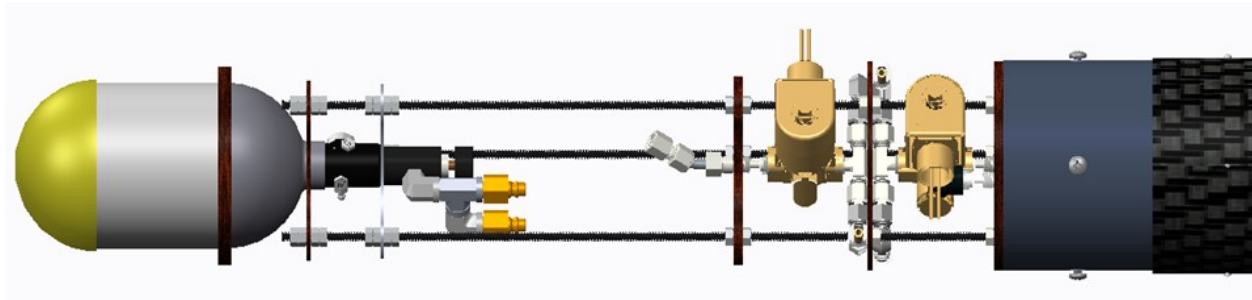


Figure 6: Payload Section CAD at FRR



Figure 7: Fullscale Launch Vehicle Payload Section

To counteract the weight increase caused by the new payload design, the non-load-bearing bulkheads were optimized to reduce overall mass. This will be further detailed in Section 4.1.5. The resulting longer launch vehicle's SSM at rail exit of 2.94 meets the NASA SL requirement of greater than a 2.0 SSM, and VADL remains confident that the launch vehicle will be able to complete the proposed experiment as desired.

3.3 Design & Construction of Launch Vehicle

Over the course of the last 2 months, VADL has been hard at work fabricating the fullscale launch vehicle from scratch. It was a focus this year to bring manufacturing back in-house and give the undergraduate students a chance to get hands-on experience. Additionally, in-house manufacturing reduces cost relative to custom purchases, thereby giving VADL a larger budget for innovative projects to pursue. The fullscale launch vehicle was completed February 15th, 2017, leaving time to complete the integration tests before our February 19th launch date. This section will step through the fabrication process from nose to tail. The fullscale launch vehicle can be seen in Figure 8 sitting on the launch rail.



Figure 8: Fullscale Launch Vehicle on Launch Rail

3.3.1 Nosecone

The purpose of the nosecone is to add an aerodynamic shape to the forward end of the launch vehicle, and be able to integrate effectively with the rest of the airframe. Additionally, VADL has chosen to house the compressed air tank needed to complete its payload experiment inside of the nosecone - this adds the additional requirement that the nosecone must be retrofitted to constrain and add structural stability to the air tank. Fabrication of the nosecone focused on this latter requirement. A schematic of the fullscale nosecone and its internal components can be seen in Figure 9 , below.

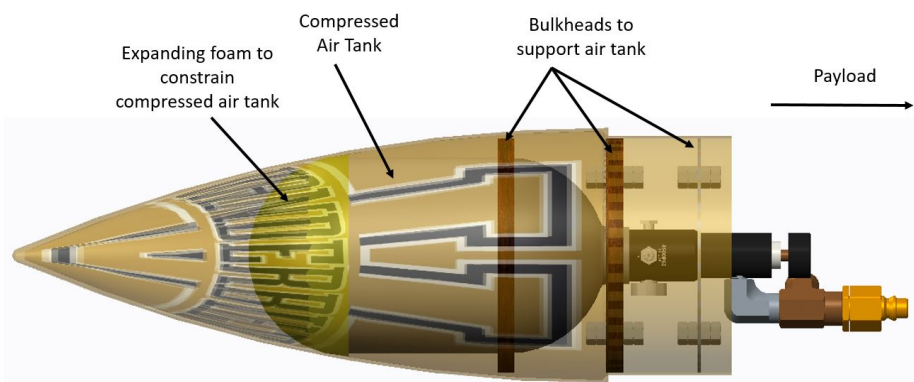


Figure 9: Fullscale Nosecone CAD Schematic

The nose cone is a 5.38" polypropylene plastic nose cone manufactured by LOC Precision Rocketry (Figure 10). Its tangent ogive shape is the most common shape for hobby rocketry outside of a simple cone. Since the launch vehicle flying well below the speed of sound (Mach 0.55), the nose cone pressure drag is essentially zero and the majority of the drag comes from the friction drag. The friction drag is dependent upon the wetted area, surface roughness, and discontinuities in shape - all of which were under careful scrutiny when selecting and preparing our nosecone.

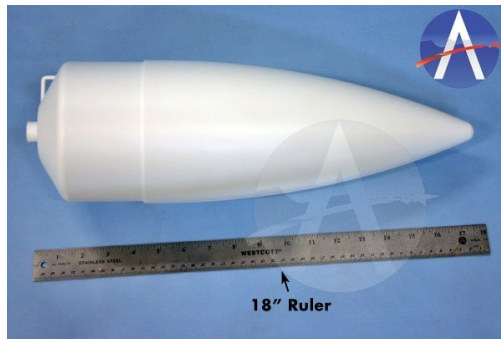


Figure 10: Purchased Nosecone - Photo from ApogeeRockets.com

In order to prepare the nose cone for our launch vehicle's design, a laser cut $\frac{1}{4}$ " birch plywood retaining ring for the air tank was epoxied with Loctite inside the nosecone. Because polypropylene doesn't bond well to epoxy, the surface was sanded with coarse sandpaper (100 grit). Then, holes were drilled in the retaining ring and drinking straws were pushed through the holes for venting (Figure 11a). The air tank was wrapped in plastic, and expanding foam was poured into the top of the nose cone. The foam was allowed to expand around the air tank, helping to constrain it vertically during takeoff and landing.

The next step in preparing our nose cone was to epoxy it to the body tube (Figure 11b). A large number of small holes were drilled into the tapered part of the nose cone. Then, the nose cone was sanded along with the interior Blue Tube where it would interface. Loctite epoxy was added around the rim and the nose cone was twisted into the body. Then, epoxy was added to the interior of the tapered part. Since the epoxy now surrounded the holes, it effectively created a mechanical lock for the nose cone.



(a) Nosecone Prepped for Foam with Epoxy & (b) Nosecone Finalized and Epoxied onto Body Venting Straws

Figure 11: Nosecone Fabrication

The nose cone was sanded down and painted with Rustoleum Metallic Gold paint. While typically used for art projects and not outdoor use, its use was justified since the rocket will only be in flight two or three times and otherwise used as a display piece. The completed nosecone can be seen in Figure 12.



Figure 12: Completed Nosecone

3.3.2 Airframe Fabrication

There are three main body tubes that make up the launch vehicle, displayed below in Figure 13. The process for creating these outside body tubes is the same, and that process is detailed below.



Figure 13: Sections of the Fullscale Launch Vehicle

This year, it was decided to move from custom-ordered carbon fiber airframes to carbon fiber reinforced Blue Tube. This combination of materials creates an ideal composite for model rocketry, as it is much lower in cost than pure carbon fiber while still maintaining carbon fiber's durable and high strength qualities. The switch to in-house fabrication gives VADL undergraduates valuable experience in carbon fiber layups.

The process of rolling the body tubes starts with cleaning a glass surface with acetone to ensure it is free of particulates which may otherwise weaken the structure. Then, the 5.5" Blue Tube is cut to length (with extra on each ends to be cut off later) and sanded to promote adhesion. The carbon fiber weave is cut to the proper length and taped to the table. Wooden bulkheads are loaded onto a 1/2" threaded rod and inserted into the Blue Tube to help it keep its shape during the compressive forces applied by the carbon fiber process. Paintbrushes are selected for the epoxy, and the loose bristles are removed. The epoxy resin is mixed with the hardener in the proper ratio, and applied generously to the carbon fiber. After the fibers are saturated with epoxy, the excess is scraped off using putty scrapers. A light brushing of epoxy is applied to the Blue Tube. Then, the tube is placed on the carbon fiber sheet and carefully rolled, being sure to keep tension in the fibers. This process can be seen in Figure 14.

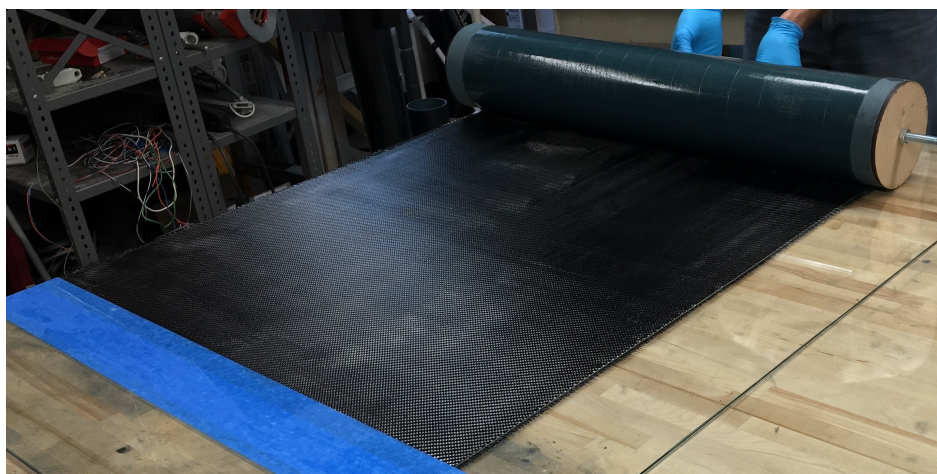


Figure 14: Rolling the Carbon Fiber Tubes

After the tube is rolled, the fiber is cut before the tape at the end, and a layer of perforated shrink tape is applied. The shrink tape contracts at high temperature, squeezing the excess epoxy out and producing a high gloss on the carbon fiber. The epoxy we use, Fiberglass System 2000, has a pot

life of 120 minutes and requires heat treatment to obtain optimum qualities. In order to achieve an ideal cure temperature, we built the "Hotbox" - a large temperature-controlled curing chamber. We used this opportunity as a practice session for ROSMOD and BeagleBone Black, our software and hardware system. For more information on the fabrication of this Hotbox, see the PDR. A picture of the Hotbox with an airframe inside can be seen in Figure 15, below.

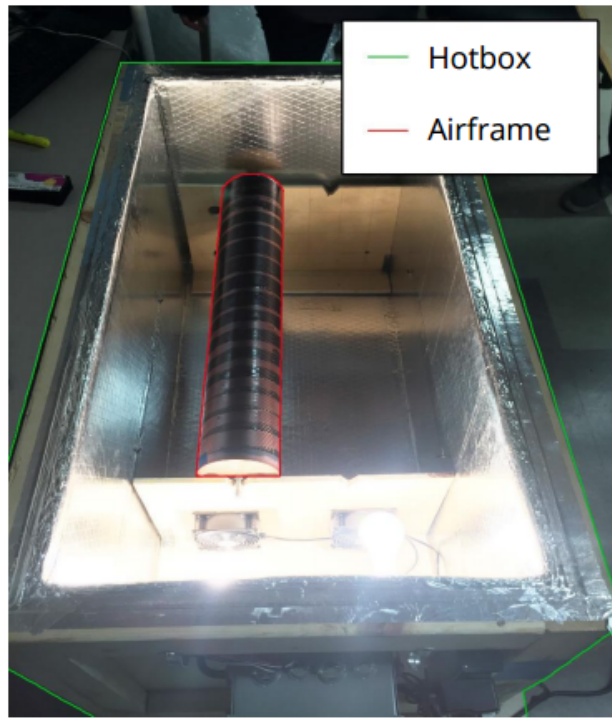


Figure 15: Hotbox with Airframe Curing Inside

After placing the tube in the Hotbox utilizing the threaded rods, the lid is latched and the airframe is left to cure for 12 hours. A brief period is spent at 190°F to allow the shrink tape to compress, before throttling down to the optimum curing temperature, around 160°F. Here, the box cycles the heating elements (lights) on and off to maintain the temperature for around 12 hours, at which point the lights are turned off and the sealed Hotbox is allowed to ramp down to room temperature. Following Hotbox curing, the tube is taken out and the shrink tape is removed.

The last step in fabricating the post-Hotbox airframe is to remove the burrs caused by excess epoxy exiting through the perforated shrink tape. These are sanded until the tube is smooth, finishing at 1000 grit. A photo of a burred tube can be seen in Figure 16.

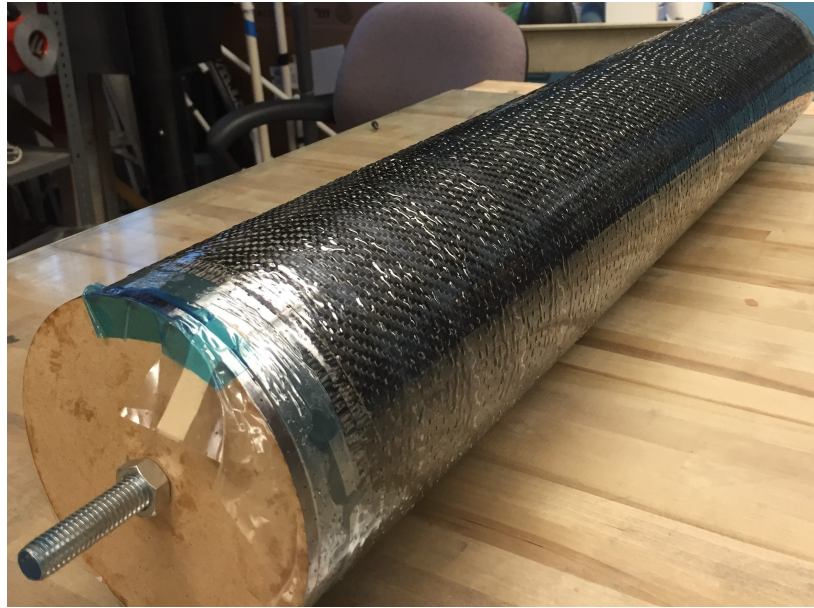


Figure 16: Airframe Directly after Exiting Hotbox

After sanding, the tube is cut to the proper length. An example of a completed airframe section is shown below in Figure 17.



Figure 17: Completed Airframe Section

3.3.3 Payload & Avionics Section

The payload is mounted within the combined nosecone-payload airframe assembly. The avionics are mounted separately in the avionics airframe. This section describes how these systems are constrained and connected.

3.3.3.1 Payload Section

This year's payload section houses the thruster system and translates the rotational torque from the thrusters onto the remaining launch vehicle body. A "payload skeleton" runs through the inside of this section. The payload skeleton is comprised of a series of bulkheads and threaded rods that support all of the components used in the experiment, including the compressed air tank,

cold gas air thrusters, and payload electronics. The fabrication of the internal components of the payload section will be discussed later - see 4 for more details. A conceptual view is shown in Figure 18 below to aid in understanding of this section.

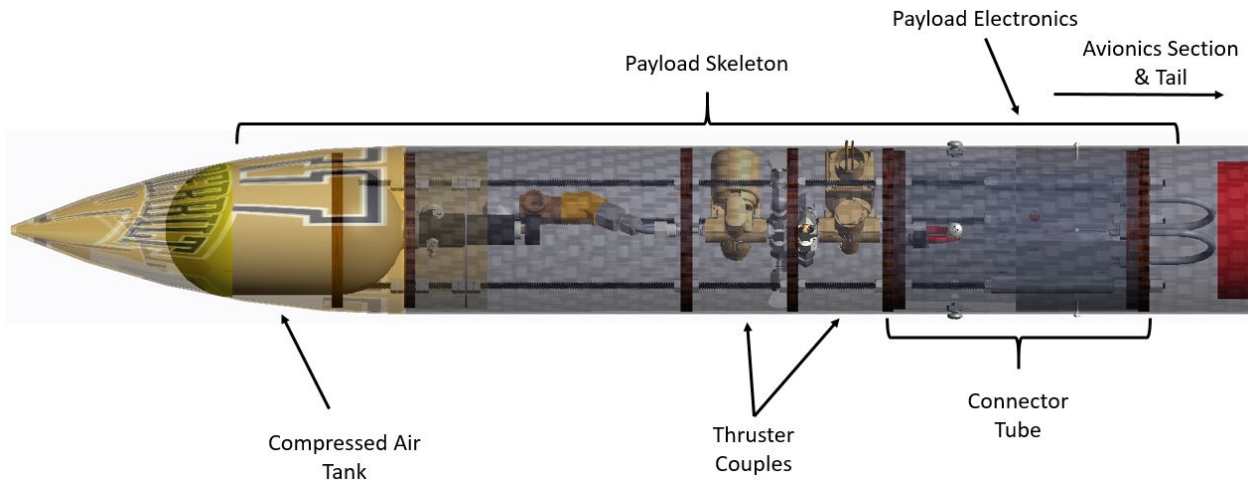


Figure 18: Diagram of Nosecone & Payload Sections

A picture of the completed payload airframe and attached nosecone can be seen in Figure 19, below.



Figure 19: Fabricated Nosecone & Payload Section

Seen in the figure above, the payload section features a number of holes: nine in total. The first four are for the outlet plume of the cold gas thrusters. They are measured from the bottom of the tube, and drilled using a $\frac{1}{4}$ " drill bit. A Dremel sanding bit is used to open the holes to the proper size for the thruster outlet. The next hole is for a 4-40 bolt that inserts into a nut epoxied into the payload skeleton. This bolt ensures that the skeleton does not rotate within the airframe. The final four holes are for $\frac{1}{4}$ "-20 steel bolts that go through the airframe and into the 5.5" Blue Tube Coupler, which is compressed by the payload skeleton and connects the payload and avionics sections together. Coupler tube will be discussed in more detail in Section 3.3.3.2 below.

3.3.3.2 Avionics Section

The purpose of the avionics section is to house the parachutes and avionics electronics that control deployment. The avionics airframe must give sufficient structural support for load transfer

under blast charge detonation and parachute deployment - this analysis is discussed in Section 3.6.1. High ease-of-assembly and modularity is of key importance. In order to aid in accomplishing these goals, a robust avionics bay has been built. The avionics bay is comprised of two bulkheads, U-bolts to transfer parachute loads, and a 3D printed sled to mount the needed electronics. The avionics bay slides into the fore end of the avionics airframe and is secured using $\frac{1}{4}$ "-20 steel bolts into $\frac{1}{4}$ "-20 aluminum coupler nuts that have been welded on to an aluminum bulkhead. This process is discussed later in Section 3.3.4. While a full description of the avionics bay's internals and construction can be found in Section 3.6.5, a general overview can be seen in Figure 20, below.

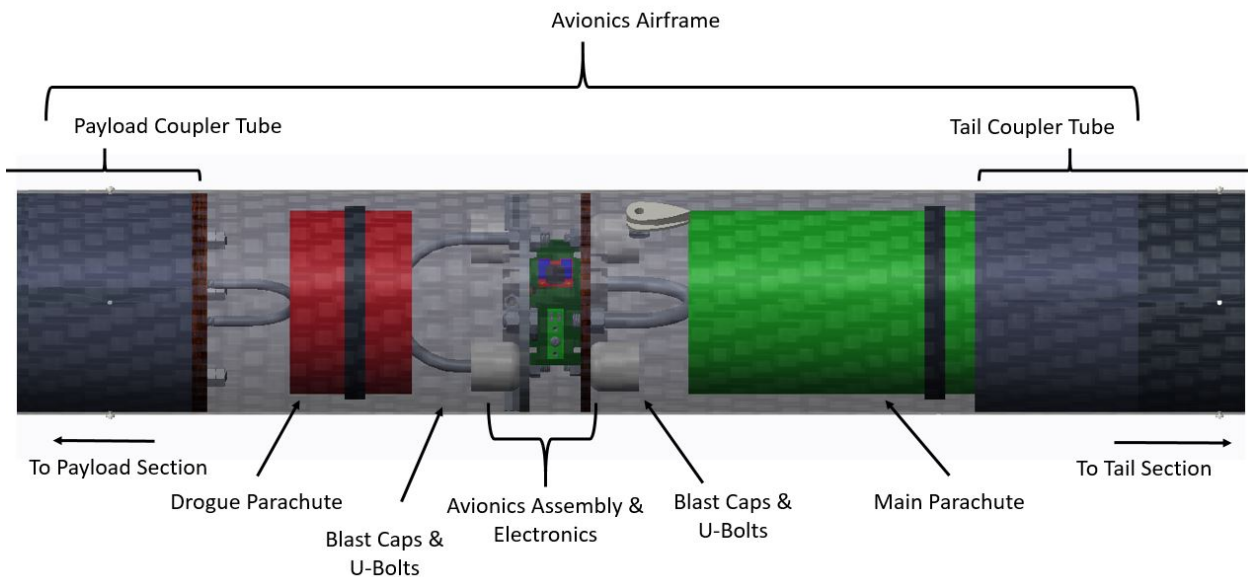


Figure 20: Diagram of Avionics Sections

Coupler Tube As mentioned in Section 3.3.3.1 above, a coupler tube is needed on either side of the avionics airframe to connect it to the other two sections. The coupler tube has two purposes: (1) to keep the launch vehicle rigidly supported on the way up to apogee, and (2) to allow for complete separation during parachute deployment. Each coupler tube is an 8" section of 5.5" Blue Tube Coupler, tubing with slightly smaller diameter than the main airframe. The fore 4" of each coupler tube is connected to its respective section more permanently, while the aft 4" of coupler tube is held with shear pins to allow for separation.

The fore coupler tube connects the payload and avionics sections. The front 4" is held to the payload section via 4x $\frac{1}{4}$ "-20 steel button head bolts into $\frac{1}{4}$ "-20 steel weld nuts. The weld nuts were bent, sanded, and cleaned to fit the Blue Tube before applying JB Weld epoxy (Figure 21, below). The structural considerations are discussed more thoroughly in Section 3.6.1. The bottom 4" is connected to the avionics section via 4x 4-40 nylon shear pins that go through the avionics airframe and into the Blue Tube Coupler that is compressed by the payload skeleton. The pins

shear upon drogue parachute deployment, allowing the coupler tube to remain with the payload section while the avionics section separates at 1 second after apogee.



Figure 21: Coupler Tube with Weld Nuts Installed

The aft end of the avionics section houses the other coupler tube. The fore 4" is sanded and attached to the aft end of the avionics section using Fiberglass epoxy, allowing the coupler tube to remain with the avionics section while the tail section completely separates at 750 ft. AGL. The aft 4" of the coupler is connected to the tail section via 4x 4-40 nylon shear pins, which break following main parachute deployment. The shear pins go through the tail airframe and into the coupler. A picture of the completed avionics section can be seen below, in Figure 22.

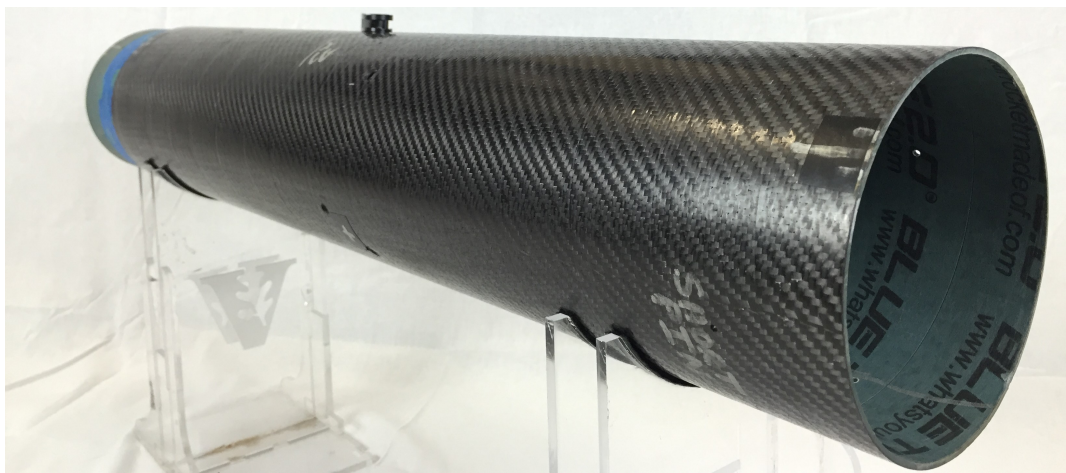


Figure 22: Finished Avionics Section

3.3.4 Aluminum Bulkheads

The launch vehicle contains three aluminum bulkheads, machined by hand from a $\frac{1}{4}$ " aluminum plate. From fore to aft end, they are:

1. Avionics Bulkhead: This bulkhead fits snugly within the main diameter of the airframe and is bolted through the airframe with the use of 4x $\frac{1}{4}$ "-20 aluminum coupling nuts that have been welded on.
2. Main Parachute Tail Bulkhead: This bulkhead sits on top of the motor tube, centering it within the airframe. It also holds the $\frac{5}{16}$ " U-bolt for the main parachute. It is epoxied along its perimeter to the airframe.
3. Fin Centering Bulkhead: This bulkhead centers the fins with the motor tube and the airframe. It is epoxied to the outside of the motor tube and the inside of the airframe.

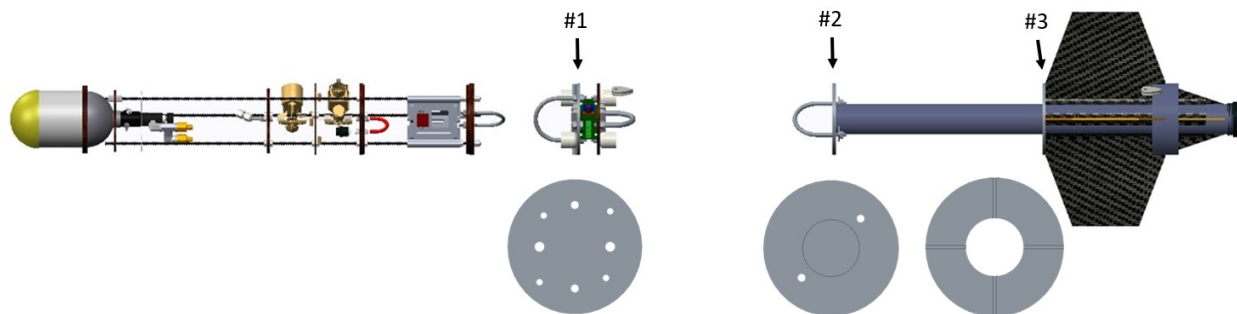
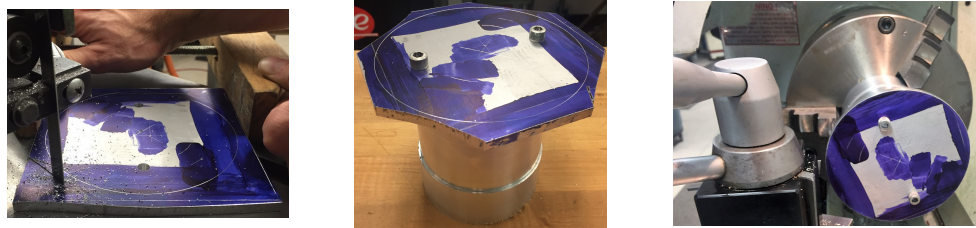


Figure 23: Fullscale CAD with Aluminum Bulkheads

The process to start the bulkheads is the same for all three. First, a jig to hold the plate was machined from a piece of cylindrical aluminum stock. The jig was turned in the lathe to make it concentric, then taken to the mill and put in a V-block clamp before finding the center using a dial indicator. Two $\frac{5}{16}$ "-18 holes were drilled and tapped the center-to-center distance of the chosen U-bolt. The edges of the holes were deburred to help the fitment of the jig and the plate.

To start the creation of the three bulkheads, bounding squares were marked up on the flat aluminum plate with layout fluid and cut using a bandsaw. Approximate geometric centers of the bulkheads were found by scribing lines across the diagonals of the squares. The bulkheads were mounted on the mill with two parallels, and two $\frac{5}{16}$ " holes were drilled. Then, the band saw was used to clip the corners of the bulkhead to achieve a roughly circular shape. One by one, each bulkhead was bolted to the jig using $\frac{5}{16}$ "-18 bolts and inserted into the lathe. The bulkheads were turned down to the proper outside diameter (until they fit the inside diameter of the Blue Tube). This process can be seen in Figure 24.



(a) Cutting Rough Shape on Bandsaw (b) Attaching the Bulkhead to the Jig (c) Turning the Bulkhead on the Lathe

Figure 24: Aluminum Bulkhead Fabrication

Here, the process deviates for the avionics (1) and tail bulkheads (2,3). The avionics bulkhead (1) was taken to the mill, where holes were drilled to allow the U-bolts, wires, and blast caps to pass through. Finally, aluminum coupler nuts were welded on with the assistance of our rocketry mentor. A more in depth description of the avionics bay's construction can be found in Section 3.3.3.2. The completed avionics bay can be seen below, in Figure 25.



Figure 25: Completed Avionics Bay

For the tail bulkheads (2,3), a parting bit was used to create grooves on the outside of the bulkhead that would allow the epoxy to set inside. The cutter was then changed and the inside concentric circle was cut. For the main parachute bulkhead (2), this concentric circle extended $\frac{1}{8}$ " into the $\frac{1}{4}$ " plate, while for the centering bulkhead (3), the circle was cut through the full length of the plate to allow the motor tube to pass through. The fit of these holes was checked against the motor tube to ensure a snug fit. At this point, the main parachute bulkhead (2) was finalized. This process can be seen in Figure 26.

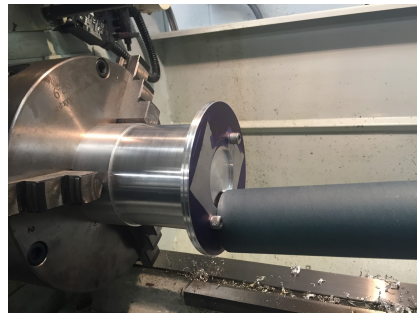


Figure 26: Checking the Fit of the Motor Tube

The fin centering bulkhead (3) was brought to the mill. After finding the center using a dial indicator, a 1/8" end mill was mounted and the grooves that house the fins were cut. Small passes were taken to keep the end mill bit from breaking, cutting only 0.02" at a time. The bulkhead seen in Figure 27 from the subscale was constructed in the same fashion and has attributes of both the main parachute bulkhead and fin centering bulkheads.



Figure 27: Parachute/Centering Bulkhead (Subscale)

3.3.5 Tail Section

The tail body section is the most complicated part of the rocket body. It contains space for the parachute, motor tube, and fins. The fabrication consists of 3 parts:

1. Creating the Motor Tube Assembly
2. Slotting the Tail Airframe
3. Securing the Motor Tube Assembly Within the Airframe

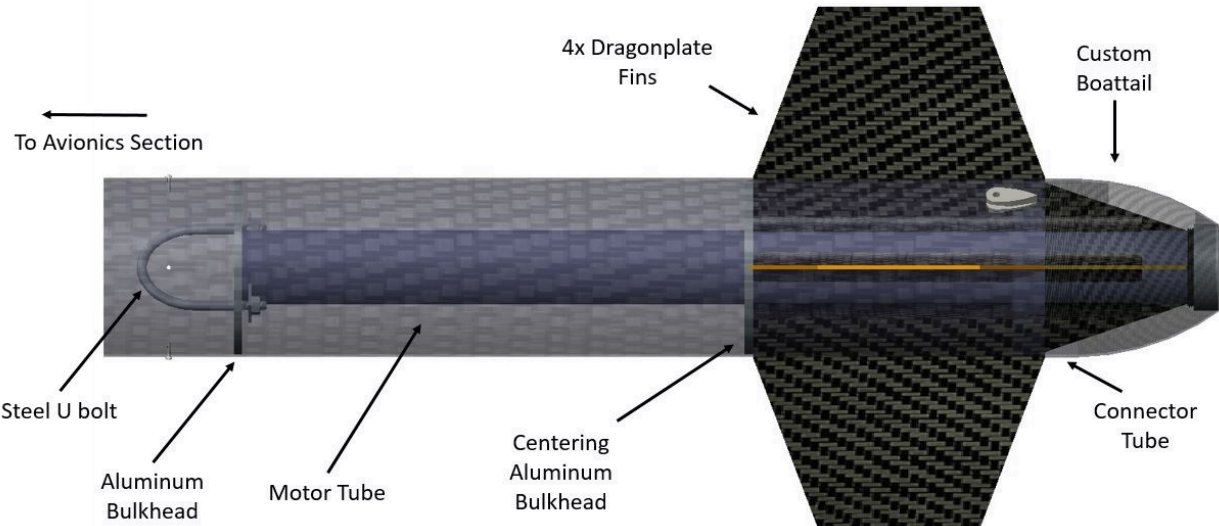


Figure 28: CAD Diagram of Tail Section

Creating the Motor Tube Assembly The first step of the tail fabrication process is to create the motor tube assembly. The motor tube was cut to 30" from 54mm Blue Tube. The fins were water jet cut from $\frac{1}{8}$ " carbon fiber plate. This is performed locally by Loftis Steel and Aluminum. Then, a fin mounting jig was designed and laser cut from medium-density fibreboard (MDF) to align the fins and aluminum bulkheads together. The jig (Figure 29a below) ensures that all fins are mounted at 90° to each other, and allows them to be held in place during assembly. After assembling the jig using $\frac{1}{2}$ " threaded steel rods, the motor tube was sanded and Loctite epoxy was used to mount the fins together with the motor tube and bulkheads. The assembly was compressed using the jig and allowed to dry. The result is shown in Figure 29b.



(a) The Fin Mounting Jig in Operation



(b) The Finished Motor Tube Assembly

Figure 29: The Construction of the Motor Tube Assembly

The finished assembly was then prepared for a carbon fiber fillet process (Figure 30, below). The carbon fiber fillets give the motor tube the needed strength to transmit the high thrust to the exterior of the rocket body. Fiberglass System 2000 epoxy and 2120 hardener was prepared and brushed onto the motor tube between the fins. Small carbon fiber filaments, taken from scrap, were laid into the groove between the motor tube and the fin for extra rigidity. Then, two layers of carbon fiber were added between the fins and motor tube with more epoxy in between. The carbon fiber was laid up slightly onto the centering bulkhead in order to assure its fixation to the motor tube. Following the carbon fiber, perforated peel ply and a cotton-like material called bleeder breather were layered. The perforated peel ply keeps the epoxy from sticking to anything but the surface of the assembly and carbon fiber, while allowing excess epoxy to absorb into the bleeder breather. The entire assembly was wrapped in green vacuum bagging plastic, and sealed using grey sealant tape. A vacuum nozzle was attached to assembly on top of an extra piece of bleeder breather, and the entire layup was compressed using a vacuum pump. The vacuum was propagated across the assembly thanks to the porous quality of the bleeder breather. After making sure there were no leaks, the assembly was transported to the Hotbox and allowed to cure for 12 hours at 160°F.



Figure 30: Applying Carbon Fiber Fillets to the Motor Tube Assembly

Slotting the Tail Airframe A jig was constructed in order to slot the tail section body tube. The slots are needed for the body tube to slide over the motor tube-fin assembly. The jig (Figure 31) is designed to be reusable for the future; it allows different lengths of slotting and features a resizeable interior for different tube sizes. It also allows us a flat surface to cut the tubes against.



Figure 31: The Laser Cut Fin Slotting Jig

After taping the jig to the airframe, an up-shear $\frac{1}{8}$ " end mill was used in the Dremel to cut the fin slots. This process is shown in Figure 32 below. Since the jig is essentially a box with four flat surfaces, it ensures that the slots are all aligned at 90° to each other.



Figure 32: Paul Slots the Tail Airframe

Securing the Motor Tube Assembly Within the Airframe Following the slotting of the tail section body tube, it was slid over the fin-motor tube assembly. Loctite epoxy was used to secure the aluminum bulkhead and the fins to the tail section body tube. A 2" coupler tube that will hold the tail cone was cut and epoxied inside the body tube.



Figure 33: Nina applies Loctite Epoxy to Secure the Motor Tube Assembly

After the epoxy had cured, a similar process as before was performed, adding carbon fiber fillets to strengthen the bond between the fins and the body tube.



(a) The Tail Section Prior to Airframe Fillets



(b) Carbon Fiber Fillets are Compressed Onto the Airframe

Figure 34: Securing the Motor Tube Assembly to the Airframe

A closeup image of the resulting fillets can be seen in Figure 35 below.

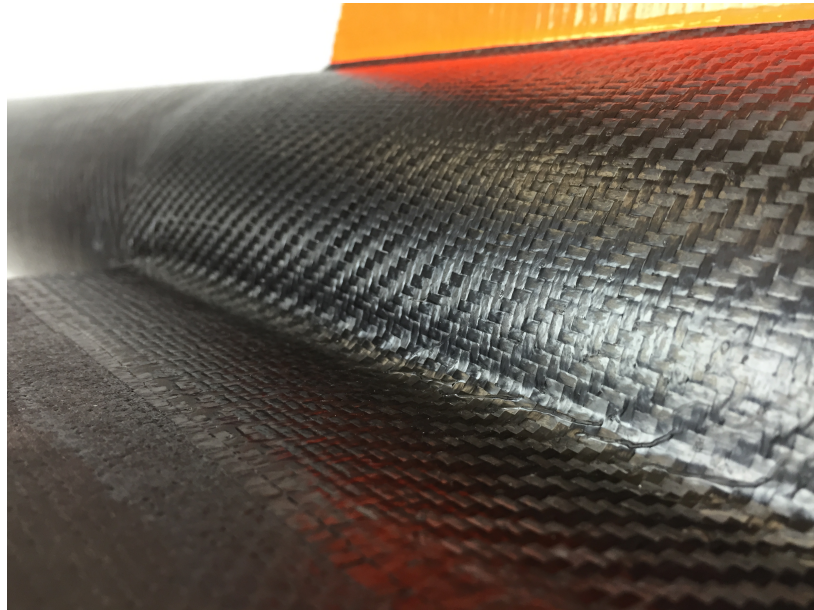


Figure 35: Closeup of The Carbon Fiber Fillets

3.3.6 Tailcone

The final part of the body is the tail cone. First, a fiberglass mold had to be created. A solid model of the tailcone was 3D printed, waxed with paraffin wax, and placed onto a waxed acrylic surface. Then, a white epoxy gel coat was applied to the surface of the tailcone. After the gel coat had

dried but was still tacky, about seven layers of fiberglass and epoxy were applied. Following the curing of the fiberglass, the ABS tail cone was extracted from the mold. Then, the mold was wet sanded up to 1000 grit sand paper. After a few more coats of wax, a PVA polymer spray was applied to keep the final part from sticking. A hole was drilled in the and a small steel plate was placed in the bottom of the mold to be able to ram the part out in case it became mechanically locked. The tailcone mold and ABS model used to create the mold can be seen in Figure 36 below.



Figure 36: The Tailcone Mold and ABS Model

Finally, the carbon fiber process started. Enough trapezoidal pieces to cover seven layers were cut and placed inside the mold. Epoxy was applied generously with each layer. Then, the carbon fiber was covered with perforated peel ply and bleeder breather before enclosing the entire mold in a vacuum bag. The carbon fiber was cured under vacuum compression in the Hotbox for twelve hours. Finally, the carbon fiber piece was extracted using the ramming rod. It was trimmed to size and secured to the tail section through 4 axisymmetric shear pins. The finished tailcone can be seen in Figures 37 and 38 below.



Figure 37: The Finished Carbon Fiber Boattail

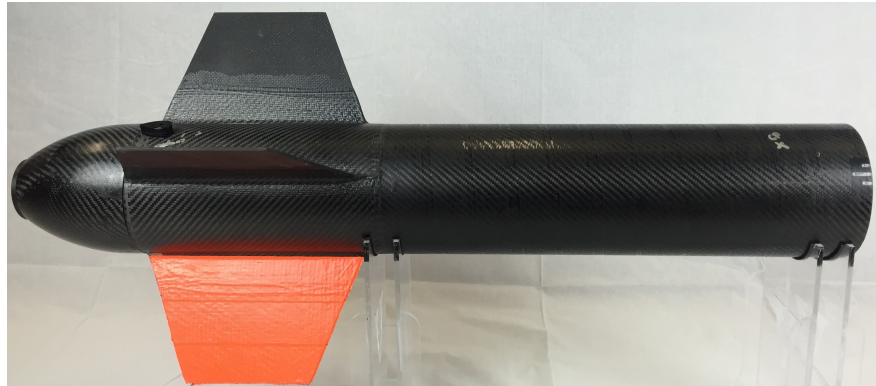


Figure 38: The Finished Carbon Fiber Boattail Integrated Onto the Tail Section

3.3.7 Final Assembly

The final step to assembly was to install the launch lugs that guide the vehicle along the launch rail. One launch lug is located as far aft as possible on the tail section, to ensure that the vehicle stays in light with the rail for as long as possible. It can be seen in Figure 38 above. The second lug is located on the avionics section near the CG, to minimize the effect of outside torques. Airfoil shaped launch lugs were chosen for their aerodynamic properties, and bolted through the airframe with the use of $\frac{1}{4}$ "-20 steel weld nuts affixed with JB Weld epoxy in the same manner as in the coupler tube (shown in Figure 21). One of the most important parts of assembly is the indexing of airframe sections - this ensures a perfect fit each time the airframe is assembled. Index marks are made as soon as the airframe pieces are cut to size to ensure that there are no alignment issues. High-visibility tape was added to one of the fins to help the chance of roll-visualization during flight and ground based testing. A full list of assembly procedures is detailed in Section 6. The final vehicle in its fully assembled state is shown in Figure 39 below.



Figure 39: The Completed Assembly of the Fullscale Launch Vehicle

3.4 Critical Design Features

3.4.1 Structural Elements

The main structural area of concern during takeoff is the tail section. The motor itself is held in the motor mount with a standard screw-cap positive retention system, which makes it impossible for the motor to come loose unexpectedly during flight or recovery. This transmits all of the motor force through the thrust ring onto the carbon fiber Blue Tube motor tube. The four 1/8" carbon

fiber plate fins are mounted directly to the motor tube with carbon fiber fillets and extend through the tail section airframe, also attaching with carbon fiber fillets. The strength of the carbon fiber and large surface area of connection make this an effective mode of force transfer. In addition, the fins taper down onto the motor tube, increasing the bonding area of the fins and reducing the chance of column buckling of the motor tube by introducing a gradual area change from the thrust ring to the airframe. Centering rings, attached with Loctite epoxy just fore of the fins and on the top of the motor tube provide a backup mode of force transfer, and assist in precision fin alignment. Figure 40 shows how the force of the motor is transmitted throughout the rocket body.



Figure 40: Block Diagram of Thrust Transfer

All vehicle airframe structures will be made of carbon fiber reinforced Blue Tube. This combination of materials creates an ideal composite for model rocketry, because it is lower cost than pure carbon fiber while still being a durable, high strength alternative to the phenolic tubing commonly used in rocketry. Using this carbon fiber reinforced Blue Tube for the airframe also moves manufacturing in-house, giving VADL undergraduates valuable experience.

To ensure the carbon fiber reinforced Blue Tube is an appropriate material, two compression tests were performed. The first tested the solid carbon fiber reinforced Blue Tube. The failure load of this airframe was 10,880 lbs force, which correlates to a stress of 6468 psi. Its stress-strain diagram is shown in Figure 41.

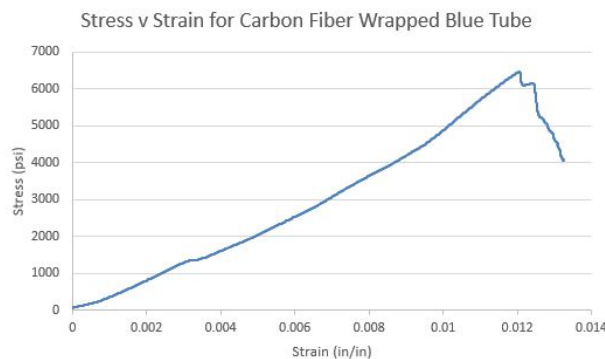


Figure 41: Stress-Strain Diagram for Solid Body Tube

The second compression test took into account airframes with holes in them. Holes will be drilled into the launch vehicle airframe for a variety of reasons, such as exhaust holes to prevent over-pressurization in the payload section, or access holes in the avionics section. This drove our

decision to test a second body tube to characterize the strength of the carbon fiber reinforced Blue Tube containing stress concentrations caused by the holes. As expected, the airframe failed along the lines of the holes. This is shown in Figure 169.

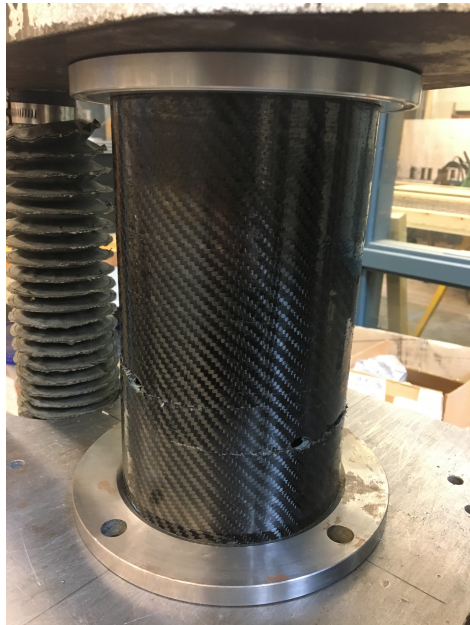


Figure 42: Failure Points for Bodytube with Stress Concentrations

The failure point of this tube is 9,790 lbs force, which correlates to a stress of 5827 psi. The stress-strain diagram is shown in Figure 43.

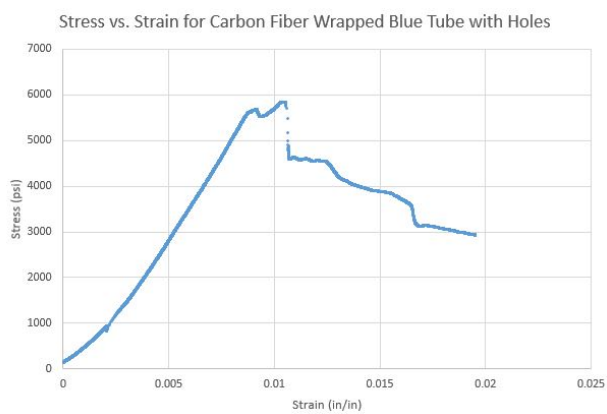


Figure 43: Stress-Strain Diagram for Bodytube with Holes

This test proved that holes in the airframe somewhat decrease the failure load. In order to prove that the carbon fiber wrapped Blue Tube can stand up to inertial effects of rocket acceleration, a

worst case scenario was analyzed. The acceleration of the rocket is greatest at takeoff. If the takeoff acceleration was 18g's, healthily above the predicted 15g's, and the isolated tail section instantaneously hit the rest of the rocket body, there would be an inertial force of 334 lbf. This is well below the experimental deformation value of 9,790 lbf. The airframe will withstand all inertial forces during takeoff and the duration of the launch, thereby making the carbon fiber wrapped Blue Tube an appropriate material choice for the airframe.

Discussion of the bulkheads and loading from recovery operations is reserved for Section 3.6.1.

3.4.2 Vehicle Electrical Elements

There are two electronic subsystems aboard the flight vehicle: the payload electronics subsystem and the recovery subsystem. Each subsystem is self-contained, and secured to the rocket vehicle using 3D printed sleds. See Sections 4.3 and 3.6.5 for renderings of the payload and recovery bays, respectively. ABS plastic is a strong, lightweight insulator, ideal for electronics. Because they are 3D printed, the sleds have been optimized for wire routing, low mass, structural strength, ease of assembly, and accessibility. Shielded wires and cables are routed through the center cavity of the payload sled to prevent wire pinching during assembly. All electronic boards are secured to the sleds using integrated standoffs and 4-40 nylon screws.

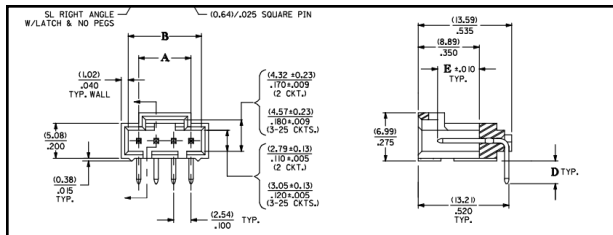
Electrical interconnects between the components of each subsystem are made using XT60 drone connectors (Figure 44) for wire-to-wire connections and Molex locking right-angle connectors (Figure 45) for wire-to-board connections. These locking connectors improve reliability and reduce the off-board height of the electrical systems. Tests are performed on these connectors by the manufacturer, including vibration endurance and mechanical shock tests (Figure 46). The manufacturer requires that electrical continuity must be maintained during stress for the connector to pass the test.



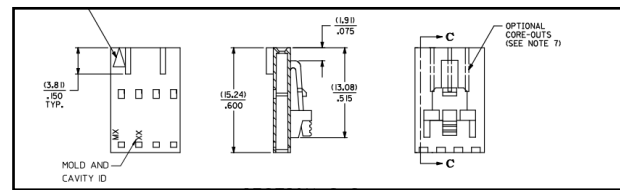
Figure 44: XT60 Connector for Wire-to-wire Connections

Each subsystem is independently powered. The two rechargeable Li-Ion payload electronics batteries each weigh 120 grams, and are secured in tight compression to their sled using zip ties routed through strategic holes. See Section 4.3 for CAD renderings of the payload electronics bay. Two Lithium 9V batteries power the recovery subsystem's altimeters and blast charges. These batteries are secured in compression between the two bulkheads that seal the avionics chamber. See Section 3.6.5 for CAD renderings of the recovery system.

Both subsystems are armed from outside the assembled rocket using screw switches manufactured by Missile Works, as pictured in Figure 47. When the screw head is tightened against the exposed trace, the two terminals are shorted together.



(a) Molex Locking Connector (Female)



(b) Molex Locking Connector (Male)

Figure 45: Technical Drawings of the Molex 4 Pin Locking Connector for Wire-to-board Connections

Vibration Mil-Std-1344 Method 2005.1 Condition 1	Amplitude: 1.50mm (.060 inch) peak to peak Sweep: 10-55-10 Hz in one minute Duration: 2 hours in each X-Y-Z axis. (Test module shall be per Section 7.0)	Contact Resistance: 10 milliohms Maximum Change from Initial Discontinuity: not greater than one microsecond
Mechanical Shock Mil-Std-1344 Method 2004.1 Condition A	50 g's with three 1/2 sine wave form shocks in each X-Y-Z axis. (Test module shall be per Section 8.2)	Contact Resistance: 10 milliohms Maximum Change from Initial Discontinuity: not greater than one microsecond

Figure 46: Manufacturer's Mechanical Test Requirements for Molex Right Angle Connector

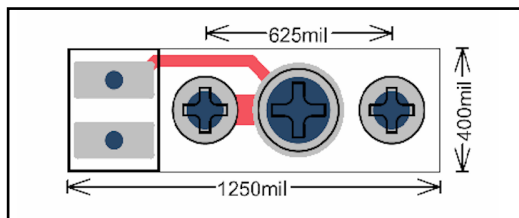


Figure 47: Screw Switch for Electrical System Arming

3.5 Flight Reliability Confidence

3.5.1 Mission Statement

The VADL 2016-2017 team mission is to successfully build, test, and fly a rocket carrying an attitude control payload which will enable valuable in-flight experimentation and data collection. The objective of this attitude control payload is to induce roll about the rocket's vertical axis post motor-burnout, rotating the rocket in one direction and then returning it back to the original position with a counter roll. After the experiment is completed, the launch vehicle will reach apogee (5280 ft) and land safely, ready to be launched again in the same day.

3.5.2 General Mission Success Criteria

First and foremost, for the mission to be a success, it must be conducted in accordance with all NASA imposed requirements and regulations, from planning to construction to final execution. Beyond this however, the Vanderbilt Aerospace Design Lab has identified a list of additional requirements and mission success criteria. These mission success criteria are not exhaustive in

nature, and only apply to the vehicle and recovery systems. The payload success criteria is addressed specifically in Section 4. A fully exhaustive list of all requirements and mission objectives can be found in Section 7.2.

3.5.3 Launch Vehicle Mission Success Criteria

1. The launch vehicle shall attain a target altitude of 5280 ft AGL
2. When fully assembled on the launch pad, the launch vehicle must be structurally stable once the nosecone and payload airframe are removed, so as to allow for payload manipulation
3. All sections of the post-chute deployed rocket must remain structurally stable when in free fall
4. All sections of the launch vehicle must be able to be assembled within 4 hours, from the time the Federal Aviation Administration flight waiver opens
5. The launch vehicle must be capable of remaining in launch-ready configuration at the pad for a minimum of 1 hour without losing the functionality of any critical on-board component
6. No structural vehicle failures across all launches
7. All parts of the rocket are recoverable and reusable (able to launch again on the same day without modifications or repairs).

3.5.4 Recovery System Mission Success Criteria

1. The recovery system must be designed to be armed at the launch pad.
2. The drogue/main chute must deploy within 2.0 sec after apogee is reached.
3. The landing energy of the heaviest section of the rocket must be less than 75 lbf-ft

3.6 Recovery Subsystem

3.6.1 Structural Elements

Vehicle integrity during parachute deployment is a main priority for VADL. Each bulkhead of the avionics system (including payload and tail bulkheads which connect to the parachutes) must sustain loads of charge ignition and parachute deployment. Working aft from the fore section of the rocket, potential points of failure under these loads will be analyzed.

First the payload skeleton drogue parachute bulkhead will be analyzed. This bulkhead is made of 3/8" plywood, and uses a 5/16" steel U-bolt to secure the paracutte. The primary load on this bulkhead will be the tension it experiences as the drogue parachute is ejected and opens. This load is transferred from the U-bolt to the bulkhead using aluminum nuts and washers. Although this is the most likely point of failure for this bulkhead, it has been successfully tested in both the subscale and full scale flights. In order to experimentally determine the strength of this bulkhead

configuration, a similar configuration was tested in the Vanderbilt Materials Science load frame. The set up of the tensile test is shown in Figure 48.

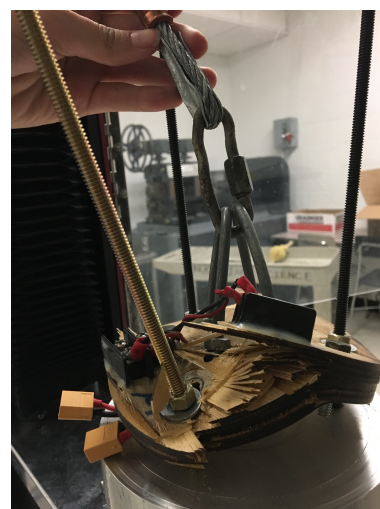


Figure 48: Wooden Bulkhead Test Set-up

A constant tensile force was applied to the bulkhead until it was permanently deformed. The point where the U-bolts began to deform occurred at 1,235.4 pounds, which is much higher than their rated failure load of 850.0 pounds. Although only one U-bolt will be flown, we are confident that this U-bolt will withstand the estimated drogue parachute force of 15.15 pounds, because it is rated to 425 pounds. This deformation continued until 2,221.0 pounds, which is the official failure point of the configuration as defined by the point that the bulkhead is deformed so much that the rocket will not be able to launch again. The bulkhead at this point is shown in Figure 49a. The tensile force was continually applied until the bulkhead reached an ultimate failure point where the plywood separated completely. This occurred at 4,353.6 lbs. An image of the bulkhead at this point is shown in Figure 49b.



(a) Wooden Bulkhead Failure Point at 2,221 Pounds



(b) Wooden Bulkhead Ultimate Failure at 4,335 Pounds

Figure 49: Plywood Bulkhead Failure Testing

This test proved that the wooden bulkhead could withstand the force of 15.15 lbs exerted as the drogue parachute opens with a safety factor of over 15. Furthermore, this test proved that the wooden bulkhead could withstand the 570 pound load from separation of the avionics and nose section of the rocket.

The blast charge detonation that deploys the drogue parachute exerts approximately 570 pounds of force. The 1/4" - 20 weld nuts that affix the payload electronics coupler tube to the nose section airframe are attached using JB-Weld. If these nuts are ripped from their bond during deployment, the nose section would fall to the ground unhindered. The bonding area of the weld nuts is 2.53 in^2 . JB-Weld's published Tensile Lap Shear strength is 1040 psi, giving a load capacity of 2,600 lbs. This is well below the force experienced by the coupler tube during deployment and validates the integrity of the weld nuts and use of JB-Weld epoxy.

In the avionics section, one 1/4" aluminum bulkhead must endure the force of the black powder explosion and the forces of the drogue and main parachute deployments. ANSYS was used to analyze the total stress and deformation on the avionics aluminum bulkhead as a result of the black powder ignition force, 570.0 lbs. The total equivalent stresses and deformation is shown in Figures 50 and 51.

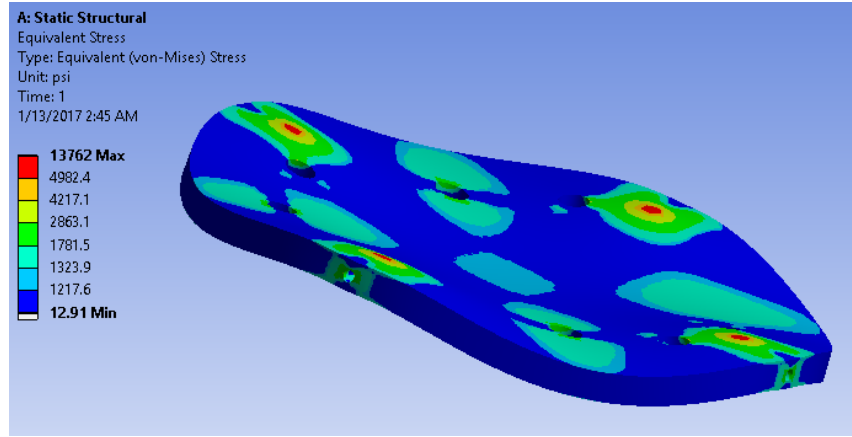


Figure 50: Equivalent Stresses Due to Black Powder Ignition

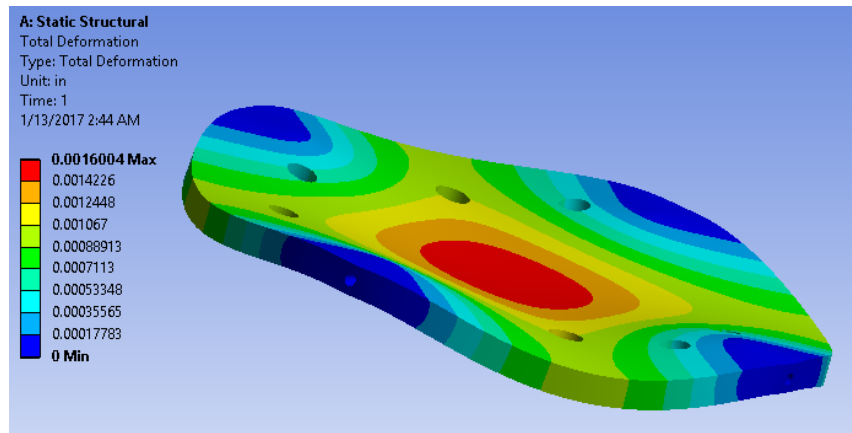


Figure 51: Bulkhead Deformation Due to Black Powder Ignition

These models show that the bulkhead can withstand the black powder ignition force with a safety factor of 2.95. 52 shows the safety factor at each point on the rocket. As can be seen in Figure 50 and 51, the areas around the four fixed supports deform the least and experience the maximum stress of about 13.7 ksi. This analysis shows that aluminum is an appropriate material selection for this bulkhead.

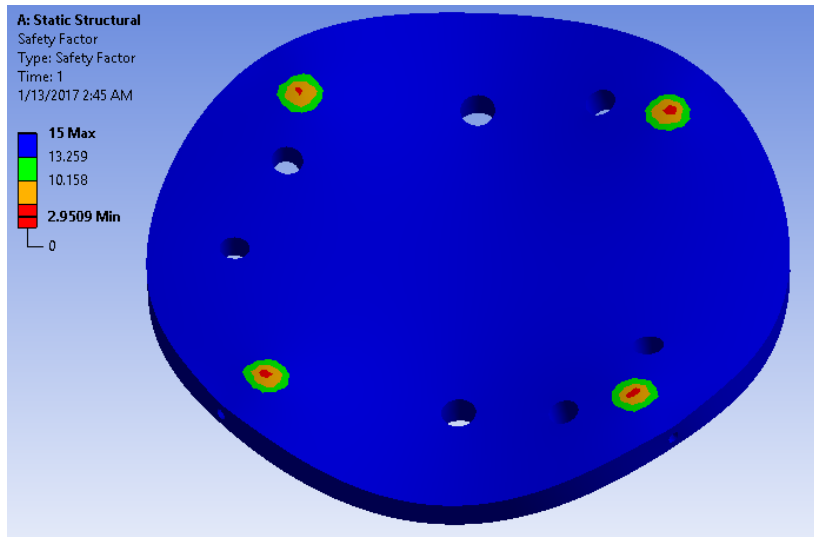


Figure 52: Avionics Bulkhead Safety Factor Graphic

The wooden bulkhead in this section must withstand the black powder ignition force as well. The forces and wooden bulkhead/U-bolt configuration are the same as discussed previously, and therefore the wooden bulkhead analysis can be applied here to show plywood as an appropriate material.

In the tail section, a 1/4" aluminum bulkhead is secured to the main parachute using a 5/16" steel U-bolt, and secured to the airframe using Loctite epoxy. The epoxy bond between the tail aluminum bulkhead and the airframe must not fail, otherwise the tail section will fall to the ground unhindered. The bonding area of the epoxy is 2722.2 mm^2 , and the epoxy's lap shear strength is 13.7 N/mm^2 . Assuming perfect adhesion to surfaces, this epoxy bond can withstand up to $37,294 \text{ N}$ or 8,384 lbs, which is much greater than the maximum force that will act as a result of the black powder ignition and parachute deployments. Another potential point of failure is the U-bolt during main parachute deployment. This U-bolt is rated up to 600 lbs, so it will be strong enough to withstand the expected deployment force (conservatively 140 lbs) by a safety factor of 4.3.

3.6.2 Recovery System Electrical Elements

The recovery system includes an electrical subsystem, which is made up of two StratoLogger altimeters, two manual screw switches, and two lithium 9V batteries, wired according to Figure 53. These components form two redundant altimeter assemblies: one primary assembly, and one backup assembly. Since the full scale vehicle has a dual-parachute recovery system, each altimeter fires two charges: one for the drogue parachute, and one for the main chute. The specific timing of the blast charges for parachute deployment is programmable; more information can be found in subsequent sections.

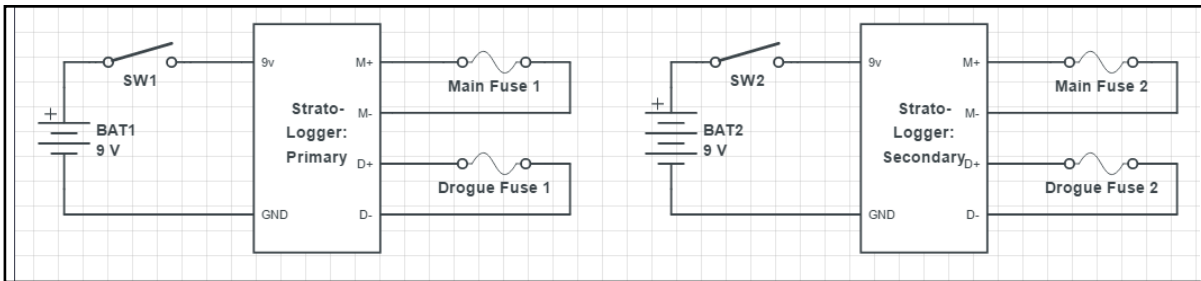


Figure 53: Recovery Electronics Schematic

All electronics mentioned above are secured to an optimized 3D printed sled using nylon 4-40 screws. The sled is then secured to the recovery bulkheads by threading it onto the extended posts of two long eye-bolts, which are used to secure the main parachute to the avionics bay. Nuts tightened down on the eye-bolt posts compress the two bulkheads together, ensuring battery retention and transferring stress to the aluminum bulkhead, rather than the plywood bulkhead. See Section 3.6.5 for renderings of the recovery system.

The recovery system also features an RF transmitter, which allows for directional sensing of the rocket's location from several miles away. The transmitter is secured to the main parachute's shock cord to allow for signal transmission from outside the shielding of the launch vehicle's carbon fiber body during recovery. More information concerning the transmitter can be found in Section 3.6.6.

Screw switches are accessible from outside the rocket, allowing for arming on the launch pad. See Figure 47 for a diagram of the switch.

3.6.3 Redundancy Features

Recovery is one of the most important aspects of the rocket design process to be considered. It is not a successful flight if the rocket can not be safely recovered so that the vehicle can be preserved and the data can be extracted. To ensure a safe recovery, proper redundancies must be established to increase the safety factor of the system. Figure 54 displays the logic used to establish redundancy in the recovery system.

Two altimeters will be used, one serving as the main with the second serving as the backup. The main altimeter is set to sense 1 second after apogee and a main parachute deployment altitude of 750 ft. The backup altimeter is set to sense 2 seconds after apogee and a main parachute deployment altitude of 550 ft. Each altimeter will be connected to a blast charge per parachute needed to deploy. Further details of the recovery process are outlined in Figure 55.

This chart displays the redundancies established in the system in order to avoid failure of the parachutes as well as the failure of the overall recovery system.

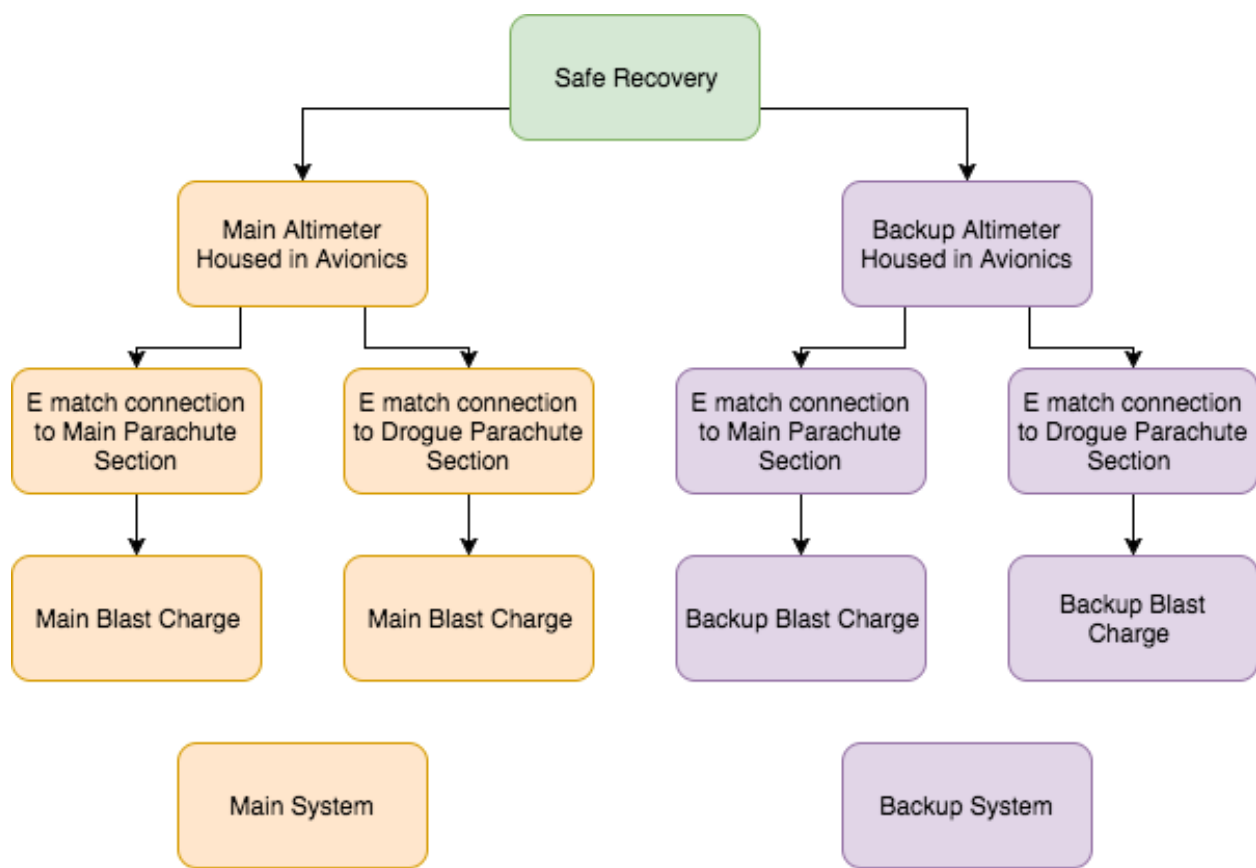


Figure 54: Systematic Redundancies Flowchart

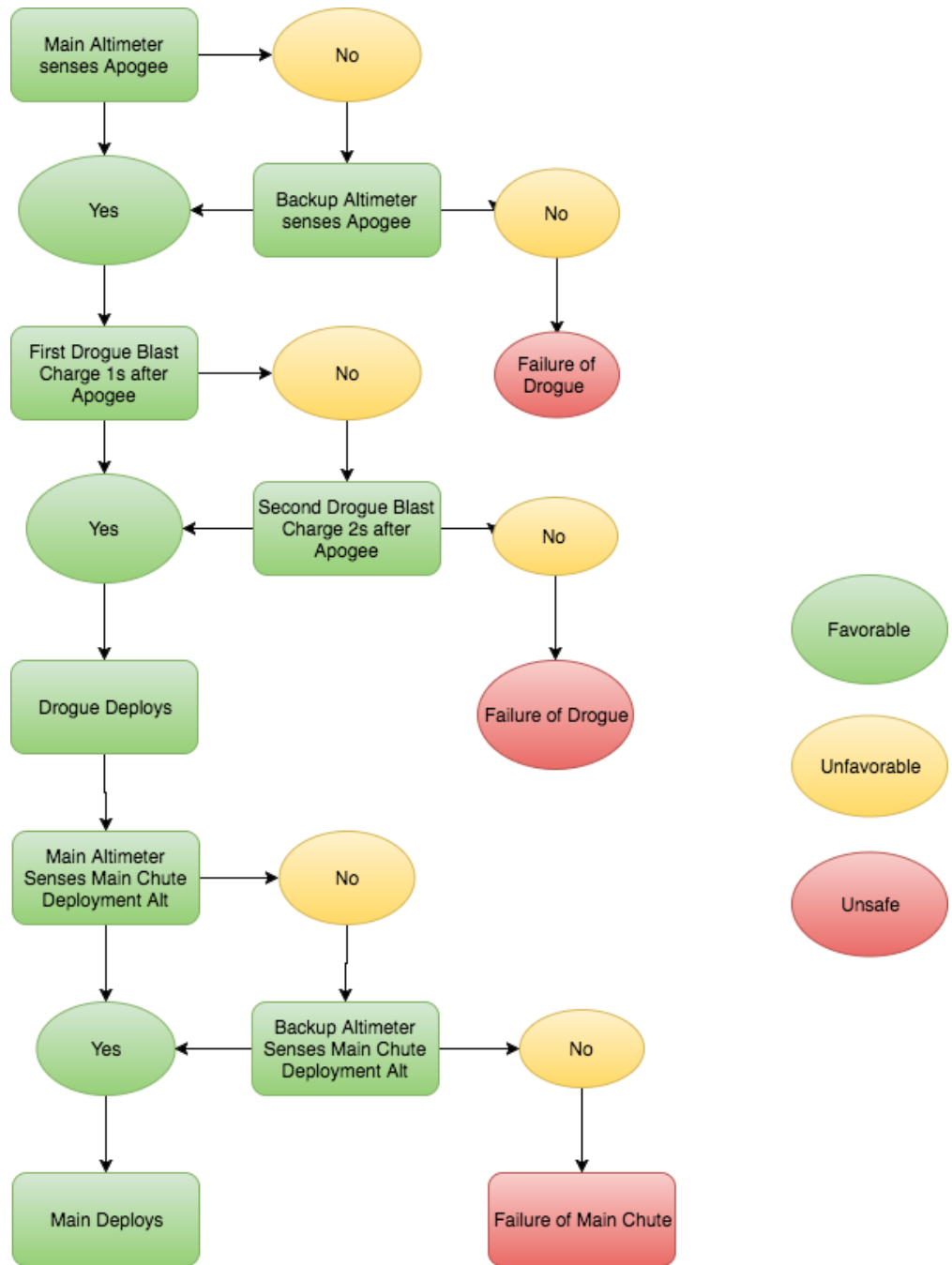


Figure 55: Recovery System Flowchart

3.6.4 Parachute Sizes and Descent Rates

It is vital to size the parachutes for the altitude regime in which we choose operate. With a goal of 4500 ft, the team will make use of a dual deployment parachute system featuring a drogue and main chute. Table 2 shows the differences in the main and drogue parachutes for our full scale flight. The team generated plots which helped the team gain an understanding of the safety behind our preselected parachute. Figure 56a shows the velocity at which the rocket falls varying with the apogee delay. Force is plotted in Figure 56b. These graphs allow the VADL team to ensure that the force on the U-bolt and bulkhead will not result in structural failure.

Table 2: Parachute Parameters

Parachute	Main	Drogue
Diameter	96"	18"
Shape	Toroidal	Elliptical
Cd	2.2	1.5
Source	FruityChutes	FruityChutes
Altitude	750'	Apogee +1s
Backup Altitude	550'	Apogee +2s
Descent Speed	15.1 fps	75.1 fps
Shock Cord Length	18', 25' (43')	15', 25' (40')
Shock Cord Material	Kevlar	Kevlar
Kinetic Energy of Heaviest Section	49.6 lb-ft	1416 lb-ft
4F Black Powder Charge Mass	4.5 g (5.0 g)	1.5 g (2.0 g)
Fire Retardant Blanket	Nomex	Nomex

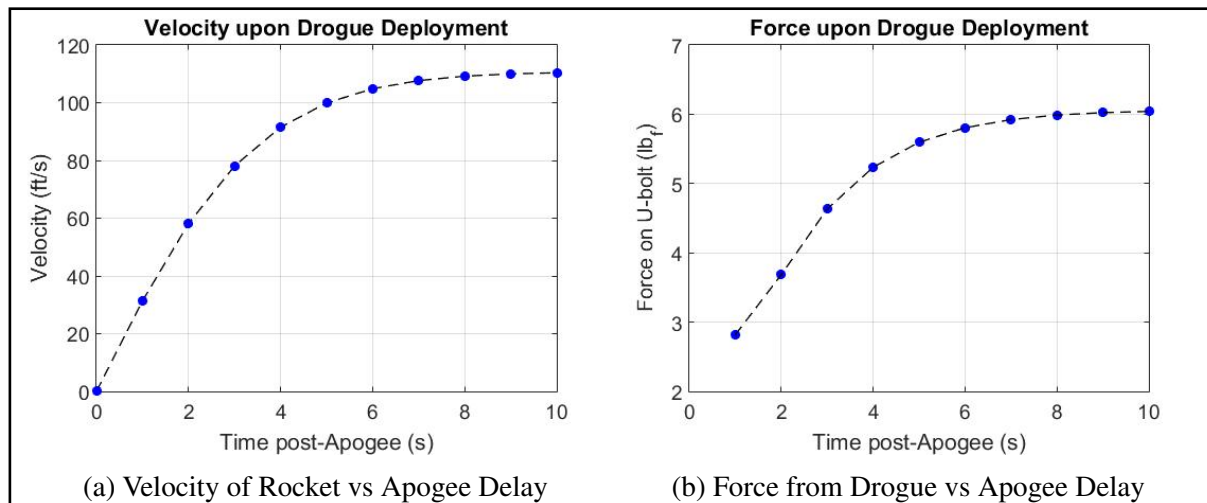


Figure 57a shows that a longer opening time of the main parachute produces less force on the U-bolt and bulkhead. As illustrated by Figure 57b, deploying the main parachute at a lower velocity similarly reduces the risk of structural failure.

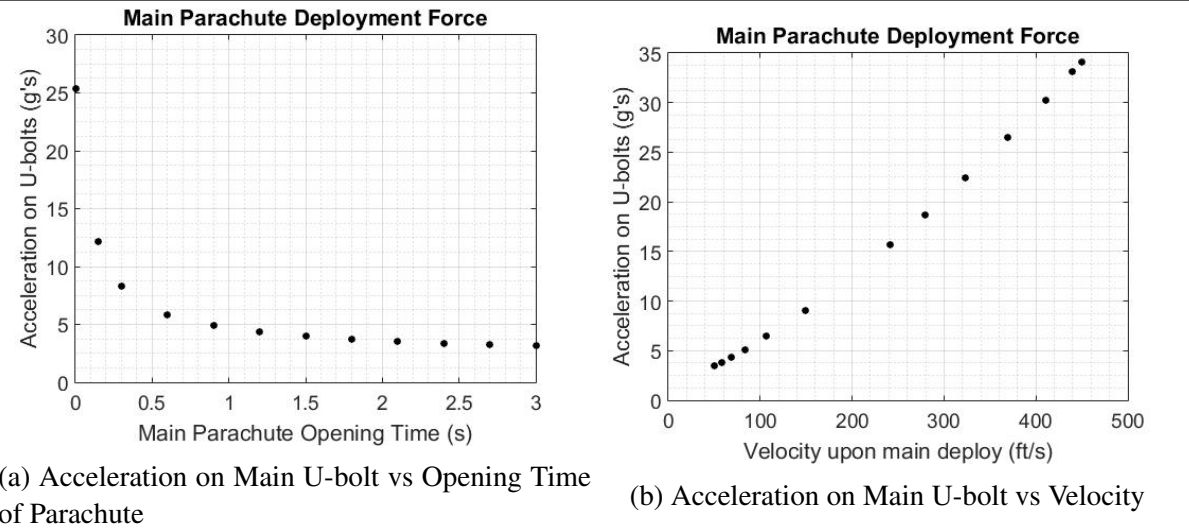


Table 2 shows the differences in the main and drogue parachutes. The first separation event occurs +1s after the rocket reaches apogee and initiates the drogue recovery process. Drogue recovery will use an 18" diameter fruity-chute elliptical parachute. This will provide a stabilized descent at approximately 78 ft/sec for a rocket of weight 31 lb. after motor burn off. When calculating the descent velocity under the drogue parachute, the drag coefficient of both the chute and the rocket body itself must be taken into account. Falling speed with an 18" drogue from 4500 ft. to 750 ft is calculated as follows:

$$V_d = \sqrt{\frac{mg}{0.5\rho(C_{DAP} + C_{DAR})}} = \sqrt{\frac{31lb * 32.17ft/s^2}{0.5 * .0765lb/ft^3 * (1.5 * 1.76ft^2 + 1.2 * 1.66ft^2)}} = 75ft/s^2 \quad (3.1)$$

A Nomex/Kevlar parachute protection pad will surround the parachute to prevent it from being burned by hot ejection gases. For moderate to high wind conditions an 18" drogue chute is ideally suited to forestall excessive wind drift. The drogue parachute will attach to 15 and 25 ft. Kevlar 1/4" shock cords via quick links. The shock cord connects to a short 1/4" wide Kevlar harness near the ejection charges where fireproof material is needed. The shock cord, rated minimally at 3000lb, will tether the drogue parachute to the upper body tube and to one end of the avionics bay, again using quick links. Furthermore, nine 43" nylon shroud lines (86" continuous) will attach the parachute to the shock cord. A cross stitch seam type using #400 flat line threads will connect the nylon parachute sections. These parachute materials will be lightweight but also strong enough to safely return the rocket to the ground. Using quick links, the shock cord will tether the parachute to the coupler tube and the forward section (rigidly bolted to the body tube) via one aluminum U-bolt. The main parachute will be connected to two aluminum eye bolts. The avionics assembly can be viewed in Figure 58.

The second separation event occurs at 750ft. and initiates the payload recovery process. Payload recovery will use a 8 ft. diameter iris ultra parachute. This will provide a stabilized descent at approximately 15.1 ft. /sec. These parachutes were both purchased from Fruity Chutes, a reliable

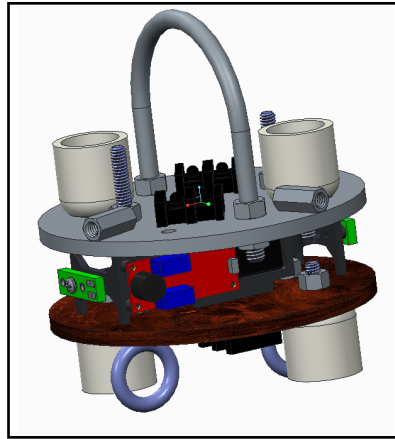


Figure 58: Avionics Full Assembly

parachute maker. They have been selected for its consistent success in deployment and minimization of failure modes and risk to recovery. Figure 59 shows a successful deployment of the team's recovery system.



Figure 59: Successful Full-Scale Recovery

The landing speed of the rocket after main parachute deployment was calculated as follows:

$$V_d = \sqrt{\frac{mg}{.5\rho(C_D A_P + C_D A_R)}} = \sqrt{\frac{31lb * 32.17ft/s^2}{.5 * .0765 * (2.2 * 50.25ft^2 + 1.2 * 0.0008ft^2)}} = 15.1ft/s^2 \quad (3.2)$$

Figure 60 shows a successful deployment of the team's 8 ft Iris Ultra parachute free from scars. This is the same parachute the team used for it's full scale flight. The team will use this design for our competition launch as well. The main parachute will be connected with a quick link to a 15 ft., 1/4" wide Kevlar shock cord reinforced with nylon rated minimally at 1500lb. This 15 ft shock cord is connected to the avionics section, which holds the avionics bay. The shock cord connects to a nomex blanket near the ejection charges where fireproof material is needed. A second 25 ft, 1/4" wide kevlar shock cord is connected by quick link to the parachute and tethers the parachute to a U-bolt bulkhead deep in the aft section. Furthermore, nine 200" nylon shroud

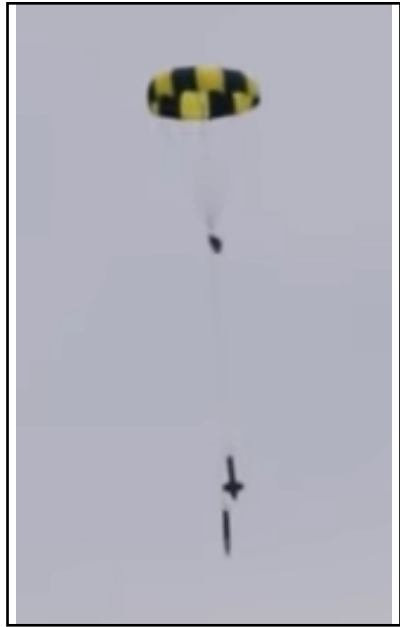


Figure 60: Subscale Parachute Deployment

lines (400" continuous) will attach the parachute to the shock cord. A Nomex/Kevlar parachute protection pad will surround the parachute to prevent it from being burned by hot ejection gases. A fireball anti zipper device will also be used on the connection to the avionics section to prevent damage to the rocket body.

The heaviest section is the payload section weighing in at 14.0 lb. The landing energy of the heaviest section is:

$$KE_{landingenergy} = \frac{\frac{W}{g} * V^2}{2} = \frac{14.0 * 15.1 f\text{ps}^2}{2 * 32.17} = 49.6 lb_f - ft < 75 lb_f - ft$$

Where KE is kinetic energy, W is weight, g is gravity, and V is velocity of descent. The landing energy assumes absolutely no ground wind; however, our experience has been that the ground wind speed contributes to lofting and the actual landing speeds with the main are substantially lower. These calculations give confidence in the design of the main parachute for the full scale design and will be fully vetted and scrutinized in the full scale test launch.

3.6.5 Drawings and Schematics

Figure 61 shows a diagram of the full scale vehicle, with the recovery bay (shown here as *avionics bay*) and parachute locations indicated. The recovery bay houses two independent altimeters each with a drogue and main blast charge, shown below in Figure 62. Fuses in the schematic represent electronic matches which ignite an amount of black powder charge sized according to the volume of the parachute cavity.

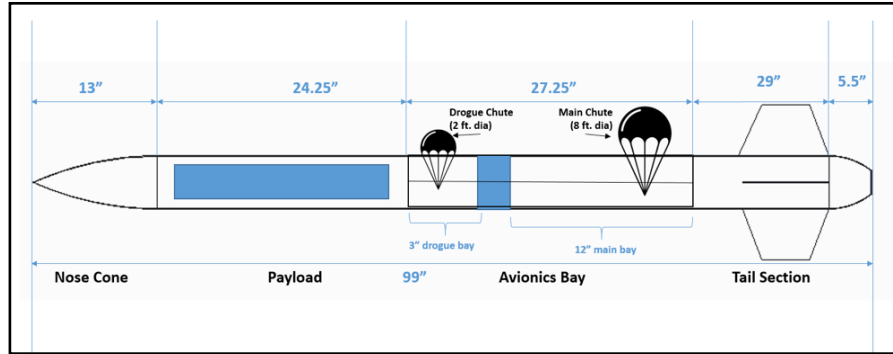


Figure 61: Recovery System Vehicle

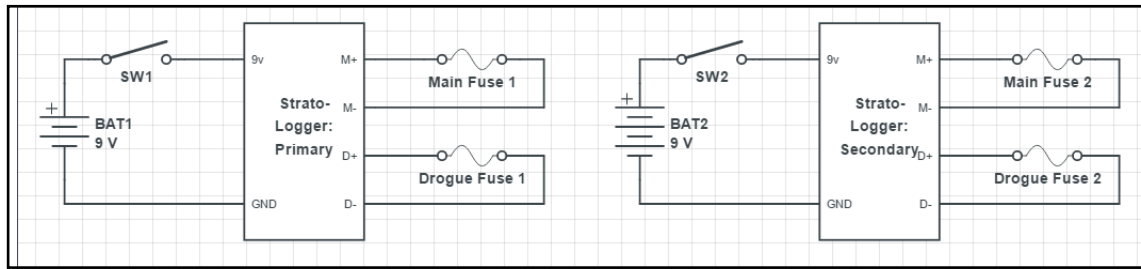
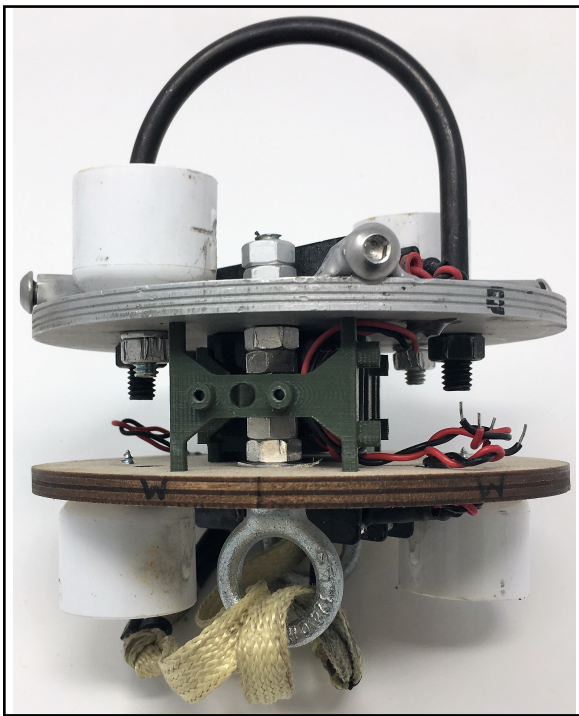


Figure 62: Recovery Electronics Schematic

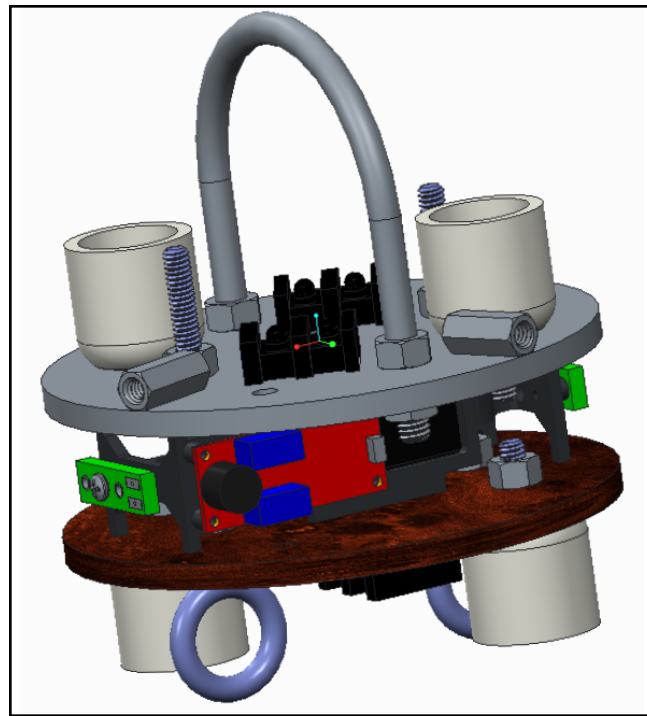
This schematic is physically arranged as depicted below in Figure 63. The aluminum bulkhead is 1/4" thick, and the majority of the loads from parachute deployment and recovery during descent. PVC blast caps are secured to this bulkhead using 1/4" - 20 bolts, and to the 1/4" plywood bulkhead using wood screws. These blast caps hold black powder deployment charges, which are ignited by the fuses attached to altimeter deployment ports. A 5/16" steel U-bolt secures the drogue parachute to the bay, and two 1/4" steel eye-bolts secure the main parachute while also holding the bay in compression by threading through the recovery electronics sled and the aluminum bulkhead.

Perhaps the most important part of the recovery bay is the method by which it is secured to the rocket's airframe. The bay is anchored to its carbon fiber enclosure by four 1/4" steel button bolts each threaded through the airframe and into an aluminum coupling nut welded to the aluminum bulkhead. Repeatable spacing between the bulkheads, which is critical for alignment of the recovery bay with the airframe, is ensured by threading four spacer nuts on each eye-bolt between the sled and the bulkheads.

All holes in the bulkheads have been sealed to prevent pressure leaks into the altimeter bay. Pressure sampling holes have been cut in the airframe according to the PerfectFlite StratoLogger User's Manual.



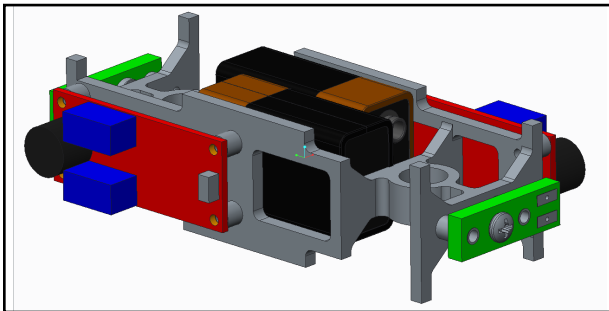
(a) Full Assembly of Recovery System Bay
(Electronics Not Shown)



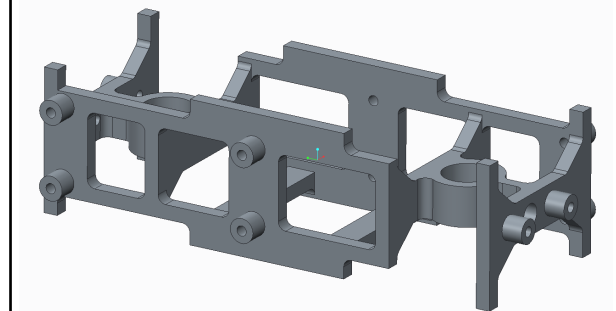
(b) Full Assembly of Recovery System Bay (CAD Render)

Figure 63: Physical and CAD Assemblies of Recovery Bay

Figure 64 below shows the assembly of electrical components of the recovery system on a 3D printed sled. StratoLogger altimeters are pictured in red, and screw switches in green.



(a) Recovery Sled, Shown with Components



(b) Recovery Sled, Shown without Components

Figure 64: CAD Renderings of 3D Printed Recovery System Sled

Figure 65 shows an image of the fabricated avionics section airframe, which contains the parachutes and the recovery system. Figure 66 shows the allotted space for each parachute. The green section represents the space allotted for the main parachute while the red is for the drogue.



Figure 65: Recovery System Airframe, Fabricated in House

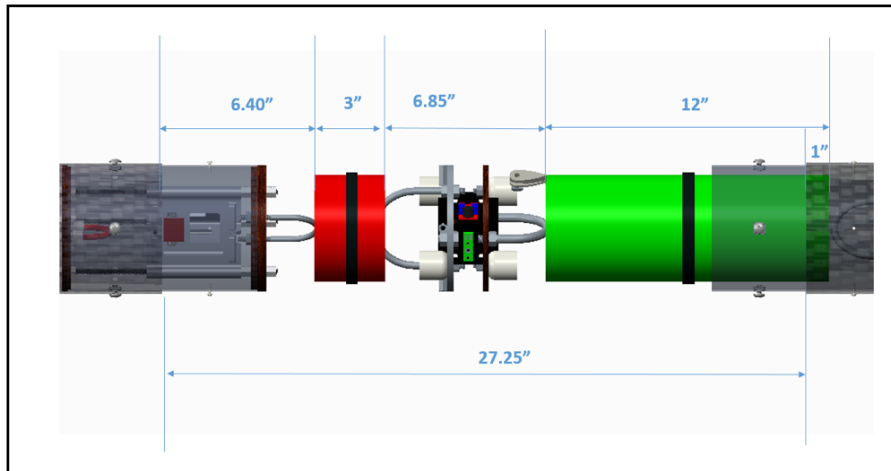


Figure 66: Recovery System CAD Rendering

This system was tested and proven to be reliable. Deployment tests were done before the full scale launch to ensure the rocket would separate. The full scale vehicle was safely recovered after the full scale test flight.

3.6.6 Rocket-Locating Transmitters

A launch vehicle precision location device is incorporated into the launch vehicle on competition day in order to make the recovery efforts as efficient as possible. If line of sight with the launch vehicle is broke at any time, the telemetry electronics will aid in a rapid recovery of the launch vehicle. The device used will be the Big Red Bee Transmitter pictured in Figure 67.

The BeeLine TX is a small radio device that sends an RF signal to a handheld radio. The device will transmit under the call sign AA4VU. The user can then use a directional antenna to detect the general direction of the launch vehicle and commence recovery operations. This device weighs 1 ounce. The handheld radio to be used is a Kenwood TH-F6 radio. This radio is a commercially available radio and features an LCD screen for ease in rocket recovery.

As in previous years, the transmitter will be mounted to a portion of the rocket parachutes shock cord. The transmitters small size and low weight means that it has no impact on the performance of the rockets recovery system, as proven by multiple years of successful rocket recovery while mounting the transmitter in this fashion. The transmitter is also placed here to reduce possible signal interference with the carbon fiber wrapped blue-tube. The team seeks full signal visibility.

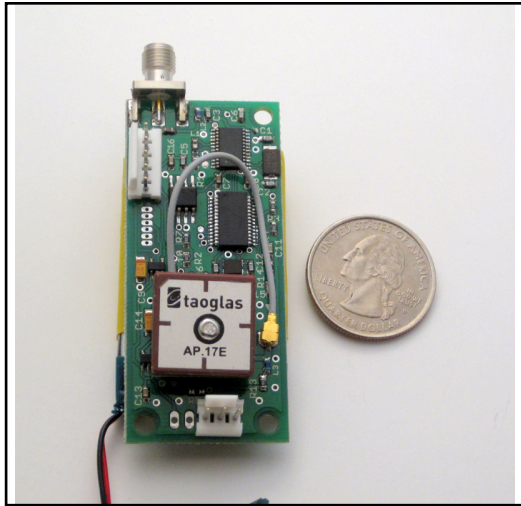


Figure 67: Big Red Bee BeeLine Transmitter

The transmitter will broadcast pulses on the amateur band (70cm) at a frequency of 425.0 MHz. It can also be programmed to broadcast at any frequency between 420.0MHz and 450.0MHz in 250Hz increments. The transmitter is powered by a small lithium ion battery heatshrunk to the package. The battery connection is interruptible to prevent unnecessary power loss. When the transmitter broadcasts at full power (+12dBm) it has a transmitting range of up to 5 miles.

3.7 Mission Performance Predictions

3.7.1 Mission Performance Criteria

The rocket and payload performance should be indicative of successful implementation of the design, build, and test process. The team understands that a safe and stable rocket flight is a prerequisite to any innovation in payload design. The following are quantitative requirements that must be met in simulation and testing to signify a safe competition flight:

- The target altitude for the launch vehicle is 5,280 feet. A ceiling of 5,600 feet is not to be exceeded.
- The final drift of the launch vehicle should be kept to a minimum to facilitate safe and simple recovery.
- The launch vehicle shall accelerate to a minimum velocity of 52 fps at rail exit.
- Each independent section of the rocket shall land with a kinetic energy of less than 75 ft.-lb_f.
- The launch vehicle shall have a minimum static stability margin of 2.0 at the point of rail exit.
- Following main engine cutoff, the launch vehicle shall perform 2 revolutions around its main axis. Then it shall maintain its angular position at 2 revolutions with alternating thrust and counter-thrust. The experiment shall be completed prior to apogee.

3.7.2 MATLAB Flight Simulation

Production of an overall flight profile is crucial in understanding the role various launch conditions play on the flight targets. Theoretical results can be used to validate design choices and provide a benchmark for comparison with experimental data. For these reasons, a MATLAB script was created to simulate the entire rocket flight from launch to touchdown. The following sections detail the important components of the flight simulation.

3.7.2.1 Trajectory Equations

The simulation numerically integrates the standard set of flight equations with thrust and drag to determine acceleration, velocity, and position over the course of the rocket's trajectory. For simplicity, only two dimensions are modeled—vertical (z) and horizontal (x)—though a third dimension could be readily added if needed. Table 3 defines the variables in Equation 3.3.

Table 3: Rocket Equations Symbol Definitions

Symbol	Definition
a_z	Vertical acceleration (m/s^2)
a_x	Horizontal acceleration (m/s^2)
v_j	Velocity in either the z or x direction (m/s)
v_d	Drag velocity (differs from total velocity due to wind)
j	Position in either the z or x direction (m)
ϕ	Angle of rocket axis relative to vertical (rad)
T	Thrust (N)
D	Drag (N)
W	Weight (N)
m	Rocket mass (kg)
w	Side wind velocity (m/s)
dt	Time step (s)
i	Index variable

$$a_{z,i} = \frac{(T - D) \cos \phi - W}{m_{i-1}} \quad (3.3a)$$

$$a_{x,i} = \frac{(T - D) \sin \phi}{m_{i-1}} \quad (3.3b)$$

$$v_{j,i} = v_{j,i-1} + (a_{j,i-1})(dt) \quad (3.3c)$$

$$j_i = j_{i-1} + (v_{j,i-1})(dt) + \frac{1}{2}(a_{j,i-1})(dt)^2 \quad (3.3d)$$

$$\cos \phi = \frac{v_z}{v_d} = \frac{v_z}{\sqrt{v_z^2 + (v_x + w)^2}} \quad (3.3e)$$

$$\sin \phi = \frac{v_x + w}{v_d} = \frac{v_x + w}{\sqrt{v_z^2 + (v_x + w)^2}} \quad (3.3f)$$

3.7.2.2 Drag

Drag force, D , is calculated as the sum of two separate sources of resistance: pressure drag, D_p , and skin friction, D_s (Equation 3.4).

$$D = D_p + D_s \quad (3.4)$$

Pressure Drag Pressure drag is given as Equation 3.5, where C_D is the drag coefficient, A is the largest cross-sectional area of the rocket, and the remaining variables are as described in Section 3.7.2.1. For a cylindrical rocket with a nose cone such as fabricated by VADL, the drag coefficient typically has a value close to 0.35; the apogee altitude of the subscale launch was found to be best approximated with a C_D of 0.27 (Section 3.7.4.1).

$$D_p = \frac{1}{2} C_D \rho A v_d^2 \quad (3.5)$$

Skin Friction The equation for skin friction follows the same form as for pressure drag (Equation 3.6), except the friction coefficient is generally much smaller than the drag coefficient. In which C_f is the friction coefficient and A is the rocket's total surface area parallel to the flow¹,

$$D_s = \frac{1}{2} C_f \rho A v_d^2 = \frac{1}{2} C_f \rho (A_{cyl} + 4A_{fin}) v_d^2 \quad (3.6)$$

The value of the friction coefficient varies as a function of the Reynold's number and the state of the boundary layer. The Reynold's number for a flat plate is defined as in Equation 3.7, where L is the length of the rocket and ν is the kinematic viscosity of air^{3.7.2.2}:

$$Re = \frac{v_d L}{\nu} \quad (3.7)$$

¹ Welty, J. R., Wicks, C. E., & Wilson, R. E. (1969). Fundamentals of Momentum, Heat, and Mass Transfer. New York: J. Wiley.

For Reynold's numbers less than 2×10^5 , the flow is laminar, and the mean friction coefficient over the length of the plate is given by Equation 3.8^{3.7.2.2}:

$$C_f = \frac{1.328}{\sqrt{Re}}, Re < 2 \times 10^5. \quad (3.8)$$

For turbulent flow ($Re > 2 \times 10^5$), many correlations have been developed to approximate the skin friction coefficient; the simulation here uses the Prandtl-Schllichting formula². Equation 3.9 is only valid for Reynold's numbers up to 10^7 ; while the fullscale vehicle will reach a maximum Reynold's number of $Re \approx 2 \times 10^7$, the correlation is assumed to hold for the entire simulation.

$$C_f = \frac{0.455}{[\log_{10}(Re)]^{2.58}}, 2 \times 10^5 < Re < 10^7 \quad (3.9)$$

The kinematic viscosity of air at 277 K is about $1.36 \times 10^{-5} \frac{m^2}{s}$, and the length of the fullscale rocket is around 2.5 m, leading to a laminar boundary layer only for velocities less than $\approx 4 \text{ m/s}$. Therefore, the majority of the rocket's flight occurs with a turbulent boundary layer and augmented skin friction coefficient, though skin friction contributes about two orders of magnitude less than pressure drag to the overall drag force felt by the rocket.

3.7.2.3 Side Wind

Another consideration when evaluating the rocket's trajectory is the effect of a side wind. The simulation assumes a constant ground wind velocity acting in only the horizontal (x) direction. Wind enters the simulation in two ways: weathercocking or weathervaning, and drift from the parachute.

The wind is input as its speed at a reference height of 10 meters, high enough to ignore the boundary layer on the ground. A wind amplification scheme is followed that increases the velocity of the wind by Equation 3.10 based on altitude. Where w is wind velocity, z is height above ground level, and α is the wind speed amplification constant³,

$$w = w_{ref} \left(\frac{z}{z_{ref}} \right)^\alpha = w_{ref} \left(\frac{z}{10m} \right)^{\frac{1}{7}} \quad (3.10)$$

With wind amplification established, the effect of weathercocking becomes apparent. The term "weathercocking" refers to a slow turning of the rocket into the wind as a result of a positive stability margin. While the fins are present to correct for any pitching motion of the launch vehicle, only very large axial velocities can prevent a gentle angling in the direction of the side wind. Weathercocking is important primarily during the motor burn phase of the launch because any angling of the motor tube causes the rocket to acquire an extra velocity in the direction opposite the wind. It is counterintuitive that the rocket would speed up when traveling into the

² https://www.cfd-online.com/Wiki/Skin_friction_coefficient

³ Elliott, D.L., C.G. Holladay, W.R. Barchet, H.P. Foote, and W.F. Sandusky, 1986, Pacific Northwest Laboratory, Richland, WA. Wind Energy Resource Atlas of the United States

wind, but acceleration generated by thrust is much greater than the resistive acceleration of the wind. As was discussed in Section 3.7.2.2, the wind does factor into calculation of the drag velocity. Refer to Figure 68 for a visual depiction of weathercocking; the black triangle represents the velocity vectors at the beginning of a time step, and the red lines show the resultant angle and drag velocity.

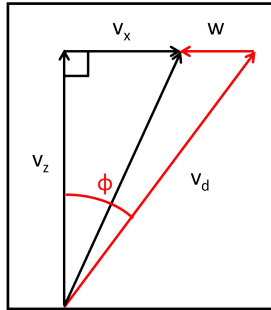


Figure 68: Instantaneous Flight Velocity Component Diagram

3.7.2.4 Standard Atmosphere Model

While the Earth's atmosphere varies little throughout the first mile of altitude, it is good practice to include an atmosphere model applicable to much greater altitudes. Therefore, the International Standard Atmosphere⁴ is used in the simulation, the main output of which is air density (though temperature and pressure are also calculated in the process). The launch pad elevation, z_0 , is taken as an input, and the 1976 U.S. Standard Atmosphere is interpolated to estimate the initial density ρ_0 ⁵. The ambient ground air temperature is also an input and varies with altitude as Equation 3.11a, where T_0 is the ground temperature, z is the altitude, and β is a constant. At altitudes below the tropopause (11 km), temperature decreases linearly by 6.5°C for every 1000 meters in altitude^{3.7.2.4}. The local pressure is then calculated from Equation 3.11b, where R is the gas constant ($286.9 \frac{J}{kg \cdot K}$ for air), and the local air density comes from Equation 3.11c.

$$T = T_0 - \beta \frac{z}{1000}, \quad \beta = 6.5 \quad (3.11a)$$

$$p = p_0 \left(\frac{T}{T_0} \right)^{\frac{g}{R\beta}}, \quad g = g_0 \left(\frac{r_0}{r} \right)^2, \quad r = r_0 + z_0 + z \quad (3.11b)$$

$$\rho = \frac{p}{RT} \quad (3.11c)$$

3.7.2.5 Compressibility

Compressibility effects on air density are assumed to be negligible under Mach 0.3⁶. The maximum fullscale launch velocity approaches Mach 0.55, so compressibility must be considered.

⁴ M. Cavcar, The International Standard Atmosphere (ISA), Anadolu University, Turkey, 2000.

⁵ U.S. Standard Atmosphere, 1976, U.S. Government Printing Office, Washington, D.C., 1976

⁶ <https://www.grc.nasa.gov/www/k-12/airplane/machrole.html>

The stagnation equations for isentropic flow could be employed to deduce the effective change in air density⁷. However, because the effective density is only used for the pressure drag calculation (Section 3.7.2.2, a correction for the drag coefficient will be used instead⁸. In Equation 3.12a, $C_{d,0}$ is the drag coefficient at zero velocity, M is the Mach number (Equation 3.12b, with a the local speed of sound, γ the specific heat ratio, and T the local temperature).

$$Cd = \frac{C_{d,0}}{\sqrt{1 - M^2}} \quad (3.12a)$$

$$M = \frac{v_d}{a} = \frac{v_d}{\gamma RT} \quad (3.12b)$$

3.7.2.6 Motor Burn Profiles

The launch is dictated by the published thrust and mass profile for the Loki Research L1400 motor⁹. Figures 69a and 69b display the experimental data input to the simulation.

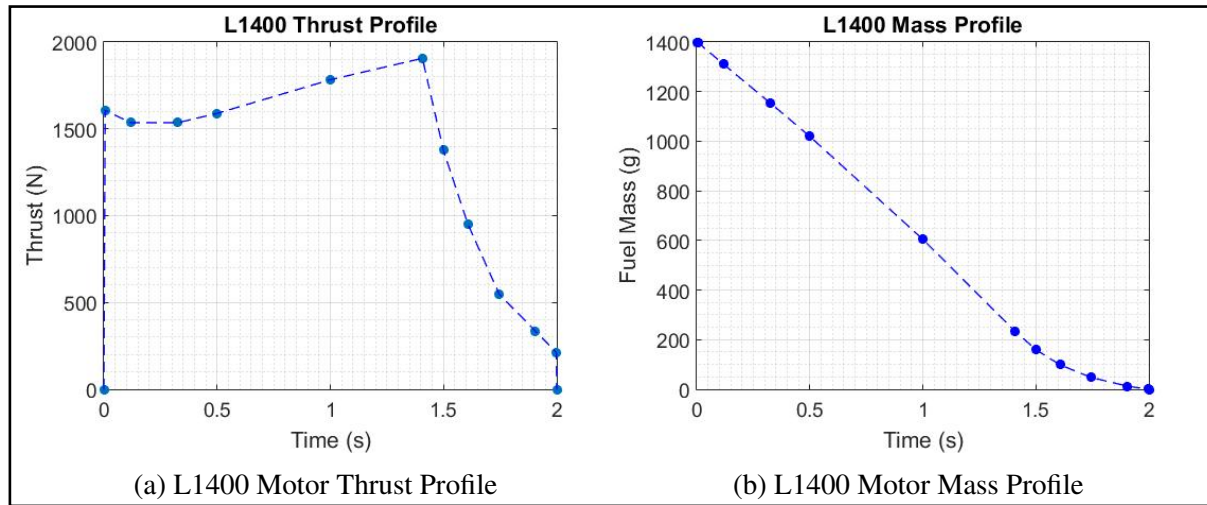


Figure 69: Loki Research L1400 Motor Data Profiles

The published data features points spaced by time periods greater than the time step of the model, and the points do not correspond exactly to times that occur during the simulation. Therefore, as shown by the dashed lines in Figure 69, the data is linearly interpolated to determine thrust and fuel mass values at times between two given points.

3.7.2.7 Parachute Deployment

The fullscale flight features the deployment of two parachutes: a drogue with diameter of 2 ft. and a main with diameter of 8 ft. The drogue is released soon after apogee to decrease the launch

⁷ <https://www.grc.nasa.gov/WWW/BGH/isentrop.html>

⁸ Cramer M.S. (2002) Foundations of fluid mechanics. Cambridge University Press.

⁹ <http://www.thrustcurve.org/motorsearch.jsp?id=403>

vehicle's terminal velocity; this reduces the force on the U-bolts upon main parachute deployment. The simulation accepts either a time-after-apogee or an altitude input to initiate drogue deployment. Main parachute deployment is signaled by an altitude input, likely near 800 ft. to minimize drift but still allow the system to achieve its terminal velocity. Neither parachute opens instantly, so an opening time for each is factored into the simulation as well. During this time period, the parachute diameter is assumed to expand linearly so that the drag area increases quadratically.

The same equations as in Section 3.7.2.1 are used to track the system's acceleration, velocity, and position over time. However, because of the relatively slow velocity, the parachute is assumed to remain in an upright position such that horizontal and vertical movement can be treated independently. A separate drag coefficient is applied to the x- and z-components, and the drag area can be calculated simply from the hemispherical shape of the parachute. While separating the components may not exactly describe experimental results, any deviations are overwhelmed by the unpredictable motion generated as the parachute deploys. The latter is not simulated; overall effects are instead captured empirically by the chosen drag coefficients.

3.7.3 MATLAB Payload Experiment Simulation

The payload experiment performed for the 2016-2017 project is also capable of being simulated. The roll control experiment is modeled simultaneously with the rocket's trajectory. The cold gas thruster system was designed to not interfere with the rocket's flight, so the two simulations are treated independently despite happening concurrently. All of the rolling and counter-rolling of the launch vehicle occurs following a specified time after MECO and before the rocket reaches apogee.

3.7.3.1 Rotation Equations

Standard Newtonian physics are employed to simulate the rotation of the launch vehicle. The equations in Equation 3.13 are numerically integrated at the same time as Equation 3.3 with an identical time step. Only the rotational dimension about the vehicle long axis is examined (see Figure 70¹⁰); perturbations in the pitch and yaw directions are ignored but may factor into empirically determined drag coefficients. Table 4 defines the variables in Equation 3.13.

$$\tau = Fr = I\alpha \quad (3.13a)$$

$$\alpha_i = \frac{\tau_{cg} - \tau_d}{I} \quad (3.13b)$$

$$\omega_i = \omega_{i-1} + (\alpha_{i-1})(dt) \quad (3.13c)$$

$$\theta_i = \theta_{i-1} + (\omega_{i-1})(dt) + \frac{1}{2}(\alpha_{i-1})(dt)^2 \quad (3.13d)$$

¹⁰ <http://sciencelearn.org.nz/Contexts/Rockets/NZ-Research/Rocket-control>

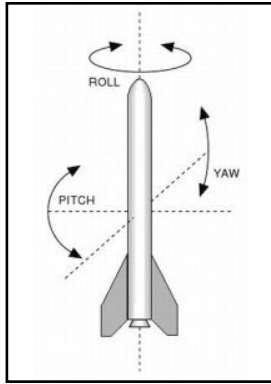


Figure 70: Roll, Pitch, and Yaw of a Rocket

Table 4: Rotational Equations Symbol Definitions

Symbol	Definition
α	Angular acceleration (rad/s ²)
ω	Angular velocity (rad/s)
θ	Angular position (rad)
τ	Net torque (N-m)
τ_{cg}	Thrusting torque (cold gas thrusters, N-m)
τ_d	Resistive torque (drag, N-m)
F	Force (N)
r	Length of moment arm (m)
I	Rotational inertia (kg-m ²)
dt	Time step (s)
i	Index variable

3.7.3.2 Thrust

The rolling motion is generated by a pair of cold gas thrusters that provide a torque to the vehicle. The design of the cold gas thrusters is described in the Preliminary Design Review (PDR) report, but analysis and testing of the actual output of the thruster system can be found in Section 7.1.1; due to regulator droop, the torque from the system does not maintain a constant value as the pressure in the compressed air tank decreases. A curve fit to the test data for a nominal pressure of 4000 psi has resulted in the thrust profile in Equation 3.14 that gives the expected thrust based on the total time that the solenoid valve has been open continuously. Where T is thrust and t_{op} is the total operational time,

$$T = (-6.56 \times 10^{-4})t_{op}^4 + (0.0103)t_{op}^3 - (0.0531)t_{op}^2 - (0.181)t_{op} + 12.3 \quad (3.14)$$

3.7.3.3 Resistive Torque

Rotation of the rocket is opposed by three different forces, mostly involving resistance to fin movement: pressure drag (τ_q), skin friction (τ_s), and jet-fin interaction (τ_{jf}), and the total resistive torque (τ_d) is the sum of the individual torques (Equation 3.15).

$$\tau_d = \tau_q + \tau_s + \tau_{jf} \quad (3.15)$$

Pressure Drag Of the three torques, pressure drag is the most obvious resistance and is significant because of the large axial velocity of the launch vehicle. The side wind can be ignored as its net effect is zero for a rocket with symmetrical fins. As the rocket rolls, a resistive moment acts on the fins, the value of which increases radially outward on the fin. An integration must be performed across the height of the fin to calculate the total torque based on the dynamic pressure. The fin is assumed to be a flat plate with dimensions given in Figure 71.

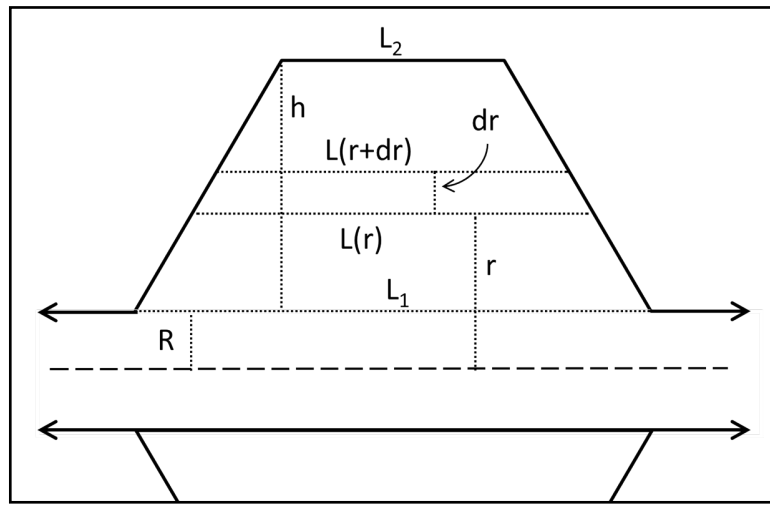


Figure 71: Trapezoidal Fin Schematic

Following the procedure outlined in the OpenRocket documentation¹¹, we begin with the definition of pressure drag and prepare an integral for the resistive torque, where η is the instantaneous angle of attack of the fin into the flow ($\eta = 0$ for non-rotating, vertically-aligned fins), v_0 is the total velocity of the fin v_d is the axial velocity, and v_ω is the horizontal velocity:

$$\begin{aligned} \tau_q &= Fr = \frac{1}{2} C_{d,fin} \rho A v_0^2 \eta = \frac{1}{2} C_{d,fin} \rho \left(\sqrt{v_d^2 + v_\omega^2} \right)^2 r A(r) \frac{v_\omega}{v_d} \\ &= \frac{1}{2} C_{d,fin} \rho v_d^2 r A(r) \frac{\omega r}{v_d}, \quad v_d \gg v_\omega \Rightarrow v_0 \approx v_d \\ &= \frac{1}{2} C_{d,fin} \rho \int_R^{R+h} (v_d)(\omega r) r [L(r)] dr \\ &= \frac{1}{2} C_{d,fin} \rho v_d \omega \int_R^{R+h} r^2 \left[\frac{(L_1 - L_2)(r - R)}{-h} + L_1 \right] dr \end{aligned}$$

¹¹ S. Niskanen, OpenRocket technical documentation, for version 13.05, 2013.

The magnitude of τ_q varies linearly with both angular velocity and axial velocity and depends on the geometry of the fin, which arises as the constant Z_{fin} . Equation 3.16 describes the total pressure drag acting on four fins that opposes the torque from the cold gas thrusters.

$$\begin{aligned}\tau_q &= (4 \text{ fins}) \left[\frac{1}{2} C_{d,fin} \rho v_d \omega Z_{fin} \right] \\ Z_{fin} &= \int_R^{R+h} \left[\frac{(L_1 - L_2)(r - R)}{-h} + L_1 \right] r^2 dr \\ Z_{fin} &= \frac{1}{4} \frac{L_2 - L_1}{h} [(R+h)^4 - R^4] + \frac{1}{3} \left(L_1 - \frac{L_2 - L_1}{h} \right) [(R+h)^3 - R^3]\end{aligned}\quad (3.16)$$

Skin Friction Skin friction is calculated in the same manner with the same friction coefficient as in Section 3.7.2.2, though the area relevant solely to resistive torque excludes the fins. The viscous drag occurs on the body of the cylinder, so the moment arm length is the radius of the rocket. Equation 3.17 is used.

$$\tau_s = F_s R = \frac{1}{2} C_f \rho A_{cyl} v_d \omega R \quad (3.17)$$

Jet-Fin Interaction The final source of resistive torque, jet-fin interaction, refers to aerodynamic effects from vortices created by interference between the cold gas thruster stream and the axial flow. The magnitude of the effect is not well understood, but it has been approximated for a certain set of conditions through experiment¹². Just as in other forms of drag, jet-fin interaction is characterized by a coefficient, C_{CT} . The countertorque coefficient is defined by Equation 3.18, where τ_{jf} is the countertorque due to the interaction vortices, A is the cross-sectional area of the vehicle, and d is the vehicle diameter¹².

$$C_{CT} = \frac{\tau_{jf}}{q_\infty Ad} \quad (3.18)$$

However, if the countertorque coefficient is known from other methods, the torque can be computed directly from Equation 3.18. A correlation between the coefficient and the jet-to-freestream dynamic pressure ratio, J , has been established for $J < 40$ ¹². In Figure 72, the solid blue curve best approximates the conditions of the VADL rocket, namely its subsonic nature and the fins' uncanted alignment.

Unfortunately, the launch vehicle operates at values of $J > 40$ for all but the first 2 seconds of the experiment, so Figure 72 cannot be used without extrapolation. Instead, a factor F_{jf} is applied to the resistive torque, in which F_{jf} accounts for all jet-fin interaction and any other inconsistencies in drag. As a result, Equation 3.15 becomes the following:

$$\tau_d = \tau_q + \tau_s + \tau_{jf} \approx F_{jf} (\tau_q + \tau_s) \quad (3.15)$$

¹² S. Beresh, et al., Planar Velocimetry of Jet/Fin Interaction on a Full-Scale Flight Vehicle Configuration, AIAA Journal (45-8), 2007.

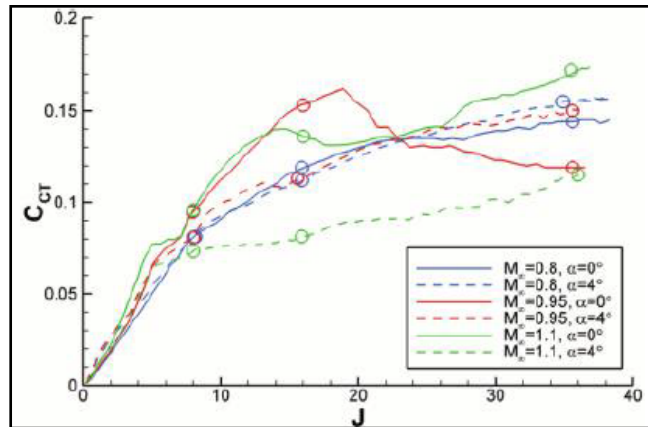


Figure 72: Jet-Fin Interaction Countertorque Coefficient

3.7.3.4 Computational Modeling

The results of subscale flight allowed VADL to realize the significance that the axial flow plays in the damping of roll induction. To better characterize these effects, Computational Fluid Dynamics (CFD) models were run using ANSYS Fluent, a popular modeling software. The goal of these simulations was to visualize the resistive torque on the fins via a pressure distribution plot, and to verify the mathematical models that VADL used to estimate the resistive torque as a function of angular velocity.

Pressure Distribution To visualize the resistive torque caused by the axial flow, it was necessary to visualize the pressure distribution across a plane perpendicular to the main axis of the rocket that passes through the fins. Figure 73 shows the distribution on this plane at varying angular velocities. The simulation was run with a fluid rotating at a varying angular velocity and a constant axial velocity of 100 m/s.

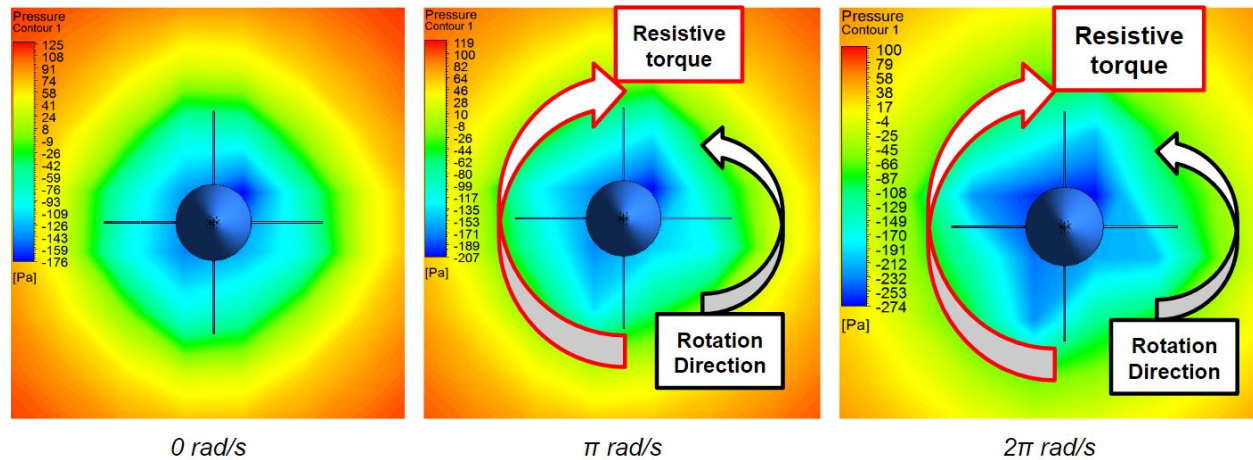


Figure 73: Pressure Distribution at Fins for Various Angular Velocities

As discussed in Section 3.7.3.3, the dynamic pressure on either side of the fins has a significant effect on the ability of the rocket to rotate. This CFD analysis shows the pressure difference that

forms across the fins of the rocket during rotation which adds to this resistive torque. To quantify this effect, a moment analysis was performed on the rocket about its main axis for various angular velocities. The results were compared to the damping coefficient calculated from Equation 3.16, which found a relationship between the damping torque and the angular velocity. The resistive torque is a function of both angular and axial velocity, so to describe the torque as a function of angular velocity alone, an axial velocity of 100 m/s was used in all calculations. The damping coefficient was found to be $T_d = .16\omega$. Figure 74 shows the results of the torque analysis from ANSYS, which produced a damping coefficient of .15, which supports the mathematical model and therefore the team's justification for the unsuccessful roll experiment.

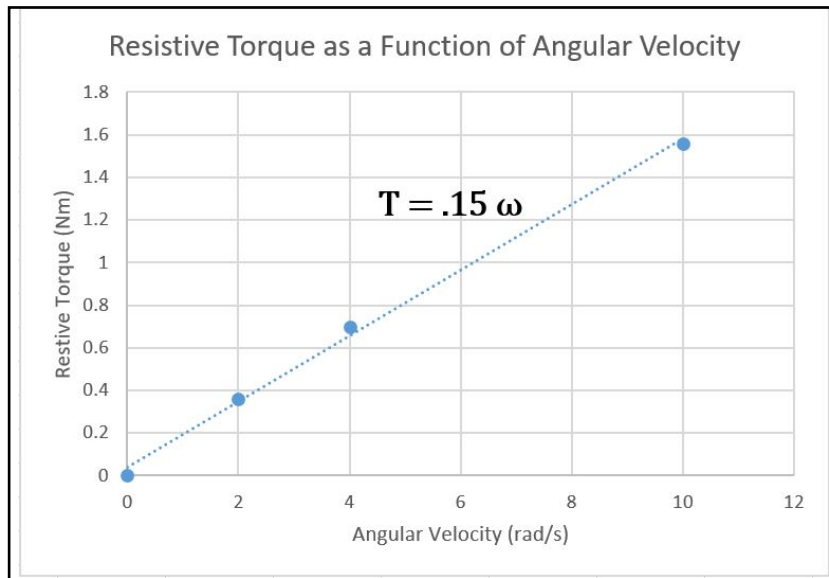


Figure 74: Damping Coefficient at an Axial Speed of 100 m/s

3.7.3.5 Solenoid Actuation Properties

Whenever the cold gas thrusters are activated, the solenoid valve must be actuated at least twice-at the beginning and end of the pulse. Actuation of the solenoid valve is not an instantaneous event, so the mass flux and thrust should not be instantly toggled between zero and full output. The valve is therefore assumed to open and close linearly such that the mass flux and thrust are directly proportional to the first power of the time since actuation:

$$T, \dot{m} \propto t - t_{actuation} \quad (3.19)$$

A different function may better capture the boundary properties of the solenoid valve performance, but a linear approximation is sufficient for the short time scale of actuation. A fast-actuating solenoid was chosen specifically to avoid the variable and unknown flow properties involved with a valve in between states.

3.7.4 Flight Test Validation

Currently, three flight tests - two subscale and one fullscale - have been conducted, all of which have contributed to and validated the integrity of the flight simulation. Both the trajectory analysis and the payload simulation have been updated after each flight test, and the effect of the flight analysis will be described in the following sections.

3.7.4.1 Initial Subscale Flight

The first subscale flight occurred on December 14, 2016 and served as the first validation of the flight model. Primary takeaways from the data include an estimation of the drag coefficient and a substantially improved model of resistive torque opposing the rotation of the payload experiment.

As was described in the Critical Design Review (CDR) report, the drag coefficient from the subscale apogee altitude was estimated to be 0.27. A computational analysis of the rocket's flight confirmed the C_D value. Previous years' flights have produced drag coefficients around 0.3-0.4, so the drag coefficient from the 2016-2017 launch was not unexpected. Figure 75 combines the altitude flight data from subscale launch, a predicted simulation prior to flight with $C_D = 0.35$, and the simulation post-flight that matches apogee by decreasing drag.

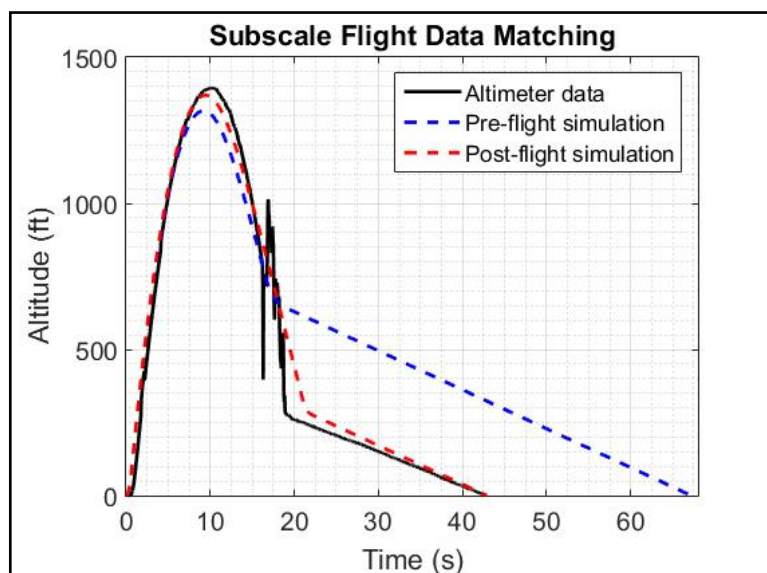


Figure 75: Subscale Altitude Drag Coefficient

In regard to the payload experiment, the model that had been developed prior to the initial subscale flight operated under the assumption that the axial and rotational directions were independent. The results from the subscale flight disproved that assumption, prompting further analysis into the pressure drag resulting from axial flow. The model presented in Section 3.7.3.3 represents the greatest outcome from the subscale flight. Figure 76 illustrates the significant improvement in the experiment model compared with the subscale flight data.

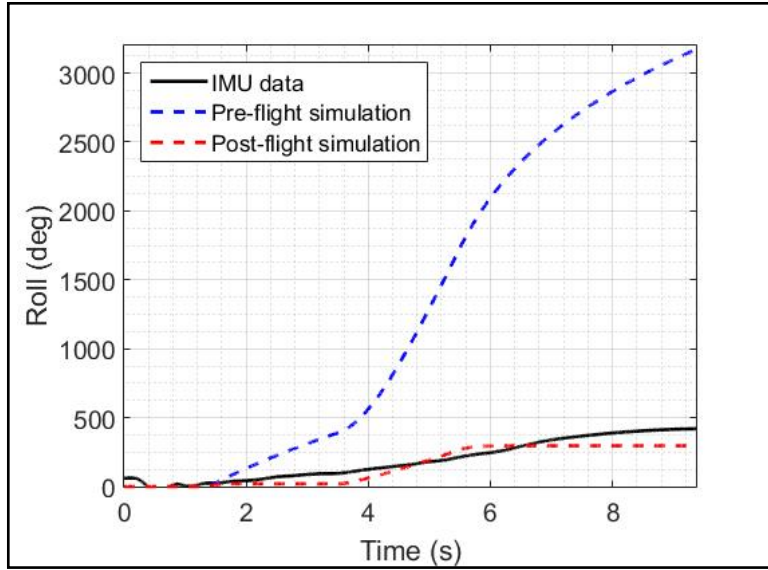


Figure 76: Improvement to Resistive Torque Model

3.7.4.2 Fullscale Flight

The fullscale test flight occurred on February 19, 2017 and is discussed in Section 3.8. The flight was considered an overall success due to the safety and success of launch and recovery; however a non-nominal motor burn and mechanical actuation failure of the solenoid valve proved the upward flight difficult to use for modeling purposes. Primary improvements from fullscale flight data were focused on the recovery system - specifically the opening time of the drogue and main parachutes. The drogue parachute opening time was reduced from 1 second to 0.5 seconds, and the main parachute opening time was reduced from 3 seconds to 1 second. While the longer opening times stemmed from previous years' vehicles, the fullscale flight and initial subscale flight indicated a quicker deployment, perhaps due to slight differences in recovery bay design or more effective parachute packing.

3.7.4.3 Second Subscale Flight

The subscale relaunch occurred on February 26, 2017. As is explained in Section 3.8, the purpose of this flight was to prove the mechanical actuation failure of the solenoid valve during fullscale flight had been rectified. In addition, experiment flight data was gathered with the same hardware, electronics, and logic as was flown for the fullscale test. In terms of flight modeling, though, the flight was quite useful in validating the trajectory simulation.

Figure 77 shows the altimeter data compared to the pre-flight altitude prediction and the matched altitude. In matching the altitude, the model remained unchanged from the predictive analysis; the only difference between the two simulations is the incorporation of the empirical thrust profile from launch and an additional drag factor of 1.5 to the parachute descent. On all three test flights, the main parachute has descended at a slower rate than expected, likely due to unpredictable updrafts into the parachute that do not affect the drag coefficient but do increase drag.

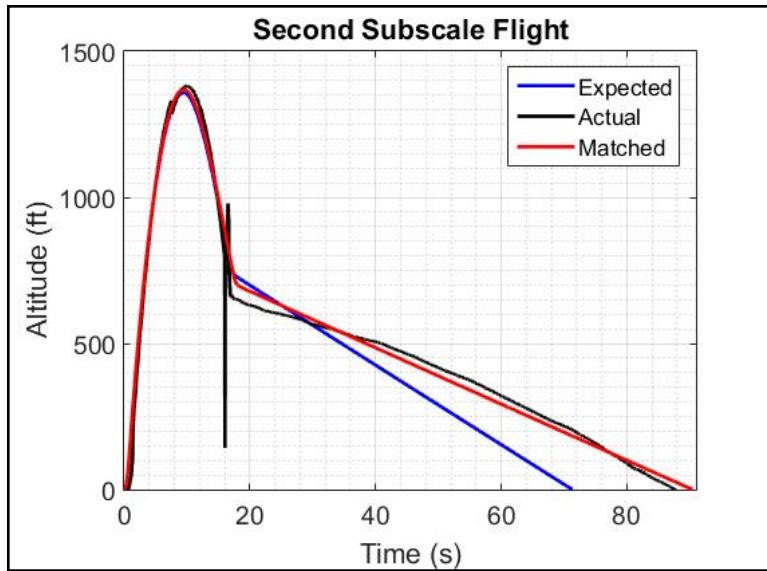


Figure 77: Second Subscale Flight Altitude Analysis

The Cesaroni J1520 motor burned for about 12% longer than expected, but its total impulse was similar to as published. Figure 78 compares the published thrust profile with the acceleration experienced at launch. With the inclusion of the empirically derived thrust, the flight simulation matched the altitude curve and apogee without any further tuning. Though drift throughout the flight is not tracked, the simulation produced a final of drift of 297 feet, just a 15% discrepancy to the 260 feet of drift measured in the field.

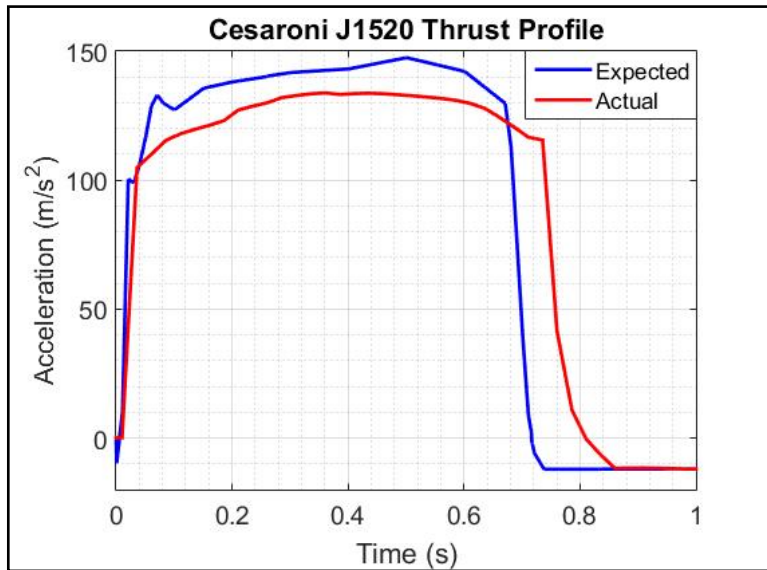


Figure 78: Second Subscale Flight Thrust Analysis

3.7.5 Example Simulation

To illustrate the type of results generated by the simulation, a case study is presented here. Table 5 shows the input parameters to the example simulation. The flight conditions are intended to be representative of a typical fullscale flight under moderate conditions; however, no conclusions regarding future success or failure of the competition launch should be drawn from this example. Analysis of the fullscale launch is also omitted from this section in favor of the previous analysis in Section 3.8.

As the simulation runs, milestones along the flight path are indicated on the display screen to give the user a sense of the progress of the simulated launch vehicle. A time stamp is printed with each event to facilitate analysis involving initial conditions, completion of the payload experiment, and the final state of the rocket. Figure 79 illustrates the simulation output.

Table 5: Example Simulation Input Parameters

Input Parameter	Value	Notes
<i>Flight Parameters</i>		
Diameter	5.5 in	
Length	99 in	
Mass	34.0 lb	15.4 kg
Side wind	10 mph	
Launch angle	5°	Into wind
Drag coefficient	0.27	See Section 3.7.4.1
Motor	Loki L1400	See Section 3.7.2.6
Single fin area	0.0237 m ²	
Launch rail length	12 ft	
Elevation	528 ft	Huntsville, AL
Temperature	80°F	April in Huntsville
Drogue parachute	2 ft elliptical	
Drogue C_D	1.5/0.3	Vertical/horizontal
Drogue deploy	1 s after apogee	
Drogue opening time	1 s quadratically	
Main parachute	8 ft toroidal	
Main C_D	2.2/0.3	Vertical/horizontal
Main deploy	800 ft altitude	
Main opening time	1 s quadratically	
<i>Payload Parameters</i>		
Tank pressure	4000 psi	air + N ₂
Thrust	nominal 12.3 N	Based on tank pressure
Moment arm	2.13 in	
Thrust oscillation condition	$\theta = 4\pi = 720^\circ$	Alternate thrust to hold position
Thrust cutoff condition	14 seconds	End of experiment window
Solenoid actuation time	30 ms	
Z_{fin}	5.04×10^{-4}	
Fin drag coefficient	1.28	Flat plate ¹³
Air tank mass loss	nominal 18.0 g/s	Based on regulator and nozzle

```

Wind velocity = 10 mph
Launch angle = 5 degrees
Mass = 34.0 lb

0.00 s, Liftoff

0.29 s, Launch rail cleared; Rail exit velocity = 84.66 fps

2.00 s, MECO; Velocity at MECO = 553.34 fps

4.001 s, Roll initiated

8.524 s, Counter-roll initiated

9.105 s, Stopping mechanism initiated

9.222 s, Roll stopped; All thrusters off

15.960 s, Apogee; Altitude at apogee = 4006 ft

16.96 s, Drogue parachute deployed

59.07 s, Main parachute deployed, Drogue velocity = -75.34 ft/s

60.57 s, Parachute fully opened

107.25 s, Touchdown!, Main velocity = -15.09 ft/s

Apogee = 4006 ft
Final drift = 706 ft
Max velocity = 553 ft/s
Max acceleration = 12.25 g's

```

Figure 79: MATLAB Simulation Output

In addition to real-time output of launch checkpoints, the simulation environment stores all flight variables over the duration of the flight so that they can be accessed following completion of the simulation. Figure 80 shows examples of the post-flight analysis that can be performed on each simulation.

The trajectory plot is the most intuitive output from the flight simulation (Figure 80a); both axes are position, so the curve represents the expected path of an associated rocket launch. Regarding this particular set of conditions, it is clear that the side wind has decreased the potential apogee through weathercocking. Furthermore, the drift is relatively sensitive to the main parachute deployment altitude in that the system drifts about 150 feet for every 100 feet above ground level that parachute is released. Drift correlated with deployment altitude will be explored in Section

3.7.6.3. The second plot (Figure 80b), the acceleration of the launch vehicle, showcases four clear milestones during the flight. The thrust profile manifests itself within the first two seconds of flight; at MECO, drag force adds 20% to the acceleration of gravity. Deployment of the drogue parachute at 18 seconds puts little stress on the recovery subsystem, and the system reaches steady quickly. Significant stress is applied to the U-bolts constraining the main parachute during deployment at 85 seconds, but the system is able to withstand the load and ensure survivability of the launch vehicle and IMU data (see Section 3.3).

Figure 80c in the lower left simply mirrors the acceleration profile. Both the vertical and horizontal components of velocity are depicted, and one can see the reduction in terminal velocity from the drogue to the main parachute. In addition, the contribution of wind becomes clear, as the sideways velocity rapidly decreases post-apogee to match the wind speed. Finally, the mass profile in Figure 80d shows only pre-apogee flight as the total mass remains constant following completion of the payload experiment. Throughout the motor burn phase, the launch vehicle exhausts nearly 3.1 lbs of solid fuel, causing the center of gravity to move towards the nose. During the time period in which the cold gas thrusters fire, mass is lost from the air tank as well, though the exact amount is undetermined and will vary based on flight conditions and control capabilities. The air tank holds 0.76 lbs of air and nitrogen at 4000 psi, so the rocket mass should not decrease by more than about 0.5 lbs, assuming not all the air is needed to successfully achieve the desired roll and counter-roll.

As was previously mentioned in Section 3.7.3, the roll control experiment is modeled in parallel with the rocket flight. Figure 81 illustrates the expected results of the experiment to be performed in the competition launch. While ideally the rocket would achieve two rotations before holding an angular position, the MATLAB simulation is employed only to guide the control system programming and should be taken at face value. In other words, the simulation is a tool used to suggest control parameters and predict feasibility of the experiment.

This example simulation uses continuous thrust to roll the vehicle 720 degrees, followed by alternating continuous thrust to hold an angular position, in this case arbitrarily set to 720 degrees. The alternating thrust is clear in Figure 81a, which reports the angular acceleration of the rocket as it responds to torques and countertorques applied by the cold gas thruster system. The angular velocity (Figure 81b) increases accordingly with the angular acceleration; when the thrust switches direction, the angular velocity changes sign quickly due primarily to the large dynamic pressure of the air surrounding the fins (Equation 3.16). During the latter portion of the flight, the axial velocity of the launch vehicle decreases substantially post-MECO, resulting in smaller resistive torque and smaller oscillation when holding an angular position. Regardless of the decrease in pressure drag, less than a quarter-second of continuous thrust is required to reverse rotation. Angular position (Figure 81c) is shown to increase and decrease in a quadratic manner. It is important to note that holding an angular position requires continuous alternation of the thrust direction and is quite difficult in terms of controls and logic. While the simulation is built for continuous thrust, the actual control scheme applied in flight may employ a combination of continuous thrust with pulse schemes to achieve the desired experiment.

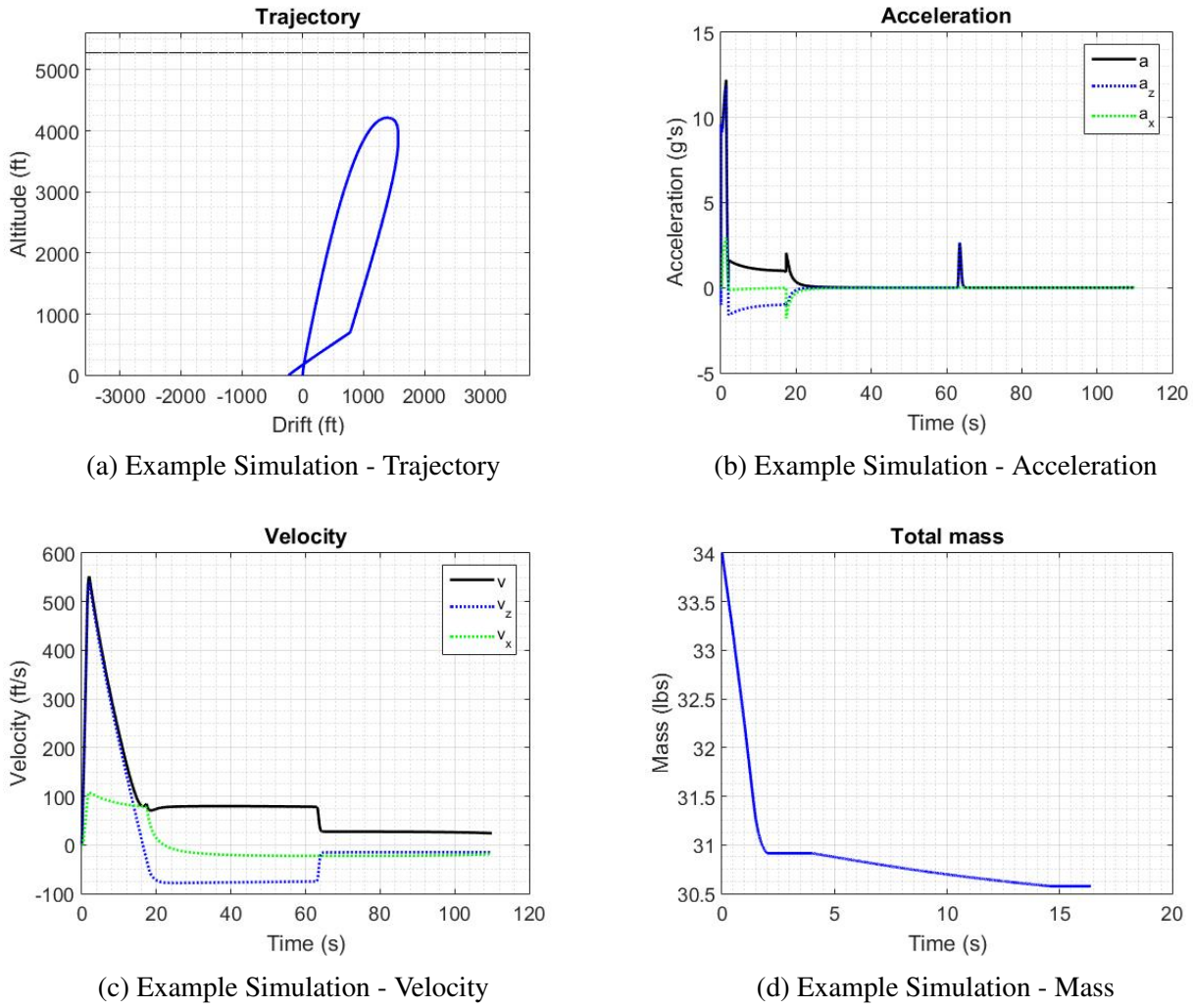


Figure 80: Example Simulation - Rocket Flight

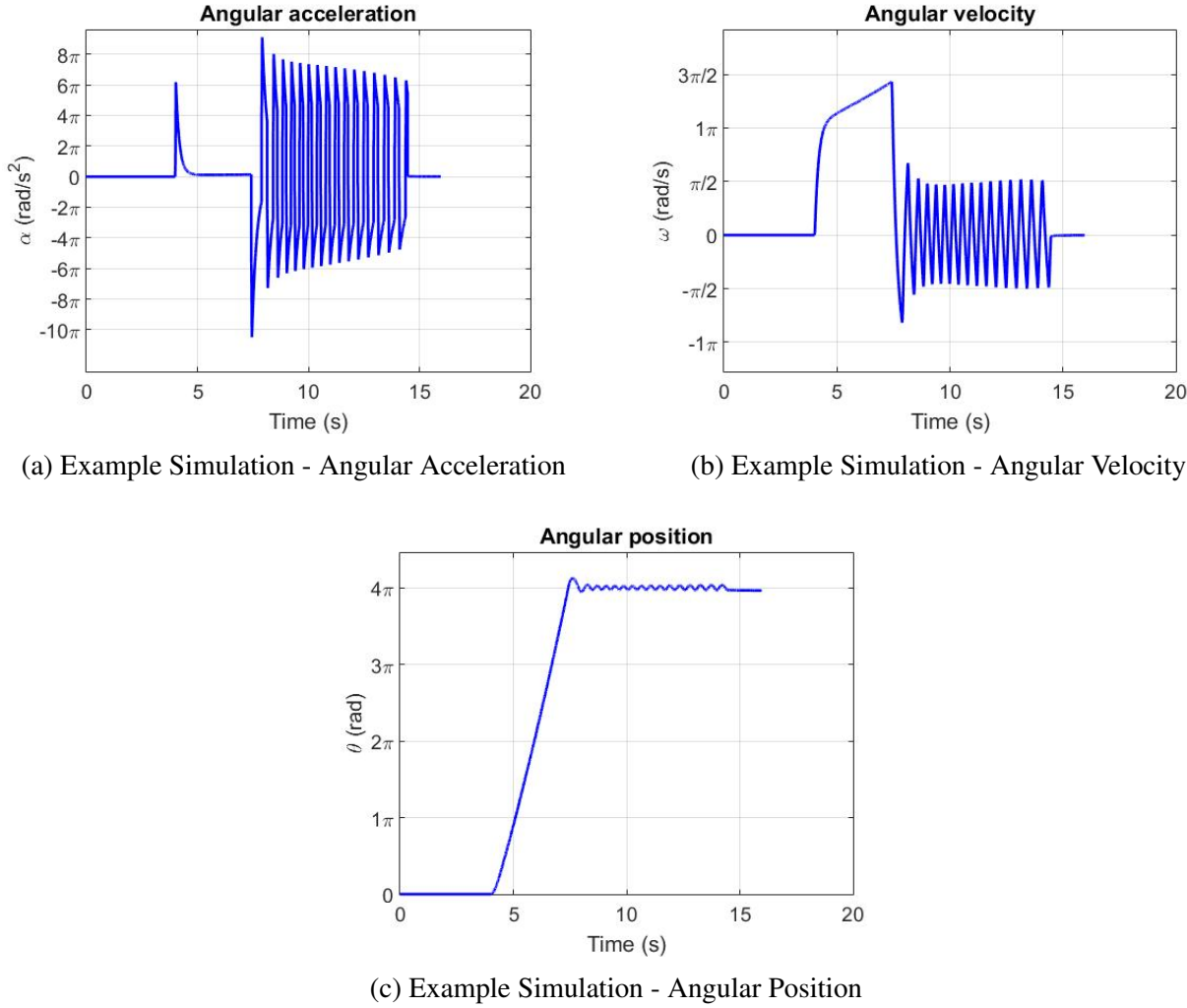


Figure 81: Example Simulation - Payload Experiment

3.7.6 Fullscale Flight Predictions and Sensitivity Analysis

The simulation described in Section 3.7.2 was validated by the subscale flight results (see Section 3.7.4.1) and can therefore be used to predict performance of the fullscale flight vehicle. A supplemental simulation was employed to obtain information regarding the stability margin and to verify the relatively straight flight of the rocket. Parameters such as side wind velocity, exact motor output, and mass, however, will not be known exactly until final rocket assembly or after launch, but they factor into important design choices. Therefore, ranges of these parameters and their effects on the flight must be explored to validate the chosen design and verify that the launch and payload experiment can be completed successfully.

3.7.6.1 Launch Stability

Calculations of the static stability margin arise from simulation in Rocksim and CFD. Figure 82 shows the estimated locations of the center of gravity and center of pressure. With the CG at 52.2 inches and the CP at 65.6 inches from the nose, the static stability margin on the launch pad is

$2.43 ((65.6 - 52.2)/5.5 = 2.43)$. Following motor burn on the launch rail, the stability margin increases to 2.94 at rail exit. Figure 83 describes the variation in stability margin as the launch vehicle travels from the pad to apogee. Furthermore, the rail exit velocity of the vehicle is 84.7 ft/s, meeting the requirement of a minimum rail exit velocity of 52 ft/s.

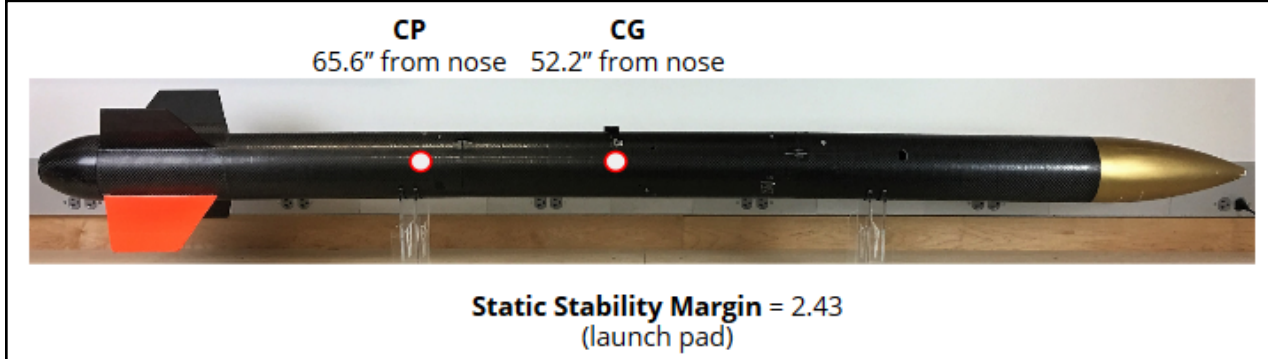


Figure 82: Location of CP and CG

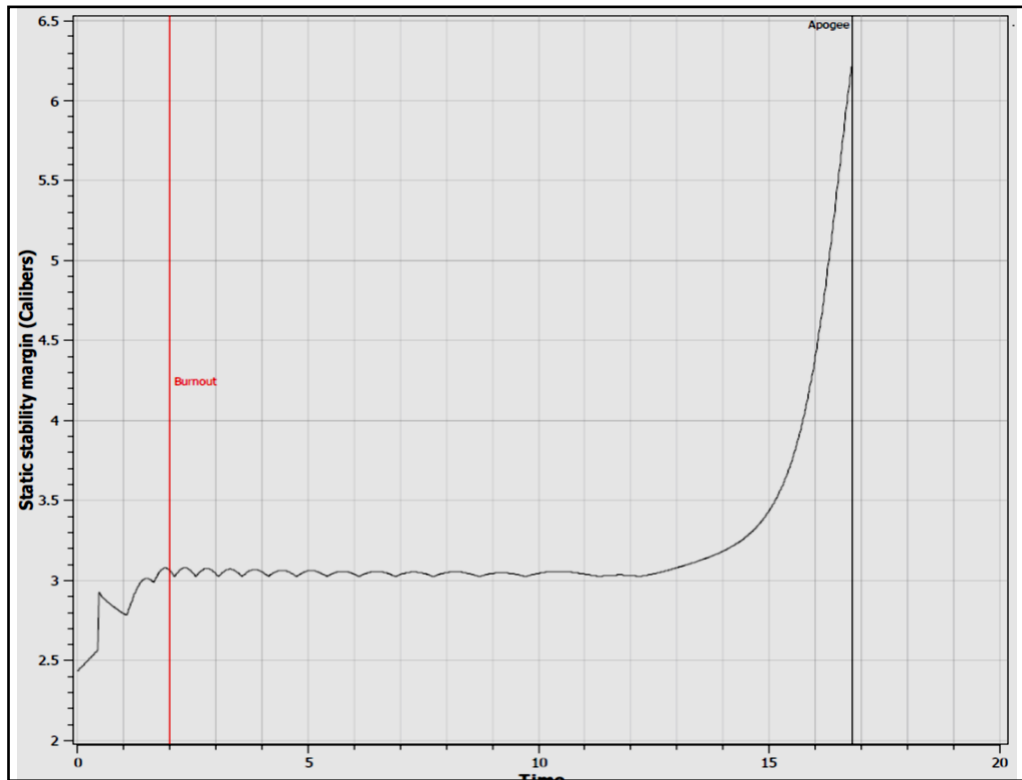


Figure 83: Variation in Static Stability Margin

3.7.6.2 Landing Kinetic Energy

One of the mission requirements, defined in Section 3.7.1, is that the landing kinetic energy of all independent and tethered components must not exceed 75 ft-lbs. The VADL rocket has three sections: nosecone/payload (14.45 lb dry), avionics (7.00 lb), and tail (9.15 lb dry), all of which are tethered together upon landing. The drogue parachute deploys approximately one second post-apogee, splitting into two sections: nosecone/payload (14.0 lb) and avionics/tail (16.15 lb). The main parachute deploys at an altitude of 750 ft, separating the avionics and tail section. The terminal velocity of the system under an 8-foot Iris Ultra toroidal main parachute is approximately 15.1 fps, based on the expected dry mass of 30.15 lbs. Table 6 details the landing kinetic energy of each of the three sections. Given the choice of parachute and the expected launch mass, none of the sections will land with more than 75 ft-lbs of energy, satisfying the safety requirement.

Table 6: Landing Kinetic Energy of Components

Component	Estimated Mass (lb)	Landing Energy (ft-lb)
Nosecone/Payload	14.0	49.6
Avionics	7.00	24.8
Tail	9.15	32.5

Figure 84 displays the kinetic energy of each separated section throughout a simulated fullscale flight. The energy of the launch vehicle is quite large during the thrusting phase of flight but decreases monotonically from MECO to touchdown.

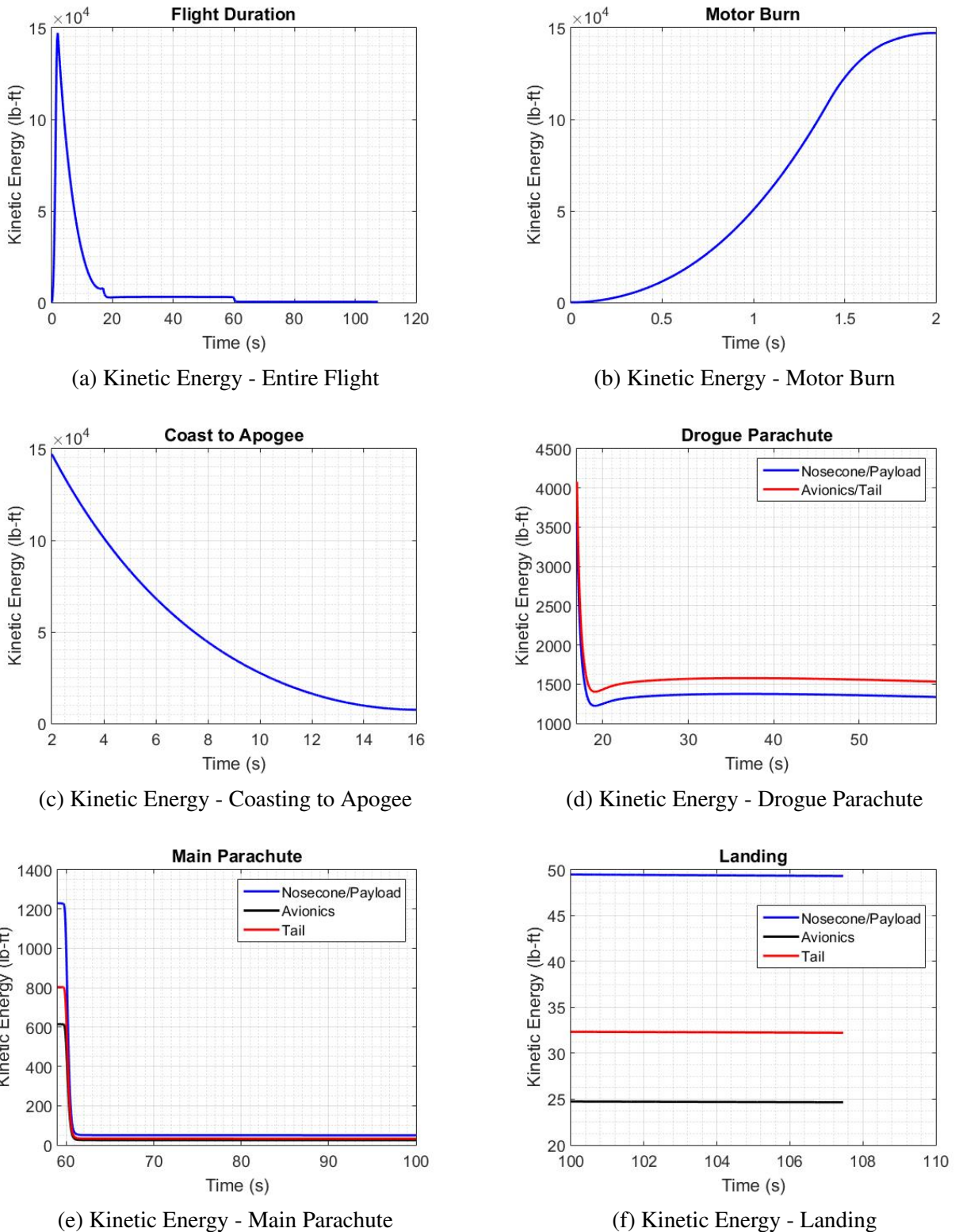


Figure 84: Kinetic Energy Management

3.7.6.3 Side Wind

Side wind is notably one of the most difficult aspects of the launch for which to prepare, and little can be done to mitigate process hazards arising from non-steady and non-uniform wind. The launch vehicle must be robust enough to deal with a range of wind conditions, and a wind speed ceiling must be established at which the launch is canceled. Historically, the maximum wind speed for launch in the NASA Student Launch competition has been 20 mph, and VADL will adhere to this limit in all test and competition launches. The primary hazard posed by side wind is the extreme drift conditions, though parachutes are chosen for the rocket to minimize drift and landing speed under moderate weather conditions. Table 7 indicates the final values of drift for winds of 0, 5, 10, 15, and 20 mph for both vertical launches and launches angled 5 degrees into the wind, and Figure 85 graphically demonstrates the effect of the side wind on drift. Furthermore, apogee altitude is affected by the magnitude of the side wind as well; simulation results are shown in Figure 86. The launch angle will be chosen anywhere between 0 and 5 degrees depending on the wind conditions on launch day.

Table 7: Drift for Various Wind Conditions

Wind speed (mph)	Drift (ft) - vertical launch	Drift (ft) - 5 degree launch
0	0	-1514
5	-126	-1156
10	231	-709
15	617	-244
20	1006	217

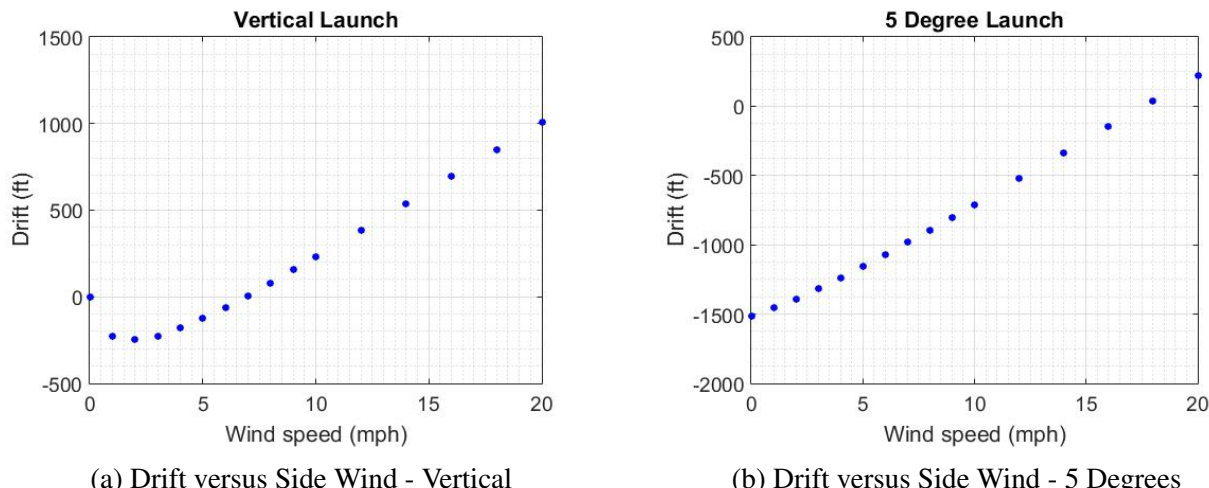


Figure 85: Effect of Side Wind on Drift

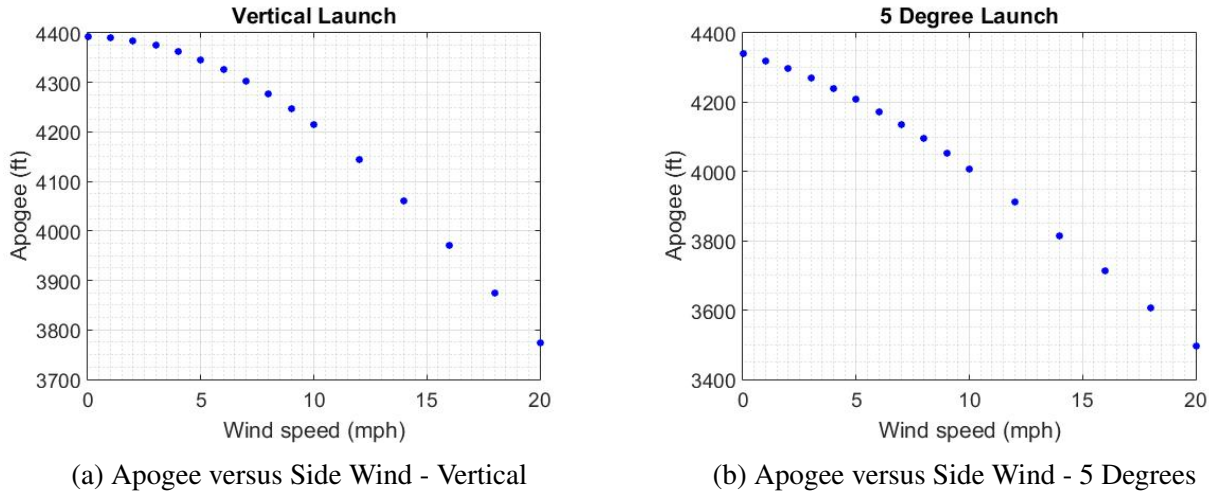


Figure 86: Effect of Side Wind on Apogee

3.7.6.4 Motor Thrust Variability

Another parameter that is unknown prior to launch is the thrust output by the motor. While the published data for the motor must be taken at face value in the absence of statistical testing, knowledge of the sensitivity of the flight to the motor output is important. In particular, because a target altitude exists and overshooting the target by a few hundred feet is not allowed by competition rules, a plot of altitude based on actual thrust is useful. Figure 87 shows the expected apogee versus the percentage difference in thrust compared to the published data (Section 3.7.2.6). These data were produced for a vertical simulation with no wind, so they represent ideal launch conditions. The maximum altitude of the launch vehicle varies approximately 80 feet for each 1% increase or decrease in thrust compared to published values. Assuming the actual thrust profile falls within 5% of expected thrust under moderate weather conditions, the flight should be considered a success in terms of the target altitude.

3.7.6.5 Launch Mass Variability

Finally, a parameter that will be known in the field prior to launch is the exact mass. The apogee altitude is quite sensitive to launch mass, and the capability to add a ballast near the center of gravity is designed into the vehicle. Figure 88 illustrates the variation in apogee with total mass. The mass range explored is centered around the expected mass of 34.0 lb, and the simulations are run with a 5 degree angled launch into a 10 mph wind.

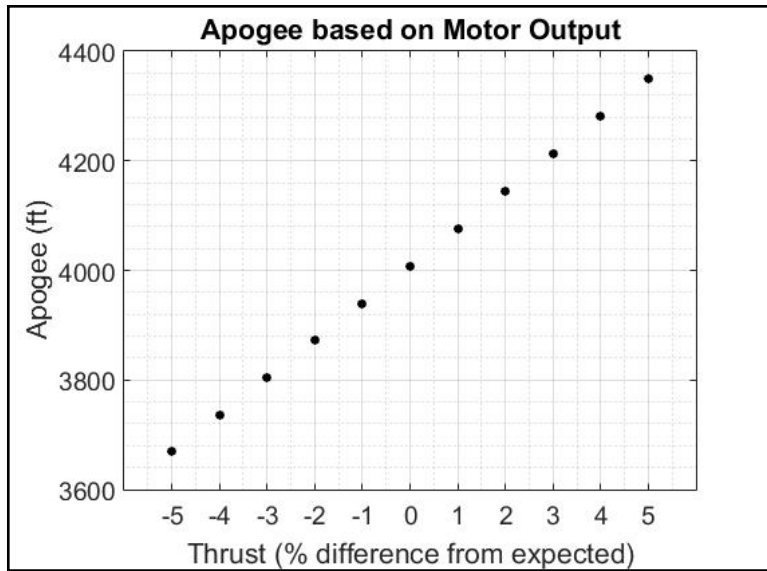


Figure 87: Variation in Apogee due to Variability in Thrust

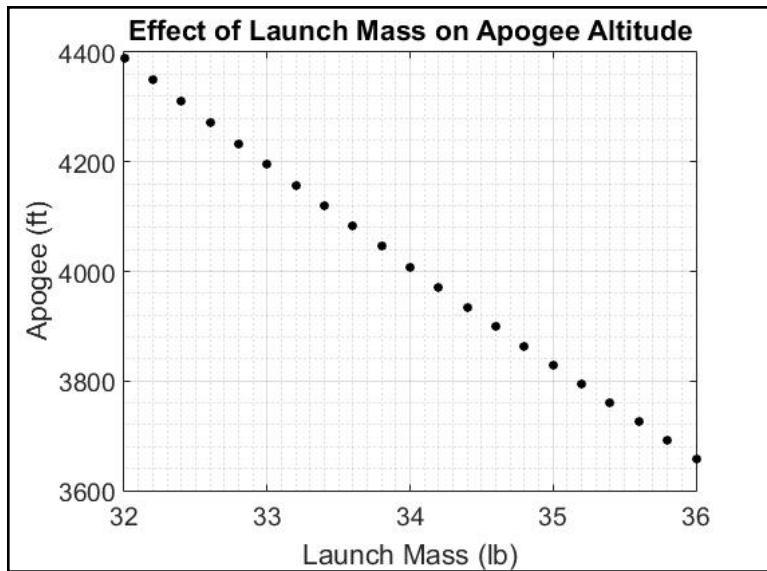


Figure 88: Variation in Apogee due to Changes in Launch Mass

3.8 Fullscale Flight Results

3.8.1 Introduction

In order to demonstrate the functionality of our fullscale flight vehicle, a launch was performed on Sunday, February 19th. VADL is pleased to report that the flight was a success, with:

1. Successful drogue and main parachute deployment (see Figure 89)
2. Safe recovery of all onboard systems
3. Limited Drift

4. Validation of payload's control logic evident through IMU data gathered

Additionally, the fullscale launch brought to attention the presence of significant natural roll during fullscale vehicle flight, which occurs even in the absence of active roll control.

In order to supplement the data gathered during the fullscale launch, our subscale flight vehicle was launched for a second time on Sunday, February 26th. The goal of this launch was to:

1. Verify payload thruster actuation by onboard electronics during flight
2. Develop an improved understanding of how the natural roll of the flight vehicle and axial flow damping affect the payload's ability to induce two full rotations in a limited timeframe.

Furthermore, the data gathered during the supplemental launch has allowed the team to optimize the roll control system in the presence of natural roll.

Overall, two successful launches have been conducted since the Critical Design Review, validating the construction of the fullscale launch vehicle and payload, and supplying the VADL team with an improved understanding of the variables associated with the roll control payload experiment.



Figure 89: Full Scale Recovery

3.8.2 Comparison of Flight Data and Simulations

Despite achieving ideal deployment and safe recovery of the fullscale flight vehicle, the peak altitude experienced during fullscale launch was significantly lower than predicted. Figure 90 demonstrates the discrepancy between the pre-launch simulations and the actual altimeter data. As is demonstrated in the figure, a revised model has been generated based on thorough analysis of all variables associated with altitude. The revised model is nearly identical to the flight data, which validates that a thorough understanding of the lack of altitude has been reached. The factors that contributed to the lack of altitude will be discussed in the subsequent sections.

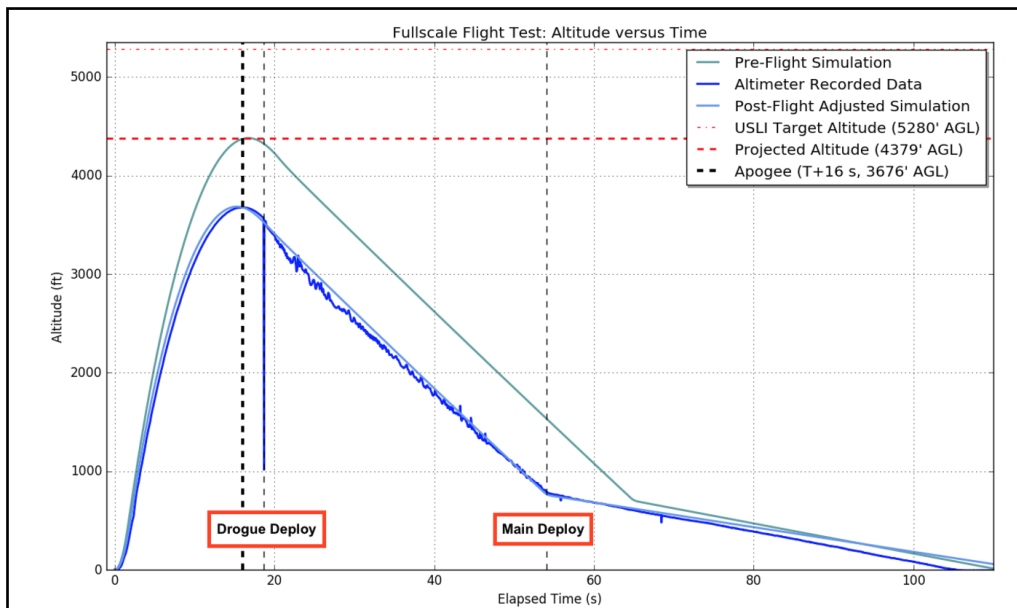


Figure 90: Fullscale Launch Altimeter Data vs Projected Altitude

3.8.3 Motor Thrust Analysis and Associated Altitude Loss

As can be seen in Figure 90 above, the fullscale flight vehicle failed to reach the projected altitude. One major cause for this shortcoming lies in the motor thrust profile. Figure 91 compares the manufacturer specified thrust profile of Loki L1400 motor with an approximated thrust profile experienced during fullscale. The approximated thrust data is based on IMU z-axis acceleration data and takes into consideration variables such as the change in mass throughout the motor burn period of flight. Accordingly, the team is confident that the data presented in Figure 91 is accurate and warrants analysis.

Clearly, there are a number of differences between the thrust profile provided by Loki Research and the approximated thrust profile based on IMU data. Most notably, the motor burned for 10% longer than the manufacturer data suggested, and the peak thrust was significantly lower than predicted. Additionally, the initial thrust increase was far more gradual than the almost immediate thrust increase published by the manufacturer.

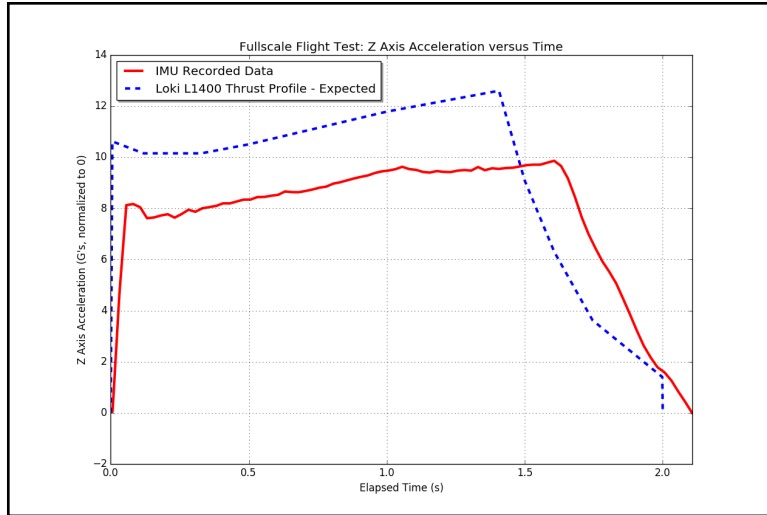


Figure 91: Thrust Profile Comparison

The poor motor performance experienced during fullscale launch has also been analyzed to determine its effect on the flight vehicle's peak altitude. Figure 92 shows an altitude comparison using the manufacturer provided thrust data and the fullscale launch z-axis IMU acceleration data. This simulation isolates the thrust profile as the only independent variable, and assumes a simplified flight environment with no side winds and a vertical launch. This simulation is not meant to match fullscale launch conditions, but rather to demonstrate how the two thrust profiles affect altitude. This figure indicates that the thrust profile discrepancy discussed above translates to a significant peak altitude disparity. Based on this analysis, it is clear that the Loki L1400 motor used during fullscale launch significantly underperformed.

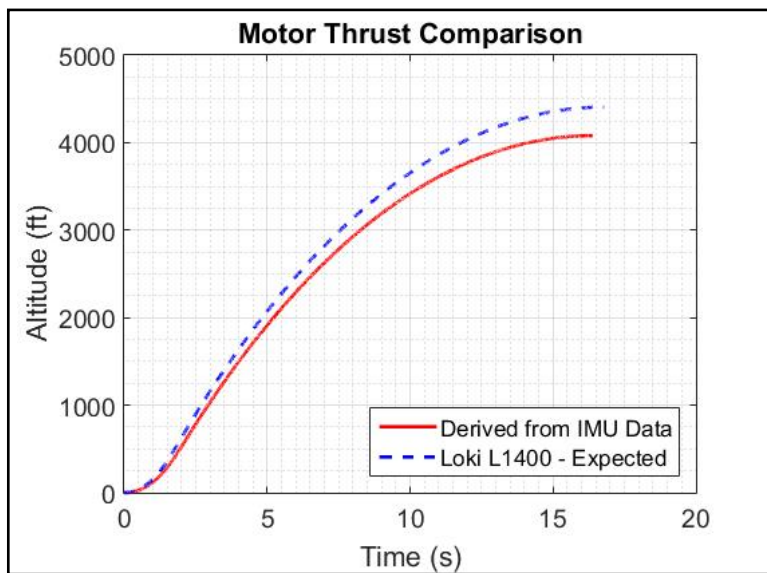


Figure 92: Altitude Comparison Based on Thrust Profiles

Loki Research has acknowledged the poor performance of the motor they provided and has

agreed to provide a motor that is more consistent with their published thrust data. The replacement motor will be the same motor as chosen at CDR, except that the manufacturer will have verified that its thrust profile agrees with their published data. In addition to providing VADL with a motor that is closer to their specifications, Loki Research recommended the use of a Fat Boy igniter by Quickburst. Loki advised that this would ensure a uniform burn throughout the long grain of the motor, and should address the slow initial thrust increase experienced during fullscale launch. As can be seen in Figure 93, 1.25 seconds elapsed between the motor ignition and the beginning of liftoff. While immediate liftoff is not expected, this uncharacteristically long amount of time points to an issue with ignition. A likely explanation for this behavior is that igniter was unable to cause the entire surface of the grain to begin to burn at the same time, thus resulting in a slow initial thrust increase.

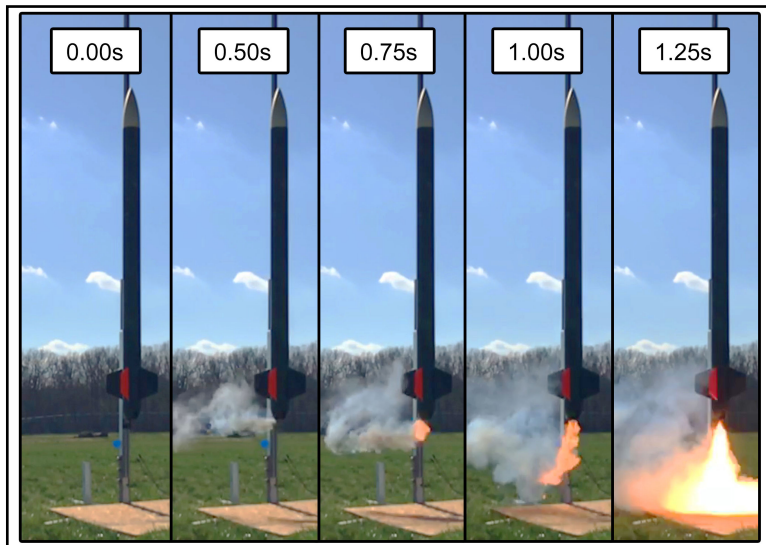


Figure 93: Fullscale Motor Slow Ignition

Overall, the Loki L1400 motor used during fullscale launch significantly underperformed, resulting in a reduction in altitude of approximately 320 feet. In order to address this, Loki Research will provide VADL with an L1400 motor that is closer to the specifications they have provided. Additionally, VADL will use the recommended Fat Boy igniter to ensure uniform grain burning and reduce initial thrust increase time. VADL is confident that after implementing these changes the altitude of the launch vehicle will be much closer to the predicted value.

3.8.4 Effective Drag Coefficient and Associated Altitude Loss

Due to the slower burn time of the motor, the launch vehicle was more susceptible to the effect of side winds soon after rail exit. As a result, the vehicle experienced a relatively large torque near the beginning of the motor burn phase, leading to a series of over-corrections provided by the stability margin of the vehicle. While this wobbling during motor burn will not be expected when flying a motor with the published specifications, the effective drag coefficient during the fullscale test launch was nearly doubled from 0.27 to 0.46. Variability in the drag coefficient and incident area for pressure drag substantially increased the magnitude of the drag force on the launch

vehicle, thus decreasing the apogee altitude. Figure 94 illustrates the correlation between drag coefficient and altitude. From this figure, it is evident that significant altitude loss of approximately 350ft was caused by the increased drag coefficient.

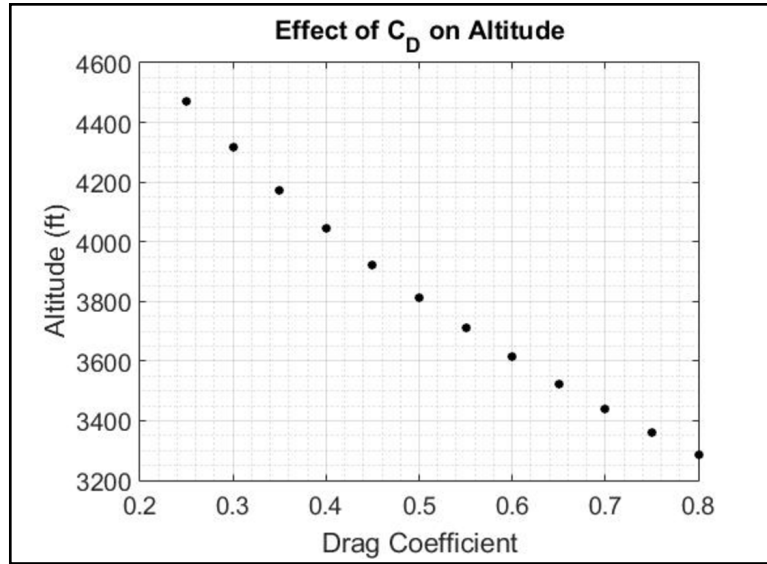


Figure 94: Effect of Drag Coefficient on Altitude

3.8.5 Flight Altitude Conclusions

After thorough analysis of all aspects of the flight vehicle affecting peak altitude, a robust understanding of the various shortcomings of the fullscale launch has been developed. The combination of poor motor performance and increased effective drag coefficient reduced the peak altitude by approximately 670 feet as compared to simulation. After incorporating all of these factors into a model with conditions identical to the fullscale launch, the team is confident that a full understanding of the altitude deficiency has been achieved. Figure 95 compares our improved model that incorporates these factors to the actual altimeter data from the fullscale launch. It is clear that the new model agrees with the data collected during fullscale launch. More importantly, each factor that contributed to loss of altitude has been addressed and mitigated in order to prevent such shortcomings from happening again. Overall, the factors that contributed to altitude loss have been analyzed, understood, and addressed so that the same issues will not persist during future launches.

Other goals of the fullscale launch included actuation of the thruster system, IMU data collection, and verification of the control system logic. Figure 96 shows the vehicle's roll over the duration of the flight overlaid with the solenoid pulsing scheme of a thruster.

3.8.6 Fullscale Roll Analysis

Preliminary analysis of Figure 96 confirms successful IMU data collection and verification of the control system logic. The goal of the control system was to initiate roll 2 seconds after MECO in the same direction of natural roll and then to use the counter thrusters to keep the rocket within 5°

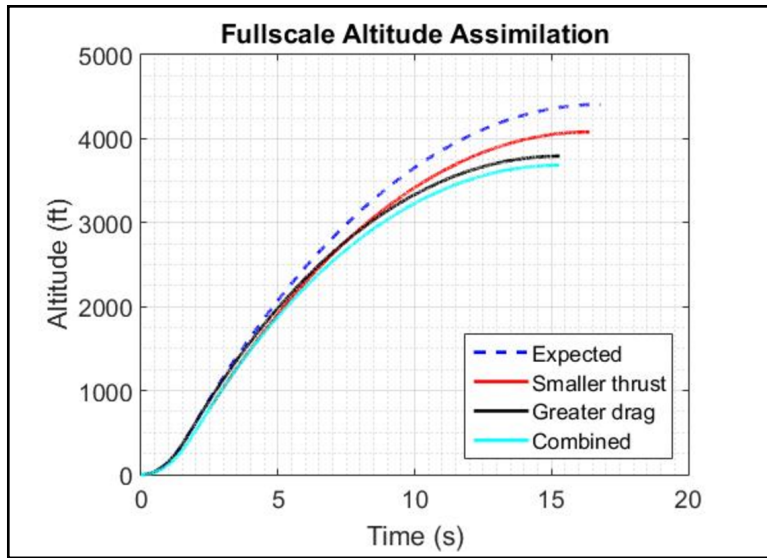


Figure 95: Combination of Factors Leading to Reduced Altitude

of the 720° rotation goal. The solenoid pin diagram shows this system behaving exactly as expected. The team is thrilled with the verification of this essential component of the payload system.

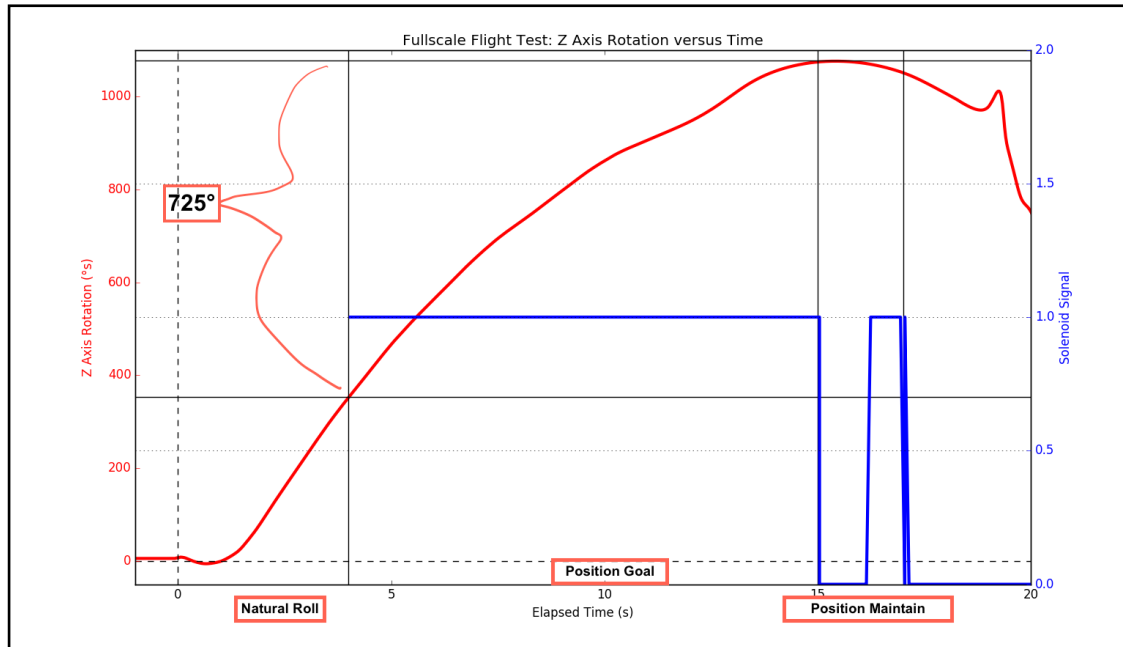


Figure 96: Fullscale Flight: Roll Data

Further analysis of the vehicle and data showed that, despite the verification of the software, there was no thruster actuation during the fullscale flight. This was noted by the lack of pressure loss in the compressed air tank and by examining the concavity of the roll data, which shows negative angular acceleration during the experimental phase (Figure 97).

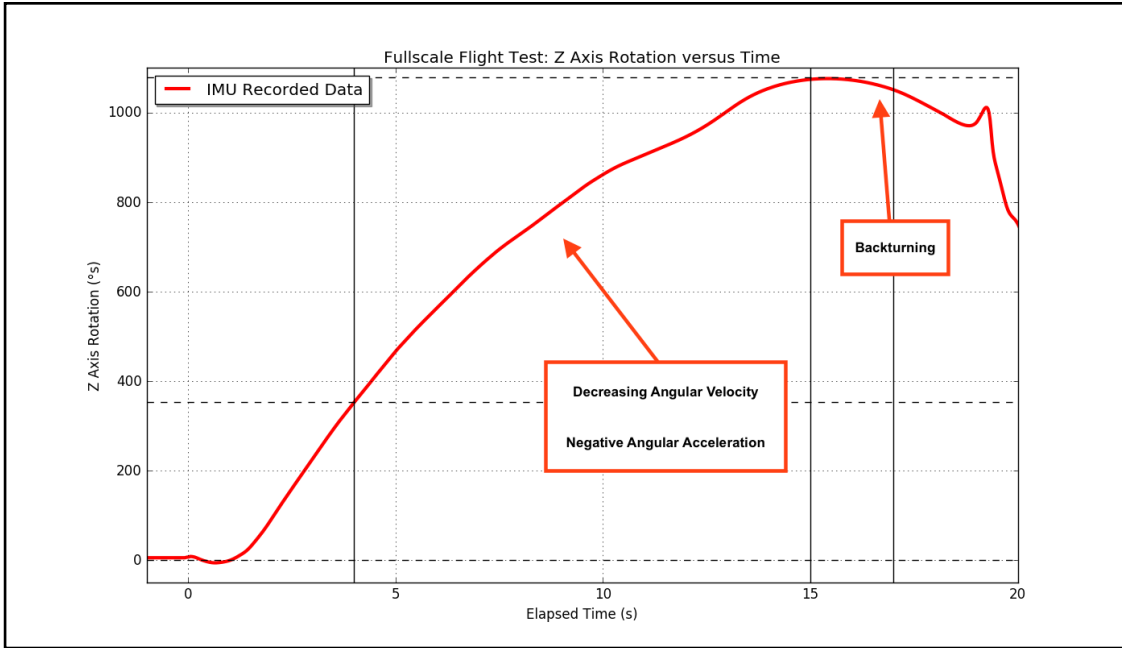


Figure 97: Fullscale Flight: Annotated Roll

Upon making this realization the team began a comprehensive failure analysis, examining every component between the solenoid pin and the thruster, in order to identify the root cause. It was not long before a faulty solder connection on an essential electrical component was found. The connection was easily fixed, however to verify that this was an isolated issue the team decided to relaunch the subscale vehicle using the updated payload electronics. This flight was also used to provide the team with more information about the system dynamics and performance of the thruster system.

3.8.7 Subscale Relaunch

The subscale relaunch was a success, with full actuation of the solenoid in accordance with the control scheme and with safe recovery. The angular rotation, velocity, and acceleration data can be seen in Figure 98.

The thruster system achieved over 200° of rotation in opposition to natural roll. Examining the angular acceleration shows that the acceleration was only positive while the thruster system was firing. The successful actuation of the solenoids also leaves the team confident about their identification of the root cause of the lack of solenoid actuation from the fullscale launch.

Figure 100 demonstrates an extrapolation of the data collected during subscale. The blue line shows the expected roll data if the solenoids were left on for the same time as is planned in the fullscale vehicle, and predicts that the thruster system is able to achieve over 500° of rotation in opposition to natural roll in just over 12 seconds. The team will be actuating the thrusters in the direction of natural roll - identified by the robust control system - and expects to be able to complete the experiment well within the experiment window.

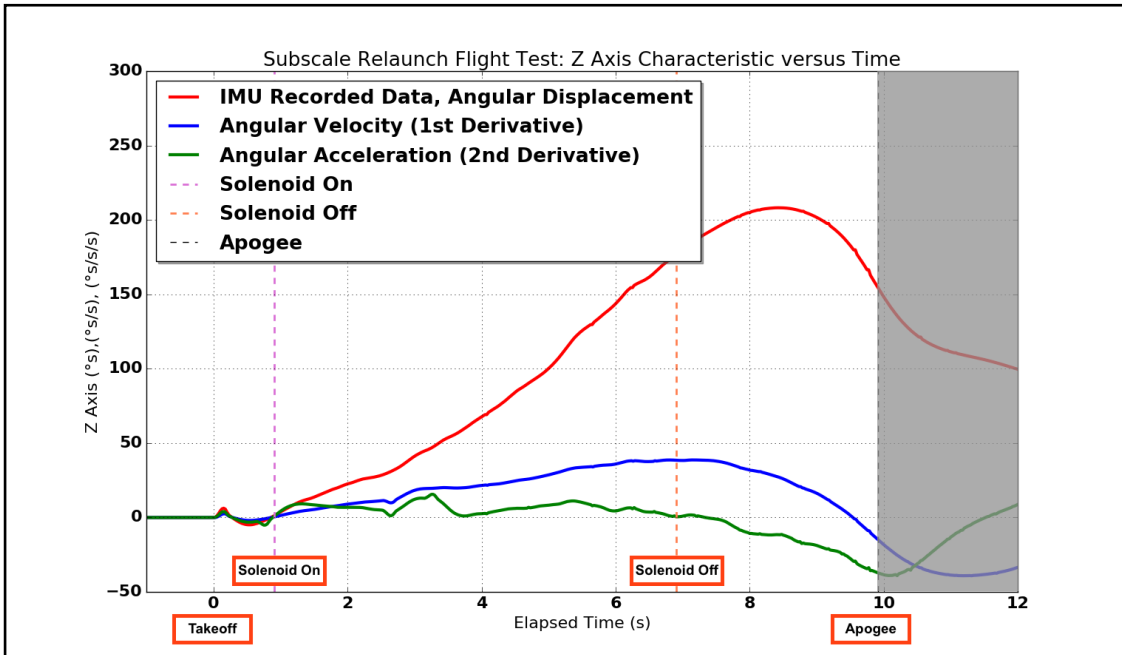


Figure 98: Subscale Relaunch: Z Axis Characteristics vs Time

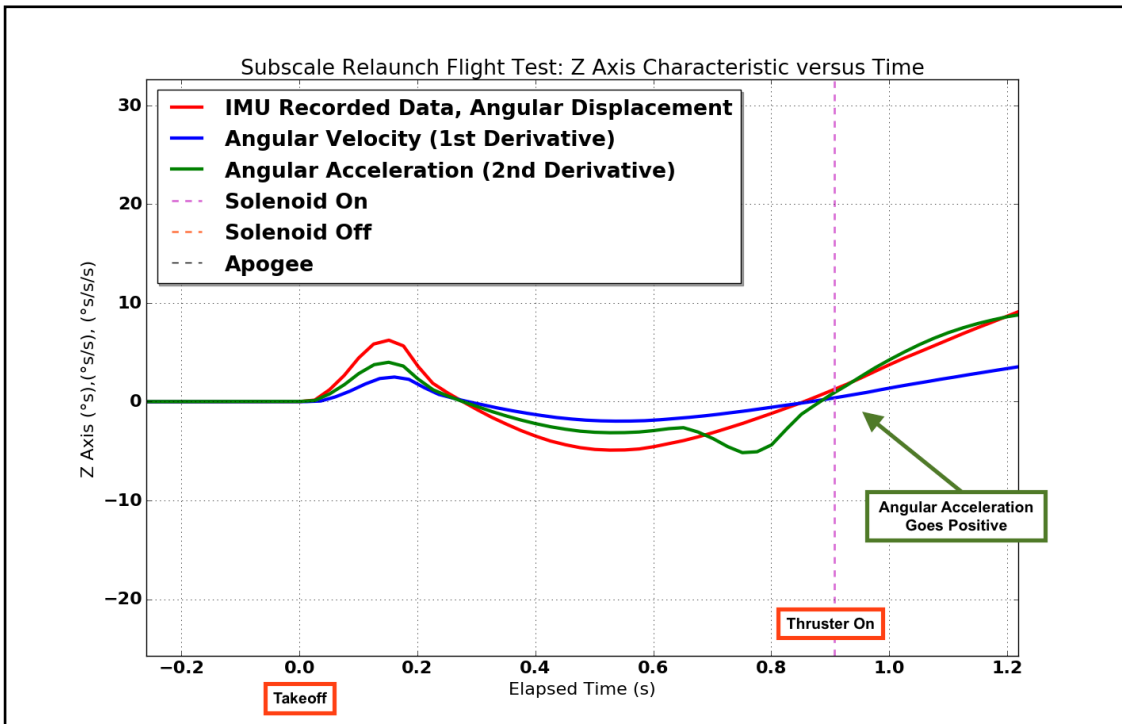


Figure 99: Subscale Relaunch: Z Axis Characteristics vs Time, Zoom

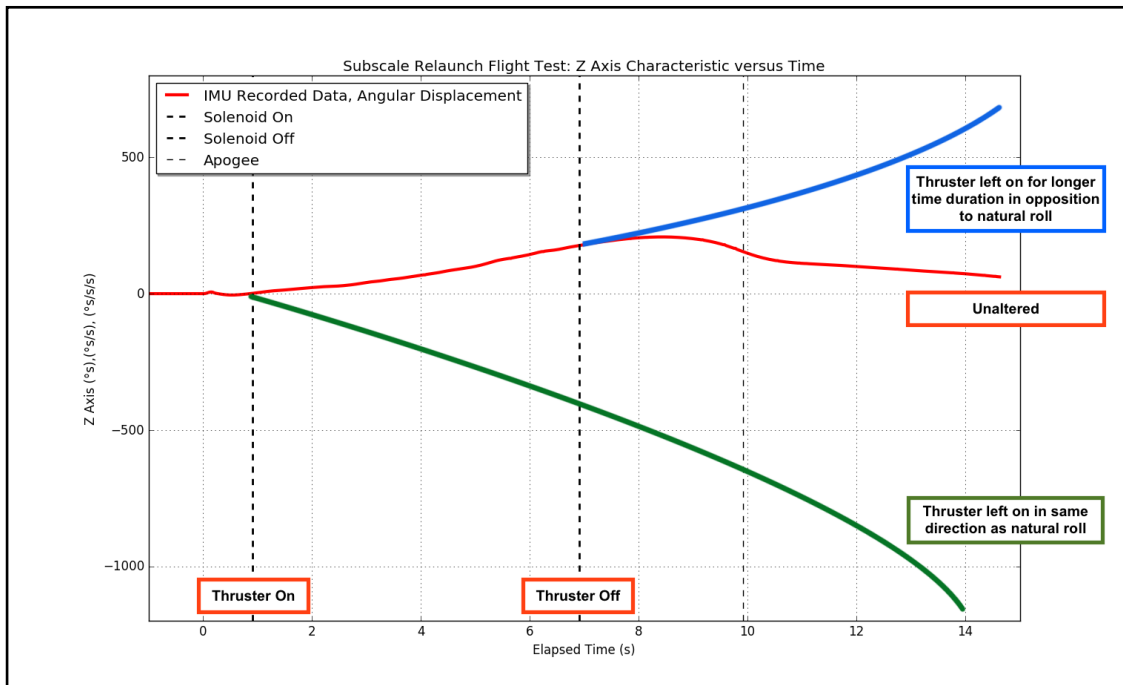


Figure 100: Subscale Relaunch: Roll Direction Analysis

3.8.8 Conclusions and Moving Forward

VADL had a successful fullscale launch, with verification of the vehicle design and successful recovery. The launch also proved the validity of the control system logic and allowed the team to recognize and remedy a failure point in the electronics system. The natural roll data collected during this flight will be valuable moving forward for improving the drag model of the FRAME and creating a realistic hardware-in-the loop simulation. The team followed their fullscale launch with a successful subscale relaunch, which verified the fix in the electronic subsystem and again provided the team with valuable damping and thrust data. The team is confident in our vehicle and our ability to accomplish the payload experiment. The team intends to continue to analyze this data and apply what we learn to improve our simulations and FRAME model.

Furthermore, there is an opportunity to relaunch the fullscale vehicle in March, which would allow the team to collect more data to improve our aerodynamic models for better understanding of axial flow in flight and to test the bidirectional control system with in-flight conditions.

4 Payload Criteria

4.1 Design and Construction

4.1.1 Design Selection

When approaching the flight experiment of roll control, VADL analyzed various actuator design solutions such as tangential thrusters, magnetic torque application, gravity-gradient torque, aerodynamic torque, solar radiation pressure, mass movement, momentum wheels (MWs), control moment gyroscopes (CMGs), as well as many others.¹⁴

Several of these were eliminated given that they are more suitable for use in high altitude flight, specifically those solutions of magnitudes suitable for satellite or long-distance spacecraft positioning over long time periods. These solutions include solar radiation pressure, gravity-gradient torque, and external magnetic torque. Other alternatives such as MWs and CMGs were eliminated due to the fact that the size of component needed for these two methods to produce adequate torque violated the size constraints of our launch vehicle.¹⁵

Furthermore, mass movement devices were eliminated due to their inherent characteristics such as mechanical complexity, single-use application, and low compatibility with an active control scheme.¹⁶

Also eliminated after consideration were the aerodynamically induced applications of fin-based rotation control (i.e. thruster vanes and aerodynamic control surfaces) for many reasons, the most pressing of which were the high cost of construction and a needed active burn scenario for the case of thruster vanes and the difficulties in ground-based testing and mechanical complexity for the case of control surfaces.

Lastly, VADL analyzed the use of tangential cold gas thrusters. Despite the drawbacks of needing to carry compressed propellant within the flight vehicle, VADL feels that the high impulse and short time frame of the post-MECO and pre-apogee flight for USLI make this the best option for our roll control payload experiment. Additionally, the ground-based testability of this method offers superior characterization abilities for the system in terms of control and this ground-based analysis reduces the costs of relying on full scale launches alone for testing purposes. Figure 101 shows a summary of the weighted evaluation of the attitude control alternatives. More detailed information on the analysis of these alternatives can be found in the VADL Preliminary Design Review 2016-2017.

For these reasons, VADL has chosen to move forward with the use of a tangential cold gas thruster system to induce and control our roll and counter roll during launch.

¹⁴ Fortescue, Peter, Graham Swinerd, and John Stark. *Spacecraft Systems Engineering*. 4th ed. (301-306)

¹⁵ Gurrisi, Charles, Raymond Seidel, Scott Dickerson, Stephen Didziulis, Peter Frantz, and Kevin Ferguson. "Space Station Control Moment Gyroscope Lessons Learned." *Proceedings of the 40th Aerospace Mechanisms Symposium*

¹⁶ Fortescue, Peter, Graham Swinerd, and John Stark. *Spacecraft Systems Engineering*. 4th ed. (307)

Attitude Control Method	Torque Potential	Ground-Based Testability	Ease of Manufacture	Verdict
Thruster	10	8	8	Proceed
Magnetic Torque	1	5	4	Abandon
Gravity-Gradient Torque	1	3	4	Abandon
Aerodynamic Torque	10	3	8	Abandon
Solar Radiation Pressure	1	1	2	Abandon
Mass Movement	5	3	7	Abandon
Momentum Wheel	3	5	5	Abandon
Control Moment Gyroscope	3	5	5	Abandon

Figure 101: Weighted Evaluation of Attitude Control Alternatives

4.1.2 Payload Mission Requirements Overview

When designing this year's roll control system, meeting all payload mission requirements was of top concern. The combination of two independently actuated thruster couples, an inertial measurement unit, on-board computer, and a robust control system help make sure the payload requirements set forth for the 2017 NASA USLI are met by this year's VADL payload design. Table 8 describes how our payload meets these mission requirements.

Table 8: Mission Requirements Evaluation Overview

NASA SL Payload Requirement	Team Design Solution	FRR Section Reference
Teams shall design a system capable of controlling launch vehicle roll post motor burnout.	A robust control system has been designed and validated through both ground-based and flight tests. The control system is hard-coded not to begin the experiment until the on-board IMU senses MECO.	Control System: Section 4.4
The systems shall first induce at least two rotations around the roll axis of the launch vehicle.	A thruster couple oriented tangential to the rocket main axis with exhaust ports in the airframe will induce this roll. Ground-based tests, flight, and simulations have verified the 720 degree induction capabilities.	Thruster System: Section 4.1.5
After the system has induced two rotations, it must induce a counter rolling moment to halt all rolling motion for the remainder of launch vehicle ascent.	A thruster couple oriented tangential to the rocket main axis with exhaust ports in the airframe will induce this counter roll with the control system firing each couple to maintain position for the remainder of the ascent. Ground-based tests, flight, and simulations have verified the counter roll control capabilities.	Thruster System: Section 4.1.5 Control System: Section 4.4 Ground-based Testing: Section 7.1.4
Teams shall provide proof of controlled roll and successful counter roll.	The on-board inertial measurement unit will measure the roll, pitch, yaw, and acceleration of the vehicle in real-time and record this data on the on-board computer.	IMU: Section 4.3.2.4 Flight Computer: Section 4.3.2.2

Mission Requirements Evaluation Overview

NASA SL Payload Requirement	Team Design Solution	FRR Section Reference
Teams shall not intentionally design a launch vehicle with a fixed geometry that can create a passive roll effect.	All construction operations were performed to create a symmetric and flight-worthy vehicle to safely and accurately validate our payload experiment.	Vehicle Construction: Section 3.3
Teams shall only use mechanical devices for rolling procedures.	All roll and counter roll operations are performed by custom designed and fabricated conical nozzles fed by compressed air and N ₂ actuated by independent pilot-operated solenoids.	Thruster System: Section 4.1.5 Solenoids: Section 4.3.2.1

4.1.3 Cold Gas Thruster Nozzle Design

The cornerstone of the cold gas thruster system is the converging-diverging nozzle which accelerates the propellant flow from stagnation conditions at the outlet of the air tank regulator to supersonic speeds at the nozzle exit, providing the thrust required to achieve the scientific payload objective.

For Student Launch, VADL plans to use identical nozzles as used in fullscale flight testing, which have the same design validated through subscale flight test. The nozzle design was determined through an analysis of isentropic flow equations and various design constraints (such as perfectly expanded conditions at 3000 ft and stagnation conditions equal to tank pressure and temperature values). The design also took into account aspects such as machinability, consistent geometry, pressure rating, and ease of mounting. Please refer to Table 9 and Figure 102 for nozzle design specifications. For further detail on the design process, please refer to VADL's Preliminary Design Review (PDR Section 6.2.3).

Table 9: Nozzle Overview

Throat Diameter	1.5 mm
Exit Diameter	3 mm
Converging Half-Angle	30 degrees
Diverging Half-Angle	10 degrees
Length	19 mm
Design Thrust	7.8 N

One key difference made since subscale in the operation of these nozzles is the choice of propellant. In order to obtain a greater thrust, VADL will be employing a mixture of air and nitrogen — specifically, 2000 psi of air and 2000 psi of N₂ for a total tank pressure of 4000 psi. This change was implemented to offset regulator droop leading to a drop in output thrust. The choice of N₂ was made due to the lack of availability of air storage tanks at pressures exceeding 2000 psi while these pressures are readily available with N₂ storage tanks.

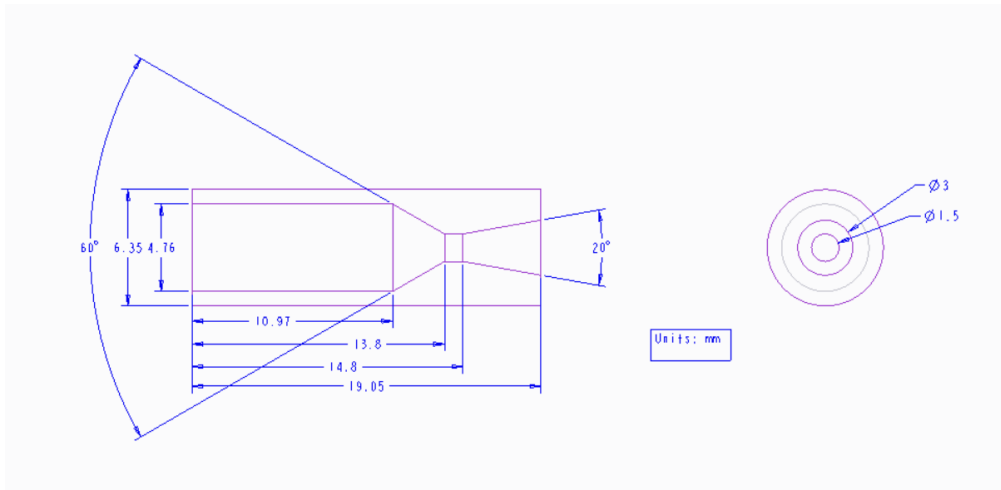


Figure 102: Nozzle Technical Drawing

4.1.4 Cold Gas Thruster Nozzle Construction

An important consideration for VADL when approaching both the vehicle and payload design for this year was the ability for all components possible to be fabricated in house. With this in mind, the conical nozzles designed were also fabricated by the team using the machining resources available at Vanderbilt.

4.1.4.1 Nozzle Fabrication Safety Measures

- The certified and university-employed shop supervisor must sign off on all procedures prior to the start of any machining operations.
- VADL members must sign-in to the shop register when entering the shop.
- Machining operations must take place during the hours of operation for the Vanderbilt Undergraduate Machine Shop.
- Any VADL team member performing a machining operation must be accompanied by an additional member to ensure safe fabrication.
- Both the VADL member performing the machining operation and the safety assistant must have been trained and approved by Vanderbilt University in all shop procedures and machines **prior** to nozzle fabrication.
- Safety glasses must be worn by both VADL members during **all** operations.
- If a VADL member is unsure of any operation procedure, the machine in question must be safely and immediately powered down until proper instruction is received by the shop supervisor.
- Duration of any machining session shall **not** exceed 4 hours to prevent any fatigue-related lapses in safety measures.

4.1.4.2 Nozzle Fabrication Machines Utilized

- Gravity Feed Horizontal Band Saw
- Lathe
- Vertical Milling Machine

4.1.4.3 Nozzle Fabrication Required Equipment

- 1/4" 12L14 steel round stock
- 0.055" HSS drill bit
- 1.5 mm HSS chucking reamer
- 10-degree tapered carbide end mill
- 3/16" HSS drill bit
- 60-degree chamfer carbide end mill

4.1.4.4 Nozzle Fabrication Steps

- **Stock Preparation Operations**

1. Use horizontal band saw to cut the stock to 0.75" length.
2. Use file to debur the resized stock.
3. Mount the resized stock in the lathe via 3-jaw chuck.
4. Set the machine speed to the proper RPM for stock size and material.
5. Face down the piece to 0.735" in length.
6. Mount center drill in the tail stock chuck and center drill both ends of the stock.
7. Remove stock from lathe and proceed to the vertical mill.
8. Verify the alignment of the vise with a dial indicator.
9. Mount a collet holder into the vise and use 1/4" collet to secure stock.
10. Use a dial indicator to center the stock with the spindle.
11. Zero the x and y axes with the digital read out (DRO).
12. Set the mill to the correct RPM for the stock size and material

- **Throat Operations**

1. Mount the 0.055" bit and zero the z axis at the top of the stock.
2. Drill 0.5" into stock making sure to use cutting fluid, proceed in small depth increments, and flush out chips to preserve work piece and tool.
3. Mount the 1.5 mm chucking reamer and re-zero the z axis.

4. Ream the hole to the same depth making sure to use cutting fluid, proceed in small depth increments, and flush out chips to preserve work piece and tool.

- **Diverging Section Operations**

1. Mount 10-degree tapered end mill and re-zero the z axis.
2. Bore to a depth of 0.2275" to create the correct nozzle outer diameter. Make sure to use cutting fluid, proceed in small depth increments, and flush out chips to preserve work piece and tool. Outside of safety emergencies, do not stop spindle while the tool is inside of the stock to preserve tool tip.
3. Flip work piece and re-zero the x and y axes with a dial indicator to begin converging section operations.

- **Converging Section Operations**

1. Mount 3/16" drill bit and re-zero the z axis to -0.0563" (to account for tip of the bit).
2. Drill 0.4169" to create the constant-diameter section before the convergence. Make sure to use cutting fluid, proceed in small depth increments, and flush out chips to preserve work piece and tool.
3. Mount 60-degree end mill and re-zero z axis to -0.1624" (to account for the tip of the end mill).
4. Bore to a depth of 0.4169". Make sure to use cutting fluid, proceed in small depth increments, and flush out chips to preserve work piece and tool. Outside of safety emergencies, do not stop spindle while the tool is inside of the stock to preserve tool tip.
5. Power off mill and remove completed nozzle.
6. Use compressed air to blow out any remaining chips in the nozzle, making sure to point nozzle away from all personnel.
7. Clean up work stations and return all tools to the proper location.

- **Securing Nozzles and Creating Thruster Couple**

1. Secure 1/4" Yor-lok elbow into vise making sure the fitting has an unused nut and crimp inside.
2. Place nozzle inside of fitting making sure that diverging section is facing outwards and hand-tighten nut.
3. Using a fine-tipped permanent pen, index both the nut and the fitting.
4. Using these indices, carefully rotate the nut 1.25 rotations using a 9/16" hex wrench.
5. Remove elbow and nozzle assembly from vise.
6. Repeat this process for second half of the couple.
7. Use the same 1.25 rotation method to connect both elbows to the Yor-lok-to-NPT Tee fitting via 1/4" smooth-bore 304 stainless steel tubing. Make sure elbows (thrusters) are facing the same angular direction.

8. Make sure finished thruster couple is level. Any re-alignment can be performed by loosening the nut, rotating fitting, and then re-tightening the nut 0.25 rotations per the manufacturer specification.

4.1.5 Payload Assembly and Rocket Integration

In designing our payload vehicle integration for this year's NASA SL, we felt accessibility both for launch day assembly and on the rail checks was of top concern. When pressurizing the air tank and arming electronics at the launch pad, the entire payload body tube and nose cone will be removed, and the payload skeleton will remain free-standing through the coupling tube fixed to the avionics body tube. This is done by utilizing the coupler tube that connects the forward and avionics sections (and contains the payload electronics) to hold the final two payload skeleton bulkheads in compression for free standing and stable configuration outside of the complete airframe. Thus, the entire payload skeleton is supported by the threaded rods and coupler tube, and the coupler tube is fixed to the payload airframe by steel button bolts and to the avionics airframe by shear pins.

The payload thruster system as well as payload control electronics are located in the forward portion of the rocket body. As shown in Figure 103, the pressurized air tank rests in the nose cone, supported by expandable polyurethane high density foam. A centering bulkhead prevents lateral movement of the tank inside the nose cone and restrains the foam during the pouring and expansion phase of fabrication. The tank will be held rigidly in place by bulkheads 1 and 2 (BH1 and BH2, respectively) as shown in Figure 104. Note that this dual bulkhead design was implemented to hold the pressure regulator in tension and thus in a stable configuration without the support of the foam and nose cone so that the propellant tank is supported by redundant systems to ensure a safe in-flight experiment. Also note that the regulator contains two burst discs — one protecting the regulator itself at 7.5 kpsi, and another protecting the outlet at 1.8 kpsi.

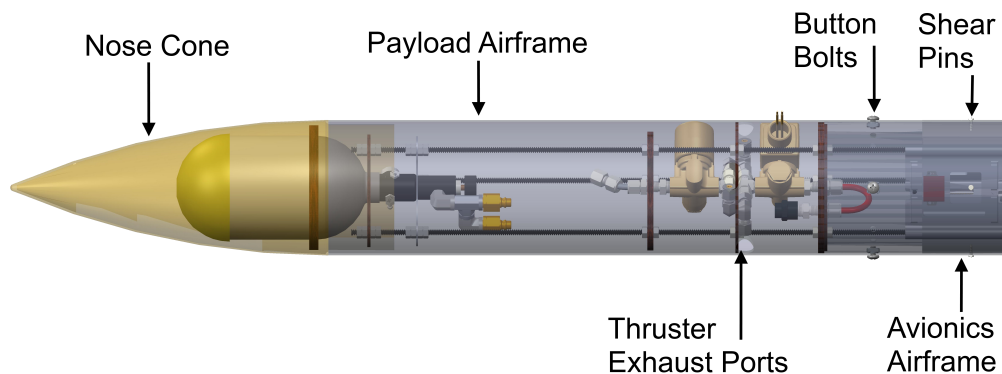


Figure 103: Payload Rocket Integration

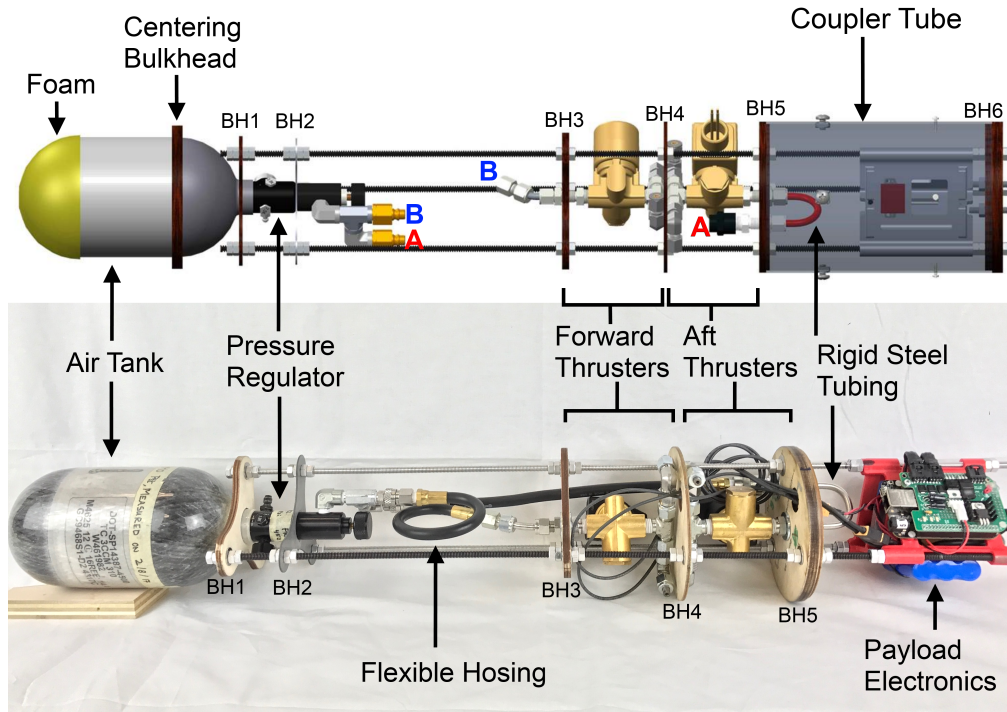


Figure 104: Payload Assembly

At the outlet of the regulator is a 1/8" NPT male to female elbow which attaches to an NPT pipe tee. From there, the propellant flow sees one of two routes depending on the active thruster couple. The control system ensure that only one route is open at a given time. See Figure 105 for the two propellant routes and the sequence of components and fittings employed. Also shown in Figure 105 is the factor of safety for and set operating pressure seen by each component.

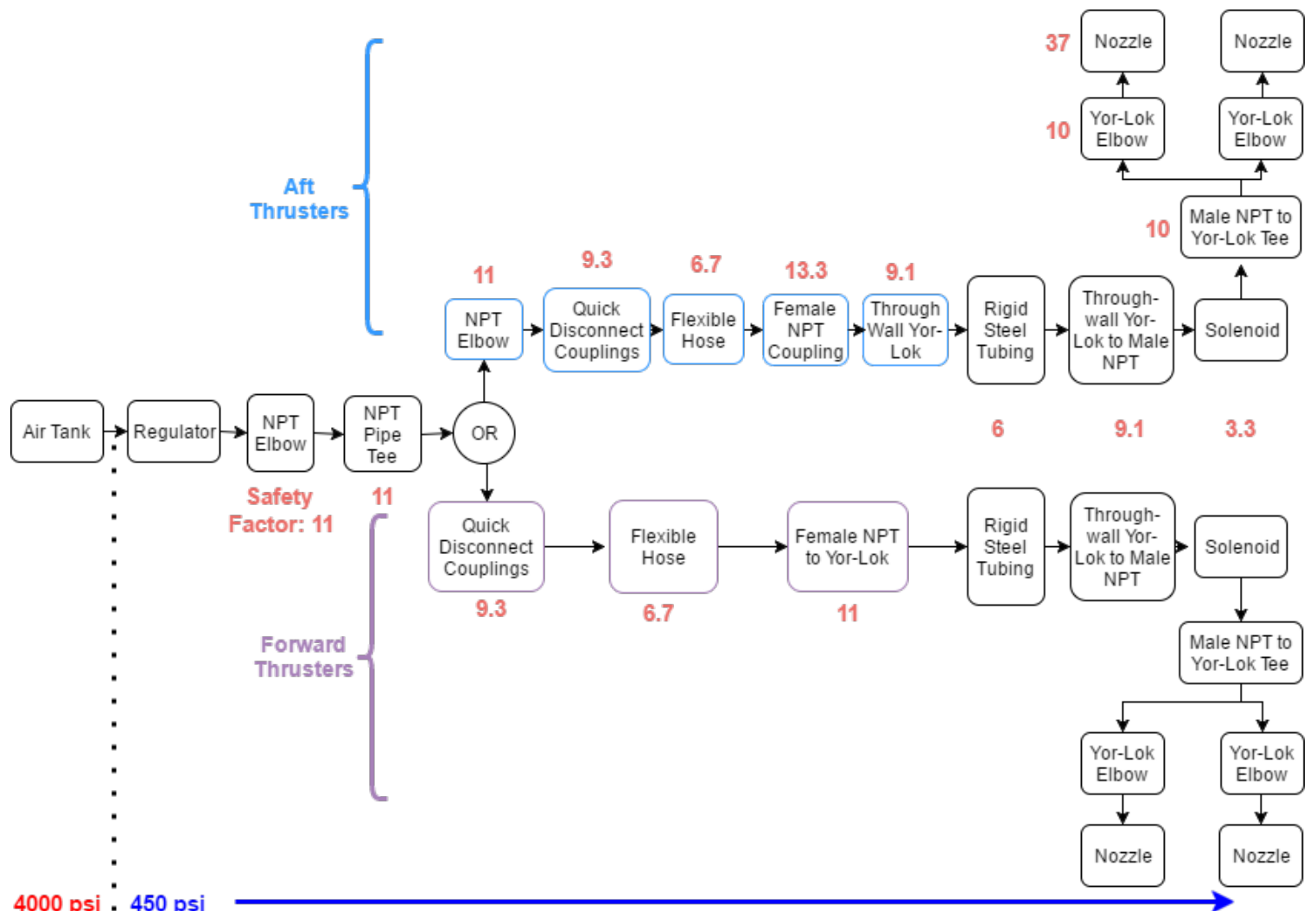


Figure 105: Payload Component Flowchart

Aft Thruster Couple For actuation of the aft thruster couple (between bulkheads 4 and 5), the flow exits the pipe tee into a male NPT to Quick Disconnect hose coupling (red A in Figure 104) and then into a flexible grease gun hose running through bulkheads 3 and 4 (BH3 and BH4, respectively). The hose is connected to a female NPT coupler and then into a through-wall Yor-Lok compression fitting adapter embedded in bulkhead 5, indicated by the red A (note that this bulkhead as well as bulkhead 6 consist of two pieces: an outer bulkhead and an inner centering bulkhead used to hold the coupler tube in place). The Yor-Lok based compression fitting design enables a modularity and interchangeability of components to the payload system as opposed to the rigidly welded thruster system in the 2015-2016 VADL project. From the Yor-Lok fitting, a section of smooth bore steel tube is bent into a "U", diverting the flow back through bulkhead 5 into a Yor-Lok to male NPT through-wall fitting and then into the solenoid. The pressure rating and bend radius limitations of this steel tubing were carefully analyzed to ensure a 4X factor of safety. The flow then passes through the open solenoid valve into a male NPT to Yor-Lok pipe tee fitting. The flow path then diverges into the two thrusters, which consist of a custom-machined converging-diverging steel nozzle held inside of a Yor-Lok elbow.

Forward Thruster Couple Actuation of the forward thruster couple (between bulkheads 3 and 4) is similar. An NPT elbow followed by Quick Disconnect coupling leads into flexible hosing, indicated by a blue B in Figure 104. The hose is then attached to a female NPT to Yor-Lok adapter. From the Yor-Lok, a bent section of steel tube takes the flow to a through-wall Yor-Lok to male NPT adapter at bulkhead 3. The bent steel tube is used to offset the fittings in order to prevent interference with the regulator knob, allowing minimal space to be used in this section. From the through-wall fitting, the flow enters the forward solenoid and exits into the atmosphere through a thruster couple identical to that of the aft thruster couple.

Note that every Yor-Lok to Yor-Lok interface contains a segment of smooth-bore steel tubing. All components' inner diameters are at least 1/8" in order to prevent any incident of choked flow (a minimum area of 0.084" is required).

Weight Cutting Measures The entire payload skeleton is held in place with one high strength steel fully threaded rod and two aluminum threaded rods. The change of two threaded rods from steel to aluminum (in addition to switching to aluminum nuts) was one measure that was taken to reduce the overall vehicle weight. Given team analysis and reference to prior year's use of these components in successful flights, we are confident that the aluminum components provide sufficient structural support and rigidity.

Another major measure taken to reduce weight occurred through redesigning several of the non-load-bearing bulkheads (no bulkheads receiving flight load were changed in material or geometry). Bulkheads 1, 2, and 3 were re-cut to the shape shown in Figure 106. Bulkheads 1 and 3 were reduced from 3/8" plywood to 1/4" while bulkhead 2 remained 0.05" high strength stainless steel. Bulkhead 4 was reduced to 1/8" plywood, and bulkhead 5 was reduced to a 1/4" bulkhead followed by a 1/8" centering bulkhead. Bulkhead 6 was untouched as it houses the drogue U-bolt, and is therefore load-bearing.



Figure 106: Bulkhead Redesign

4.1.5.1 Risk Mitigation

The entirety of the payload system is designed to accomplish the associated requirements with NASA's experimental objectives. Through isentropic analysis and precise testing of the thrusters, payload simulation through MATLAB, and rigorous testing both on the ground and in flight, VADL has verified its ability to not only induce at least two rotations about the vehicle roll axis but also control vehicle roll post motor burnout. By implementing two sets of thruster couples pointed in opposite directions, the payload will have the ability to induce a roll as well as halt that rotation through a counter-roll. The very nature of the payload as well as the vehicle design guarantees that this objective is accomplished through mechanical devices and not through some passive roll effect.

Since the thruster system uses a pressurized vessel, there is a need to meet the requirements that:

1. The system employ a solenoid pressure relief valve that sees the full pressure of the tank
 - In lieu of pressure relief valves, VADL has elected to use burst discs at regulator inlet and outlet (7.5 kpsi and 1.8 kpsi respectively). These single use pressure relief diaphragms will fully evacuate and vent the gaseous propellant into the atmosphere (through airframe venting holes built into the vehicle design) in the highly unlikely event of over-pressurization.
2. The full pedigree of the tank shall be described, including the application for which the tank was designed, and the history of the tank, including the number of pressure cycles put on the tank, by whom, and when.
 - The tank itself is a Ninja carbon fiber wrapped aluminum air tank (SKU 40668; see Figure 107) manufactured for paintball purposes (note that the intended usage would subject the tank to much more frequent impacts than it would experience in VADL's

payload). The tank has a specified minimum burst pressure of 13.5 kpsi. It was purchased in July 2016 solely for use in VADL's payload. Since then, a detailed log of every refill cycle has been kept.



Figure 107: Ninja Air Tank and Regulator

Another key requirement is that the minimum factor of safety (Burst or Ultimate pressure versus Max Expected Operating Pressure) shall be 4:1. With an operating pressure of 450 psi, the minimum pressure rating of any payload component that sees should be 1800 psi. As indicated in Table 10, all components exceed this baseline pressure except for the solenoid, which was selected due to electrical and sizing constraints. Detailed reasoning for this solenoid selection is described in the waiver attached in Appendix A.

Table 10: Payload Components and Pressure Ratings

Part	Supplier	P/N	Pressure Rating (psi)
Pressure Regulator	Custom Products	TANKREG	N/A
NPT Male to Female Reducing Adapter	McMaster	50925K511	5000
Quick Disconnect Socket	Foster	12FSS	4200
Quick Disconnect Plug	Foster	12MPS	4200
Through-wall Yor-Lok to NPT fitting	McMaster	5182K196	4100
Steel Pipe Tee	McMaster	50925K197	5000
Yor-Lok to Female NPT Fitting	McMaster	5929K45	4900
Yor-Lok to Male NPT Tee Fitting	McMaster	5929K105	4900
Yor-Lok Elbow Fitting	McMaster	5929K213	4900
Female-female NPT Pipe Coupling	McMaster	50925K211	6000
Flexible Hose	Nashville IR-G	N/A	3000
Steel Tubing	McMaster	9220K311	2700
Solenoid	Parker	73216BN2MT00	1500
Air Tank	Ninja	40668	4500

4.2 Precision Measurement

In most facets of engineering design and analysis, precision measurement plays a critical role. However, it is not always the degree of precision that is more important, but rather, the degree to which precision (and propagation of uncertainty) is known for a given instrument or system of instruments or related measurements. Herein these aspects will be examined and discussed in the context of the 2017 VADL USLI flight vehicle.

4.2.1 Measurement Devices and Propagation of Uncertainty

The 2017 VADL USLI design project entailed a widely varying array of measurements and measuring instruments in the design, fabrication, and testing of the flight vehicle and its subsystems. A summary of these measuring instruments and their associated precision and accuracy can be seen in Table 11.

Item	Model Name	Precision	Uncertainty
Digital Hanging Scale	Feedback Sports, Alpine Digital Scale	0.02 kg	± 0.01 kg
Digital Table Scale	Ohaus SD35	0.01 kg	Unknown
Caliper	Capri Tools CP20001 Platinum Series Fractional Digital Caliper	0.01 mm	±0.01 mm
Layout Rule	N/A	0.03125 in	±0.03125 in
Lathe	Republic Lagun RL Series	Crossfeed: 0.0001" Longitudinal: 0.0001"	±0.0003 inch
Knee Mill	Bridgeport Vertical Mill	x: 0.0001" y: 0.0001" z: 0.0001"	±0.0003 inch
Laser Cutter	Kern DHS100	.002"/ft	±0.0005"/ft
Compression Load Cell	Tinius Olsen 60K Super L	1 kN	Unknown
3D Printer	Stratasys Dimension 1200ES	X-axis: 600 dpi; Y-axis: 600 dpi; Z-axis: 1600 dpi	20-85 microns for features below 50 mm; up to 200 microns for full model size
Regulator outlet pressure	Ninja ProV2	50 PSI	Unknown
Regulator pressure gauge	Ninja ProV2	500 PSI	±250 psi
Testbed pressure transducer	Omega PX309 Series	1 bit	±0.25%
IMU angular position	VN-100 Rugged	0.01 °	±0.01°
IMU acceleration	VN-100 Rugged	.001 m/s^2	±0.001 m/s^2
Altimeter ADC	Stratologger CF	1 ft	±1 ft
Oscilloscope Input Impedance	Tektronix MSO 2024 Mixed Signal Oscilloscope	1 MΩ	±2%
Oscilloscope Input Impedance	Tektronix MSO 2024 Mixed Signal Oscilloscope	11.5 pF	±2 pF
Multimeter DC Volts	FLUKE 114	0.001 V	±0.5%
Multimeter Resistance (6 Ohms - 6000MOhms)	FLUKE 114	0.1 Ohms	±0.9%

Table 11: VADL Precision Measurement and Uncertainty Documentation

The chart shows metrics for uncertainty: the term uncertainty being key here. The term "error" is

often incorrectly interchanged with uncertainty. Measurements made with any form of instrumentation are not inherently "erroneous," but most definitely have an associated degree of uncertainty. Of note is that uncertainty can often exceed the smallest unit of measurement for a given instrument. That is, an instrument may be more precise than it is accurate. This matter will generally be of minimal consequence, and can often be belayed by proper calibration practices. Additionally, it must be noted that the importance of precision and accuracy for a given measurement must be evaluated before the method for measurement is decided upon: in practical engineering the requirement for accuracy and precision should always fall in line with the instrument selected.

The importance of precision in the 2017 VADL project is exemplified most clearly in the manufacture of custom nozzles used in the cold gas thruster system. Propagation of uncertainty becomes quite critical in machining of such a small nozzle: error of several thousandths invalidates the foundational equations used in the nozzle's design. A sample uncertainty propagation will be examined for the nozzle. The derived and simplified formulas used for error propagation can be seen in Table 12.

Operation	Form	Error Propagation Formula
Addition/Subtraction	$x = a + b - c$	$\sigma_x = \sqrt{\sigma_a^2 + \sigma_b^2 + \sigma_c^2}$
Multiplication/Division	$x = \frac{ab}{c}$	$\sigma_x = \sqrt{\left(\frac{\sigma_a}{a}\right)^2 + \left(\frac{\sigma_b}{b}\right)^2 + \left(\frac{\sigma_c}{c}\right)^2}$
Exponential	$x = a^z$	$\frac{\sigma_x}{x} = z \left(\frac{\sigma_a}{a}\right)$
Logarithmic	$x = \log(a)$	$\sigma_x = 0.434 \left(\frac{\sigma_a}{a}\right)$

Table 12: Simplified Error Propagation Formulas

Knowing that the nominal nozzle throat diameter is $D_t = 1.5 \text{ mm}$ and that the tools used in its boring were a high speed steel cutter of diameter $D_{cutter} = 1.5 \text{ mm} \pm 0.01 \text{ mm}$ and a vertical milling machine of ways accuracy $\pm 0.0001 \text{ in} (\pm 0.0025 \text{ mm})$, a propagation of uncertainty analysis may be completed.

Observing that herein the milling operation will be producing an arithmetically additive uncertainty, and referring back to 12, the first equation may be selected, and reformed to the context of this problem:

$$\sigma_{NET} = \sqrt{\sigma_{cutter}^2 + \sigma_{machine}^2} \quad (4.1)$$

Substituting known values and solving through, accounting for significant figures:

$$\sigma_{NET} = \sqrt{(\pm 0.01 \text{ mm})^2 + (\pm 0.0025 \text{ mm})^2} \quad (4.2)$$

$$\sigma_{NET} = \pm 0.01 \text{ mm} \quad (4.3)$$

Adding this to the initial measurement:

$$D_{t,actual} = 1.5 \text{ mm} \pm 0.01 \text{ mm} \quad (4.4)$$

If one were to propagate this uncertainty back through the initial gas equations used to calculate the thrust of nozzle using the methods proffered in 12, a total thrust uncertainty could be easily calculated. These design equations are presented in VADL's 2017 CDR and are summarized in Section 4.1.3.

4.2.2 Sampling Frequency

No discussion of precision in instrumentation is complete without mention of electrical signal sampling rate and possible aliasing due to Nyquist frequency conditions. Considering some theoretical, consistent sinusoid requisitioned for analysis, this sinusoid must be sampled at some minimum frequency in order to maintain fidelity of the ensuing discrete sample to the original waveform. This minimum frequency is known as the Nyquist frequency, which is expressed mathematically in Equation 4.5 below.

$$f_{Nyq} = \frac{f_s}{2} = \frac{1}{2\Delta t} \quad (4.5)$$

When the Nyquist frequency is less than the sampling frequency, a condition known as aliasing occurs in which a less than representative waveform is sampled. In extreme cases this can lead to a condition known as phase ambiguity as seen in Figure 108 for the condition $2f > f_s > f$.

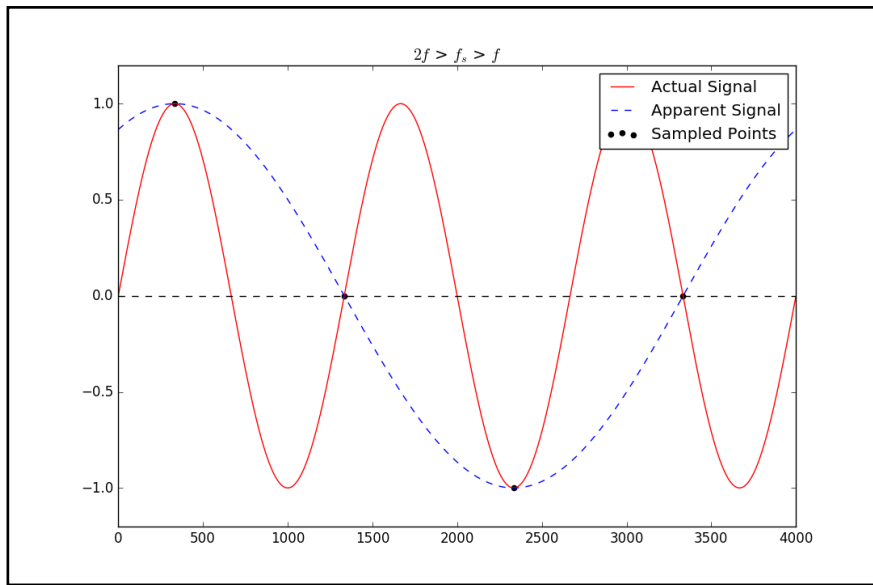


Figure 108: Nyquist Frequency: Phase Ambiguity

This discussion is important when considering the interplay of the various components mentioned in Table 13. Taking, for example, the interaction of the VN-100 IMU and the ROSMOD software that samples this resource: the IMU refreshes its quaternion data at a rate of 800 Hz and ROSMOD samples this data at a rate of 50 Hz. Here it can be seen that if the IMU data was

rapidly changing in a relatively sinusoidal fashion, a sampling frequency of over 1600 Hz would be required. However, with a healthy share of caution, the sampling criteria here may be reasoned through. The rate of change of the flight vehicle's motion will never exceed the sampling condition of 50 Hz. For example, the angular velocity of the flight vehicle would never exceed 25 full oscillations per second during ascent, and this condition (essentially 25 Hz) would represent the Nyquist frequency properly matched to a 50 Hz sampling rate. Similar assumptions can be reasoned through for the flight vehicle's other axes of motion. Summarily it should be noted that in general the Nyquist frequency of a critical signal should be taken into consideration, but in situations where that frequency might exceed the necessary sampling rate and would unnecessarily tax a processor, sampling rate may be modified with caution and knowledge of associated conditions.

Item	Model Name	Rate
IMU Data Out (Serial)	VN-100 Rugged	1 MBps (max)
IMU Sensor Sampling Rate	VN-100 Rugged	800 Hz
Software IMU Sampling Rate	ROSMOD	50 Hz
Microprocessor Baud Rate	BeagleBone Black	115200 Baud (11.52 kBps)
Oscilloscope Maximum Sample Rate	Tektronix MSO 2024 Mixed Signal Oscilloscope	500 MHz
Altimeter Sampling Rate	Stratologger CF	20 Hz

Table 13: VADL Data Rate Documentation

4.3 Payload Electronics

4.3.1 System Level Design

The electrical system aboard VADL's full scale rocket will be composed of several main components:

1. two solenoid valves,
2. a microprocessor,
3. an external circuit board,
4. two Li-Ion batteries,
5. and a mounting sled.

The system schematic (Figure 109) indicates signal paths through each component. The physical layout of the system is shown in Figure 110. Although wires have not been included in this depiction, they are a very important design factor for this project, as the payload electronics is confined between two bulkheads. Cables have been routed through the internal cavity of the mounting sleds, with each component connected appropriately using 14-26AWG insulated wire and heavy-duty drone connectors. Each component is be analyzed more thoroughly with respect to design justification, requirements, and safety below.

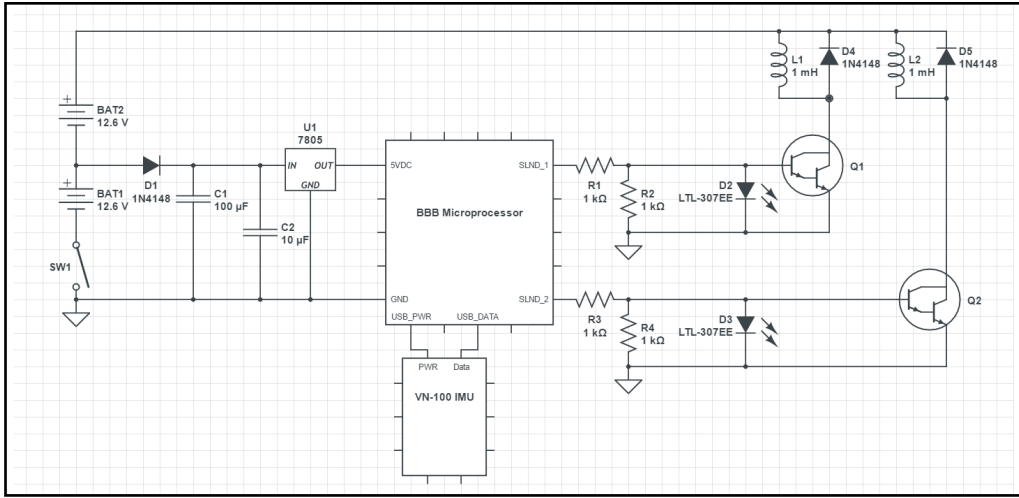
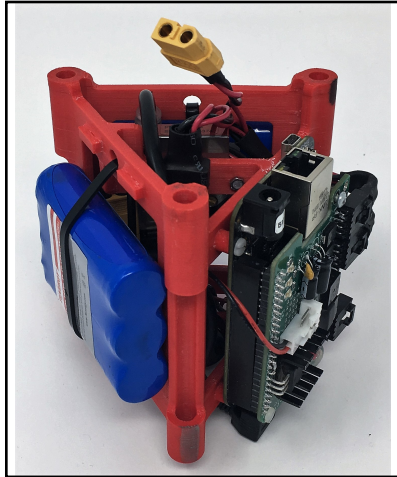
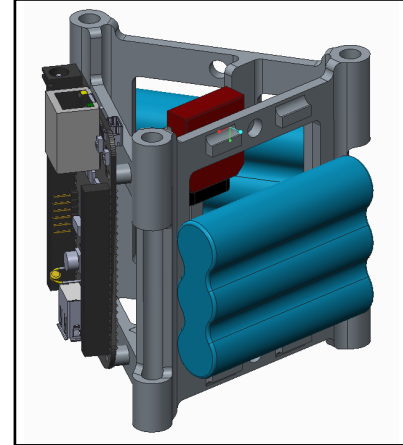


Figure 109: Payload Electronics Schematic



(a) Payload Electronics Assembly



(b) Payload Electronics Assembly (CAD Render)

Figure 110: Physical and CAD Assemblies of Payload Electronics Bay

4.3.2 Electronics - Component Detail

4.3.2.1 Solenoid Valves

Because the thrusters are pneumatically actuated, VADL's payload will be using two normally-closed solenoid valves to control the flow of gas through two pairs of axisymmetric tangential thrusters. These solenoid valves require approximately 0.75A at 24V for operation, already placing a major power requirement on the payload electronics. Solenoids also cause flyback, a large voltage spike that occurs when the solenoid's supply current is sharply reduced or cut off. A flyback diode placed in parallel with the solenoid allows the solenoid's inductive load to discharge safely when supply current is removed.

4.3.2.2 Microprocessor

The payload microprocessor is BeagleBoard's BeagleBone Black Wireless (BBB), a single-board computer equipped with a native Linux operating system. This particular microprocessor was chosen for its integrated wi-fi module, its large number of I/O ports, its compact size (85 x 50mm - slightly larger than a credit card), and because it has been used in the past for VADL projects.

The BeagleBone Black Wireless is the newest board in the BeagleBone family that replaces the 10/100 Ethernet port with onboard 802.11 b/g/n 2.4GHz Wi-Fi. It has a Texas Instruments WL1835MODGMOCT module and is an open source board utilizing Cadsoft EAGLE.

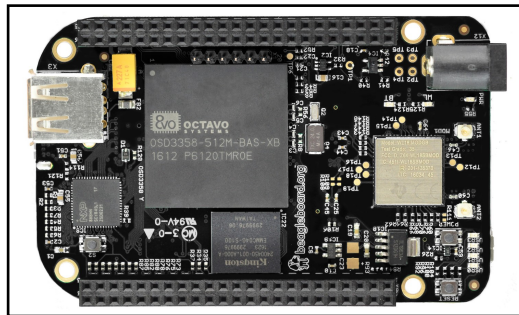


Figure 111: BeagleBone Black Wireless Single Board Computer

The microprocessor requires a power supply capable of delivering a maximum of 2A at 5V, but draws 0.4A on startup, and settles to 0.25A idle. Since the solenoids require 24V for operation, a separate 5V circuit must be regulated from a higher voltage source, using a linear voltage regulator. An arming switch connects the power supply ground node to the BeagleBone's ground node, and can be activated from outside the rocket after full assembly. During testing and launch procedures, the payload electronics bay is physically inaccessible, with the exception of this switch. Therefore, the BBB's integrated wi-fi module is an important design feature, because it allows for wireless communication between the microprocessor and ROSMOD's host servers, which are critical for fast deployment of software, experiments, and launch initialization. However, it is important to consider the reliability and safety of wireless communication. In the case of wireless communication malfunctions, hard-wired connections will be available during testing and launch, by way of a USB cable fed through clearance holes in payload bulkheads.

4.3.2.3 Auxiliary Circuit Board

An auxiliary circuit board is necessary for routing power and signals to and from the microprocessor. This circuit board was designed using Eagle Lite 7.6.0, and was sent to Advanced Circuits for fabrication, as prompted by reliability issues with earlier prototypes made in-house. Components used in the auxiliary circuit board are rated above the voltage and current levels seen during normal operation. The board was assembled with these components in house using a soldering station equipped with an infrared heating table, soldering iron, heat gun, solder and soldering paste. See Eagle layout (Figure 112), schematics (Figures 113a - 115), and bill of materials (Figure 116).

In response to the payload actuation anomaly that occurred during the full scale flight, unnecessary failure points will be removed from the circuitry, and several high impedance voltage sensors will be used to monitor and log the status of several signals, like the solenoids' driving current. These are not yet included in the layout (Figure 112) displayed, but will improve experiment integrity while not significantly altering the function of the circuit described below.

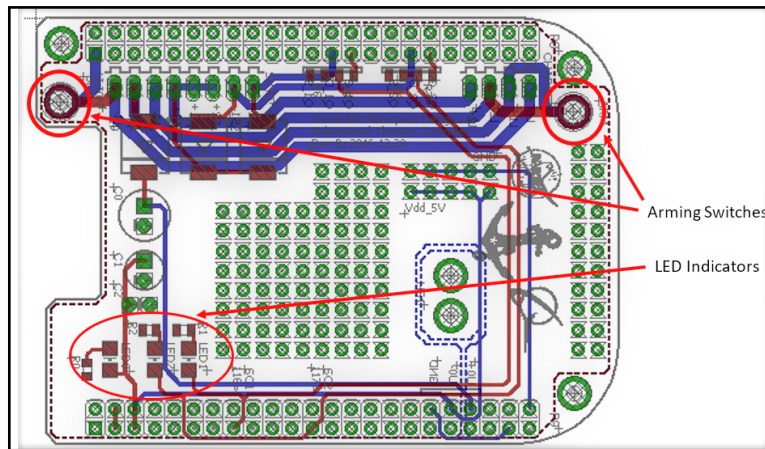
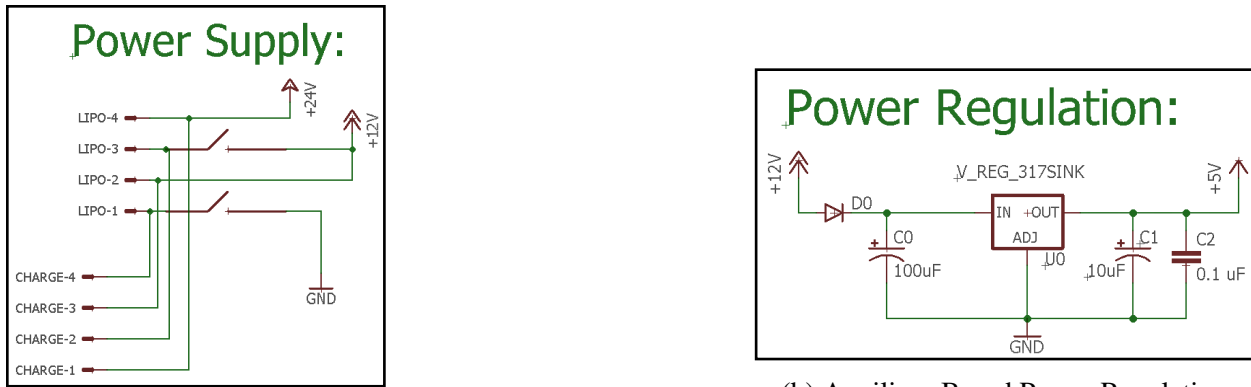


Figure 112: Auxiliary Circuit Board Layout

In the circuit (Figure 113a) below, LIPO1 - LIPO4 represent the four leads of the two batteries connecting to the board through a locking Molex connector. CHARGE1 - CHARGE4 represent the four leads that connect from a separate Molex connector on the board to the batteries' recharging circuit. Note the two switches that connect each battery's connection to ground. These are set-screw switches, and both must be closed to fully arm the payload. GND connects to the BeagleBone's ground node.

The circuit below (Figure 113b) ensures that the BeagleBone Black is connected to an appropriate 5V filtered voltage source. Capacitors provide power filtering, and a linear voltage regulator steps the voltage from 12.6V to 5V, dissipating power as thermal energy through a heatsink.



(a) Auxiliary Board Power Supply

(b) Auxiliary Board Power Regulation

Figure 113: Auxiliary Board Main Power Circuitry

This circuit (Figure 114) uses power transistors switched by 3.3V digital logic signals from the BeagleBone Black to allow current to flow from the batteries to a particular solenoid. SLND1-4 are the four leads of the two solenoids. Note the flyback diodes across the leads, which allow the solenoids to discharge safely after a sudden loss of driving current. The 24V node is connected to the output of the series connected batteries. Large pull down resistors prevent leakage current, and hold the gate at 0V.

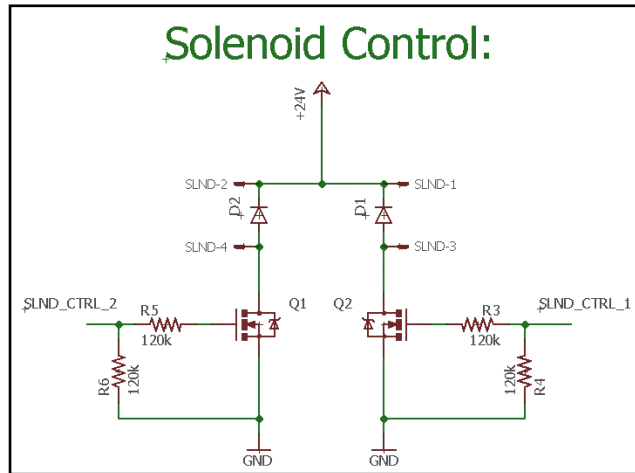


Figure 114: Auxiliary Board Solenoid Control

In Figure 115 below, LED0 indicates 5V Power. LED1 and LED2 indicate solenoid actuation. These LEDs are useful during electronics testing, by visibly indicating the presence of a digital signal.

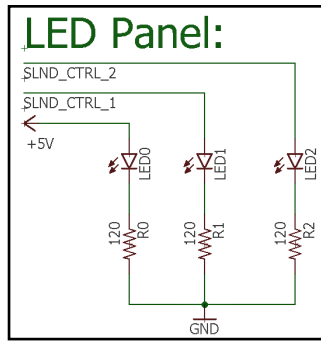


Figure 115: Auxiliary Board LED Indicators

Part Name	Manufacture	Description	Ratings/Value
LIPO, SLND	Molex	4 pin Connector @ PCB (Male) w contacts	24 AWG
LIPO, SLND	Molex	4 pin Connector @ PCB (Female)	24 AWG
D0, D1, D2	Vishay Semiconductor	Diode (smd)	3A, 600V
LED0, LED1, LED2	Lite-On, Inc.	LED (1206 smd, amber)	30mA
R0	Yageo	Resistor (0805 smd) - part of smd kit	200 Ω
R1, R2	Yageo	Resistor (0805 smd) - part of smd kit	120 Ω
R3, R4, R5, R6	Yageo	Resistor (0805 smd) - part of smd kit	120 kΩ
Q1, Q2	Fairchild Semiconductor	N-Channel MOSFET (through-hole)	60V, 32A
U0	STMicroelectronics	5V Regulator (through hole)	3A
C0	-	Polarized capacitor (through hole) - part of kit	100uF, 25V
C1	-	Polarized capacitor (through hole) - part of kit	10uF, 25V
C2	-	Ceramic capacitor (through hole) - part of kit	0.1uF, 50V
HS0	Aavid Thermalloy	T0-220 Heat Sink	2.5W @ 60C

Figure 116: Auxiliary Circuit Board Bill of Materials

The board features two integrated safety switches (highlighted in Figure 112), designed to control power flow to the microprocessor and the solenoid valves, respectively. They are simple set-screw switches, closed by tightening a screw into a nut soldered on the reverse side of the board. Once the screw head is in contact with the top surface of the board it will act as a via, connecting the switch contacts on either side of the board. Threads on the end of the screw are fouled once inserted into the nut to prevent the screw from falling out.

To improve full scale flight reliability, the series-connected switch that arms the solenoid valves may be removed. The function of the second switch will then be performed by the single remaining switch, since they are simply connected in series. These switches will also be re-constructed using more electrically conductive hardware, and a wider solder pad on both the top and bottom of the board. A redundant copy of the remaining switch may also be added to the circuit.

The board also features an integrated charging port, so that the power supply can be recharged without detaching it from the board. Each battery is charged separately on the manufacturer's charging circuit. The screw switches must be open during charging to ensure proper current flow

from the charger to the batteries. Because the second screw switch is in the current path of the solenoids, it represents a point of failure and may be eliminated due to the anomaly experience during VADL's first full scale test launch. If it is removed, batteries may be charged by opening the payload electronics bay and disconnecting the battery connector from the auxiliary board.

Another part of the auxiliary board is the voltage regulator. Overheating was one of the major problems with early subscale prototypes, causing microprocessor power failures. The linear voltage regulator on the board was attempting to step 15V down to 5V, which requires significant heat dissipation. If linear voltage regulators are not properly cooled, resistances inside the regulator will increase, generating even more heat, and reducing the output voltage. The regulator's thermal protection logic then momentarily forces the regulator to terminate power throughput, causing anything downstream to lose power.

There are three indicator LEDs on the external circuit board. LED0 indicates 5V power to the BBB. LED1 and LED2 indicate actuation of its corresponding solenoid. Each indicator draws approximately 20mA. However, the power draw of LED1 and LED2 is negligible, due to the low current consumption and extremely short duty cycle.

4.3.2.4 Inertial Measurement Unit

VADL has chosen the VectorNav VN-100 IMU for onboard sensing (Figure 118). This package exceeds all of the requirements in the payload requirements section. It provides real-time data in nine axes using a 3-axis gyroscope, 3-axis magnetometer, and 3-axis accelerometer. The VN-100 has a built-in Kalman filter, which provides quaternion-based (gimbal-lock free) data in each axis at up to 300 Hz.

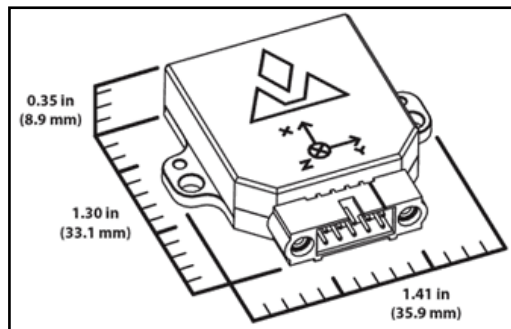


Figure 117: Dimensions of VN-100 IMU

4.3.2.5 Power Supply

The payload's power supply must provide at least 24V to operate the solenoid valves. Since batteries must be secured to the rocket, it would be best if they could be attached once and recharged as needed, rather than having to replace or remove a dead battery. 9V batteries, have

fairly short lifetimes, around 600mAh. Since the BeagleBone Black, LEDs, and IMU pull 0.6A (worst-case) during steady-state operation, these batteries would last about an hour in the armed state.

To solve these issues, two 11.1V (nominal) Li-Ion batteries, connected in series, to power the solenoids. Although large - each battery measures 70 x 55 x 18mm, and weighs 120g -these batteries are rechargeable. They are manufactured by Tenergy, have a capacity of 2200mAh, and are rated for a charge/discharge rate of up to 5A. Since the BeagleBone Black, LEDs, and IMU pull 0.6A (worst-case) during steady-state operation, the rocket, powered with these batteries, can be expected to power cycle at a little less than 4 hours. However, the solenoids require a large amount of power for operation, so the rocket should be launched within three hours of arming to prevent an airborne power failure. Together with the integrated charging port, the entire payload can now be assembled once and recharged as a unit, rather than requiring a full disassembly of the rocket for recharging.



Figure 118: Tenergy Rechargeable Li-Ion Battery (11.1V, 2200 mAh)

Large voltage sources present overheating issues for the the payload computer's voltage regulator, however. It is connected to the power source so that it sees the voltage across only one battery, instead of both. This prevents the voltage regulator from seeing the full series-connected voltage (25.2 V), which would result in significantly increased heat generation. The heat sinking requirements that arise from this problem are detailed further in 4.3.2.3. Each battery is connected to the circuit board via low-profile locking connectors, and armed using safety switches highlighted in 112.

4.3.2.6 Mounting Sled

VADL designed an innovative mounting sled for the payload electronics, pictured below. It features a triangular shape, and an inner shelf, which allows the IMU to be mounted directly on the launch vehicle's longitudinal axis. Without this particular placement, roll data would be much more difficult to interpret. Wires are routed through the inner cavity of the sled, preventing accidental shorts during assembly. Batteries will be held in firm compression to the sides of the sled using zip-ties. The microprocessor will be secured to the sled with 4-40 nylon screws.

This sled is made from ABS plastic a 3-D printer. Batteries pictured are 9V alkaline, but the actual power supply will consist of two Li-ion batteries, with one secured to each unoccupied face of the sled. The IMU is pictured in red on the center face of the sled. The sled will also feature cut outs for routing wires from the inside to the outsides of the triangular prism.

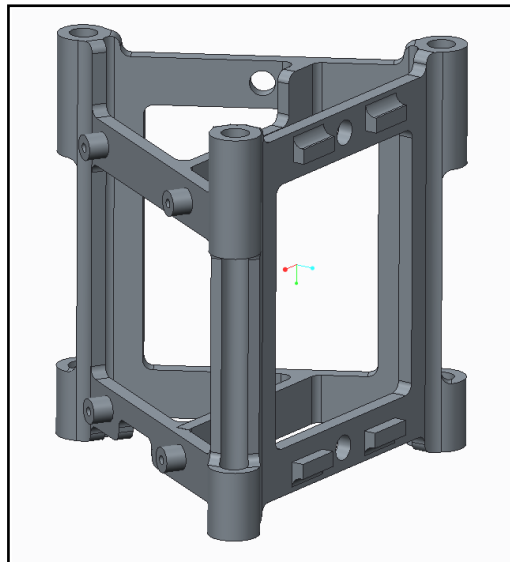


Figure 119: Payload Electronics Mounting Sled

4.4 Control Schemes

The goals of the fullscale flight were the successful actuation of the thruster system, IMU data collection, further characterization of the system response, and verification of the Bang-Bang control system. This section outlines the control system flown during the fullscale launch, the takeaways from the results, and the future tests and adjustments the team intends to make.

4.4.1 Fullscale Control System

The team flew a Bang-Bang control system during the fullscale launch. The system sensed the angular velocity defined at MECO +2 seconds and actuated the thrusters in that same direction. The system then waited until the rocket rotated 720° before firing the counter thrusters. This ensures that the rocket achieve the full rotation, which is the main requirement of the team's payload system. The next goal of the control system is to hold the rocket at this position for the duration of the flight, before releasing the rocket to natural roll prior to apogee. It accomplishes this using another Bang-Bang system. If the rocket is passed the setpoint, the counter-roll thrusters fire, and if it then returns past the setpoint, the roll thrusters fire. There was a $\pm 5^\circ$ threshold built in to this control code to allow the rocket to come to rest in this range. A MATLAB simulation was run showing the predicted results of this control system (Figure 120).

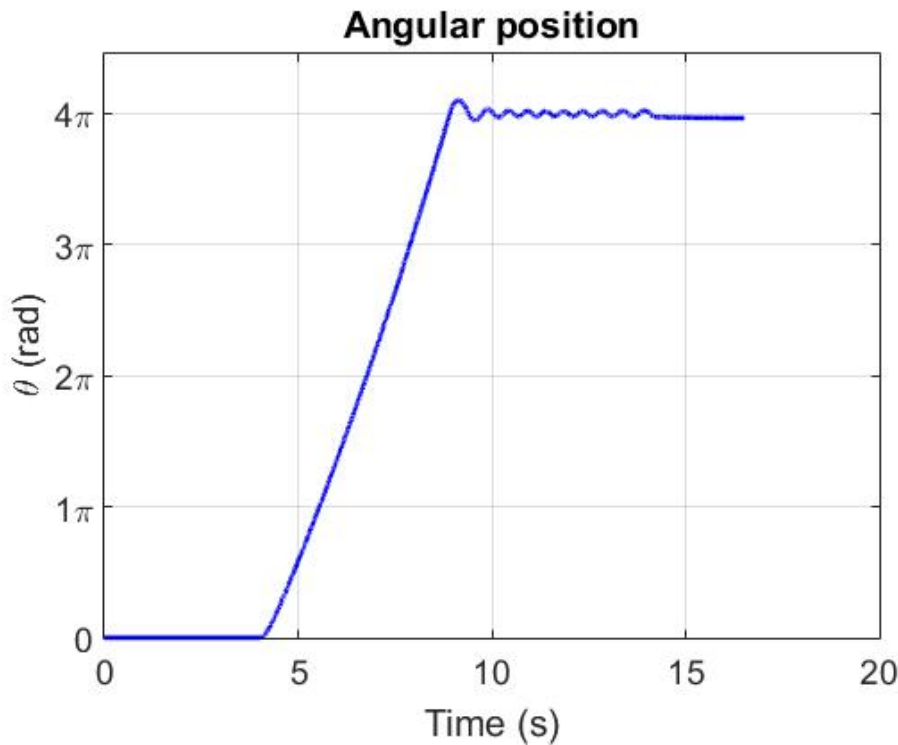


Figure 120: Simulated Bang-Bang Control With Oscillation

Due to the failure to actuate the roll-inducing thrusters during the fullscale launch, the team was unable to observe this oscillation, however due to the natural roll of the rocket, we were able to verify the logic. The logic system sensed the angular velocity at MECO, actuated the thrusters in this direction, sensed when the 720° threshold was reached, noticed it was within the $\pm 5^\circ$ threshold, and turned off both thrusters. When the rocket began to rotate in the opposite direction and the angular position fell below the setpoint, the roll thrusters were actuated again to return it to the set point. More information on these results can be found in Section 3.8.

4.4.2 Future Control System Improvements

The control system has been under constant testing and improvement since the start of this project and this will continue until the competition launch. The current control system has the goal of inducing 4π radians of roll and then maintaining this position until just prior to apogee before releasing the rocket to its natural roll. This system allows for a certain amount of overshoot, and has a settling time that increases as the rocket slows down. The team intends to perform the roll experiment as late in the flight as possible as to conserve air in the tank and minimize the effects of the resistive damping from axial flow. This means that when the rocket is intending to settle at its final position, it may see a lot of oscillation about the setpoint. In addition, a wind gust that rotates the rocket a significant amount would force the control system to fire the thrusters until the rocket returns to the setpoint. This would waste precious air and increase the oscillation if the rocket were to return to the setpoint. For this reason the team has made modifications to the Bang-Bang control system in an attempt to eliminate some of these sources of error.

Table 14: Comparison of Control Schemes

	Position-Based Control	Omega-Based Control
Rise-Time	Thrusters will be on until rotation setpoint is reached	Thrusters will be on until rotation setpoint is reached
Overshoot	Dependent on strength of counter thrusters	Dependent on strength of counter thrusters
Settling-Time	Increases as axial flow decreases	Dependent on strength of counter thrusters
Steady-State Error	No steady-state error	Dependent on strength of counter thrusters
Oscillation	Increases as axial flow decreases	Minimal
Response to Disturbances	Attempts to return to rotation setpoint	Resists disturbance until zero angular velocity achieved

The newest iteration of the Bang-Bang control system has the goal of inducing 4π radians of rotation, then bringing the rocket to a stop and maintaining a constant zero angular velocity for the rest of the flight. This control system allows for overshoot and steady-state error, however minimizes settling time and nearly eliminates oscillation. In addition, the system does not attempt to return the rocket to any specific position, and merely reacts to disturbances by firing the opposing thrusters until the angular velocity returns to zero. Table 14 compares various characteristics of the two control systems.

Both control systems have been tested on the FRAME under the same conditions and their results are shown in Figure 121.

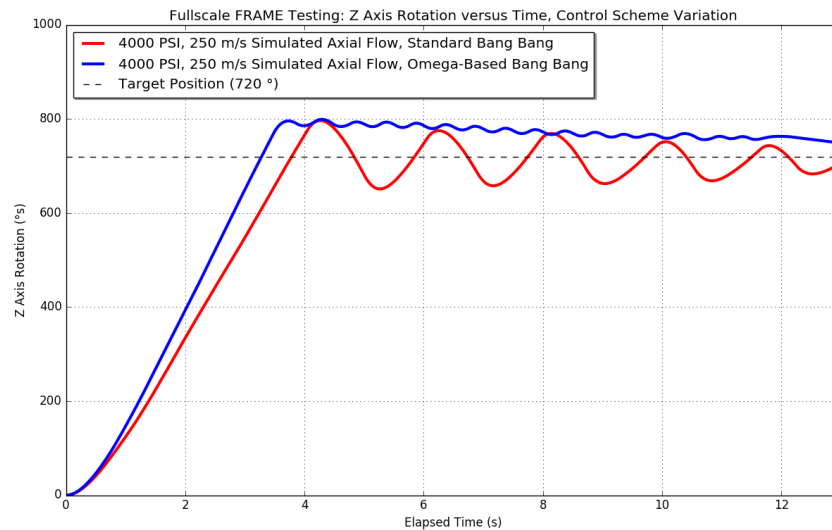


Figure 121: Comparison of Various Control Schemes

This figure clearly demonstrates the characteristics outlined in Table 14. Both systems have a

rise-time of 3-4 seconds and an overshoot of about 80° . The omega-based control settles at this overshoot value, whereas the position-based control never settles. The position-based control system has no steady-state error, whereas the omega-based control has about 80° of error. The omega-based control reduces the oscillation to a few degrees, whereas the position-based control has an oscillation of around 60° . Further FRAME tests will attempt to challenge the control systems and verify their performance under intense and random disturbances.

4.5 Payload Software

The flight software is defined by the interfaces and the controls. The interfaces are the components that interact with the environment. They can be sensors, such as the inertial measurement unit (IMU), or actuators, such as the solenoid actuators. The controls take inputs from the sensors and decide how to control the actuators. VADL uses a software modeling and execution framework called ROSMOD. All of the software is written, compiled, and executed using this environment, which uses C++ as its programming language. ROSMOD is an excellent way to visualize the communication between components in a software integrated system. Figure 122 shows a high-level diagram of the components in the VADL full scale software system and how they communicate with each other. Each component in Figure 122 is modeled individually in ROSMOD, and they communicate with each other via messages to which they can either publish or subscribe, which allows the software as a whole to be both modular and configurable. ROSMOD also allows for easy organization of components, as the sensor and actuator are within an Interfaces folder within the ROSMOD project, and the High-Level Controller (HLC) and Bang-Bang controller are in a Controls folder. As mentioned, each component can stand on its own, and thus the roles for each component can be discussed separately. The four ROSMOD components in the full scale software as listed in Figure 122 are the following:

1. VN-100 IMU
2. High-Level Controller
3. Bang-Bang Controller
4. Solenoid Actuator

VN-100 IMU The VN-100 IMU is the primary on-board sensor for the rocket. During flight, it has the following three primary functions.

1. Sense MECO and original natural roll
2. Sense when two rotations have been achieved
3. Sense velocity to match natural roll after experiment

The first function of the IMU during flight is to sense MECO. It does this using its accelerometer, as the rocket's acceleration goes from 16gs during motor burn to freefall. At this time, the IMU will sense the original natural rotation of the rocket, which serves two purposes. First, it is desired

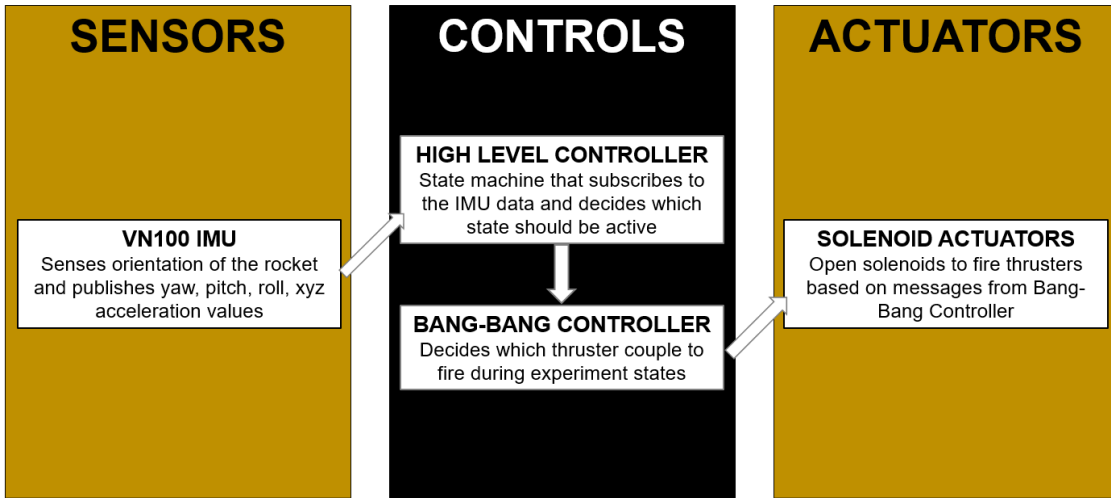


Figure 122: High Level Diagram of Flight Software

to not have to oppose the natural roll when inducing rotation, so depending on which direction the rocket starts to naturally rotate, the control system will fire the corresponding thruster couple. Secondly, after the experiment has been completed and two rolls have been achieved, the rocket shall return to its original pre-experiment angular velocity for the remainder of the ascent. The IMU must then be reporting real-time accurate information for vertical acceleration, angular position, and angular velocity. It does this via a timer built into this component in ROSMOD that publishes acceleration, orientation, and velocity messages at 50 Hz, which are read by a subscriber in the HLC.

High-Level Controller (HLC) The HLC is perhaps the most important component in the software system. It is a state machine that reads messages 40 times a second that are constantly outputted by the IMU and makes a decision as to what state the rocket should be in. Each state has a corresponding operations with respect to thruster activation. The states that the rocket goes through during flight are the following.

1. INITIALIZATION
2. LAUNCH PAD
3. TAKEOFF
4. UP-ROLL
5. DOWN-ROLL
6. MATCH VELOCITY
7. POST-EXPERIMENT

The **INITIALIZATION** state verifies proper power up of the hardware and then sets the current state to **LAUNCH PAD**. The **LAUNCH PAD** state contains a conditional statement that sets the

current state to **TAKEOFF** when the z acceleration surpasses 1 g of acceleration. The takeoff acceleration is about 16 gs so this is a reliable threshold to signal takeoff. The **TAKEOFF** state contains a conditional statement that leaves the state when the z acceleration becomes negative. After MECO the only forces will be gravity and drag which will cause the acceleration to be about -1.2 times the acceleration of gravity, so 0 is a reliable threshold. At this point, the HLC needs to decide whether to enter **UP-ROLL** or **DOWN-ROLL** depending on the direction of the natural roll. These two states are identical in function except for that they correspond to different thruster couples. Only one of these states will actually run during the experiment and the other will be skipped. This state switch also defines a variable *beginTime* which will be compared to the current time to know long it has been since the start of the experiment. If the elapsed time at any point exceeds the experiment window, then the rocket will automatically enter the **POST-EXPERIMENT** state, which turns off all thrusters so that they will not fire after apogee. The **UP-ROLL** or **DOWN-ROLL** states will fire their respective thruster couples until two full rotations have been achieved. Once this happens, the HLC will progress to the **MATCH VELOCITY** state, which will first fire the counter thrusters until rotation is halted and then fire whichever thrusters necessary to hold angular velocity through apogee. It achieves this by setting a threshold on the difference between actual and desired angular velocity. If this difference exceeds 5 degrees per second, then the HLC will fire the thrusters necessary to return to desired angular velocity. After the elapsed time defined at the start of the experiment exceeds the experimental window, the HLC will progress to the **POST-EXPERIMENT** state, where all thrusters are deactivated for the remainder of the flight. Figure 123 shows a flow chart of how the HLC changes states over the course of the flight.

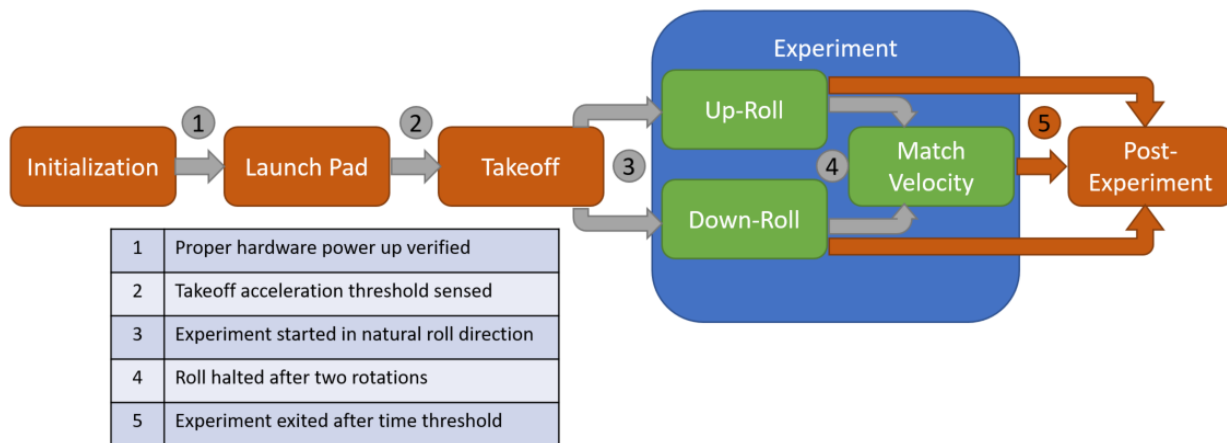


Figure 123: High Level Controller Flow Chart

Bang-Bang Controller The Bang-Bang Controller is the component that listens to messages published by the HLC and decides how to activate the thrusters by opening the solenoids. PID control was previously considered for this controller, but after the original subscale launch, it was determined that due to high resistive torque due at high rocket speeds, it was not necessary to have a more complicated control scheme that fires thrusters at different powers. Bang-bang control simply decides whether the thrusters should be turned on or off and

then fires the thrusters consistently until the HLC message changes.

Solenoid Actuator The solenoid actuator is the simplest of all components in the software. It simply receives a message from the Bang-Bang Controller to either open or close the solenoids.

5 Safety

5.1 Team Safety Structure

The Vanderbilt SL rocketry team takes individual, group, and project safety seriously. The team is continuing to follow ideologies implemented in past years to establish a functional set of safety protocols and to foster safety-focused growth of the VADL members. The team's safety hierarchy is graphically depicted in Figure 124.

The top level consists of both the Safety Administration and the Safety Documents. Four individuals are responsible for management of the safety materials and maintain the authority to make substantive changes to the protocols and safety documentation as needed. In addition, they are vested with the power to make go and no-go decisions for the team when new processes or procedures are required. The Safety Administration consists of the following people: Robin Midgett (Safety Mentor), Paul Register (Student Safety Officer), Dexter Watkins (Assistant Safety Officer), and Ben Gasser (Assistant Safety Officer). Robin is a member of the National Association of Rocketry and holds NAR Level 2 certification. Paul is a senior undergraduate student in Chemical Engineering and Physics; he will oversee the rocketry team to ensure safety precautions are taken during the design, construction and testing of all rocket materials and equipment (see Section 5.2). In this, he will also be assisted by Dexter Watkins (NAR Level 1), a graduate student in Mechanical Engineering and a five-year veteran of the Student Launch program, and Ben Gasser, the 2015-2016 Student Safety Officer. These four individuals will be informed by and will enforce the Safety Documents.

At the core of the construction and launch procedures will be a Team Operating Unit (TOU). This is a subset of the team who have been assigned a specific task (by leadership, their peers, or via volunteering) to be accomplished. For the purpose of safety and accountability, this group will never consist of less than two individuals. All TOUs are informed by the Safety Administration and Safety Documents and are expected to pause prior to beginning any task to ask a few basic questions outlined in Figure 124. First, does a protocol exist? If yes, follow it and give feedback for future improvement. If there is no protocol, does the task contain significant hazards to either person or property? If yes, write a protocol and obtain approval prior to execution of the task. For tasks with no significant hazards, it is permissible for the members of the TOU to write a safety plan and then execute the task without administration approval, provided that the members of the TOU have appropriate training with directly applicable skills. Furthermore, the TOU must generate a report following completion of the task that includes the safety plan and the members' relevant skills and training.

This team structure offers a significant safety net while also encouraging safety-oriented thinking in each individual. In addition, the common objective of safety fosters team unity, creative thinking, and problem solving skills that will promote individual and team success throughout both the Student Launch competition and in students' future careers.

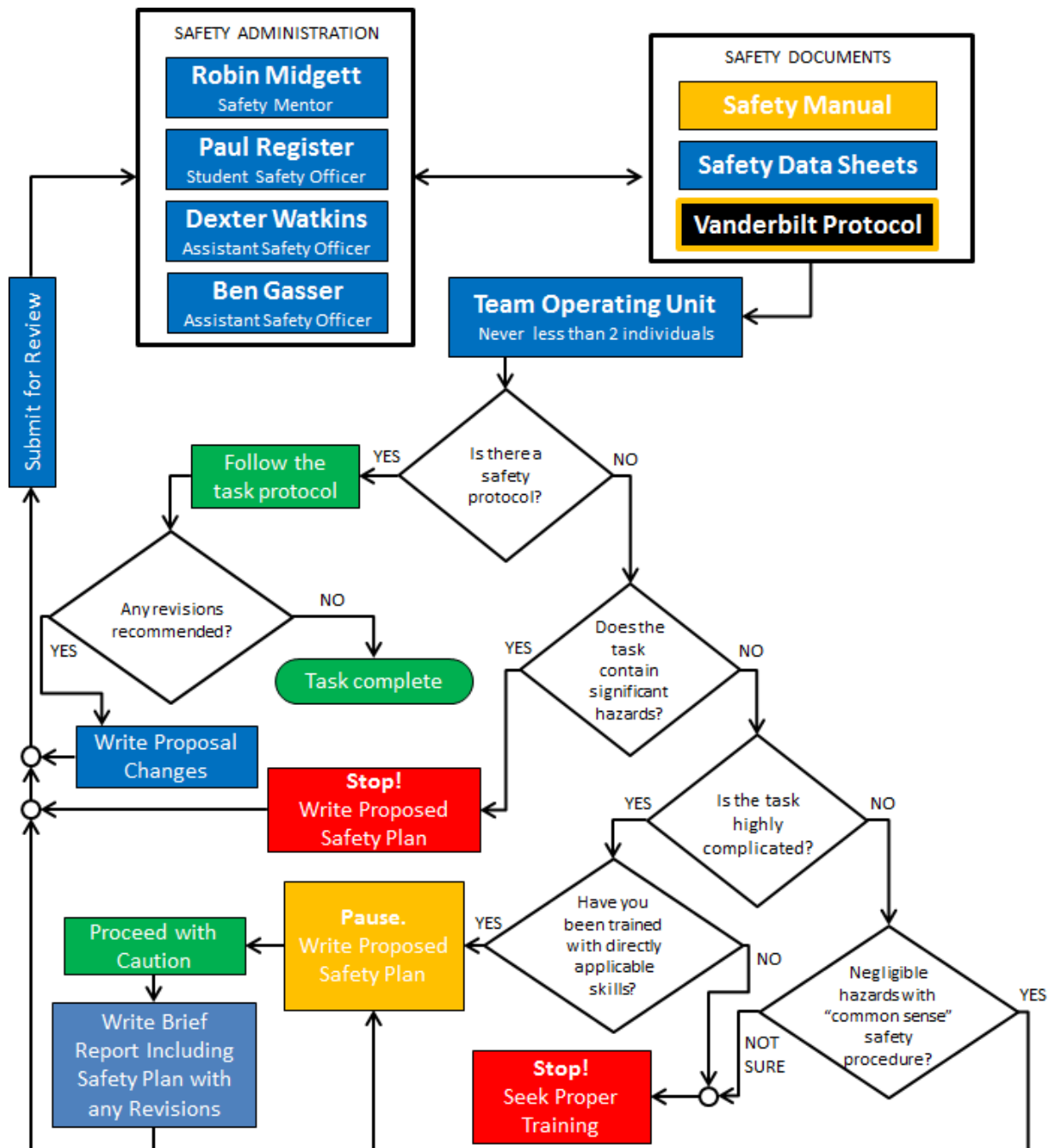


Figure 124: Vanderbilt Aerospace Design Laboratory Safety Protocol

5.2 Student Safety Officer

Paul has been designated as the Student Safety Officer. He will oversee the overall safety and launch procedures of the team and will work to fulfill the requirements listed in the SL Handbook:

- Monitor team activities with an emphasis on Safety during:
Design of vehicle and launcher

Construction of vehicle and launcher
Assembly of vehicle and launcher
Ground testing of vehicle and launcher
Sub-scale launch test(s)
fullscale launch test(s)
Launch day
Recovery activities
Educational Engagement Activities

- Implement procedures developed by the team for construction, assembly, launch, and recovery activities.
- Manage and maintain current revisions of the teams hazard analyses, failure modes analyses, procedures, and SDS/chemical inventory data
- Assist in the writing and development of the teams hazard analyses, failure modes analyses, and procedures.

5.3 Written Safety Statement

- Compliance with Huntsville Area Rocketry Association range safety inspection of rocket.
- Admission of the fact that the HARA Range Safety Officer has the final say on all rocket safety issues.
- Any team that does not comply with the safety requirements will not be allowed to launch their rocket.

A written safety statement to this effect is on the VADL website at www.vanderbilt.edu/usli and has been signed by all members of the Vanderbilt Aerospace Design Laboratory team who will be participating in rocket design and fabrication.

5.4 Safety Officer/LEUP Holder

Through outreach projects in the past, the team has made several useful contacts at a variety of local, regional, and national organizations. Robin Midgett, a Mechanical Engineering Technician at Vanderbilt, serves as the rocketry and safety mentor. Paul Register, a senior undergraduate in Chemical Engineering serves as the Student Safety Officer. Dexter Watkins and Ben Gasser, Mechanical Engineering graduate students, serve as Assistant Safety Officers.

5.5 Facilities

All facilities to be used by the team for the fabrication and assembly of rocket components and systems will be supervised by qualified personnel during the times of operation. These facilities are equipped with shop tools (both power- and hand-operated) that are commonly used by students. University personnel familiar with safe shop practices will supervise students and ensure proper operation of all equipment. All students using the machine shops at Vanderbilt will abide by the codes and rules outlined in the shop safety guidelines (see VADL website at www.vanderbilt.edu/usli).

5.6 Safety Equipment

Disposable gloves, face shields, goggles, shop aprons, and other safety apparel will be made available for use during fabrication. When applicable, SDS data will be referenced for the safe handling and storage of materials.

5.7 Injury/Emergency Situations

In the event of personal injury during the fabrication process, first aid kits are readily available in the club shop. The location of all first aid kits, fire extinguishers, and exits will be presented to all team members prior to their use of the facilities. Emergency personnel are available on campus at all hours. Fire extinguishers are located in shop areas and are inspected for readiness periodically in accordance with local fire protection regulations. Fire sprinklers and alarm systems are installed in areas where fabrication will occur.

5.8 Purchase, Storage, Transport, and Use of Rocket Motors

The design will include APCP motors. Robin Midgett, the rocketry and safety mentor, and Paul Register, the Student Safety Officer, will oversee the purchase and safe storing of these motors. The team will follow the recommendations of the local NAR chapter concerning the capability to purchase, store, transport, and use rocket motors. Necessary equipment will be purchased or built in accordance with applicable regulations regarding the handling, storage, and transportation of rocket motors. In particular, all motors, black powder, and electric matches will be purchased with the assistance of Robin Midgett. He will store these hazardous materials until the team is able to use them, at which point they will be transported in a suitable explosives magazine to the Vanderbilt University campus. Then, under Robin's supervision, the hazardous materials will be transferred to the Vanderbilt SL team's Magloc Explosives Storage Magazine, where they will remain until use. All usage of motors, black powder, and electric matches will be conducted exclusively under the supervision of the team's Safety Administration.

5.9 Transportation of Other Hazardous Materials

All hazardous materials will be handled in a fashion that is consistent with the pertinent Material Safety Data Sheet (see VADL website at www.vanderbilt.edu/usli), as well as with all federal, state, and local safety, regulatory, and environmental laws and guidelines.

5.10 NAR High Power Rocket Safety Code

The NAR High Power Rocket Safety Code was presented, discussed, and explained to all team members at a team meeting prior to initial design and is being referenced throughout design, construction, test, and launch processes. The Music City Missile Club, NAR Charter #589, advises the team regarding NAR safety requirements, the performance of hazardous materials, handling and hazardous operations, and issues pertaining to environmental laws and regulations. The Performance Guidelines for NAR personnel, along with the rest of the NAR High Power Rocket Safety Code requirements, are attached (see VADL website at www.vanderbilt.edu/usli). A copy of the Safety Code is kept in the club shop and will be referenced continuously throughout the course of the project.

5.11 Cognizance of Federal, State, and Local Laws and Regulations

The Safety Officer has briefed the team in a meeting regarding Federal Aviation Regulations 14 CFR, Subchapter F, Part 101, Subpart C; Amateur Rockets, Code of Federal Regulation 27 Part 55: Commerce in Explosives; and fire prevention, NFPA 1127 "Code for High Power Rocket Motors." Furthermore, environmental regulations will be consulted throughout the design and fabrication processes in order to ensure the team's compliance with all federal, state, and local laws. The Tennessee State Environmental Laws can be found at nasda.org. The Safety Officer has been tasked with recognizing all pertinent environmental regulations and recommendations for the handling of harmful or potentially hazardous materials and distributing this information to the team.

5.12 Safety Data Sheets

For the various potentially harmful materials that will be used in the design and construction of the rocket, Safety Data Sheets (see VADL website at www.vanderbilt.edu/usli) detail the proper handling and disposal of their associated materials. A summary of the SDS information included in the shop is provided on the VADL website at www.vanderbilt.edu/usli. The Student Safety Officer will seek out and provide the team with additional relevant regulatory or safety information for materials lacking a Safety Data Sheet and will educate all team members about proper handling and disposal of these materials.

5.13 Final Assembly and Launch Procedures

The VADL team will review system preparation requirements well in advance of the launch. Safety oversight and launch procedures are managed by the launch leader. The student safety officer, Paul, will oversee all hazardous operations involving people or the rocket. Team leaders will supervise the preparation of their respective areas. Formal integration of systems requires the launch leader's oversight. A member of NAR with appropriate certifications will oversee the assembly of the motor system. This is a quality control measure to ensure that mission-critical systems are properly prepared for launch. All launch procedures are divided into systems along with the personnel required.

5.13.1 Launch Pad, Launch Rail, and Ignition System

Launch Platform The Vanderbilt Aerospace Design Laboratory will use a standard NAR launch pad that will be constructed this year based on the specifications set forth by NAR. The launch pad is an improvement from the previous launch pad that had been in use since 2007 with its reduction in weight, increase in mobility and launch angle control, and increase in stability.

Key features of the launch platform include:

- 1/8” x 2” square aluminum tube legs and mast; aluminum base plates, stainless steel mast plate
- Stainless steel nuts and bolts to improve corrosion resistance
- Two legs that fold out from a central leg at 120° angles
- Launch rail mast that rotates on a pivot and is pinned into the stainless steel mast plate
- Rocket loaded with rail in the horizontal and then righted and pinned before launch
- Slotted hole for pin allows launch angle to be adjusted 5° in either direction from vertical
- Rail is made of two 8020 aluminum removable rails, joined together by a custom steel joint to provide straight guided path for rocket

Launch Rail The launch rail will utilize 1.5” I-shaped launch lugs that slide onto the launch rail. These will be purchased from Giant Leap Rocketry, are manufactured by Acme Conformal Rail Guides, and are made out of 6061-T6 aircraft aluminum. The base of the rail guide that interfaces with the rocket body tube will follow a 6.0” curvature (this has been shown to work for the 5.5” diameter rocket body tubes because the difference in arc length is not significant for the relatively small chord length covered by the launch lugs). The launch lugs will be permanently joined to the rocket body tube with JB weld after both the rocket body tube surface and the rail guides have been treated with 220 grit sand paper. This will ensure the JB weld has better penetration and bonding between the body tube and the launch lug. JB weld is chosen for its flexibility relative to epoxy, which will ensure resistance to small torsional loads applied while mounting the rocket to the launch rail. The launch lugs will be spaced approximately 24” apart. The tail fin section launch lug will be installed with precise measurements that guarantee the launch lugs are located halfway in between two fins. Then, two aluminum L-rods will be held in place that give machined straight lines for insertion of the second launch lug which is located on the payload section. This rig will help verify that a straight line connects both launch lugs and that there will not be misalignment issues.

Ignition System The launch ignition system consists of a 12V battery connected to 500 foot leads. The leads go through a safety switch system to the motor igniter. The safety switch ensures that no voltage differential is delivered to the electric match igniter until a key is inserted into the safety switch and a button is pressed.

5.14 Launch Operations Procedures

Launch operations procedures for all aspects of the launch preparation, vehicle assembly, and ignition are located in Section 6. Safety warnings and troubleshooting protocols are provided along with the operation procedure for each component of the launch.

5.15 Hazard Analysis

5.15.1 Risk Assessment Matrix

In order to fully assess the risks associated with the rocket and all its payloads, a risk assessment matrix (see Figure 125) is used that categorizes and ranks all risks according to the likelihood of occurrence and severity of consequence. An event's likelihood of occurrence is assigned a rating of 1, 2, 3, 4, or 5, corresponding to the designation of rare, unlikely, moderate, probable, and very likely, respectively. Similarly, an event's severity of consequence is given a rating of A, B, C, D, or E, corresponding to the designation of trivial, minor, moderate, high, or critical, respectively. When these two scales are crossed in a matrix, the resulting combinations provide enlightening information in terms of the risk level. In general, low alphanumeric combinations represent typically negligible risk, while high alphanumeric combinations tend to indicate much larger risks. Color-coding has also been included in the matrix to visually depict extent of risk. Events that fall within squares highlighted in green are considered low risk and require no mitigation or have no reasonable means of mitigation. In other words, "green" risks either occur infrequently or assume low consequence, such that serious consideration to mitigate the risk is not necessary. Similarly, squares highlighted in yellow contain events with moderate risk that should be mitigated, but the overall risk posed to the mission and general safety has been deemed acceptable. "Yellow" risks are more serious than "green" risks and could result in nontrivial consequences in terms of the success of the mission or to the safety of those involved; however, this category of risk does not necessarily represent no-go situations, assuming that potential mitigation strategies have been evaluated and implemented. The third and most critical category is highlighted in red, signifying events that pose hazardous and unacceptable risks to either mission success or personal safety. Without exception, "red" risks must be mitigated to a "yellow" or "green" level before the rocket and payload are considered safe for launch.

The explicit meanings of each of the rating designations are outlined as follows:

Likelihood of Occurrence

- 1 (Rare) - Probability of occurrence is almost non-existent. Mitigation need only exist for the most critical risks.
- 2 (Unlikely) - Probability of occurrence is very low but does exist. Mitigation should exist for high-risk consequences.
- 3 (Moderate) - Probability of occurrence is moderate. Mitigation efforts should exist for all risks resulting in greater than minor consequence.

		Consequence				
Likelihood		Trivial	Minor	Moderate	High	Critical
	Rare	A1	B1	C1	D1	E1
	Unlikely	A2	B2	C2	D2	E2
	Moderate	A3	B3	C3	D3	E3
	Probable	A4	B4	C4	D4	E4
	Very Likely	A5	B5	C5	D5	E5

Figure 125: Risk Assessment Matrix

- 4 (Probable) - Occurrence is more likely than not. Mitigation efforts should occur for all but the most trivial consequences.
- 5 (Very Likely) - Occurrence is to be expected. Mitigation is required for all but the most trivial consequences.

Severity of Consequence

- A (Trivial) - Occurrence of risk results in no effect on rocket/payload performance or safety of all persons involved. No mitigation is needed.
- B (Minor) - Occurrence of risk results in minor damage that is either easily repairable or has no effect on rocket/payload performance. No risk for injury to persons involved. Mitigation efforts should exist for the most likely risks.
- C (Moderate) - Occurrence of risks results in some damage to rocket/payload that could negatively affect performance and/or result in minor injury to persons involved. Mitigation efforts should exist for most risks.
- D (High) - Occurrence of risk results in major damage to rocket/payload that will negatively affect performance and/or result in serious injury to persons involved. Mitigation efforts should exist for all but the rarest risks.
- E (Critical) - Occurrence of risk results in catastrophic damage to rocket/payload that will eliminate performance capability and/or result in serious injury/death to persons involved or bystanders. Mitigation is necessary.

Combined Rating

- Green (Low) - Risk falls within an acceptable range of probability and consequence. Mitigation strategies should be implemented if possible but are not mission critical.

- Yellow (Moderate) - Risk may or may not be acceptable. Risk should be evaluated thoroughly for potential mitigation strategies.
- Red (Critical) - Risk has an unacceptable level of likelihood and consequence. Mission should not proceed until viable mitigation strategies are created and implemented.

All risks recognized by members of the team have been recorded and evaluated by the safety officer. Though not all risks have been encountered at the current stage of the design and fabrication process, each risk has been given an expected risk assessment rating both prior to mitigation efforts (RR) and post-mitigation (PMRR) in order to signify the safety- and reliability-oriented focus of the team. In all following risk assessment tables, each risk has been outlined along with possible causes, overall effect to the rocket/payload, mitigation strategy, verification plan of the mitigation, and risk assessment ratings for pre- and post-mitigation that have been color-coded by level of risk for easy comparison. Hazard analyses relating to the current competition has been broken into the following sections: personnel (Section 5.15.2); propulsion failure modes (Section 5.15.3); design of rocket/payload and launch (Section 5.15.4); recovery system failure modes (Section 5.15.5); vehicle failure modes not covered in the previous sections (Section 5.15.6); environmental concerns (Section 5.15.7); and project management (Section 5.15.8).

5.15.2 Personnel Hazard Analysis

Table 15 indicates possible hazards to personnel working in the shop, including risks posed by chemicals and machinery. Personnel safety is of utmost important in all construction, testing, and launch operations. Use of any equipment or chemicals requires a thorough understanding of the safety protocol and mitigation strategies for preventing and reducing the consequences of a potential failure. Information regarding safety in the shop is located on the Vanderbilt Aerospace Design Laboratory website at www.vanderbilt.edu/usli/sl-documents/.

Table 15: Personnel Hazard Risk Assessment

Risk	Cause	Effect	RR	Mitigation Strategy	Verification of Mitigation	PMRR
Shop Safety						
Electric shock	Static build-up on equipment handler	Destruction of electrical components; black powder explosion	E3	Handlers of sensitive equipment will ground themselves to discharge static build- up. Furthermore, all high voltage components will be properly marked as "HIGH VOLTAGE" and locked while in use.	Consultation of shop safety guidelines	E1

Personnel Hazard Risk Assessment

Risk	Cause	Effect	RR	Mitigation Strategy	Verification of Mitigation	PMRR
Lacerations or cuts from machines and tools	Improper use of machines/equipment	Injury potentially requiring medical attention	E3	All team members performing potentially hazardous operations will be properly trained. At least two members must be present for hazardous operations.	Consultation of safety protocol flowchart	D2
Black powder explosion/ignition while handling	Accidental connection to voltage source; Static discharge	Hearing damage; Disorientation; Personal injury	E3	Black powder handlers will only work with small amounts at a time and ground themselves prior.	Consultation of SDS	E1
Getting caught in a machine	Loose fitting clothing or jewelry; long hair not tied back	Potential for serious injury or death	E3	Those performing machining operations will never wear loose fitting clothing or jewelry. All long hair must be tied back.	Consultation of shop safety guidelines and safety protocol flowsheet	E1
Eye contact with chemicals or particulates; exposure to arc from arc-weld	Improper handling of chemicals	Discomfort and/or vision impairment	D3	Appropriate eye protection will be worn for all activities involving machinery, chemicals, and welding	Consultation of SDS, PPE: eye protection	D1
Prolonged exposure to loud machinery	Prolonged operation of heavy machinery	Disorientation and/or hearing loss	D3	Hearing protection will be worn when operating heavy machinery.	PPE: hearing protection	D1
Physical contact with hot surfaces	Leaving soldering iron on; touching welded parts immediately after welding	Burns	D3	All heat-producing tools will be turned off when not in use. Heat-resistant gloves will be worn when handling hot parts. Chemicals will be stored and handled safely.	Consultation of shop safety guidelines	D2

Personnel Hazard Risk Assessment

Risk	Cause	Effect	RR	Mitigation Strategy	Verification of Mitigation	PMRR
Inhalation of chemical fumes or carbon fiber particulates	Improper handling of chemicals	Discomfort and/or damage to lungs	D3	Volatile chemicals will only be handled in well-ventilated rooms and under a fume-hood when possible. A respirator will be worn when cutting, drilling, and sanding carbon fiber.	Consultation of SDS before use; PPE: eye protection, respirator	D1
Contact with flying debris from machining operations	Standard or improper tool use	Burns, abrasions, irritation of eyes or skin	C3	Closed-toed shoes and long pants will be worn at all times in the shop. All members present during cutting operations will wear eye protection.	PPE: clothes that cover the body, eye protection	C2
Contact with falling tools/parts	Improper storage of tools/parts	Personal injury	C3	All team members will wear closed toed footwear and long pants while machining in the shop.	Consultation of shop safety guidelines involving cleanup; PPE: clothes that cover the body	C2
Tripping over loose cords	Long power cords/wires being run across the shop floor	Personal injury	C3	Power strips have been installed near all machines/workspaces that may require a power outlet.	Consulation of shop safety guidelines	C1
Exposure to chemicals/allergens	Improper handling of chemicals and known allergens	Chemical burns, irritation of skin, allergic reaction	C2	Latex or vinyl gloves will be worn when handling chemicals or known allergens.	PPE: chemically resistant gloves	C1
Testing on the FRAME (formerly Ground-Based Test Facility)						
Shop fire	Overheating or short in motor controller	Potential for serious injury or death	E4	Follow electrical codes in wiring; run continuity checks to make sure no connections are shorted.	Consultation of safety guidelines for handling motor controller electrical components	E2

Personnel Hazard Risk Assessment

Risk	Cause	Effect	RR	Mitigation Strategy	Verification of Mitigation	PMRR
Catastrophic failure of air tank and regulator	Damage to air tank causes structural failure at normal pressure conditions	Potential for serious injury or death	E3	Thorough inspection of tank before every refill and proper padding and packing when transporting	PPE: eye protection and clothes that cover the body; consultation of safety protocol for refilling and transporting pressure tank	B2
Runaway torque motor input	Improper control pin value write due to power cycling	Rocket dislodged; potential for serious injury	D5	Connect or disconnect torque motor during nominal operation of controlling computer; incorporation of a hard off switch on the motor input	Design analysis of FRAME hardware; following of testing procedure	C2
Personnel caught in motor belt	Belt plastic failure and/or improper placement in operation whilst operator is adjusting the FRAME	Potential for injury to operating personnel	E2	Perform all belt operations while power is disconnected. Inspect belt before each use for damage. Stay clear of FRAME during testing operation.	Design analysis of FRAME hardware; following of testing procedure	C2
Catastrophic failure of air tank and regulator	Accidental overpressurization while refilling tank	Potential for serious injury or death	E2	Installment of 6 kpsi burst disc on air tank; air tank refilled by trained personnel under supervision of safety officer; large refill tank only pressurized to the design pressure (1/2 of air tank pressure rating)	PPE: eye protection and clothes that cover the body; consultation of safety protocol for refilling pressure tank	D1
Fall while securing nosecone interface	Unstable ladder base; unsafe practices	Potential for serious injury	D3	Optimal positioning of step ladder; visual monitoring of ladder movement while in use	Consultation of shop safety guidelines	E1

Personnel Hazard Risk Assessment

Risk	Cause	Effect	RR	Mitigation Strategy	Verification of Mitigation	PMRR
Rocket dislodged	Improper axial constraint	Potential for serious injury	D3	Ensure tight compression fit of top and bottom mounts; be ready to adapt setup to different vibrational situations	Design analysis of FRAME; following of testing procedure	E1
Structural failure	Excessive vibration; joint failure	Potential for injury to operating personnel	D3	Monitor construction; ensure proper joint tightness; maintain safe distance from test facility during tests	Design analysis of FRAME; following of testing procedure to ensure structural stability of system prior to experiment deployment	C2
Runaway thruster input	Control anomaly; runaway motor input	Rocket dislodged; potential for serious injury	D2	Incorporation of a hard off switch on the motor input	Design analysis of FRAME, including ease of access to manual override switch	C2
”Live” situation with thruster tank; potential for unplanned thruster firing	Experiment deployment failure coupled with software misunderstanding	Potential for injury to operating personnel	B3	Repeated verification of software integrity; secure handling of rocket (a person can easily constrain the output torque if expecting it)	PPE: eye protection	C2
Hotbox						
Electric shock	Improper shielding of control system	Potential for serious injury or death	E4	Follow electrical codes in wiring; maintain safe distance from hotbox while in use. Furthermore, the compartment containing high voltage electronics is marked with a warning sign and locked while the hotbox is in use.	Consultation of safety guidelines for handling high voltage components	C1

Personnel Hazard Risk Assessment

Risk	Cause	Effect	RR	Mitigation Strategy	Verification of Mitigation	PMRR
Shop fire	Runaway heating	Potential for serious injury or death	E3	PTC Thermistor used to cut off power to hotbox; webcam to monitor progress; digital thermometer included for redundancy in measurement; fire extinguishers kept in shop.	Design analysis of Hotbox prior to use; visual monitoring during initial uses	D1
Shop fire	Improper wiring or mounting of light bulbs	Potential for serious injury or death	E2	High power circuitry completed with safety officer present; fire extinguishers kept in shop	Design analysis of Hotbox prior to use; visual monitoring during initial uses	D1
Shop fire	Overheating of components	Potential for serious injury or death	E2	Maximum temperature possible greater than temperature ratings of every part exposed to heat; fire extinguishers kept in shop.	Design analysis of Hotbox; consultation of SDS for components to be heat-treated	D1
Thruster Test Stand						
Catastrophic failure of air tank and regulator	Damage to air tank causes structural failure at normal pressure conditions	Potential for serious injury or death	E3	Thorough inspection of tank before every refill and proper padding and packing when transporting	PPE: eye protection and clothes that cover the body; consultation of safety protocol for refilling and transporting pressure tank	D1
Loose pressure vessel in shop	Accidental and uncontrolled thruster firing	Potential for serious injury	E2	Select normally-closed solenoid; hardwire manual power switch to test stand; clamp system to table	Consultation of safety protocol; design analysis of test stand; PPE: eye protection and clothing that covers the body	C1

Personnel Hazard Risk Assessment

Risk	Cause	Effect	RR	Mitigation Strategy	Verification of Mitigation	PMRR
Thruster rupture in shop	Over-pressurization of thruster components	Potential for serious injury	E2	Hydrostatic testing with a safety officer present	Consultation of safety protocol flowchart; PPE: eye protection and clothing that covers the body	C1
Catastrophic failure of air tank and regulator	Accidental overpressurization while refilling tank	Potential for serious injury or death	E2	Installment of 6 kpsi burst disc on air tank; air tank refilled by trained personnel under supervision of safety officer; large refill tank only pressurized to the design pressure (1/2 of air tank pressure rating)	PPE: eye protection and clothes that cover the body; consultation of safety protocol for refilling pressure tank	D1
Hearing damage from thruster actuation	Prolonged exposure to test stand without hearing protection	Disorientation and/or hearing damage	D3	Hearing protection will be worn when operating thruster test stand	PPE: hearing protection	D1
Eye damage from thruster actuation	Thruster becomes dislodged from hose clamp supports	Eye damage or other serious injury	D3	Safety glasses will be worn around the pressurized system	PPE: safety glasses	D1
Personnel harm from N2 inhalation	Confined environment without ventilation for testing	Dizziness or lung damage from prolonged exposure	D2	No personnel is within 3 ft of thruster exhaust during actuation. A fan is on during all testing to push exhaust towards room vents	Consultation of safety guidelines for handling pressurized N2	D1
Personnel harm from N2 inhalation	Leak in pressurized components during filling of tank	Dizziness or lung damage from prolonged exposure	D2	Ventilation masks are worn with eye protection during all refills of tank	Consultation of safety guidelines for handling pressurized N2	D1

5.15.3 Propulsion Failure Modes

Table 16 displays modes of failure primarily concerning the rocket motor and propellant.

Table 16: Propulsion Failure Modes

Risk	Cause	Effect	RR	Mitigation Strategy	Verification of Mitigation	PMRR
Propellant fails to ignite	Improper motor packing; faulty propellant grain; damage during transportation	”Live” situation; rocket does not launch; necessary replacement	E3	Proper ignition setup; safety advisor oversees motor packing by student safety officer	Consultation of strict safety protocol regarding motor and propellant issues	D1
Premature propellant burnout	Improper motor packing; faulty propellant grain	Altitude estimate not reached; main parachute may not deploy	E3	Proper motor assembly; obtain motor only from reputable source	Static fire testing; consultation of safety protocol	E1
Improper assembly of motor	Incorrect spacing between propellant grains; motor case improperly cleaned; end caps improperly secured	Motor failure; unstable flight; target altitude not reached; damage or loss of rocket	E3	Ensure proper training and supervision by safety advisor for motor assembly by student safety officer	Consultation of strict safety protocol regarding motor and propellant issues	E1
Motor mount fails	Insufficient mount strength; damage during previous launch or transportation	Motor launches through rocket; damage to/loss of rocket; unstable flight	E3	Proper motor mount construction; load verification testing; test launches	Load verification testing; design analysis of motor mount; pre- and post-flight inspections of motor mount	E1

Propulsion Failure Modes

Risk	Cause	Effect	RR	Mitigation Strategy	Verification of Mitigation	PMRR
Transportation/ handling damage	Improper protection during transportation/ handling	Unusable motor; incapable of safe launch; potential damage to/loss of rocket	E3	Proper storage overseen by safety advisor and student safety officer; certified member handling	Consultation of strict safety protocol regarding motor and propellant issues	E2
Center ring failure	Unable to withstand motor force during launch; weak ring; poor seal to body and motor tube	Reduced stability; damage to/loss of vehicle	E3	Proper ring size and construction; sufficiently strong materials used(6061-T6 aluminum); redundant load path design that can sustain failure of fins or centering rings and still retain motor	Finite element modeling to verify rings to hold conservative thrust loads using von Mises failure criterion	E2
Propellant explodes	Improper motor packing; faulty propellant grain; damage during transportation	Destruction of motor casing; catastrophic failure of rocket; potential injury to personnel	E2	Proper motor assembly; safety advisor oversees motor packing by student safety officer	Consultation of strict safety protocol regarding motor and propellant issues	E1
Propellant burns through casing	Improper motor packing; faulty propellant grain; damage during transportation	Loss of thrust; loss of stability; catastrophic failure of rocket	E2	Proper motor assembly; safety advisor oversees motor packing by student safety officer	Static fire testing to verify proper motor assembly	E1
Motor tube dislodges from rocket body during launch	Failure of fin attachment, exposing motor tube connection	Catastrophic launch failure, uncontrolled flight	E2	Thorough construction of motor tube mounting through fins. For the motor tube to tear out, the fins would have to tear through the carbon fiber and blue tube body	Design analysis of tail section structure; visual inspection of tail section pre-flight	E1

Propulsion Failure Modes

Risk	Cause	Effect	RR	Mitigation Strategy	Verification of Mitigation	PMRR
Motor is misaligned	Centering rings misaligned; fins assembled to motor tube at an angle	Unexpected flight trajectory; unstable flight	C4	Careful machining of center rings on lathe with order of magnitude higher tolerance than laser cut plywood; proper assembly of tail section using centering rings and fin alignment jig	Design analysis of motor alignment equipment; pre-flight visual inspection of motor alignment	C1
Motor igniter fails	Faulty/incorrect igniter	"Live" situation; rocket does not launch; necessary replacement	C2	Proper igniter selection setup; proper power source	Adherence to safety protocol	C1

5.15.4 Payload/Control Failure Modes

Table 17 describes possible modes of failure of the cold gas thruster payload system and associated electronics and controls.

Table 17: Payload and Related Control Failure Modes

Risk	Cause	Effect	RR	Mitigation Strategy	Verification of Mitigation	PMRR
Insufficient space between parachute and blast charge installment	Designing to save mass and space without consideration of the recovery system integration into the vehicle body	Severe damage to recovery system	E3	Ensure proper parachute installment practices are followed per manufacturer instructions and testing	Design analysis; deployment testing	E1
Avionics power loss	Disconnection in cables or wiring	Loss of competition-required data, failure to actuate parachutes	E2	Thorough testing on the ground will help to reduce doubts about the reliability of the power supply	Testing on the FRAME proves the reliability of the payload electronics	E1
IMU dislodged	Improper connection of IMU to payload sled; heavy vibration of vehicle during flight	Catastrophic disturbance to guidance algorithm, loss of control of rocket	E1	Secure attachment of the IMU should be taken as a serious priority. Failure here would prove disastrous. Additionally, software lockouts could be introduced for scenarios like this in which IMU data is wildly off of predicted values	Design analysis to verify the IMU is securely attached	E1

Payload and Related Control Failure Modes

Risk	Cause	Effect	RR	Mitigation Strategy	Verification of Mitigation	PMRR
Thruster chain failure	Improper fitting of joints	Air stream leakage, possible damage flight vehicle	D3	Care in assembly and pressure testing to safety factor prior to use will help to ensure safety and reliability of the thruster chain	Design analysis of safety measures built in to regulator and pressure assembly; PPE: eye protection during testing	D2
Regulator failure	Improper fitting of joints; unexpected structural failure; defective part	Catastrophic loss of pressure; potential damage to flight vehicle	D2	Keeping the regulator operating at safe pressures as stated in its datasheet will mitigate possibility of failure. Employ burst discs of appropriate ratings and venting holes on the airframe to rapidly depressurize in the event of overpressurization failure.	Design analysis of safety measures built in to regulator and pressure assembly; adherence to safety protocol, stand at safe distance; PPE: eye protection during testing	D1
Air tank fracture	Overuse; impact history; defective part	Catastrophic loss of pressure. Potential damage to flight vehicle	D2	While highly unlikely, air tank cracks could indeed prove catastrophic. Visual monitoring of the tank prior to use in launch activities and careful regulation of witnessed pressure will be the best measures taken to guarantee success and safety here.	Design analysis of safety measures built in to regulator and pressure assembly; up-to-date refill log history of air tank; adherence to safety protocol, stand at safe distance; PPE: eye protection during testing	D1

Payload and Related Control Failure Modes

Risk	Cause	Effect	RR	Mitigation Strategy	Verification of Mitigation	PMRR
Failure of NASA marked altimeter	Improper handling of altimeter; dead battery	Inability to report official flight altitude for competition	D2	Test and verify proper altimeter operation before each test flight. Assure robustness of electronics configuration and avionics bay pre-flight.	Testing of the altimeter in the field before launch	C1
Thruster misalignment	Thrust torquing the nozzle about fittings	Thrust vector is not fully tangential to rocket. In the severe case, exhaust is cut off at the thruster portholes and is not fully ejected into the atmosphere. Both cases result in lost torque.	D2	Crimp compression fittings as tightly as possible without deforming rigid tubing. Secure thruster chain (particularly at the nozzle) to the bulkhead.	Design analysis to verify alignment of thrusters; test data on the FRAME confirms the desired thrust output	D1
Excess pitch and yaw	Heavy gusting; understability or overstability in terms of stability margin	Potential instability introduced to flight vehicle. If moved far past vertical, loss of control possible	C3	While gusting is out of control of the launch team, testing of the launch vehicle control system on the ground and CFD simulations will help to characterize this type of behaviour	Testing of the launch vehicle on the FRAME with application of simulated resistive torque	B3
Thruster structural failure	Unexpected structural failure; defective part	Loss of directional stability	C2	Pressure testing to safety factor and care in assembly will help to mitigate risk here	Testing of pressure apparatus; adherence to safety protocol	C1

Payload and Related Control Failure Modes

Risk	Cause	Effect	RR	Mitigation Strategy	Verification of Mitigation	PMRR
Blue Tube expansion-contraction from moisture	Excess humidity	Debonding of flight vehicle body, rapid unplanned disassembly of body components under launch/flight loading	C2	Thorough studies will be completed of moisture cycling of carbon fiber reinforced Blue Tube materials in order to characterize performance. If stabilizing chemical agents can be added to reduce any expansion effects, these measures will be taken.	Compression testing	B2
Flight computer power loss	Disconnection in cables or wiring	Loss of control, interruption of control algorithm	C2	Thorough testing on the ground will help to reduce doubts about the reliability of the power supply	Testing on the FRAME proves the reliability of the payload electronics	D1
One or more thruster nozzles become clogged	A small amount of dirt or debris is sufficient to plug up the nozzles	Roll control is unsuccessful and in the case of a single nozzle, the unbalanced couple could alter flight path	C2	Care will be taken in thruster system assembly to ensure no contaminants are introduced to any part in the flow path of the propellant	Consultation of launch operations procedure to ensure nozzles are clear prior to launch	C1
Wildlife interference	Launch vehicle flies through a flock of birds	Catastrophic disturbance to flight vehicle	D1	One of the most unpredictable failure events, little can be done to mitigate this risk during flight	Consultation of launch operations procedure to ensure clear launch field prior to flight	D1
Solenoid stuck open	Electronics or physical failure	Continuous thrust, loss of roll control	B3	Thorough testing prior to launch will help to ensure proper functioning of solenoid valves	Testing on the thrust stand and FRAME	B2
Solenoid stuck closed	Electronics or physical failure	No roll induction or roll control possible	B3	Thorough testing prior to launch will help to ensure proper functioning of solenoid valves	Testing on the thrust stand and FRAME	B2

Payload and Related Control Failure Modes

Risk	Cause	Effect	RR	Mitigation Strategy	Verification of Mitigation	PMRR
Air leak in hosing or fittings in thruster system	Improper fitting of joints; unexpected structural failure; defective part	Roll control is unsuccessful and air buildup could cause failure of other payload skeleton components	B2	Ground-based testing of all pressurized components will verify proper sealing. Venting holes will also be placed in all bulkheads and rocket exterior.	Testing on the thrust stand and with hydrostatic pressure testing	B1
Loss of thrust control	Empty air tank	Thruster use no longer possible	A4	This failure will not cause drastic issues with the mission unless rotation of the rocket is still necessary. Fueling the tank to maximum safe levels before flight will be the best mitigation strategy	Design analysis to verify the quantity of air in the tank is sufficient to complete the experiment	A2

5.15.5 Recovery System Failure Modes

Table 18 indicates hazards associated with failure of the parachute and recovery systems. All mitigations of risk are verified by consultation of launch operations procedure and testing through the subscale flight.

Table 18: Recovery System Failure Modes

Risk	Cause	Effect	RR	Mitigation Strategy	PMRR
Deployment failure	Putty not added to seal bulkhead holes	Parachute chamber artificially large	E4	Backup charges; consultation of launch operations procedures	C2
Rocket ripped apart upon chute deployment	Zippering effect of parachute harness	Catastrophic failure of recovery system; damage to/loss of rocket and payload	E3	Use Fireball anti-zippering device to distribute load to body	E1
Low battery of avionics electronics power supplies	Old, untested batteries used in avionics bay assembly	Failure to power flight altimeters throughout flight; failure to fire drogue and/or main ejection charges	E3	Pre-launch checklist assures battery testing and replacement if necessary	E1
Parachute sections come apart	Inadequate parachute design; poor stitching between sections	Catastrophic failure of recovery system; damage to/loss of rocket and payload	E3	Use semi-flat felled seam between sections; verification testing of recovery system	E2
Shroud lines become unattached	Weak stitching or materials	Catastrophic failure of recovery system; damage to/loss of rocket and payload	E3	Sew reinforcement onto shroud lines	E2
Parachute breakaway	Harness failure; weak mounting of recovery system to rocket body	Loss of parachute; catastrophic damage to/loss of rocket/payload; potential damage/injury to property/persons on ground	E3	Design strong retention system with shock absorption; load testing; multiple body attachment points	E2

Recovery System Failure Modes

Risk	Cause	Effect	RR	Mitigation Strategy	PMRR
Drogue parachute deployment failure	Drogue parachute fails to eject upon separation event; weak/failed blast charges do not eject parachute	High descent rate from apogee; unlikely successful main parachute deployment; damage to/loss of launch vehicle	E3	Ground-based deployment testing; backup drogue chamber ejection charge firing with a 1 second apogee delay	E2
Main parachute deployment failure	Parachute fails to eject from nosecone upon separation event; weak/failed blast charges do not eject parachute	Excessive landing energy for successful recovery; damage to or loss of launch vehicle	E3	Ground-based deployment testing; backup drogue chamber ejection charge firing at a slightly reduced altitude from desired main deployment altitude	E2
Separation failure	Excessive shear pin holding strength; inadequate/failed ejected charge; altimeter failure	Damage to or loss of the launch vehicle; potential damage/injury to property or personnel on the ground	E3	Ground-based deployment testing; proper shear pin sizing/strength and blast charge calculations ground and flight based altimeter testing; redundant charges for both separation events; factor of safety application for blast charge size	E2
Altimeter failure	Circuitry failure due to wiring failure; loss of or insufficient power to operate altimeters and fire ejection charges; arming switch failure	Failure to ignite drogue and/or main ejection charges; deploy parachutes at undesired altitudes or lack of deployment altogether; damage to/loss of launch vehicle	E3	Main-backup altimeter scheme; individual power supply module for each redundant altimeter; fully ground-based altimeter testing before each flight	E2

Recovery System Failure Modes

Risk	Cause	Effect	RR	Mitigation Strategy	PMRR
Arming switch failure	Faulty screw-switch component; miswiring of power supply, switch, and altimeter; short-circuit condition; switch changes out of NO state before or during flight; insecure soldering of wires to screw switches	Failure to activate the altimeters pre-launch	E3	Ground-based testing of each arming switch; ground-based deployments tests; flight test of altimeter arming switch; securing solder with small amounts of epoxy	E2
Shock cord failure	Faulty shock cord	Parachute disconnect from rocket; catastrophic damage to/loss of rocket	E3	Inspect shock cord before packing parachutes	E2
Shroud lines or shock cords tangle after deployment	Shock cords too long	Potential for parachute to not fully deploy; catastrophic damage to/loss of rocket	E3	Maximize cord length to tail section; flight testing	E2
Shroud lines or shock cords tangle after deployment	Excess rocket rotation	Potential for parachute to not fully deploy; catastrophic damage to/loss of rocket	E3	Minimize shock cord length to nose cone; flight testing	E2
Parachute or shroud line tangle	Improper transportation, storage, or packing	Decreased parachute performance leading to potential damage to or loss of rocket	D4	Proper packing of recovery system; proper and consistent method of folding and storing after each use	C2

Recovery System Failure Modes

Risk	Cause	Effect	RR	Mitigation Strategy	PMRR
Parachute melts	Improper separation of/insulation between charges and parachute; improper storage	Decreased parachute performance leading to potential damage to/loss of rocket	D4	Proper shielding from ejection charges; ground-based testing	D2
Lack of adequate space for parachutes	Improper budgeting of rocket space; poor translation of requirements to rocket design	Incapable of safe launch	E2	Clear outline of rocket design; verification of design needs met	D1
Parachute tear	Parachute snags upon separation; improper transportation/storage	Decreased parachute performance leading to potential damage to/loss of rocket	D3	Inspect material for defects; proper and consistent packing technique; removal of potential snags within parachute compartment	C2
Avionics bay not properly sealed	Holes in rocket body or avionics bay; gaps between sections	Incorrect detonation of drogue and/or main ejection charges; failure to reach desired altitude; damage to/loss of launch vehicle; errored altitude sensing	D3	Putty used to seal edges between avionics bay bulkheads and airframe; putty used to seal holes used for wiring	D2
Descent rate too fast	Parachute C_d too low; cross-sectional area too small	Potential damage to or loss of rocket or payload	D3	Verification testing of recovery system	D2
Onboard fire in parachute compartments	Combustible material near separation charges	Potential damage to or loss of launch vehicle and internal components; failure to deploy parachutes	D2	Isolation of ejection charges from flammable material; ground-based deployment testing and subscale flight	D1
Descent rate too slow	Parachute C_d too high; cross-sectional area too large	Potential to land outside of authorized zone	C3	Verification testing of recovery system	C2

5.15.6 Miscellaneous Failure Modes

Table 19 shows modes of failure relating to the rocket body and its components that do not fall into the other hazard analyses.

Table 19: Miscellaneous Failure Modes and Hazard Analysis

Risk	Cause	Effect	RR	Mitigation Strategy	Verification of Mitigation	PMRR
Premature rocket separation	Faulty separation charge wiring; shear pins too small; altimeter malfunction	Unstable flight; recovery failure; unable to reach target altitude; potential loss of vehicle	E3	Proper shear pins selection; ground-based deployment and altimeter testing	Design analysis of shear pins; testing on the FRAME; altimeter testing	E2
Buckling or shearing of airframe	Shear pins do not shear; bulkheads unable to withstand force from motor during launch; poor seal to rocket body and/or motor tube	Unstable flight; potential loss of vehicle	E3	Selection of strong airframe materials; proper manufacturing techniques; finite element stress analysis modeling	Design analysis of airframe components under high stress; testing of body tube material	E1
Bulkhead failure	Unable to withstand motor force during launch; weak ring; poor seal to body and motor tube	Damage to/loss of avionics, payload, or rocket; unstable flight	E3	Aluminum and steel bulkheads for critical components; proper construction; test for stability	Design analysis of bulkhead selection; finite element modeling; failure testing	E2
Structural failure despite stress modeling	Stress model underestimates true flight stress and overestimates factor of safety	Damage to vehicle or components; flight failure	E3	Verify the model with multiple experimental tests; use conservative design safety factors; use model uncertainty factors	In addition to finite element analysis, compression testing and validation from test launches	E1

Miscellaneous Failure Modes and Hazard Analysis

Risk	Cause	Effect	RR	Mitigation Strategy	Verification of Mitigation	PMRR
Rocket comes loose from launch pad	Rail buttons not securely mounted to rocket; extreme wind; team error in aligning rocket while attaching to pad	Rocket breaks free during initial phase of launch; potential damage to rocket, bystanders, and property; potential loss of vehicle and payload	D4	Rail buttons used on rocket for secure attachment; careful precision of alignment while guiding rocket on launch rail	Design analysis to align rail buttons; validation from subscale flight	C2
Premature section separation	Failure of shear pins	Deploy at incorrect altitude; potential damage to/loss of vehicle	E2	Proper shear pin sizing/strength	Design analysis of shear pin selection; deployment testing prior to launch	D1
Vehicle component not brought to launch site	Component not packed	Rocket does not launch	E1	Follow launch inventory and checklist; bring duplicates of smaller components like fasteners	Consultation of launch operations hardware checklist	D1
Carbon fiber joint failure	Weak adhesion; loss of material strength	Unstable flight; damage to/loss of vehicle	D3	Follow proper procedure for applying carbon fiber joints, including proper surface preparation, epoxy selection, and vacuum bagging technique	Consultation of fabrication protocol for rolling carbon fiber	B2
Fin failure or weakness	Damage in landing of previous launches or during travel; improper sealing from environmental hazards	Unstable flight	D3	Correct construction techniques; evaluate structural integrity after and before each launch; protective epoxy coating	Design analysis of fin choice; testing of carbon fiber strength	D2

Miscellaneous Failure Modes and Hazard Analysis

Risk	Cause	Effect	RR	Mitigation Strategy	Verification of Mitigation	PMRR
CG is too far aft	Poor overall rocket and section design; unnecessary weight	Insufficient stability for reliable flight	C3	Proper simulation of rocket characteristics using RockSim; add ballast to forward section of rocket if needed	Design analysis with simulation environment	B2
CP is too far forward	Poor overall rocket and section design; fin area too small	Insufficient stability for reliable flight	C3	Proper simulation of rocket characteristics using RockSim; increase fin size to move CP further back.	Design analysis with simulation environment	B2
Nosecone damage	Damage in landing of previous launches or during travel; improper sealing from environmental hazards	Unstable flight; unstable nosecone structure	C3	Strong nose cone selection; evaluate structural integrity after and before each launch; protective paint coating	Design analysis in choice of nose cone; validation from subscale launch	B2
Excess friction between rocket and launch rail	Misalignment or poor installation of launch lugs; misalignment of launch rail; improper lubrication or debris on launch rail	Rocket does not reach desired altitude	A3	Use of jig to align launch lugs; follow rail assembly procedures, checking for correct alignment and using acceptable lubrication	Verification from subscale launch; pre-flight inspection of alignment of rail buttons	A2

5.15.7 Environmental Effects Analysis

Tables 20 and 21 show interactions between the rocket and the environment during launch. While many of the risks listed are potentially hazardous to personnel at the launch sight, this section focuses on the interplay between weather, wildlife, and other environmental hazards with the rocket. Safety hazards related to the environment can be unpredictable and must be characterized as broadly as possible prior to launch. Especially as the scale of the mission increases in terms of vehicle mass and projected altitude, the potential environmental consequences of a vehicle failure become more relevant. Also, at the smaller scale of the Student Launch rockets, the effect of the environment on the rocket can be devastating. Therefore, robustness in design and an understanding of all potential process safety hazards are crucial to a successful mission. All environmental hazards are verified to be mitigated before and during launch procedures by strict adherence to the launch procedures checklist, in which safety hazards are specifically demarcated with the appropriate procedural steps (see Section 6).

Table 20: Environmental Impact on Rocket

Risk	Cause	Effect	RR	Mitigation Strategy	Verification of Mitigation	PMRR
Structural failure; launch pad fire	High temperature or exposure to sunlight	Overheating of electronics; warping of body tube or structural components	E3	Prior to placement on launch pad, rocket assembled in tent-shaded area; time from setup on pad to launch minimized if possible	Study of launch operations procedure to minimize field time; body tube integrity verified by previous exposure to Hotbox during curing process; battery temperature tested on pad prior to launch. NO-GO IF BATTERIES ARE OVERHEATED	C1
Extreme weather-cocking	Excessive wind	Unexpected vehicle trajectory; vertical launch compromised	D4	Vehicle has a stability margin that minimize risk of both understable and overstable flight	Design analysis of fins and mass distribution to procure favorable stability margin; consultation of launch operations procedure to verify SSM on launch pad; subscale flight test validates choice of SSM. NO-GO IF STEADY WIND SPEED EXCEEDS 20 MPH	B1

Environmental Impact on Rocket

Risk	Cause	Effect	RR	Mitigation Strategy	Verification of Mitigation	PMRR
Structural or component damage; misalignment of rocket axis; unintended ignition of vehicle	Contact with animals, particularly cows in a farm setting	Unexpected vehicle trajectory; damage to vehicle components or launch pad	E2	All structural and electrical components located internal to rocket body; launch pad leveled immediately prior to launch; ignition actuator not located within distance specified by minimum distance table	Design analysis of structural components; adherence to launch procedures; visual monitoring of launch pad area from final setup until launch. NO-GO IF ANIMALS TAMPER WITH LAUNCH PAD SETUP	C1
Damage to rocket body; parachute destruction	Excessive wind; nearby obstacles in field	Vehicle drags along ground due to large horizontal velocity; components may snag on obstacles; drift exceeds size of launch field	D3	Launch vehicle body kept void of protuberances; launch only occurs in field clear of destructive obstacles	Design analysis of external vehicle profile; certification of robustness of external components; consultation of launch operations procedure in choosing launch location. NO-GO IF STEADY WIND SPEED EXCEEDS 20 MPH OR LAUNCH FIELD NOT CLEAR OF OBSTACLES	B2
Launch pad not level	Pad sinks due to soft ground conditions; pad not leveled properly upon setup	Unexpected vehicle trajectory	D3	Plywood boards to prevent the launch pad legs from sinking into the ground; level brought to launch site	Consultation of launch operations procedure, which incorporates multiple verifications of the launch pad condition. NO-GO IF LAUNCH PAD IS NOT LEVEL	B2

Environmental Impact on Rocket

Risk	Cause	Effect	RR	Mitigation Strategy	Verification of Mitigation	PMRR
Difficulty assembling vehicle components in the field	Excess humidity	Swelling or warping of body tube and internal components, particularly wooden bulkheads	D2	Inner surface of body tube and internal components weatherproofed with polyurethane spray; sandpaper taken to launch field as potential minor resizing tool	Adherence to fabrication design; consultation of launch hardware list. NO-GO IF VEHICLE ASSEMBLY NOT POSSIBLE WITHOUT MAJOR MODIFICATIONS	A1
Ice buildup on vehicle body; sealing of vent holes	Below freezing temperatures and precipitation	Increased vehicle mass; uncharacterized changes in aerodynamic drag; pressure buildup inside rocket body	D2	Final assembly performed under tent; vehicle wrapped in blanket until immediately prior to launch; sandpaper taken to launch field to scrape off ice buildup	Visual inspection of vehicle prior to launch. NO-GO IF ICE VISIBLE ON VEHICLE BODY	C1
Launch pad fire	Wet conditions compromise integrity of the electronics or wiring	Electronics short circuit	C3	Electronics enclosures sealed with putty to prevent water exposure; weatherproofing of inner surface of body tube	Consultation of launch operations procedure; adherence to fabrication design. NO-GO IN CONDITIONS OF HEAVY PRECIPITATION	B2
Untethered hardware blown around	Excessive wind	Final vehicle assembly made more difficult; personnel hazard	B2	Minimization of hardware requirement on launch day; securement of hardware in labeled boxes	Design and consultation of launch hardware list. NO-GO IF WIND PREVENTS SAFE VEHICLE ASSEMBLY	A1

Environmental Impact on Rocket

Risk	Cause	Effect	RR	Mitigation Strategy	Verification of Mitigation	PMRR
Excessive launch rail friction	High temperatures or exposure to sunlight, low humidity; misalignment of rail buttons	Unexpected vehicle trajectory	B2	Rail coated in Vaseline; rail buttons aligned properly	Design analysis and testing confirms alignment of rail buttons; consultation of launch operations procedure with inspection of rail condition prior to launch. NO-GO IF LAUNCH RAIL NOT IN PROPER CONDITION FOR LAUNCH	A1

Table 21: Rocket Impact on Environment

Risk	Cause	Effect	RR	Mitigation Strategy	Verification of Mitigation	PMRR
Unsuccessful parachute deployment; parachute failure	Insufficient or excessive parachute deployment charges and/or shear pins	Destruction of launch vehicle upon ground impact; scattering of foreign debris; potential cratering	E4	Recovery system extensively ground-tested to validate deployment charge calculations, parachute wrapping technique, and deployment method	Design analysis to verify expected deployment of parachute; consultation of launch operations procedure while packing parachute	E1
Launch pad fire	Heat from main engine ignites dry vegetation surrounding the launch pad	Damage to vegetation and potential hazard to nearby team members	E2	Launch conducted in area clear of excess underbrush and vegetation; launch aborted in extremely dry conditions; fire extinguisher taken to launch site	Consultation of launch operations procedure during launch. NO-GO IF DRY CONDITIONS PRESENT FIRE HAZARD	D1

Table 21: Rocket Impact on Environment

Risk	Cause	Effect	RR	Mitigation Strategy	Verification of Mitigation	PMRR
Mid-air explosion of rocket or components	Internal failure of payload or main engine	Widespread scattering of vehicle debris	E1	All payload components with explosive potential rated with a safety factor of 4; motor is sourced from a reliable, commercial supplier	Design analysis of components seeing pressure; hydrostatic testing of house-made nozzles	B1
Vehicle strikes people or structures outside planned launch area	Excessive wind; improper timing of main parachute deployment, possibly due to buildup of pressure near avionics bay	Vehicle drifts outside launch field	C2	Vent holes cut in bulkheads and vehicle body to eliminate pressure buildup; large launch field chosen in case of early parachute deployment	Design analysis to verify pressure venting and reduce pressure leaks from thruster system; simulation testing to predict drift under non-ideal conditions; launch operations procedures followed in choosing launch field. NO-GO IF WIND SPEED EXCEEDS 20 MPH	B1
Harm to environment from litter	Improper disposal of trash; failure to setup up designated trash bag	Poisoning, strangulation, or suffocation of wildlife	B5	Deployment of trash bags at launch site; documentation of hardware taken to site	Adherence to launch operations procedure; consultation of launch hardware checklist	B2

Table 21: Rocket Impact on Environment

Risk	Cause	Effect	RR	Mitigation Strategy	Verification of Mitigation	PMRR
Injury to wildlife	Animals contact launch pad or vehicle; rocket impacts wildlife during flight or upon landing	Animal wounds, contusions, or death	D1	Launch conducted in area clear of wildlife or obstacles	Adherence to launch operations procedure; visual monitoring of launch pad from setup until launch	A1
Chemical poisoning of ponds or ground water	Leakage of battery fluid or excess fuel	Electrical components provided extra separation from environment within body tube; rocket recovered quickly to minimize exposure time; launch site chosen away from bodies of water	D1	Consultation of launch operations procedure before and after launch. NO-GO IF BODY OF WATER WITHIN 2500 FEET OF LAUNCH PAD		B1
Injury to wildlife	Animals ingest components (trash or tools) at tent while team is at launch pad	Animal wounds, contusions, or death	D1	Launch conducted in area clear of wildlife or obstacles. If wildlife present, personnel will be left at tent while members go to the launch pad.	Adherence to launch operations procedure; visual monitoring of launch pad from setup until launch	A1
Damage to sod (if applicable from location)	Team walks through field to retrieve rocket	Damage to sod	B3	Minimal members of team will walk to retrieve launch vehicle taking the shortest route to limit surface area of sod covered.	Adherence to recovery operations procedure	A1

5.15.8 Project Management

Table 22 details difficulties that may be encountered while the team attempts to meet both self-imposed and NASA criteria/deadlines.

Table 22: Project Management Risk and Mitigation

Risk	Consequences	RR	Mitigation Strategy	PMRR
Vehicle testing failure	Vehicle parts are destroyed or damaged during ground testing or flight testing. Could lead to ordering new materials late in the year and running the risk of not completing the project on time.	E3	Design the vehicle components after extensive mathematical and physics analysis in order to ensure that a damaging failure will not occur. Only conduct tests with the potential to cause damage once a robust design has been developed and implemented. Set up an inventory of spare parts and components for building a second rocket within a week	E1
Weather launch delays	Inability to meet CDR and FRR timelines and obligations	D4	Have multiple possibilities for launch by working with launch clubs in the Tri-State area of TN, AL, and KY.	C2
Rushed timeline	Low quality in manufacturing, vehicle safety, payload safety, and risks to mission success in all aspects	D3	Well defined component verification metrics and workmanship standards, internal launch readiness reviews, no culture of go fever	D1
Communication breakdown between team members	Failure to meet deadlines; failure to show results	D2	Frequent meetings to improve team morale and stress the importance of timelines, and chain of command. Recalibration of deliverables based on progress.	B1
Delays in critical path	If a portion of the project that is necessary to complete the next portion takes longer to complete than expected, there could be delays in project development.	C3	Make sure that realistic expectations are set for completion of elements along the critical path.	B2
Ambiguous product lead time	If the amount of time it takes for parts to ship is ambiguous or unknown, there could be unexpected delays in project development.	C3	Ensure somebody is responsible for knowing the lead times on all parts, and trying to eliminate all the ambiguity.	B1

Project Management Risk and Mitigation

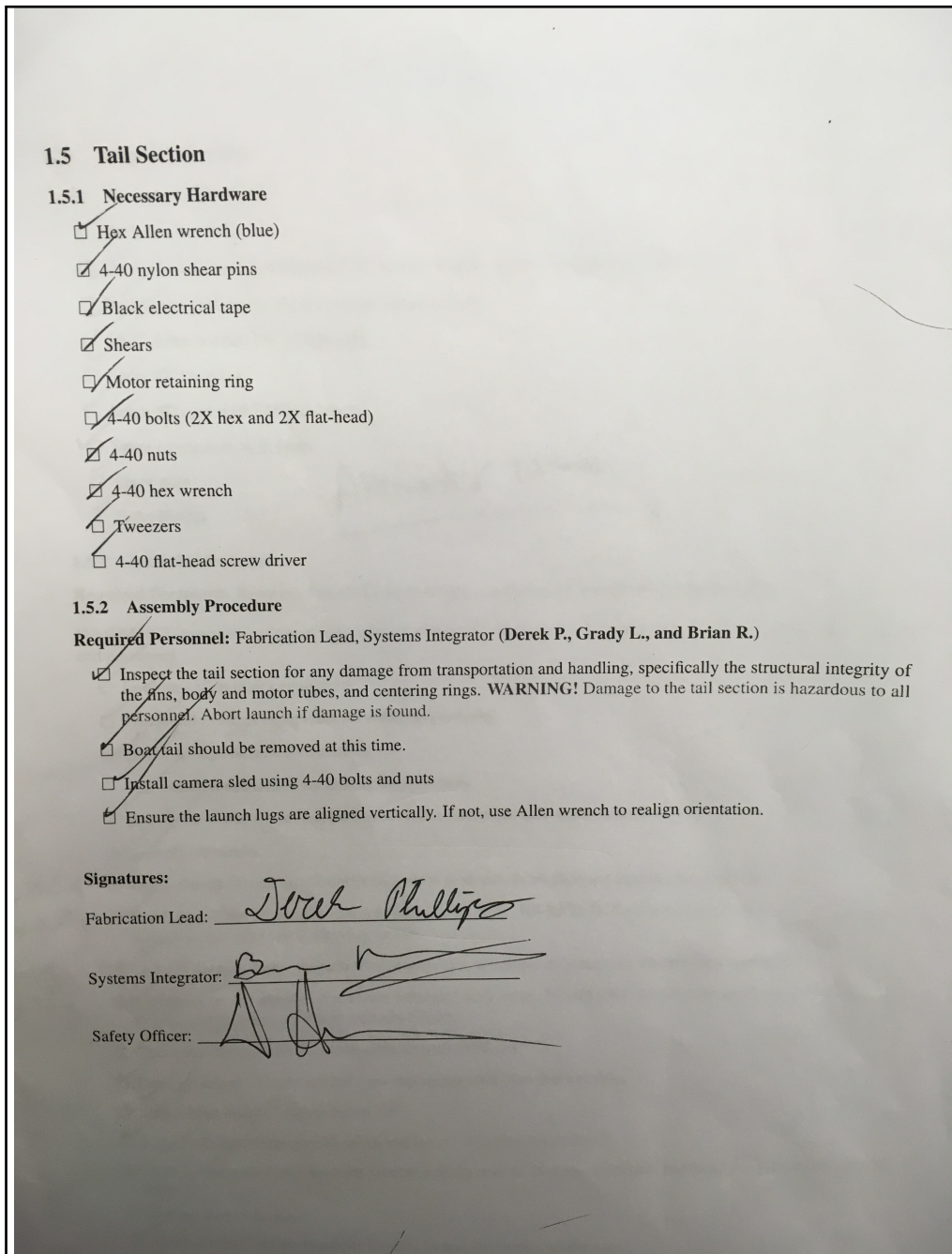
Risk	Consequences	RR	Mitigation Strategy	PMRR
Excessive academic responsibility	Fabrication, testing, or launch deadlines would be compromised	C2	Weekly team meetings cover individual availability to ensure adequate personnel are available for each scheduled task	C1
High budget costs	Could threaten the feasibility of the project, as well as a violation of the rules of the competition.	C2	Keep a detailed budget and projected budget to minimize the chance of overspending. Make sure that every purchase is justified.	C1
Misplaced or lost component	Cause delays in construction of the rocket and payload. Loss of time in searching for misplaced component. Incurs redundant cost in the event of reordering.	B4	Routinely organize shop. Delegate sections of the shop for components/equipment of various sections of the rocket (i.e. mechanical payload section, payload electronics section, recovery section, etc.). Order in excess when fiscally reasonable for vital components. Take care to place vital components in designated, labeled areas.	A4
Equipment breakdown	Machine shop or laboratory equipment breakdown could cause a slowdown in production and threaten the timely completion of the project.	C1	Ensure that the team has access to multiple machine shops in case equipment in one place fails. Also, ensure that equipment is used and stored properly to minimize the likelihood that such a failure will occur.	B1
Unavailability of parts or delays in parts delivery	Delays in construction of the rocket and payload attachment scheme; rushing through work or settling with parts that are not compatible with the ideal design	B3	Start the design process very early, and allow room in the design for the use of parts other than those initially selected: flexibility in design without the compromise of safety or science value	A2
Limited access to machine shops	Delays in fabrication of various parts or rushed work. Impact on timely completion of the project.	B2	Ensure that contact with the machine shop operators is constant, and that available times for access are established.	B1
Personnel shortage	Student or faculty members could be unavailable, which can lead to higher workloads for others, or the lack of technical knowledge of some system aspect.	B2	Make sure that the knowledge of rocket construction and testing techniques is known by the entire team. Make sure that the schedule is known by everyone so that people are not voluntarily absent/unavailable at inopportune times.	B1

Project Management Risk and Mitigation

Risk	Consequences	RR	Mitigation Strategy	PMRR
School holidays	Slows down the project and threatens timely completion and available times for testing.	A2	Ensure that the schedule for work and testing is designed with school holidays in mind, such that the team does not expect to have full access to equipment or personnel during those times.	A1

6 Launch Operations Procedures

A pre-launch checklist has been developed to ensure safety and success in all aspects of the flight. For each independent section of the launch field process, a list of necessary hardware, and a detailed breakdown of the assembly process is included. Procedures on troubleshooting and post-flight steps are also detailed for convenience. Figure 126 shows an example of part of the launch checklist signed off on at fullscale launch.



The image shows a handwritten signed launch checklist. The document is organized into sections with headings and lists of items. There are several signatures at the bottom, indicating approval from different personnel. The text is in black ink on a light-colored background.

1.5 Tail Section

1.5.1 Necessary Hardware

- Hex Allen wrench (blue)
- 4-40 nylon shear pins
- Black electrical tape
- Shears
- Motor retaining ring
- 4-40 bolts (2X hex and 2X flat-head)
- 4-40 nuts
- 4-40 hex wrench
- Tweezers
- 4-40 flat-head screw driver

1.5.2 Assembly Procedure

Required Personnel: Fabrication Lead, Systems Integrator (**Derek P., Grady L., and Brian R.**)

- Inspect the tail section for any damage from transportation and handling, specifically the structural integrity of the fins, body and motor tubes, and centering rings. **WARNING!** Damage to the tail section is hazardous to all personnel. Abort launch if damage is found.
- Boat tail should be removed at this time.
- Install camera sled using 4-40 bolts and nuts
- Ensure the launch lugs are aligned vertically. If not, use Allen wrench to realign orientation.

Signatures:

Fabrication Lead: Jordan Phillips

Systems Integrator: [Signature]

Safety Officer: [Signature]

Figure 126: Signed Launch Checklist

6.1 Launch Field General Setup

WARNING! Always handle pressurized tanks with care. The pressurized air tank and its spare are stored in a protective, padded case on the journey to the launch site. Any refilling must be executed with safety mentor oversight.

Necessary Hardware

- | | | | |
|---|--|--|--|
| <input type="checkbox"/> Tent | <input type="checkbox"/> Dustin's thruster box | <input type="checkbox"/> Metal file | sealing all holes between payload and electronics |
| <input type="checkbox"/> Tarps (2) | <input type="checkbox"/> Paul's nuts and bolts bag | <input type="checkbox"/> Box cutter | |
| <input type="checkbox"/> Tables (2) | | <input type="checkbox"/> X-acto knife | |
| <input type="checkbox"/> Chairs (6) | <input type="checkbox"/> Tape measure (2) | <input type="checkbox"/> Gorilla tape | |
| <input type="checkbox"/> Garbage bags (2) | <input type="checkbox"/> Wire cutters | <input type="checkbox"/> Sealant tape (gray) for sealing bulkhead holes that contain wires | |
| <input type="checkbox"/> X-frames (3) | <input type="checkbox"/> Needle nose pliers | | |
| <input type="checkbox"/> Robin's toolkit | <input type="checkbox"/> Shears | <input type="checkbox"/> Sealant putty (blue) for | |
| <input type="checkbox"/> Dexter's electronics box | <input type="checkbox"/> Zip Ties | | |
| | | | <input type="checkbox"/> Epoxy kit (5-minute epoxy resin and hardener, mixing cups, popsicle sticks) |
| | | | <input type="checkbox"/> Drill (with spare battery and all needed bits) |

Assembly Procedure

Required Personnel: Rocketry Mentor, Safety Officer (Robin, Paul R.)

- Unload equipment and materials from van. Bring to field setup location.
- Identify expected launch pad location, and begin field assembly at least 500 feet away.
- Set up tent and secure with stakes.
- Assemble portable tables. **WARNING!** Ensure ground is level and clear from obstructions.
- Set up bags for trash collection. **WARNING!** Littering presents an environmental hazard.
- Place X-frames for each section on tables.
- Place independent sections of rocket on X-frames (payload, avionics, tail).
- Place all electronics on their own table.

Signatures:

Rocketry Mentor: _____

Safety Officer: _____

6.2 Launch Pad and Launch Rail

Necessary Hardware

- Launch pad
- Stakes for launch pad
- Adjustable wrench (2)
- Launch rail (12 ft)
- Vaseline
- Latex Gloves
- Hex Allen wrench (blue)
- Level
- Tarp

Assembly Procedure

Required Personnel: Systems Integrator (**Chris R.**)

- Place launch pad on tarp (preventing the burning of sod adjacent to pad).
- Open launch pad legs fully and bolt into place with stainless steel bolts and lock nuts. Stake into ground.
- With mast in the horizontal position, slide bottom half of launch rail onto the carriage bolts on the mast so that the bottom of the rail is flush with the bottom of the mast. Tighten nuts.
- Slide the top portion of the launch rail over the steel joint and tighten bolts, ensuring a flush fit.
- Loosen the bolts on the launch rail stop and adjust to the appropriate height. Tighten bolts.
- Fully inspect assembled launch pad and rail to ensure it provides a sturdy base for the rocket during launch. **WARNING!** This step is imperative for a straight takeoff. Postpone launch until a secure pad location is found.
- PPE Required:** Wear latex gloves. Apply Vaseline or another appropriate lube to the rail.
- Ensure there is a smooth transition from the lower to the upper rail sections.

Signatures:

Systems Integrator: _____

Safety Officer: _____

6.3 Software and Controls

Necessary Hardware

- MicroUSB cable
- Computer of Software and Controls Lead

Procedure

Required Personnel: Software and Controls Lead (**Arthur**)

- Open Virtual Machine (VM) and connect to server
- Verify the most recent version of code is being used.
- Check User configurations to ensure proper launch experiment.
- Turn off *Time-Based Enable* and increase takeoff acceleration threshold. **WARNING!**
Failure to do so can result in premature thruster firing - damage to personnel.
- Check system model to ensure proper hardware mapping.
- PPE Required:** safety glasses. Run test experiment.

Required Tests

- Ping BeagleBone and listen for "echo" buzzer.
- Arming pin test.
- Stream specs and boot source.
- Time-based deployment to validate solenoid actuation.
- Check for nominal data logging.
- Ensure no abhorrent timing behavior.
- Confirm acceleration-based deployment for launch.

Signatures:

Software and Controls Lead: _____

Safety Officer: _____

6.4 Payload Skeleton and Electronics

Necessary Hardware

- | | |
|---|---|
| <input type="checkbox"/> 7/16" wrench (2) | <input type="checkbox"/> Wire stripper/cutter |
| <input type="checkbox"/> 9/16" wrench | <input type="checkbox"/> Crimpers |
| <input type="checkbox"/> 5/8" wrench | <input type="checkbox"/> Needle-nose pliers |
| <input type="checkbox"/> Adjustable wrench (2) | <input type="checkbox"/> Electronics allen wrench |
| <input type="checkbox"/> Spare pressurized tank and regulator
(with wooden retaining bulkhead) | <input type="checkbox"/> Phillips screw driver |
| <input type="checkbox"/> 1/4"-20 hex nuts | <input type="checkbox"/> Small precision flat-head screw driver |
| <input type="checkbox"/> Washers | <input type="checkbox"/> 1/4" bolts (4) |
| <input type="checkbox"/> Grey sealant tape | <input type="checkbox"/> 4-40 bolt (1) |
| <input type="checkbox"/> Blue sealant putty | <input type="checkbox"/> Torx wrench |
| <input type="checkbox"/> Thread seal tape | <input type="checkbox"/> 4-40 shear pins |
| <input type="checkbox"/> Spare Li-ion batteries (two 14.8 V, one
11.1 V) | <input type="checkbox"/> Allen wrench for 4-40 bolt |

Assembly Procedure

Required Personnel: Payload Lead, Fabrication Lead, Electrical Systems Lead (**Jimmy, Derek, Brad**)

- Make sure forward section is not over skeleton.
- Secure all bulkheads in flight location on threaded rods with nuts. Check lengths below by measuring along each of the three rods from bulkhead to bulkhead.
 - A1 → A2: $2 \frac{1}{8}$ "
 - A2 → P1: $9 \frac{7}{16}$ "
 - P1 → P2: $3 \frac{15}{16}$ "
 - P2 → P3: $3 \frac{3}{16}$ "
 - P3 → PE: $2 \frac{1}{4}$ "
- Verify air tank retention at the top of the payload section.
- Verify mounting of all thruster hardware. **WARNING!** Failure to secure payload hardware can result in a failed experiment and a risk of unstable flight.

- Install payload electronics sled on threaded rods, matching alignment indices. **WARNING!**
Make sure cage nuts do not interfere with electronics sled.
- Attach electrical connections. Seal bulkhead wire holes with putty.
 - Connect solenoid valve leads (Black to Black, Yellow to Yellow).
 - Ensure micro USB cable is connected to beaglebone and extending past bulkhead (P3).
 - Ensure charging leads (white and black wires) are extending past P3.
 - Seal all bulkhead wire holes with putty.
- Verify SD card is properly installed and has not been ejected.
- Add 1 washer and 2 nuts to each threaded rod to secure electronics sled.
- Slide on final 2 payload bulkheads (coupled by U-bolt) and verify witness marks between coupler tube and bulkhead.
- Compress bulkhead assembly against coupler tube with 2 nuts on each threaded rod.
WARNING! Do not over-compress coupler tube. The Blue Tube will bulge outward, rendering final vehicle assembly difficult.
- Slide on forward rocket section and check nut with bulkhead alignment mark.
- Bolt forward section to ensure proper orientation. 4-40 bolt first to constrain payload skeleton relative to airframe, then 1/4" bolts connecting airframe to coupler tube.
- Check and verify thruster alignment.

Signatures:

Payload Lead: _____

Fabrication Lead: _____

Electrical Systems Lead: _____

Safety Officer: _____

6.5 Tail Section

Necessary Hardware

- Hex Allen wrench (blue)
- 4-40 nylon shear pins
- Black electrical tape
- Shears
- Motor retaining ring
- 4-40 bolts (2X hex and 2X flat-head)
- 4-40 nuts
- 4-40 hex wrench
- Tweezers
- 4-40 flat-head screw driver

Assembly Procedure

Required Personnel: Fabrication Lead, Systems Integrator (**Derek, Brian**)

- Inspect the tail section for any damage from transportation and handling, specifically the structural integrity of the fins, body and motor tubes, and centering rings. **WARNING!** **Damage to the tail section is hazardous to all personnel. Abort launch if damage is found.**
- Boat tail should be removed at this time.
- Ensure the launch lugs are aligned vertically. If not, use Allen wrench to realign orientation.

Signatures:

Fabrication Lead: _____

Systems Integrator: _____

Safety Officer: _____

6.6 Avionics Section

Necessary Hardware

- Dexter's electronics box
- Small Phillips head (grey/orange) for screw switches (check w/ screw while packing)
- Multimeter (yellow) to check voltage across battery
- 5/64" Allen wrench for VN100 IMU
- Spare 9V batteries
- Spare SD card with BBB image
- Spare connectors with leads
- Spare wire
- Extra Kevlar

Assembly Procedure

Required Personnel: Recovery System Lead, Electrical Systems Lead, Rocketry Mentor (**Paul M., Brad, Robin**)

WARNING! Damaged equipment or improper wiring can cause recovery failure - hazard to the rocket, environment, and personnel.

- Inventory all avionics equipment.
- Inspect all avionics equipment for safety and security.
- Check voltage on new 9V batteries.
- Test switch functionality by turning on altimeters.
- Ensure the altimeters are secure and set for correct parachute deployment altitudes.
- Turn off altimeters.
- Connect main charge ignition wire (e-match) to terminals on plywood avionics bay bulkhead. **WARNING!** Ensure secure connection. Successful firing of the blast charges is crucial to recovery of the flight vehicle.
- Seal holes on the plywood avionics bulkhead with putty. **WARNING!** Insufficient application of putty may alter blast dynamics and cause recovery failure.
- Connect drogue charge ignition wire (e-match) to terminals on aluminum avionics bay bulkhead.

- Seal holes on the aluminum avionics bulkhead with putty. **WARNING!** Insufficient application of putty may alter blast dynamics and cause recovery failure.
- Check that batteries are a compression fit with bulkhead.
- Place parachute charges in blast caps and secure with blue painters tape.
- Secure blast charge wires to bulkhead.
- Inspect all separation ignition wires and ensure clearance for assembly.
- Slide avionics sled into avionics section making sure to face the aluminum bulkhead away from the coupler tube.
- Bolt the sled to the tube.
- Verify access holes are in proper location to arm electronics on the pad.

Signatures:

Recovery System Lead: _____

Software and Controls Lead: _____

Rocketry Mentor: _____

Safety Officer: _____

6.7 Drogue Parachute Assembly and Integration

Necessary Hardware

- Parachute (2 ft Classic Elliptical)
- Shock cords
- Quick-connects for shock cords
- Fireballs for anti-zippering
- Blast charges (4, pre-prepared)
- Blue 3M tape
- Nomex blanket

Assembly Procedure

Required Personnel: Recovery System Lead and Rocketry Mentor (**Paul M., Robin**)

WARNING! Failure to properly pack parachute can cause recovery failure - hazard to the rocket, environment, and personnel.

- Inspect drogue parachute for hardware defects and security.
- Visually inspect the deployment charges for secure connection.
- Insert deployment charges into labeled blast caps. **WARNING!** Ensure blast charges are placed in correct caps.
- Visually verify that deployment charges are secured in their respective blast caps.
- Connect first shock cord from top of payload electronics section to parachute.
- Connect parachute to Nomex blanket.
- Connect second shock cord from parachute to avionics section.
- Ensure all shock cord and parachute connections are in their proper locations. **WARNING!** Failure to properly connect drogue parachute will result in recovery failure.
- Load drogue parachute and shock cord, folded using a z-fold, into forward section of rocket above avionics bay.

Signatures:

Recovery System Lead: _____

Safety Officer: _____

6.8 Main Parachute

Necessary Hardware

- Parachute (8 ft Iris Ultra)
- Shock cords
- Quick-connects for shock cords
- Fireballs for anti-zippering
- Blast charges (pre-prepared)
- Blue 3M tape
- Nomex blanket

Assembly Procedure

Required Personnel: Recovery System Lead and Rocketry Mentor (**Paul M., Robin**)

WARNING! Failure to properly pack parachute can cause recovery failure - hazard to the rocket, environment, and personnel.

- Inspect main parachute for hardware defects and security.
- Visually inspect the deployment charges for secure connection.
- Insert deployment charges into labeled blast caps. **WARNING!** Ensure blast charges are placed in correct caps.
- Visually verify that deployment charges are secured in their respective blast caps.
- Connect first shock cord from bottom of avionics section to parachute.
- Connect parachute to Nomex blanket.
- Connect second shock cord from parachute to tail section.
- Ensure all shock cord and parachute connections are in their proper locations. **WARNING!** Failure to properly connect main parachute will result in recovery failure.
- Load main parachute and shock cord, folded using a z-fold, into avionics section of rocket below avionics bay.

Signatures:

Recovery System Lead: _____

Safety Officer: _____

6.9 Launch Vehicle Final Integration

Necessary Hardware

- (4) 1/4" button bolts for bolting forward body section to coupler tube (BRING EXTRAS)
- (1) 4-40 bolt to constrain rotation of payload skeleton (BRING EXTRAS)
- Torx wrench for button bolts (check with bolt while packing)
- (8) 4-40 nylon shear pins for securing tail cone and coupler tube to tail section
- Black electrical tape to cover shear pins
- Safety glasses

Assembly Procedure

Required Personnel: Fabrication Lead, Systems Integrator, Electrical Systems Lead (**Derek, Jimmy, Brad**)

- Align witness marks and slide forward section over coupler tube around payload electronics. **Verify thruster alignment with exhaust holes.**
- Confirm that altimeter switches and payload electronics switches can be reached.
- Bolt the forward section to the coupler tube first with the 4-40 bolt for rotation prevention and then with 1/4" bolts.
- Align witness marks and fasten avionics airframe to payload electronics coupler tube with 4-40 nylon shear pins.
- Align witness marks and join tail section to avionics coupler tube with 4-40 nylon shear pins.
- Align witness marks and install boat tail with 4-40 shear pins.
- Check for pressure venting holes (thruster tank and altimeters). **WARNING! Buildup of pressure in tube may alter blast dynamics and cause recovery failure.**

Signatures:

Payload Lead: _____

Electrical Systems Lead: _____

Safety Officer: _____

6.10 Motor Installation and CG Operations

Necessary Hardware

- Motor retaining ring
- Motor refuel kit
- Scale for massing rocket
- Baby powder

Assembly Procedure

Required Personnel: Fabrication Lead, Rocketry Mentor (**Derek, Robin**)

WARNING! Always perform motor installation under supervision of rocketry mentor.

- Motor should be stored in own container for transport and secured to avoid drops or impacts.
- Inspect the motor to ensure that no damage occurred during transportation or handling that could result in such failures. **WARNING!** If damage is identified, abort launch.
- Insert the Loki L1400 motor into rocket motor tube and tighten the positive screw cap retention ring. Applying baby powder to the exterior of the motor can help facilitate installation.
- Verify that the positive screw cap retention ring is securely fastened to the rocket.
- Mass rocket and mark CG.

Signatures:

Fabrication Lead: _____

Rocketry Mentor: _____

Safety Officer: _____

6.11 Launch Pad Operations

Necessary Hardware

- Laptop and cables for experiment deployment
- Torx wrench for button bolts (check with bolt while packing)
- 4-40 nylon shear pins for securing tail cone and coupler tube to tail section
- 4-40 allen-head bolt
- Allen wrench for bolt
- Screw driver for electronics arming
- Black electrical tape to cover shear pins
- Safety Glasses
- Ladder

Assembly Procedure

Required Personnel: Fabrication Lead, Systems Integrator, Electrical Systems Lead (**Derek, Jimmy, Brad**)

- Carefully carry rocket assembly to the launch pad making sure to support all sections.
- Line up the rail buttons that are attached with the rocket to the launch rail slots. Very slowly slide the launch lugs onto the rail guides making sure not to put a bending moment on the rocket.
- Remove forward section.
- Attach flexible hose from NPT fitting onto Quick Disconnect.
- Once the launch vehicle is oriented so that the tail cone is placed one foot off the launch pad, slowly raise the launch rail back into a vertical configuration and bolt down the pad so that it will not pivot.
- Use a level placed on the vertical surface of the launch rail to ensure that the desired angle is achieved in correct direction and perpendicularity with the ground is achieved.

Final Steps:

- Turn on BeagleBone
- Check for solid red beaglebone power light.
- Check for blue blinking beaglebone status lights.
- Check for green blinking IMU status light.
- Connect to BeagleBone via microUSB cable and deploy experiment.
- Listen for 5 second beep to confirm positive IMU communication.

- Disconnect from BeagleBone during beep. **WARNING!** Experiment is now live; avoid inducing large vertical acceleration, as experiment could be triggered.
- PPE Required:** safety glasses. Turn on thruster tank (twist pin depressor toward tank). **WARNING! VERIFY THRUSTER TANK IS ON OR PAYLOAD EXPERIMENT WILL NOT BE SUCCESSFUL.**
- Slide forward section onto the payload skeleton
- Use Phillips head screwdriver to tighten 4-40 allen-head bolt that will constrain rotation.
- Bolt the forward section with 1/4" bolts.
- Arm the payload electronics using a through-wall screw switch. **WARNING!** Ensure proper booting of payload electronics - failure to do so will result in experiment failure.
- Arm avionics using a through-wall screw switch. **WARNING!** Failure to do so will result in recovery failure.

Signatures:

Payload Lead: _____

Electrical Systems Lead: _____

Safety Officer: _____

6.12 Igniter Installation

Necessary Hardware

- Igniter stick
- Launch electrics (in blue tub)

Assembly Procedure

Required Personnel: Rocketry Mentor (Robin)

WARNING! Always perform igniter installation under supervision of rocketry mentor.

- Insert igniter into the rocket motor.
- Attach leads that connect igniter to the ignition trigger.
- Ensure the ignition system is wired to the power source.

Signatures:

Rocketry Mentor: _____

Safety Officer: _____

6.13 Post-Flight Inspection

Required Personnel: Rocketry Mentor, Recovery Lead, Electrical Systems Lead, Safety Officer
(Robin, Paul M., Brad, Paul R.) **WARNING!** Do not damage sod in launch field by walking on it unnecessarily.

- PPE Required:** Wear appropriate shoes and clothing for retrieval of vehicle. Locate launch vehicle and safely retrieve it - avoid hazardous areas if possible, otherwise proceed with appropriate caution.
- Return launch vehicle to field setup tent.
- Disengage compressed air tank.
- Connect to BeagleBone and stop experiment.
- Check parachutes and shock cords for damages.
- Properly dispose of any live black powder charges. **WARNING!** Risk of explosion if not done properly.
- Check compressed airframe for zippering from shock cords.
- Record apogee data from altimeters.
- Examine fins and motor tube for burn damage.
- Repack sectioned launch vehicle in same manner as brought to field for safe transportation.

Signatures:

Rocketry Mentor: _____

Electrical Systems Lead: _____

Recovery Lead: _____

6.14 Troubleshooting in the Field

- Ensure all team members keep detailed notes on their respective subsystems.
- Approach problems with a composed and organized systems engineering approach.
 - Consult relevant section leads.
 - Quickly develop a probable list of reasons for component failure.
 - Assess the feasibility of each potential failure method.
 - Assess the probability of mitigating each potential failure method.
 - Mitigate all probable failure methods if can be completed efficiently.
 - If probable causes cannot be mitigated in a reasonable period of time, abort launch.
- If problem arises on launch pad, handle situation professionally.
 - Acceleration-based enable is live, so avoid inducing large vertical accelerations.
 - Disarm altimeters and BeagleBone.
 - Carefully remove forward section of launch vehicle.
 - Close compressed air tank.
 - Lower launch rail and remove vehicle from rail.

6.15 Pack List: Full List of Necessary Hardware

- | | | |
|--|--|--|
| <input type="checkbox"/> Tent | <input type="checkbox"/> Tape measure (2) | <input type="checkbox"/> Sealant putty (blue) for sealing all holes between payload and electronics |
| <input type="checkbox"/> Tarps (2) | <input type="checkbox"/> Wire cutters | |
| <input type="checkbox"/> Tables (2) | <input type="checkbox"/> Needle nose pliers | <input type="checkbox"/> Epoxy kit (5-minute epoxy resin and hardener, mixing cups, popsicle sticks) |
| <input type="checkbox"/> Ladder (1) | <input type="checkbox"/> Shears | |
| <input type="checkbox"/> Chairs (6) | <input type="checkbox"/> Zip Ties | <input type="checkbox"/> Drill (with spare battery and all needed bits) |
| <input type="checkbox"/> Garbage bags (2) | <input type="checkbox"/> Metal file | |
| <input type="checkbox"/> X-frames (3) | <input type="checkbox"/> Box cutter | <input type="checkbox"/> Launch pad |
| <input type="checkbox"/> Scale for massing rocket | <input type="checkbox"/> X-acto knife | <input type="checkbox"/> Stakes for launch pad |
| <input type="checkbox"/> Robin's toolkit | <input type="checkbox"/> Gorilla tape | <input type="checkbox"/> Adjustable wrench (2) |
| <input type="checkbox"/> Dexter's electronics box | <input type="checkbox"/> Sealant tape (gray) for sealing bulkhead holes that contain wires | <input type="checkbox"/> Launch rail (12 ft) |
| <input type="checkbox"/> Dustin's thruster box | | <input type="checkbox"/> Vaseline |
| <input type="checkbox"/> Paul's nuts and bolts bag | | <input type="checkbox"/> Paper towels |

- Latex Gloves
- Hex Allen wrench (blue)
- Level
- Small Phillips head (grey/orange) for screw switches (check w/ screw while packing)
- Multimeter (yellow) to check voltage across battery
- 5/64" Allen wrench for VN100 IMU
- Spare Lipo batteries
- Spare SD card with BBB image
- Spare connectors with leads
- Spare wire
- USB Male-to-Male (mini to standard)
- Altimeter manual
- Brad's Toolbox
- Michael's Toolbox
- Hex Allen wrench (blue)
- 4-40 nylon shear pins
- Black electrical tape
- Parachutes (Fruity Chutes 2-ft. elliptical drogue and 8-ft. toroidal main)
- Shock cords
- Quick-connects for shock cords
- Fireballs for anti-zippering
- Blast charges (pre-prepared)
- Blue 3M tape
- Shock cords
- Quick-connects for shock cords (4)
- Fireballs for anti-zippering (2)
- Nomex blanket (2)
- 7/16" wrench (2)
- 9/16" wrench
- 5/8" wrench
- Spare pressurized tank and regulator (with wooden retaining bulkhead)
- 1/4"-20 hex nuts
- Washers
- Thread seal tape
- Spare Li-ion batteries (two 14.8 V, one 11.1 V)
- Wire stripper/cutter
- Crimpers
- Phillips screw driver
- Small precision flat-head screw driver
- Computer of Software and Controls Lead
- Motor retaining ring
- Motor refuel kit
- Baby powder
- (4) 1/4" button bolts for bolting forward body section to coupler tube (BRING EXTRAS)
- 4-40 bolt to constrain rotation of payload skeleton (BRING EXTRAS)
- Torx wrench for button bolts (check with bolt while packing)
- 4-40 Allen wrench
- Tweezers
- Safety glasses
- Igniter stick
- Launch electrics (in blue tub)
- Extra Kevlar

7 Project Plan

7.1 Testing

7.1.1 Thruster Testing

In order to conduct safe and controlled tests of our thruster nozzles, a ground-based test facility (further referred to as Thruster Test Stand) was designed. This test stand incorporates compressed propellant regulation capabilities allowing for continuous or pulsed operation of the thruster. The stand also measures post-regulator pressure (with both a digital and analog sensor) and thrust delivered by the system. A schematic showing the flow of both air and power for the system can be seen in Figure 127 below.

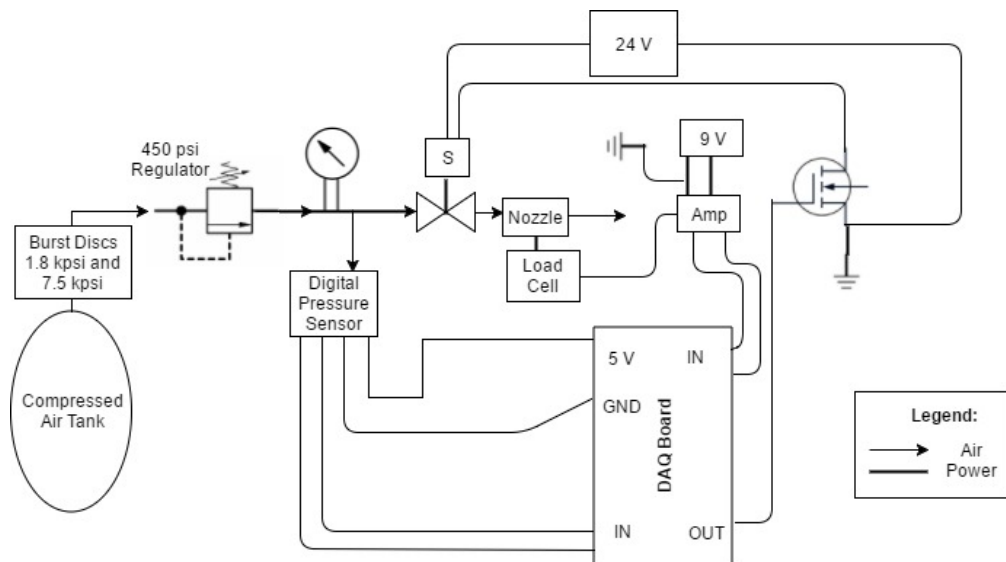


Figure 127: Test Stand Schematic

The thruster is integrated into the test stand by rigidly mounting the solenoid valve (and attached compression Yor-Lok fitting that retains the nozzle) to a plate of aluminum which is in turn suspended by two spring steel sheets. One end of each sheet is attached via L-brackets to the aluminum plate with the other end firmly attached to the roof of the outer structure of the test stand. This outer structure is made primarily of Aluminum 80/20 T-slot extrusions with a thick plate mounted on the rear two extrusions (orthogonal to the suspended solenoid mounting plate) which holds an Omega LCEB series load cell in place. Separate from this structure is a horizontal plate to which the air tank feeding the thruster system is secured with adjustable U-bolts. The load cell is set up so that a screw on the back side of the solenoid mounting plate will compress into it during thruster actuation, thus reading the reaction force felt from the thrust provided. For a more visual representation of the test stand, see Figures 128 and 129 below.

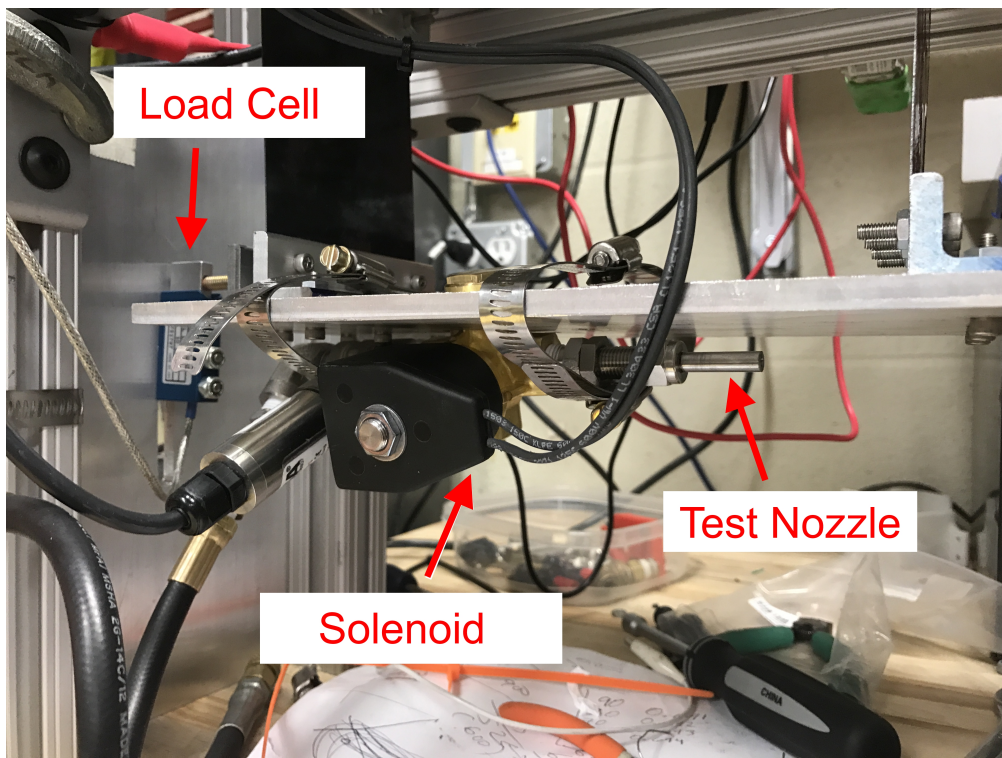


Figure 128: Test Stand Nozzle and Solenoid Mounting

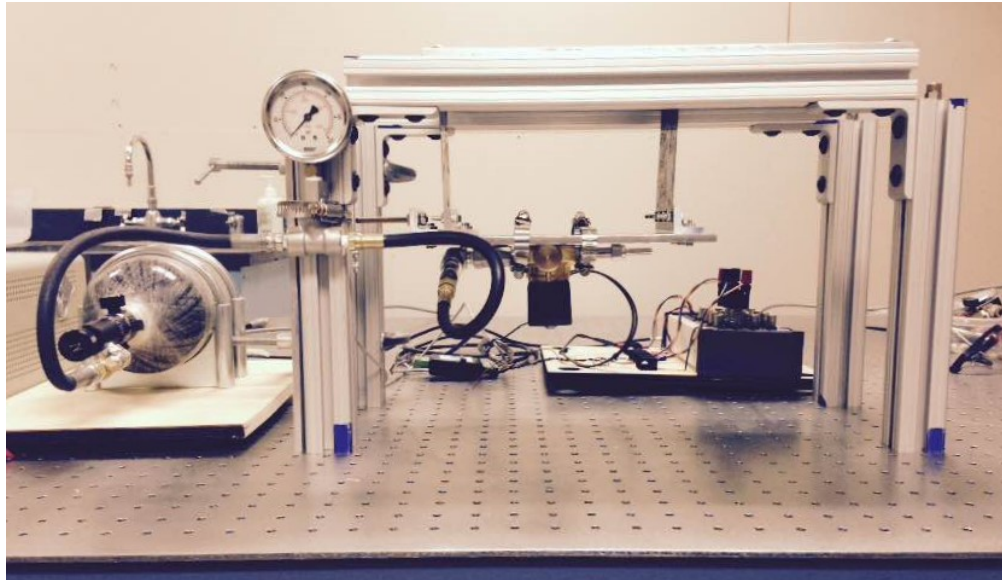


Figure 129: Test Stand Overview

The thrust test stand's load cell was calibrated before testing took place to ensure accurate results for each trial. Figure 130 shows the calibration set up for the load cell. A force sensor was mounted to the frame of the stand via an aluminum plate with rails so that a crank could incrementally push the sensor against the plate. The sensor then read reaction force values that

were recorded along with the load cell outputs (read through a NI DAQ Board and fed into LabVIEW for processing) to calibrate the system. This process was repeated incrementally by increasing force from 0 to 20 N, unloading the plate between each increment to record new zero values to ensure accuracy of the trend obtained. The calibration curve can be seen in Figure 131.

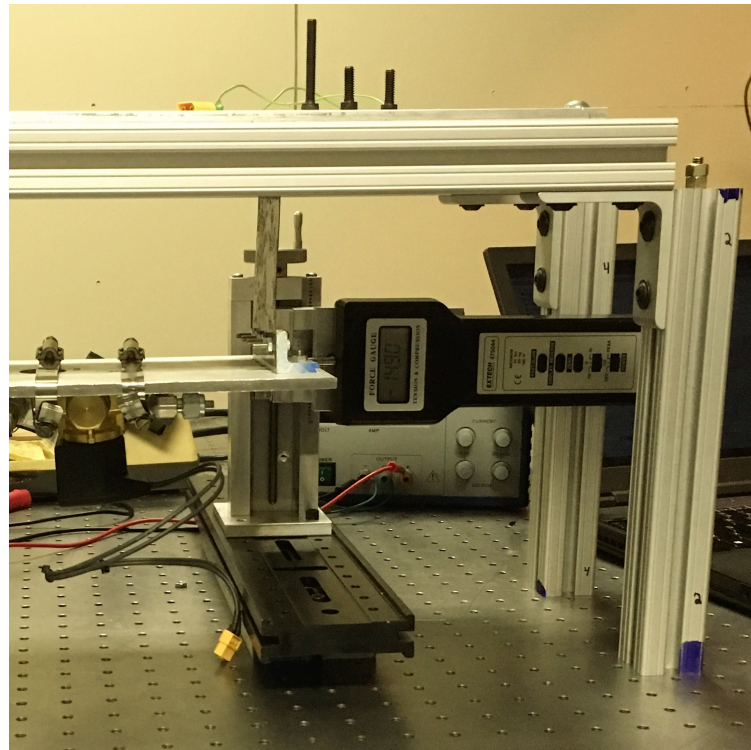


Figure 130: Test Stand Load Cell Calibration

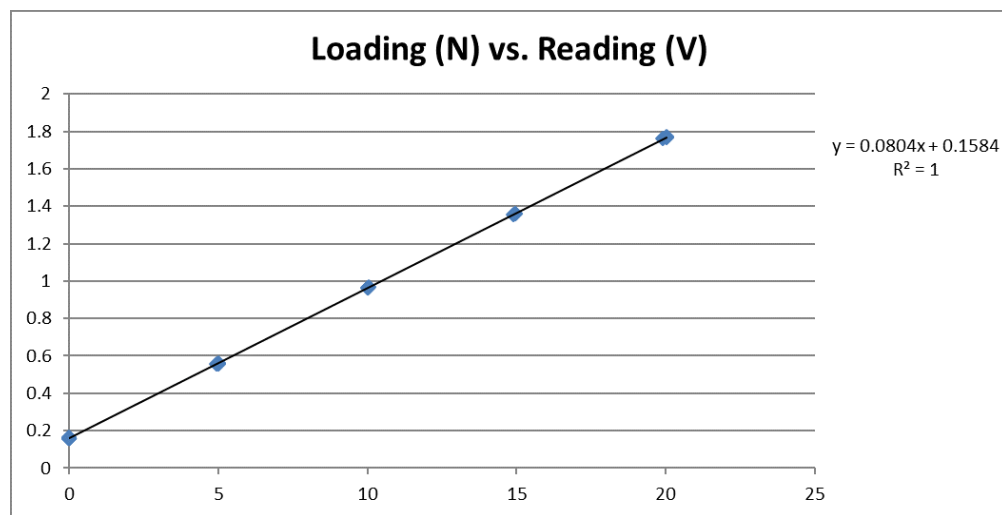


Figure 131: Load Cell Calibration Curve

The test stand was used to measure thrust for many different experimental setups, the results of which can be seen in Figures 132, 133, 134, and 135 below. The first figure shows the test results for running the thruster continuously to monitor thrust and pressure data over the time taken to empty the tank while Figures 133, 134, and 135 show pulsed conditions of various lengths. It should be noted that between each test, the tank was refilled to the same starting pressure of 2000 psi.

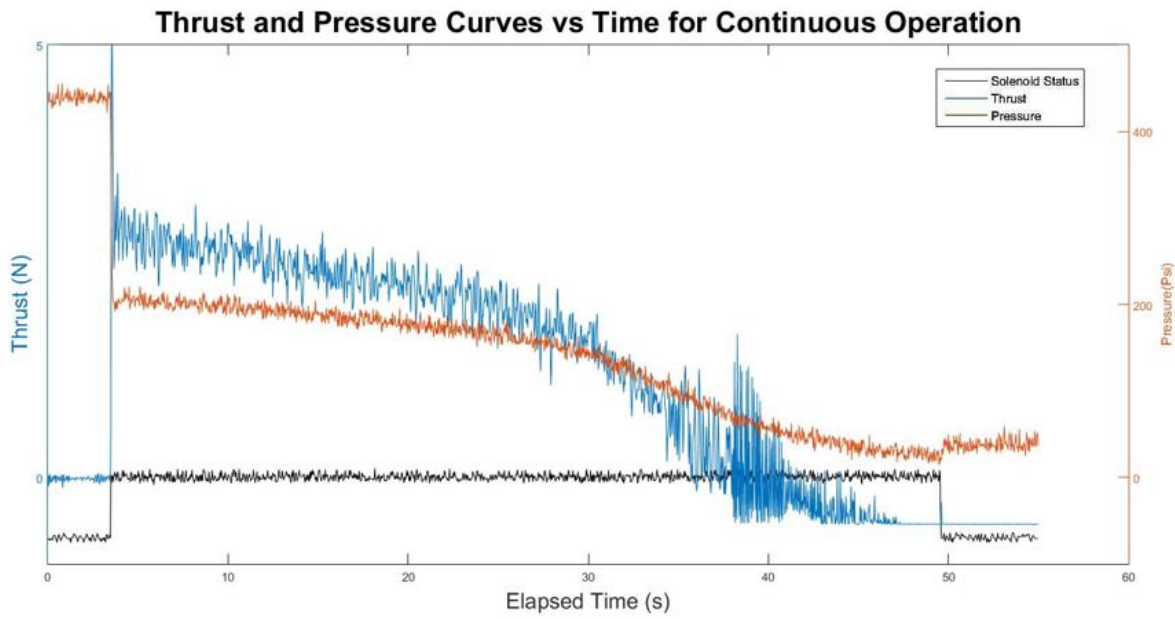


Figure 132: Thruster and Pressure vs Time, Continuous Run

The results of Figure 132 show that even with the tank pressurized only to 2000 psi, a relatively consistent thrust value was measured for 30 seconds for one thruster. With two thrusters firing simultaneously, the system runtime is reduced to approximately 15 seconds, which is optimized for the experimental duration (8 seconds).

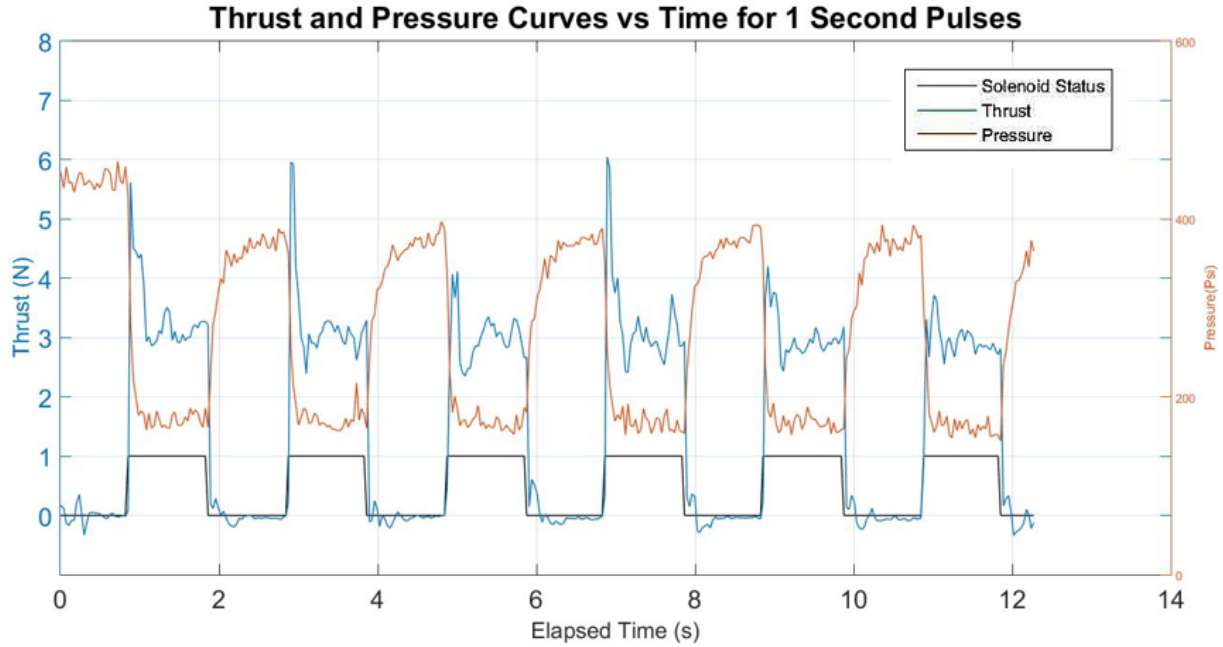


Figure 133: Thruster and Pressure vs Time, 1 Second Pulses

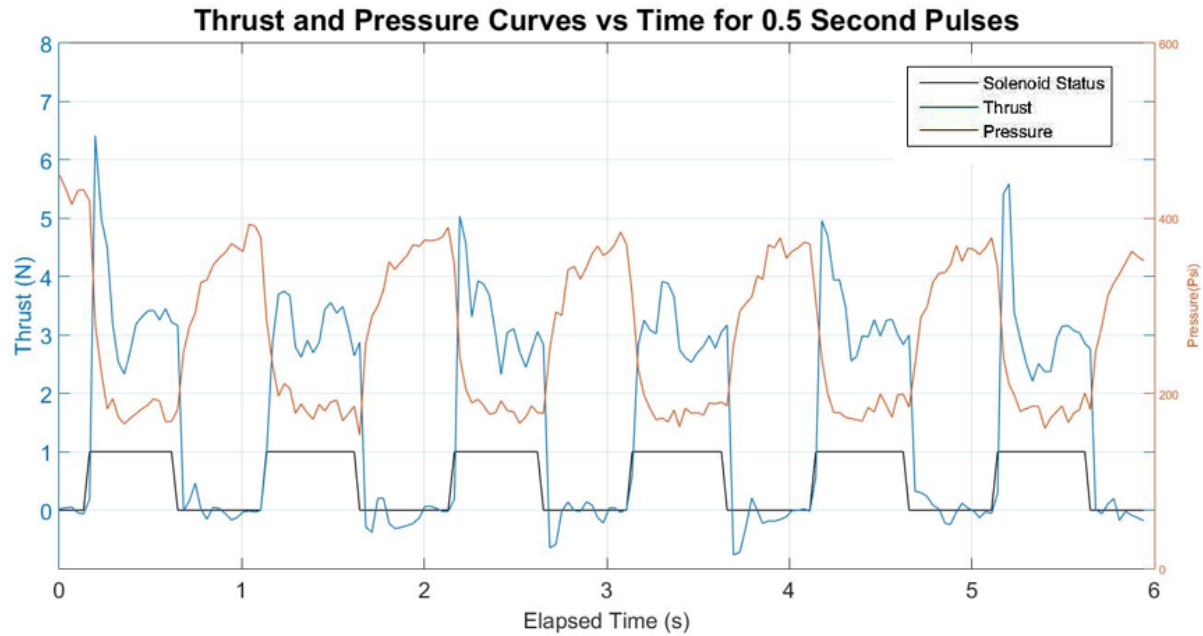


Figure 134: Thruster and Pressure vs Time, 0.5 Second Pulses

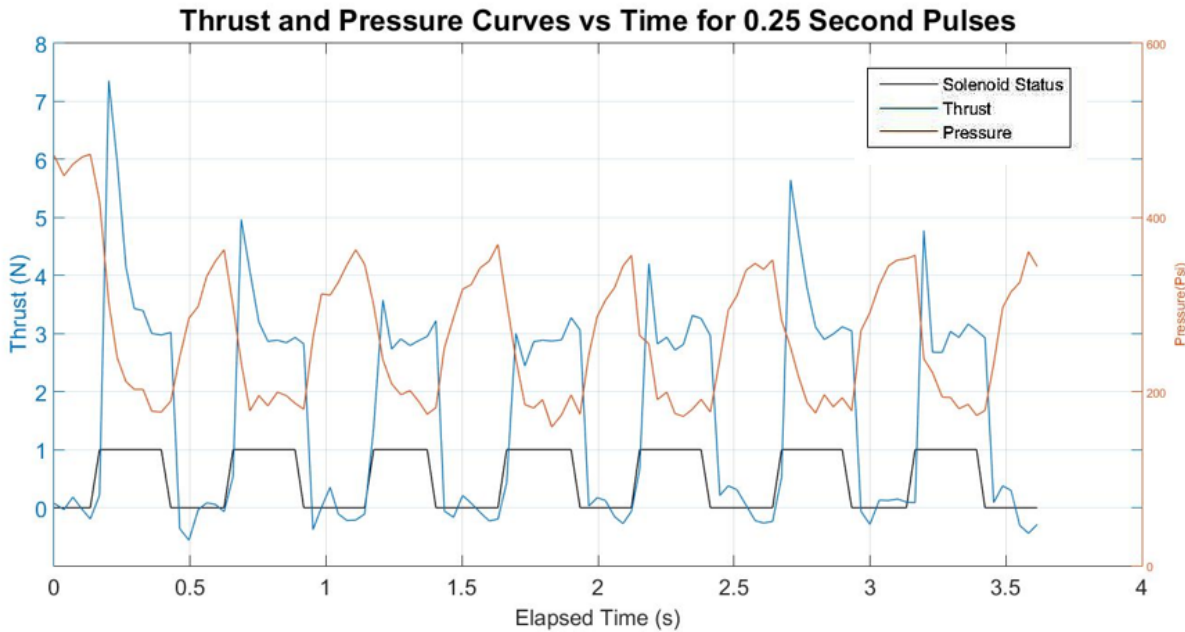


Figure 135: Thruster and Pressure vs Time, 0.25 Second Pulses

Analyzing the results of Figures 133, 134, and 135, a drop in static pressure was observed for each time stamp in which the solenoid was opened (from 450 psi tank conditions before the first pulse to approximately 200 psi during actuation). However, in order to achieve the desired thrust of 7.8 N (the 4X design thrust estimated by the team in PDR to allow our control scheme an ample operating range), consistent 450 psi static pressure is necessary at all stages of thruster operation.

Intuition points to an insufficient volumetric flow rate from the regulator as the culprit of this issue that in turn delivers an average thrust value that is less than half of the design value (3.2 N vs 7.8 N expected). However, it can also be seen by comparing the figures that regardless of the pulse length, the average thrust value of approximately 3.2 N was consistently provided for each pulse. This shows that the total pressure climb when the solenoid is closed (which varies over the three figures due to the pulse length of time) does not drastically affect the thrust obtained from each subsequent pulse.

To resolve the low thrust value, a higher volumetric flow rate regulator was ordered (prior to CDR) and installed on the test stand. After repeating the one second pulse test with this new setup, a 5 N thrust was consistently measured with a pressure drop to 300 psi as opposed to 200 psi. The 5 N thrust matches with a high degree of fidelity the design value for a 300 psi condition from the MATLAB design script, a result which we feel helps validate our fabrication methods, design script, and thruster test stand instrumentation. The results of this test can be seen in Figure 136 with the measured thrust in blue and the expected thrust (calculated by inputting the measured pressure into our MATLAB analysis script) a dotted line.

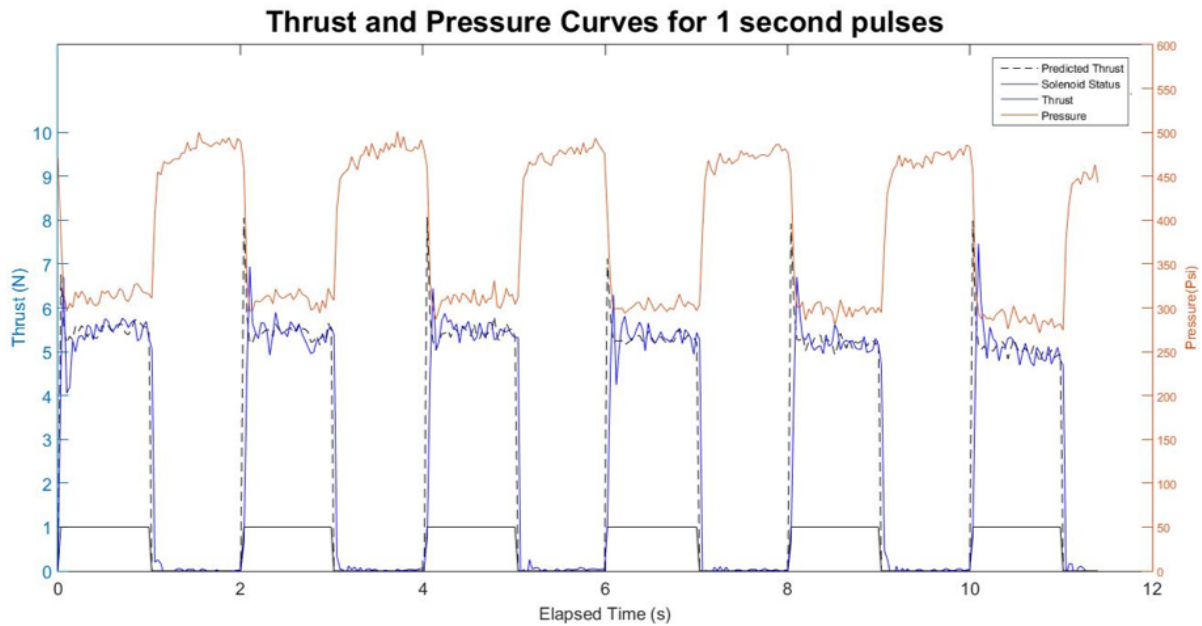


Figure 136: Thrust and Pressure vs Time, 1 Second Pulses, High Flow Regulator

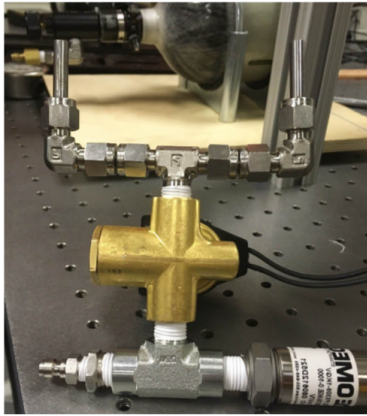
Table 23 shows a comparison between the original (pre-CDR) and current regulator for the single second test.

Table 23: Single Nozzle Thrust Comparison for Two Regulators

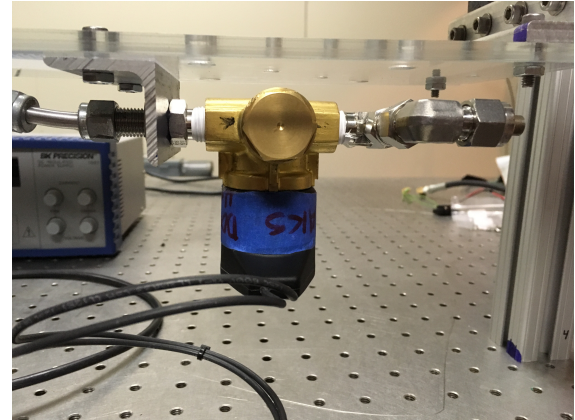
Regulator	Thrust (N)
Original	3.2 N
2nd (Ninja)	5.0 N

Furthermore, this test stand was also used to analyze the thrust of two nozzles. Figure 137 shows the two thruster arrangement while Figure 138 shows a continuous actuation test for this dual thruster setup at a tank pressure of 2000 psi.

While adding a second thruster intuitively should have yielded double the thrust of a single nozzle, a value of approximately 6.5 N was measured for two thrusters (see Figure 138). After team research into flow characteristics of propellant tank regulators, VADL feels that this lower value is due to a pressure "droop" inherent to many regulators where the delivery pressure decreases with increasing flow rate. By adding the second thruster, we increased the flow rate of air through the regulator, and this resulted in a corresponding decrease in delivery pressure. This decrease in pressure led to a lower mass flow rate through each thruster individually. It should be noted that this analysis assumes that the thrust from a given thruster is a function of flow rate alone, which VADL feels is a valid assumption given that we designed our nozzles for perfect



(a) Two Thruster Arrangement



(b) Dual Thruster On Stand

Figure 137: Dual Thruster Arrangement, On and Off Test Stand

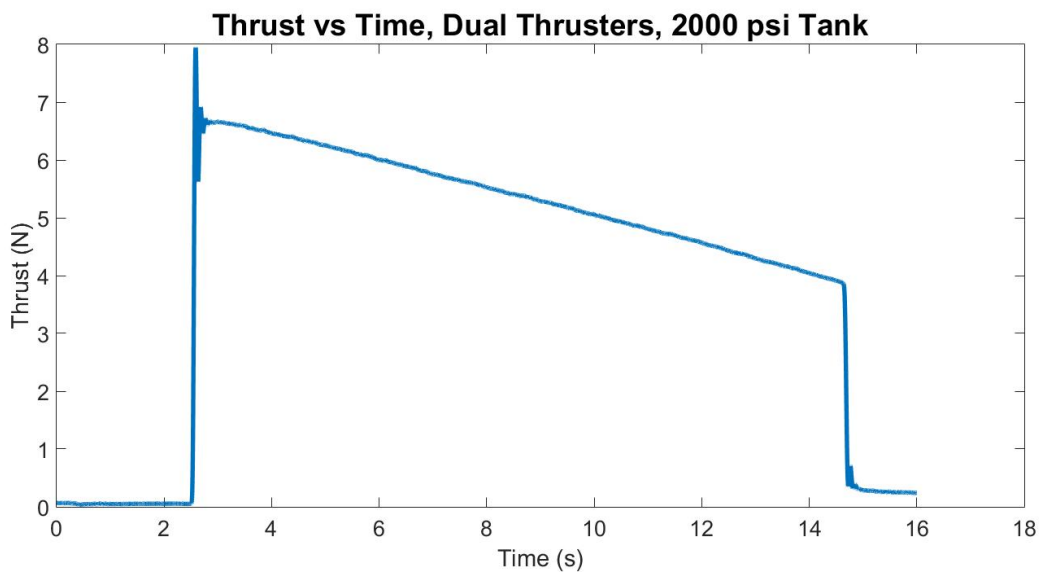


Figure 138: Thrust vs Time, 2000 psi

expansion and have not modified the thruster geometry or stagnation temperature over the course of these tests.

To address this issue, the tank pressure was incrementally increased from 2000 psi to 3000 and 4000 psi (ending here because the recommended operating pressure from the manufacturer is <4500 psi). Continuous actuation tests of roughly 12-15 seconds were performed for each pressure condition, and this resulted in a total increase of approximately 1.5 N for the highest pressure condition of 4000 psi (see Figure 139 and Table 24 for more details on the experimental results).

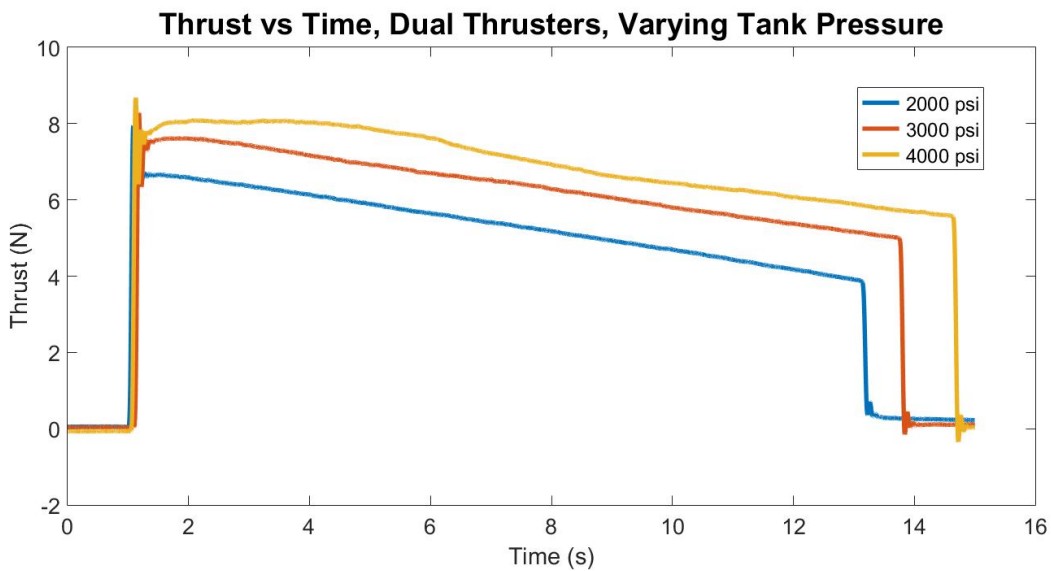


Figure 139: Thrust vs Time for Dual Nozzle Setup and Increased Tank Pressure

Table 24: Varying Pressure Thruster Test Summary

Tank Pressure (psi)	Number of Thrusters	Thrust (N)
2000	1	5.0 N
2000	2	6.5 N
3000	2	7.5 N
4000	2	8.0 N

While the increase of tank pressure succeeded in obtaining higher thrust, regulator droop still persisted, limiting the thrust output of our nozzles. After further analysis, the team determined that the second regulator (while performing better than the first) still had limitations in flow capabilities primarily from the small orifice at the regulator output. This orifice was designed to be suitable for lower flow hobby applications, thus limiting the mass flow and therefore thrust far too much for our applications. To resolve this, the team ordered a third and final regulator

(Custom Products CP Air "Super High Flow" 450 psi Regulator). This regulator is specifically designed for high flow capabilities and rugged applications with design modifications such as multiple and larger regulator outlet orifices. A comparison between the orifices of the regulators can be seen in Figure 140.



(a) 2nd Regulator Outlet Orifice



(b) Final Regulator Outlet Orifice

Figure 140: Regulator Outlet Orifice Comparison: 2nd vs Final Regulator

To characterize the performance of this new nozzle, tests were performed on the test stand with two nozzles and 4000 psi for both regulators to compare thrust outputs. The comparison of output thrust values for these two regulators can be seen in Figure 141.

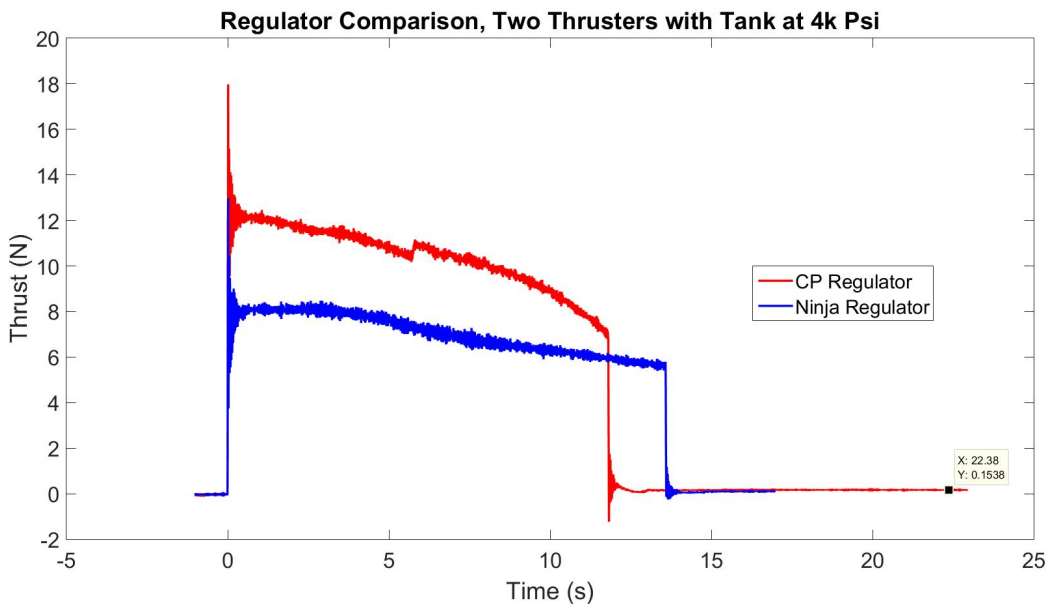


Figure 141: Thrust vs Time for Dual Nozzle, 2nd vs Final Regulator

This change in regulator alone gave the team an approximately 4 N increase in thrust, a much larger gain than the increases in tank pressure. After analyzing the results of this measured

thrust's incorporation into our payload experiment simulations (as well as flight data obtained from our onboard IMU for both the fullscale launch and subscale relaunch), we feel this thrust increase will help us achieve a safe and successful payload experiment during post-MECO and pre-apogee flight (see Section 3.7.5 for more details regarding this analysis). For a revised visual of the thrust comparisons for all pressure and regulator components, see Table 25. The final row of this table represents our final conditions that have been integrated for flight.

Table 25: Total Thruster Test Summary

Tank Pressure (psi)	Number of Thrusters	Regulator Iteration	Thrust (N)
2000	1	Original	3.2 N
2000	1	2nd (Ninja)	5.0 N
2000	2	2nd (Ninja)	6.5 N
3000	2	2nd (Ninja)	7.5 N
4000	2	2nd (Ninja)	8.0 N
4000	2	Final (CP)	12.0 N

The design and testing of this refined thruster system have taught the team many lessons regarding gas dynamics and hardware limitations, knowledge that will be highly useful in our future engineering endeavors.

7.1.2 Electronics Testing

7.1.2.1 Avionics Testing

Electronics testing comprises several processes over multiple systems. First, the more simple avionics system will be examined. The avionics system includes a rather intuitive single-board recording altimeter package powered by standard 9V batteries. A screw switch interrupts this power supply until the device is necessary for flight use. Two altimeters are used for redundancy. Each altimeter has leads to internal blast charges used for vehicle separation and parachute deployment as part of recovery operations. This system is pictured below in Figure 142. Testing this system requires validation of all electrical connections to the Stratologger CF altimeter (pictured in Figure 143), calibration of altimeter units, and verification of altimeter blast charge detonation altitudes and function. These processes are detailed in Table 26. They center around electrical testing, but stray into some mechanical systems where necessary and relevant.

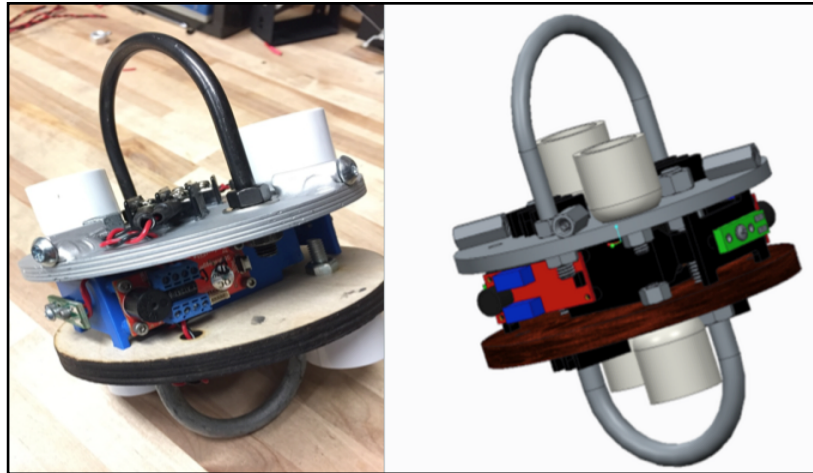


Figure 142: Avionics Bay

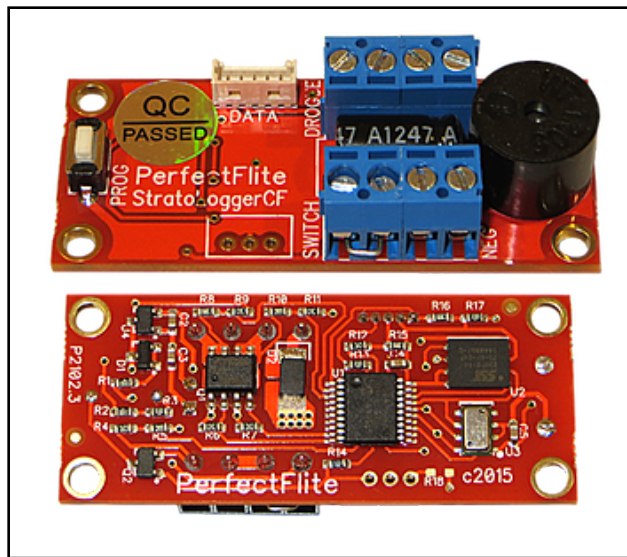


Figure 143: Stratologger CF Altimeter

Test	Procedure	Test Result	Recurrence	Modifications (if any)
Avionics battery voltage check	Using a multimeter of known calibration in DC voltage mode, place leads with proper polarity into the terminals of the 9V battery to be used, observe	Above 9.0 V: flight ready	Each time before use	Be sure to use a new battery for each flight
Avionics switch continuity check	Using a multimeter of known calibration in continuity mode, place leads across newly-soldered ends of screw switch, observe for consistent beep	Good for both switches	After any switch installation	
Avionics switch integrity check	Tighten screw switch with appropriate phillips head driver, not overtightening. Remove, observing for a snug fit, and examining the terminal for damage after removal	Good for both switches	Before any flight	
Avionics blast charge connection continuity check	Using a multimeter of known calibration in continuity mode, place leads across newly-connected ends of screw terminals and associated Stratologger screw terminal, observe for consistent beep	Good for all eight connections	After any blast lead installation	
Avionics blast charge connection integrity check	Firmly tug on each screw terminal connection to ensure that they will no slip loose under g-loading conditions or flight vibrations	Good for all sixteen connection points	After any change in blast lead connection	Be sure to use consistent terminals for reliability
Avionics calibration and function test	Program Stratologger CF for activation at flight altitudes expected for fullscale launch. Place stratologger in precision vacuum chamber, lowering pressure until the expected pressure for the given altitudes is reached, examine data after experiment to check linearity and accuracy of avionics data collection.	Within 5% for both altimeters	Before any flight	
Avionics pre-flight function check	With all avionics installed in the flight vehicle as they would be on launch day, turn on all elements and observe for pre-programmed beeps indicating target altitudes and electrical function	Good for both altimeters	Before any flight	
Avionics deployment test	With blast charges and parachutes installed as they would be on launch day, and taking all necessary safety precautions for personnel safety and safety of the flight vehicle, detonate blast charges to test for successful deployment	Good for both charges	Before first flight	

Table 26: Testing Procedure and Results for Avionics

7.1.2.2 Payload Electronics Testing

Assessing functionality of payload electronics required several tests: some purely electrical, and others electromechanical. The mission critical portion of the payload electronics system is the custom fabricated BeagleBone Black cape that can be seen in Figure 144 below. This cape required hours of work by way of surface mount component installation and through-hole soldering. The small workspace greatly increased the likelihood of a short. Extensive testing was done with a multimeter to ensure continuity where continuity was desired, and to ensure no shorting where undesirable. Two iterations of board were required before a successful model was manufactured. A full testing protocol can be seen in Table 27.

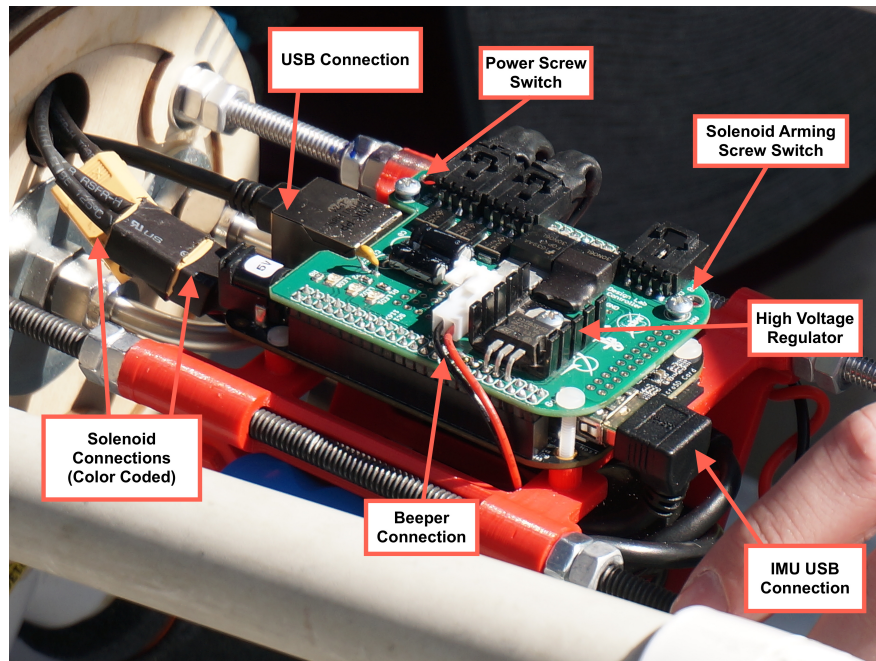


Figure 144: Payload Electronics at Fullscale Launch Test, Labeled

Test	Procedure	Test Result	Recurrence	Modifications (if any)
Payload electronics battery voltage test	Using a multimeter of known calibration in DC voltage mode, place leads with proper polarity into the terminals of the battery to be examined, observe	Above 12.25 V: flight ready	Each time before use	Be sure to test in appropriate connectors
Payload electronics series battery voltage test	Using a multimeter of known calibration in DC voltage mode, place leads with proper polarity onto the series battery leads	Above 25 V: flight ready	Each time before use	
Payload electronics beeper function check	Using a power supply set to slightly below 3.3 V, touch leads to exposed beeper connections on top of beaglebone	Audible tone flight ready	After fabrication	
Payload electronics power up check	Using a philips head driver, tighten the payload electronics power screw switch and observe for consistent blinking pattern of blue light 1 and 2s on BBB board, and for the red light on the cape to be lit.	Visible confirmation: flight ready	Each time before use	If lights blink in inconsistent pattern, BBB may have booted from flash instead of SD
Payload electronics endurance heat check	After powering the payload electronics assembly, leave it running until battery depletion while logging performance, later analyzing this performance for heat-related issues	Post-data analysis: flight ready	After fabrication	
Payload electronics communication check	Plugging the BBB into the USB port of a computer with an open terminal, ping 192.168.7.2 to ensure that the BBB powered up correctly	Positive ping result in terminal: flight ready	Each time before use	If failure, attempt to reboot from SD
Solenoid arming screw switch check	After using a philips head driver to snug the solenoid arming switch, and using a multimeter of known calibration in DC voltage mode, place leads with proper polarity onto the leads of the mosfet	Failure post-fullscale test flight	Each time before use	Issue resolved, switch replaced and tested for function
Payload electronics solenoid LED activation test	Having flashed flight software to the BBB, look for the LEDs in line with the relevant solenoid activation circuit to light up when triggered	Visual confirmation: flight ready	After fabrication and during endurance reliability testing	
Payload electronics solenoid actuation test	Having flashed flight software to the BBB, and ensuring that the solenoids are not seeing pressure, listen for quidble clicking of solenoids signalling proper function.	Audible confirmation: flight ready	Each time before flight	
Payload electronics full integration FRAME test	After assembling the flight vehicle and subsystems exactly as they would be on launch day, flash flight software and mount assembly into FRAME. Watching for visual confirmation of proper experiment execution	Visual confirmation: flight ready	Ongoing testing process	

Table 27: Testing Procedure and Results for Payload Electronics

As mentioned in Table 27, several full electronics integration test were completed on the FRAME prior to flight. Viscous drag in the rotation axis was simulated by a separate motor control microprocessor and servo controller. The rotation as sensed by the software, prompted the electronic state machine to enter one solenoid action mode or another depending on direction. The flight vehicle spun and then oscillated on the test stand as was expected of successful tests. After this test was conducted multiple times with some variation of condition the payload electronics were validated for flight.

7.1.3 Software Testing

Software reliability is one of the most essential aspects of this entire project. Without robust testing protocols we would be unable to confidently fly our rocket, actuate the solenoids, and receive usable IMU data. The testing protocol developed allowed us to individually test each aspect of the software and then combine it all together to test the HLC. The following will outline the testing procedures and success criteria for the various software components

7.1.3.1 IMU

The IMU component was tested to verify its precision and reliability. For this test, the IMU simply plotted data for roll, pitch, yaw, and xyz acceleration. The IMU was held in the configuration it would be in during flight and, with the payload electronics sled in hand, the team would shake, spin, accelerate, and vibrate the IMU. Tests were done with random motions as well as predefined and carefully executed motions to verify the precision of this component.

Success Criteria

1. Recorded data matches applied movements
2. No time delays or slow operations
3. No failure under stressful conditions
4. Proper direction and scaling of values

7.1.3.2 Solenoid Actuator

The solenoid actuator component was tested to verify its ability to actuate the solenoids based on a predefined pulse pattern. A simple control component was written such that the user could input the number of pulses, the initial delay, the pulse length, and the delay length. This was deployed to the BeagleBone to light up an LED and was proven successful. As far as software is concerned, if this LED lit up, then it could be assumed that the solenoid would fire as well.

Success Criteria

1. Actuation of LEDs in accordance with pulse pattern
2. Proper directional control based on thruster direction
3. No delays or slow operations

7.1.3.3 High Level and Bang-Bang Controllers

Testing the control components can only occur once the IMU and solenoid actuator components have also been tested, as to allow for isolation of the variables for any issues that may arise. In testing the HLC, it was necessary to verify the triggering events that move the software from one state to another, as well as the activation of the solenoid. To do this, the IMU was connected to a BeagleBone and LEDs were connected to the solenoid pins. Simply through a user-inputted upward acceleration of the IMU followed by a deceleration, all of the acceleration triggers could be verified. At MECO, the HLC must sense the angular velocity and actuate the solenoid in accordance with this direction. This angular velocity could also be applied by the user and verified for accuracy by examining the plots. By watching the LED and ensuring that its pulse pattern matches the desired pulse pattern, it could again be assumed that the same would occur during flight.

Success Criteria

1. Precise sensing of takeoff and MECO
2. Proper detection of initial angular velocity
3. Sensing of a 4π radian rotation, and toggling of solenoid
4. Correct signal sent to solenoid in accordance with rotation direction
5. No delays or slow operations

The output of the solenoid pin is automatically plotted in ROSMOD as seen in Figure 145. For incorporating this software into the full rocket integration tests on the FRAME, a time based enable feature was added to bypass the acceleration thresholds and begin the pulsing cycle after a user-defined initial delay. The goal of this was not to verify the software, but to use the software to verify the hardware, the FRAME, and the thruster system.

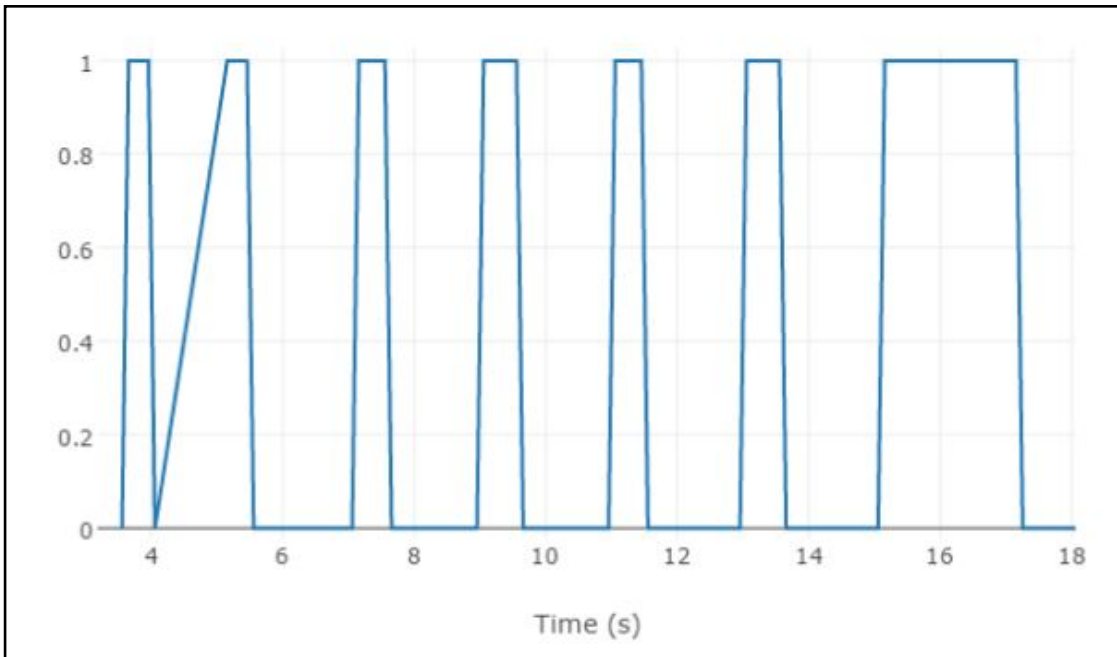


Figure 145: Solenoid Pin Value vs. Time

7.1.4 The FRAME

7.1.4.1 Introduction

In order to ensure a successful payload experiment, extensive testing is required to develop and refine the algorithms that control the attitude of the flight vehicle. Specifically, the payload must be able to precisely control the angular position of the rocket during flight such that it is able to complete two full rotations and then return to its initial angular position. This entire operation must occur in the eight seconds between MECO and apogee, necessitating a precise control algorithm to ensure efficient execution.

7.1.4.2 Purpose

The FRAME, seen in Figure 146 will allow for roll control algorithms to be developed and refined in the convenience of a laboratory setting. The algorithms will govern the actuation of two solenoids, which each activate a thruster couple to apply moments to rotate the flight vehicle. In order for the testing and refinement of these algorithms to be effective, the test and flight environments must be as similar to one another as possible. Accordingly, The FRAME must allow for flight conditions to be recreated in a ground-based laboratory setting.

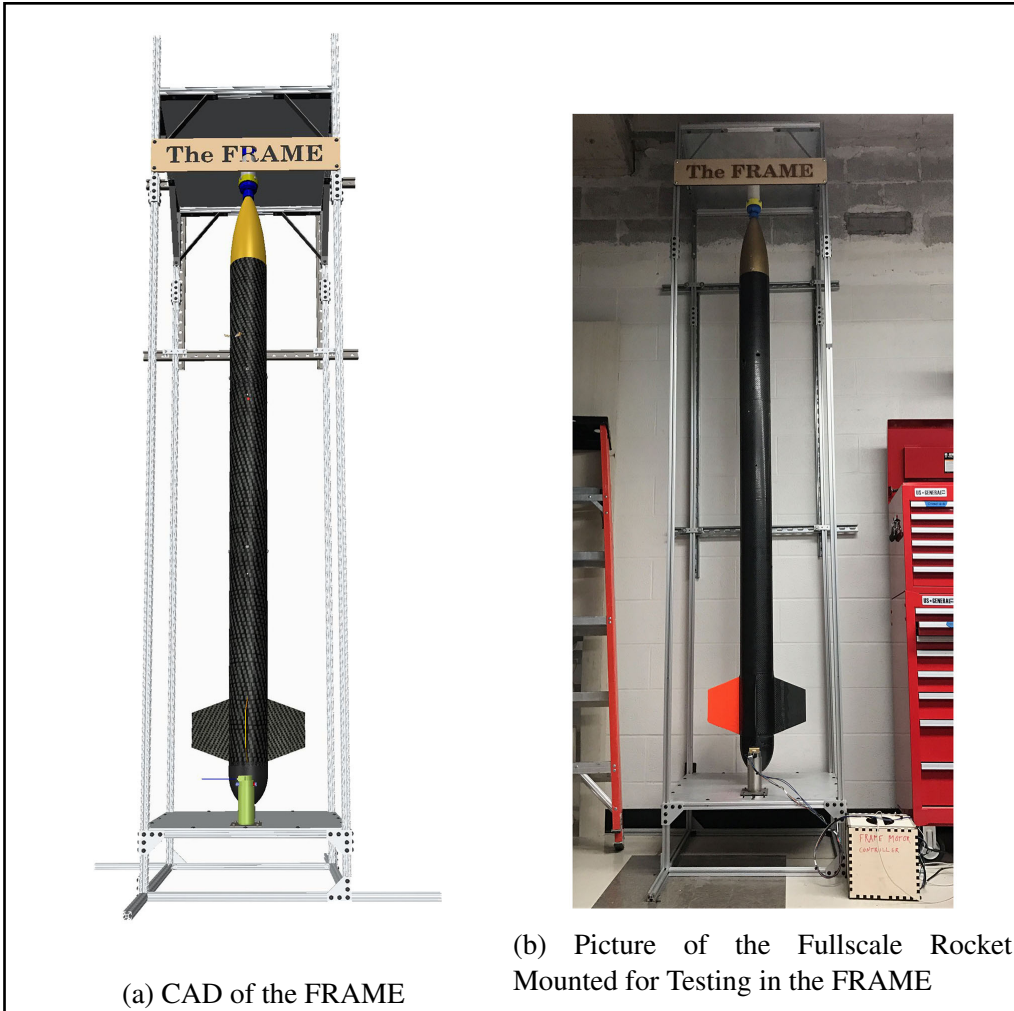


Figure 146: CAD and Picture of the FRAME

7.1.4.3 Advantages

Due to the apparent difficulty of modeling the dynamic flight environment of a rocket in a laboratory setting, it may seem more logical to conduct payload testing on practice flights. However, the cost, safety risks, and logistical difficulties associated with rocket launches make ground-based testing a much more attractive option. Specifically, it is estimated that a full rocket launch can cost as much as \$500.00, with primary contributors being transportation to a remote launch location and the cost of the single-use motor. Additionally, a single launch can take as long as 6 hours to properly execute, as preparation, transportation, and careful launch operation each take a considerable amount of time. Furthermore, the considerable safety risks of handling blast charges and rocket motors must be taken into account.

Testing the payload in a controlled, ground-based laboratory environment solves all of these problems. The total cost of The FRAME is less than the cost of two launches, and each test can be performed in approximately 10 minutes. Furthermore, the safety hazards associated with the FRAME are negligible when compared to those associated with a launch. Clearly, pursuing a

ground-based testing solution for the payload is preferred, despite the difficulties associated with proper execution.

7.1.4.4 General Criteria For Success

While it is easy to talk about accurately replicating a rocket's flight environment in a ground-based laboratory setting, it is quite another matter to actually accomplish such a feat. In order to understand exactly what must occur in order to make this happen, it is important to get a sense of the important elements of the rocket's flight environment. The following list outlines the three most important criteria that were considered when designing the FRAME to ensure that it accurately modeled the flight environment.

1. Allow for frictionless rotation of the flight vehicle
2. Ensure a vertical orientation of the flight vehicle
3. Simulate the effects of aerodynamic damping on the rotation of the flight vehicle

Perhaps most importantly, the FRAME must allow for frictionless rotation about the main axis of the flight vehicle. This is a critical feature, as the roll control algorithms can only be monitored if the payload can cause the flight vehicle to rotate. The frictionless nature of this rotation is vital, as the flight vehicle will experience no opposition to its rotation during flight other than aerodynamic forces. Additionally, the flight vehicle must maintain a vertical orientation during testing, as it will throughout the payload experiment window of the flight. This vertical orientation during flight is ensured by the selection of a high impulse motor that burns for a short duration. Simulations and subscale flight have confirmed this expected flight path, and the FRAME must mirror this condition in order to properly model the flight environment. Finally, the aerodynamic forces that will act on the flight vehicle at high velocities must be properly understood and incorporated during testing. The FRAME must be able to accurately reproduce the rotational damping effect of air resistance. While there will be some inherent drag when testing in a ground-based laboratory setting, the tremendous airspeed experienced by the flight vehicle during the payload experiment significantly increases the rotational drag as discussed in Section 3.7.3.3. Accordingly, this behavior must be modeled during testing in order to ensure that the roll control algorithms are optimized to function in a realistic flight environment.

7.1.4.5 Design Choices

Frictionless Rotation In order to ensure that the three primary criteria for successful tests are met, a number of design choices were made when building the FRAME. First, in order to ensure frictionless rotation, a bearing system was constructed using radial and thrust bearings. As can be seen in Figure 147, rotation about the main axis of the flight vehicle aligned with a vertical shaft, highlighted in blue. The shaft is supported by two radial bearings, which are highlighted in green. A thrust bearing, highlighted in red, supports vertical loads, ensuring smooth rotation even when supporting the full weight of the flight vehicle. The entire assembly is contained within a custom machined bearing cup, highlighted in yellow, which is bolted directly to the bottom plate of the FRAME to ensure stability.

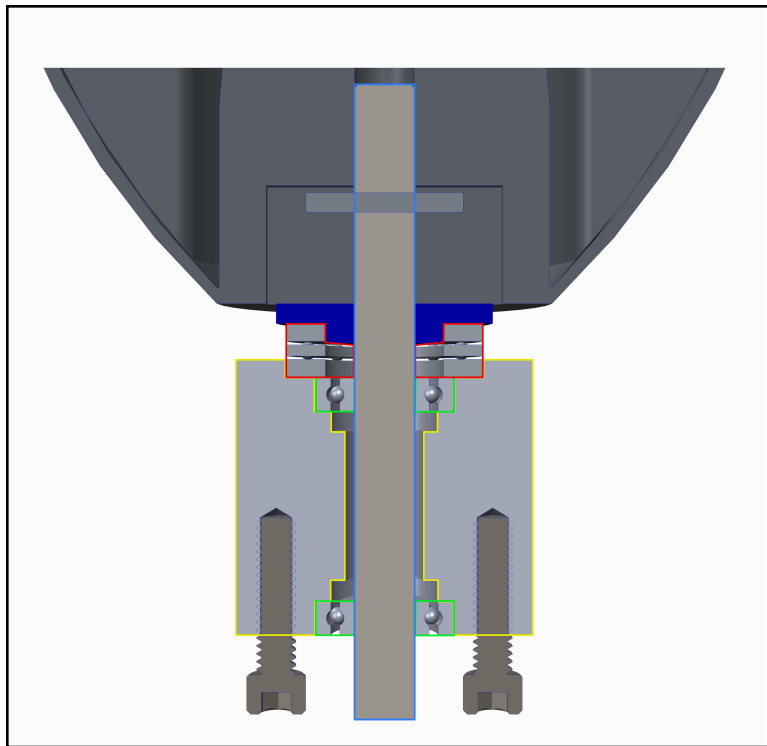


Figure 147: Cross Section View of Bearing System Enabling Frictionless Rotation

Vertical Orientation To preserve the vertical orientation of the flight vehicle during testing, a dual support system was implemented, constraining the nose cone and tail of the rocket. The top and bottom support systems can be seen in Figure 148. These independent supports are each aligned with the central axis of the flight vehicle and bolted to custom machined aluminum plates. Each of these plates features four identically placed holes that are accurate within hundredths of an inch, ensuring perfect vertical alignment of the two support systems. In order to ensure that the flight vehicle aligns precisely with each of the support systems, both were designed to specifically interface with components of the rocket.

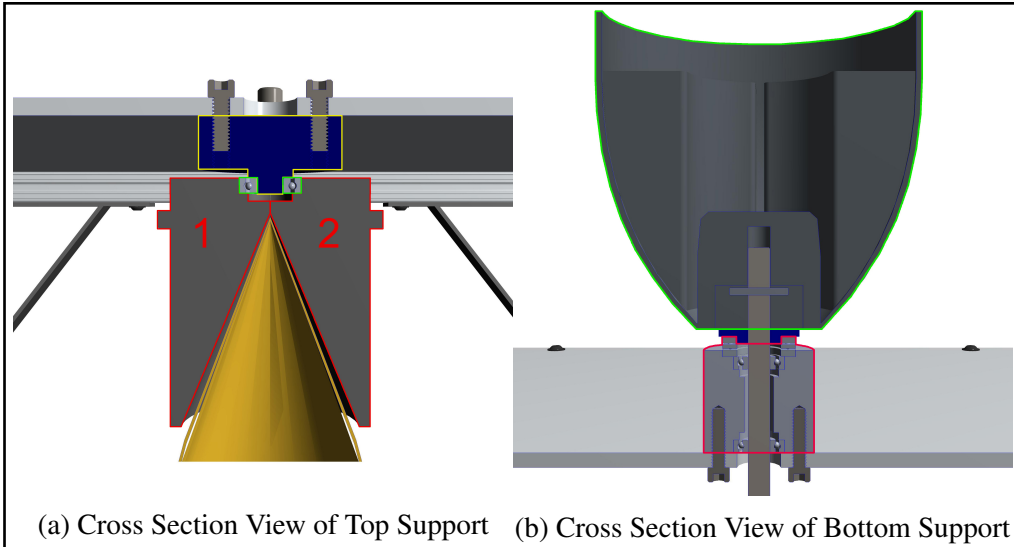


Figure 148: Top and Bottom Supports Enabling Vertical Orientation

The top support features a nose cone gripper, seen in Figure 148a. This two-part rapid prototyped component, highlighted in red, encloses the nose cone of the rocket, and is clamped into place during testing. It is clamped around a radial bearing, highlighted in green. The radial bearing is fit onto a rapid prototyped part, which is highlighted in yellow, and is bolted to the top plate of the FRAME to secure the top support in place. The conical interior of the nose cone gripper acts to center the tapered nose cone with the axis of rotation of the top support, while the clamp allows for easy assembly as well as a snug interface with the nose cone. Figure 148b shows the bottom support, which consists of a rapid prototyped fin gripper, highlighted in green, and aforementioned bearing assembly, highlighted in red. While the primary function of the fin gripper is to transmit torque to the rocket, it also serves to center the flight vehicle to ensure a vertical orientation. The central column of the fin gripper was specifically designed to fit snugly within the motor tube of the rocket. With the boat tail disassembled, the flight vehicle slides vertically down into the fin gripper, centering itself with the bottom support.

7.1.4.6 Motor Characterization

One of the essential requirements of the FRAME is the accurate simulation of the aerodynamic effects experienced by the rocket during flight. In order to accomplish this, a motor is used to apply resistive torques to the rocket during the experiment. The following section will outline the various hardware and software components utilized to accomplish this task.

System Overview Figure 149 shows a high-level overview of the motor control system. During FRAME testing, KSP and the IMU will be publishing various values necessary in calculating the resistive torque from aerodynamic effects to the BBB, which will calculate the output necessary to provide this torque. To simulate an analog voltage, the BBB sends a PWM signal to the op-amp, which provides a gain and offset, mapping this 0-3.3 V signal to a $\pm 5V$ signal. The output voltage of the op-amp is inputted into the motor controller, which provides a 2

A/V gain, mapping the input to a ± 10 output to the motor. This range will allow for sufficient counter-torque to resist entirely the torque from the thrusters, in addition to adding any disturbances the team wants to apply.

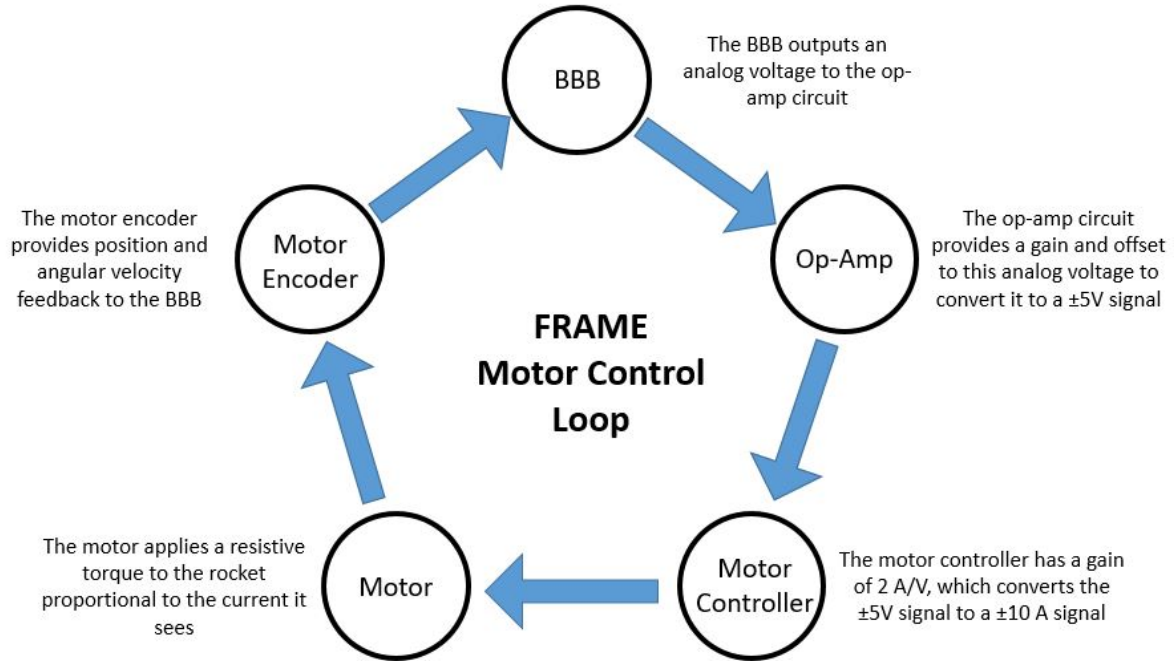


Figure 149: High-Level Overview of Motor Control System

Motor Selection There were various factors considered when selecting the FRAME motor, including maximum torque, maximum power, cost, size, encoder resolution, and reliability. Table 28 lists various quantities that are essential to have accurate motor characterization and control.

Operational-Amplifier Circuit In designing an op-amp circuit, two important values to calculate are the gain, m , and the offset, b . The gain is calculated using Equation (7.1) and the offset is calculated using Equation (7.2).

$$m = \frac{V_{out\max} - V_{out\min}}{V_{in\max} - V_{in\min}} \quad (7.1)$$

$$b = V_{out\min} - m * V_{in\min} \quad (7.2)$$

Where V_{in} is the output voltage from the BBB, and V_{out} is the output of the op-amp. From the gain and offset, the resistor values needed to fill in the circuit shown in Figure 150 can be calculated. These calculated values are ideal, and must be replaced with real resistors, which introduces error to the calculations. These resistor values were tested and adjusted to produce the optimal output voltage range.

Table 28: Brushed DC Motor Specifications

Motor Characteristic	Value
Supply Voltage	24V
Continuous Output Torque	0.35 N-m
Output Speed at Cont. Torque	2810 RPM
Current at Cont. Torque	6 A
Continuous Output Power	300 W
No Load Current	0.3 A
No Load Output Speed	331 (rad/s)
Peak Current	41 A
Peak Output Torque	2.9 N-m
Motor Torque Constant	0.0706 N-m/A
Motor Voltage Constant	0.0919 N-m/ \sqrt{W}
Rotor Inertia	0.000047 kg-m ²
Viscous Damping Factor	0.000017 N-m s

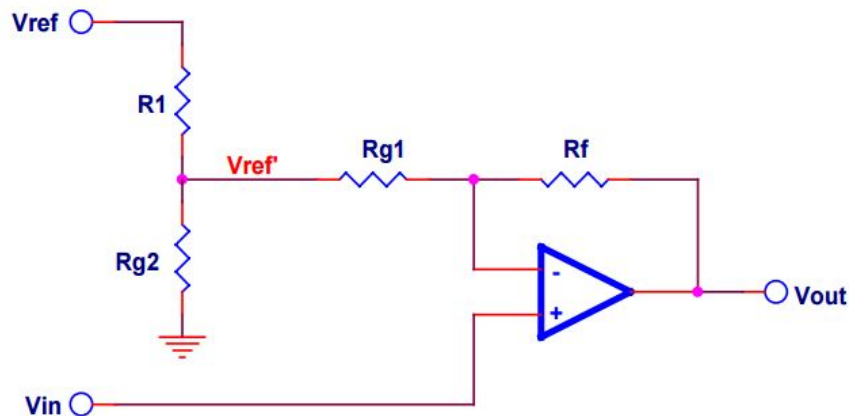


Figure 150: Operational-Amplifier Circuit for Motor Control

V_{ref} is a 5V supply voltage from the BeagleBone, and V_{in} is an input signal from the BeagleBone between 0 – 3.3V. The op-amp rails are powered via $\pm 15V$ output terminals from the motor controller. The output of this op-amp circuit is inputted to the motor controller, where a known gain of $2A/V$ will be applied. The output range of the op-amp circuit was calculated via nodal analysis to be $\pm 5V$, which corresponds to an output current of $\pm 10A$.

Linear Servo Motor Controller The Aerotech 4020 Linear Servo Controller (Figure 151) was chosen due to its reliability, compact design, high output power, low noise, and ease of operation. The controller consists of a 741-type pre-amplifier with rate and position loop compensation, driving a power amplifier configured in a current feedback mode. The goal for the use of the servo controller is to have accurate and reliable current control. This controller meets all design requirements.



Figure 151: 4020 Linear Servo Motor Controller

Motor Actuation Software and Hardware As with all software that VADL develops, the software for motor control was written, tested, and executed using ROSMOD modeling framework. The software loop for the entire FRAME system is outlined in Section 7.1.4. This section will focus on the motor actuation code, which sends a PWM signal to simulate an analog voltage value. The digital pin chosen has a voltage range of 0-3.3V, so a digital PWM signal with a 50% duty cycle will behave similarly to a 1.65V signal. The BBB does not come preconfigured with PWM ready GPIO pins, so the pin had to be prepared in the device tree overlay, which is where various initialization settings can be defined and edited for the GPIO pins.

To make a more stable output voltage, a low-pass filter (Figure 152) was added to the circuit before the op-amp. A low-pass filter passes signals with a frequency lower than a certain cutoff frequency and attenuates signals with frequencies higher than the cutoff frequency.

Where V_{in} is the unfiltered PWM signal from the BBB and V_{out} is the filtered signal to be sent to the op-amp circuit. The next step in the process is selecting and tuning the R and C values to optimize the system response. It is important to have a fast response time (time constant) and a steady-state with minimal fluctuations. To tune these values, a MATLAB script was used to plot the system response based on various input parameters. After multiple iterations, the chosen values were a $.15\mu F$ capacitor and a $5.3K\Omega$ resistor. The circuit has been tested and produces a consistent and unvarying voltage at a full range of duty cycle values.

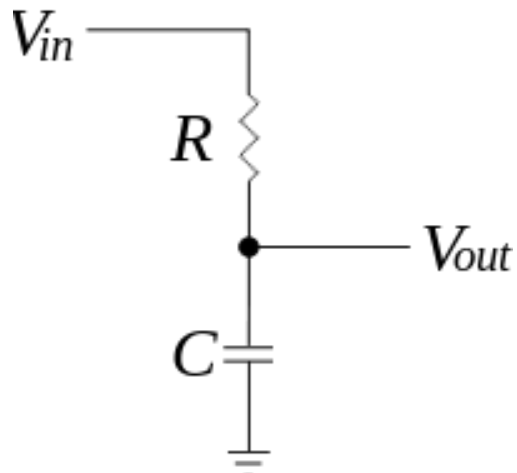


Figure 152: Low-Pass Filter Circuit

Motor Controller Containment The circuit was first designed on a breadboard where it was tested and tuned rigorously. Although this board provided the team with a great testing platform and ease of access to various components, it did not provide reliable connections and the team ran into numerous errors related to this issue. The team decided to design a protoboard shield for the microcontroller in order to organize the wires and ensure consistent connections (Figure 153).

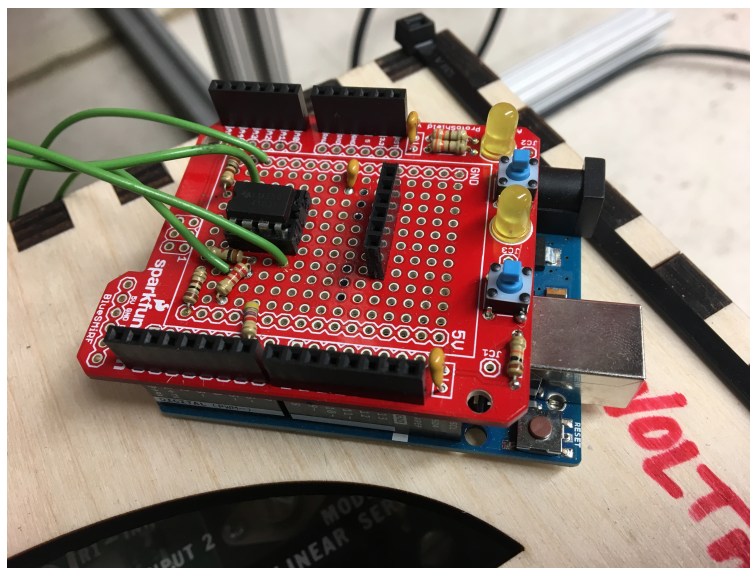


Figure 153: Microcontroller shield for FRAME motor control

This shield and the motor controller were placed inside a laser cut box (Figure 154, 155), which further served to contain the electronics. This doubled as a safety measure, as the high voltage wires connected to the motor controller were previously loosely guarded by a plexiglass cover. This box also provided ventilation holes for the motor controller and access holes for the wire connections. A switch was also placed in series with the motor as a safety mechanism. This allows the team to quickly shut off the motor in the case that the motor is actuated when it should

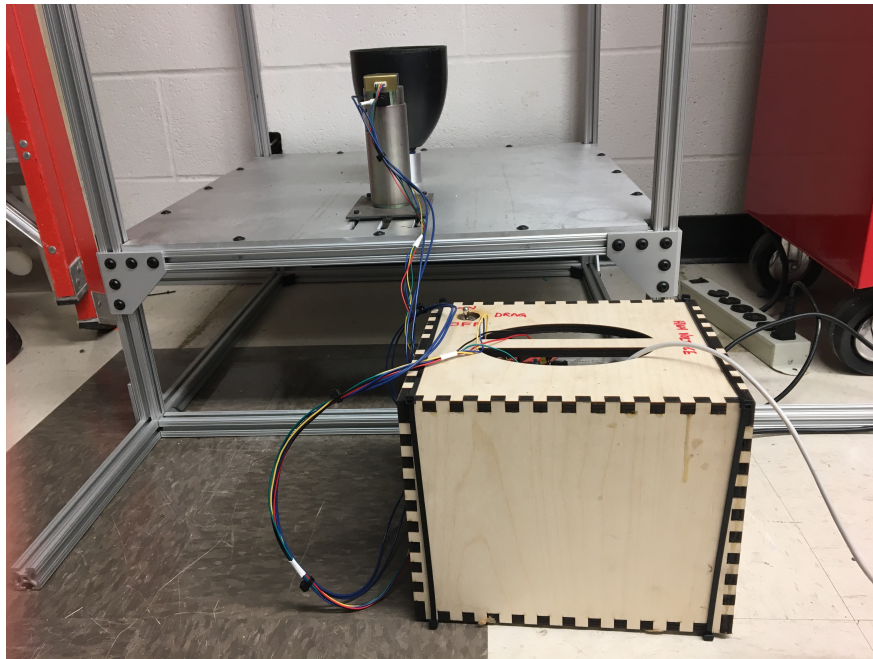


Figure 154: Motor Controller Containment

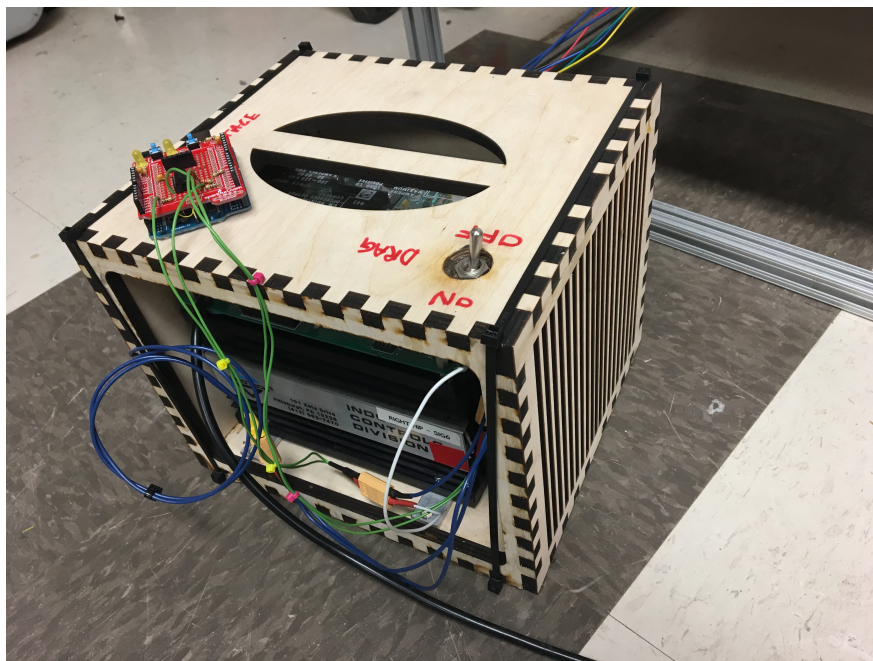


Figure 155: Motor Control Containment

not be. This feature initially served as a testing mechanism, to allow for rapid variation in the software, however the team realized quickly that a motor disconnect switch was essential to the overall safety of the system.

7.1.4.7 Torque Transmission

The aerodynamic damping torque is physically applied via DC motor, seen in Figure 156. The motor is coupled to the shaft of the bottom support via a timing belt with a gear ratio of 3:1 to allow for minimal power consumption while delivering the necessary torque. A picture of this linkage can be seen in Figure 157.



Figure 156: Picture of DC Motor Used to Simulate Aerodynamic Damping via Torque Inputs

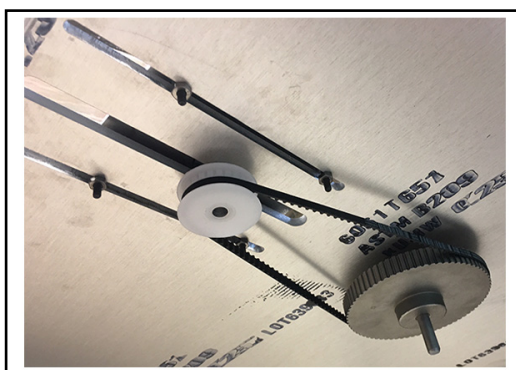


Figure 157: Picture of Pulley and Timing Belt Linkage Used to Transmit Torque from the DC Motor to the Shaft of the Bottom Support

The torque is transmitted from the motor through the timing belt to the vertical shaft. From there, the torque is transferred to the rapid prototyped fin gripper, which can be seen in Figure 158 highlighted in green. To facilitate torque transmission from the shaft to the fin gripper, a cross pin, highlighted in red in Figure 158a, was press fit through the top of the shaft, which is highlighted in yellow. In addition to serving the previously mentioned function of aligning the flight vehicle

in a vertical orientation, the fin gripper was specifically designed to transmit torque from the shaft of the bottom support to the flight vehicle. Four slots were designed to snugly grip each of the four fins, through which torque can be transmitted. Figure 158b illustrates how the tail of the flight vehicle fits into the fin gripper. The dotted red lines show the path of the fins as they plunge into the fin gripper. It is important to note that the portion of the fins that interface with the fin gripper are between the airframe and motor tube of the rocket. In order to access them, the boat tail of the flight vehicle must be removed during testing. Overall, the fin gripper facilitates the transmission of torque from the DC motor to the flight vehicle, which is needed in order to model the aerodynamic drag present during flight.

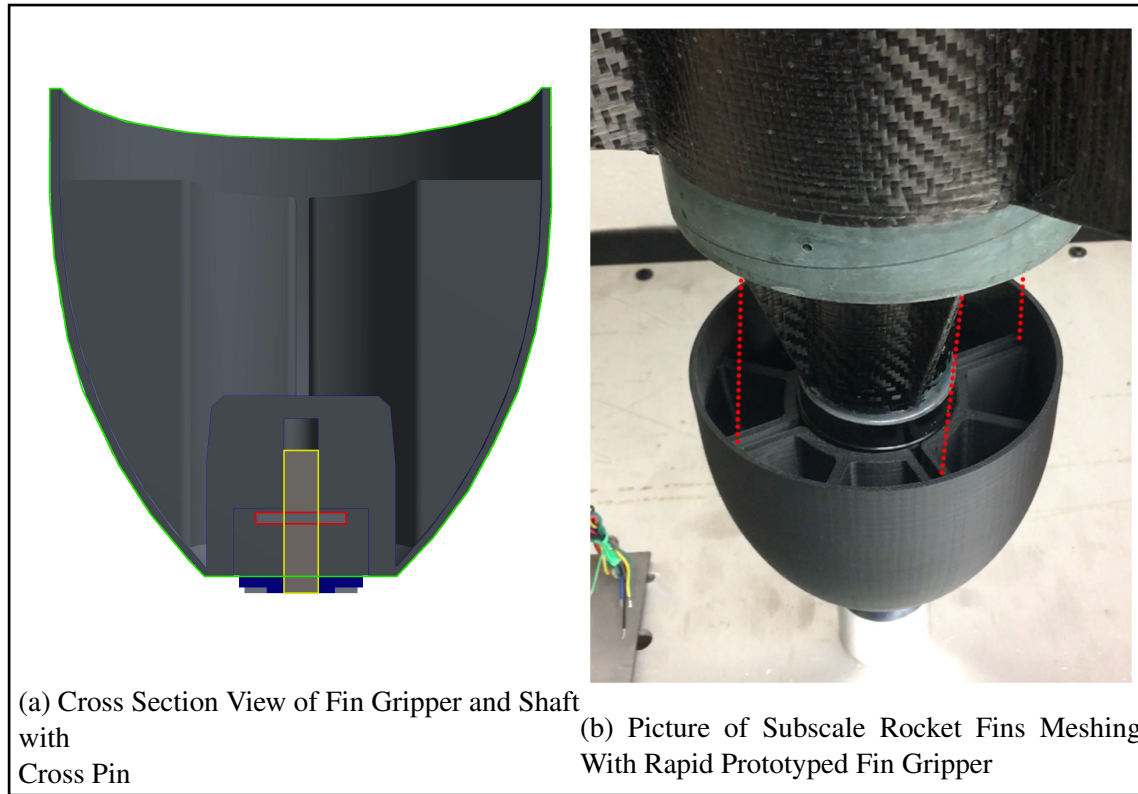


Figure 158: Fin Gripper Used to Transmit Torque to the Flight Vehicle

Using Kerbal Space Program for Real-Time Aerodynamic Modeling To produce the torque required to successfully emulate in-flight conditions, Kerbal Space Program (KSP) and ROSMOD are used. KSP is a flight simulation software with reliable physics that allows VADL to import CAD models of the rocket and assign empirically-derived material and aerodynamic properties to various parts. ROSMOD is the VADL-developed modeling and execution environment for software-integrated systems as discussed in Section 4.5.

The exact same software that was used to control the solenoid activation during flight, described in Section 4.5, is used during the FRAME testing. The high level diagram of this system is shown in Figure 159a. However, a few modifications to this software are made for ground-based testing. First, instead of using acceleration to sense takeoff and initiate the roll control algorithm, KSP's

accelerometer on the virtual rocket is used. Also, since the rocket on the frame obviously experiences no axial velocity, the motor has to be actuated to provide the correct damping torque. The high level controller (HLC) in ROSMOD is thus configured to receive vertical speed and atmospheric density input from KSP as well as rotation inputs from the IMU and calculate necessary damping torque. The HLC is then programmed to supply the necessary current to the motor to produce the equivalent torque, as well as apply point forces to the virtual rocket in KSP to make it spin synchronously with the real rocket. The high level diagram for the new software system for ground-based testing is shown in Figure 159b.

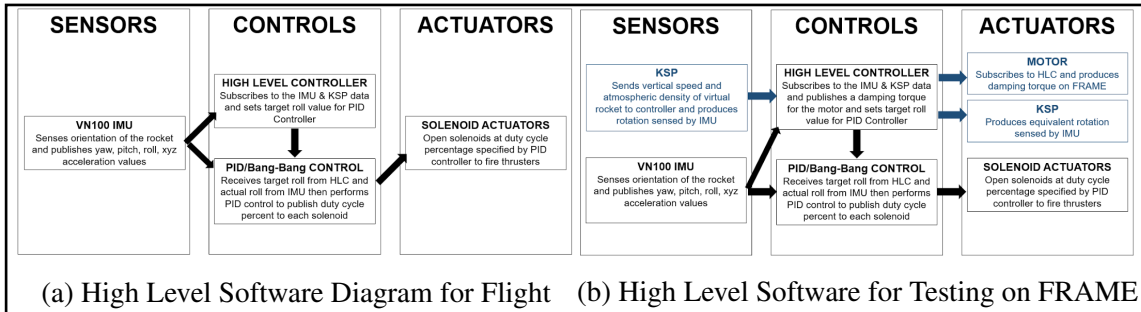


Figure 159: Comparison of High Level Software Diagrams between Testing and Flight

Equation 7.3, derived in Section 3.7.3.3, shows how to calculate damping torque to rotation as the rocket ascends.

$$\begin{aligned} \tau_d &= \tau_q + \tau_s + \tau_{jf} \approx F_{jf}(\tau_q + \tau_s) \quad (7.3) \\ \tau_q &= \frac{1}{2} N C_{d,fin} Z_{fin} \rho v_d \omega \\ \tau_s &= \frac{1}{2} C_f \rho A_{cyl} v_d \omega R \end{aligned}$$

Where τ_q is the torque produced due to pressure drag, τ_s is the torque produced due to skin friction drag, and τ_{jf} is the torque produced due to jet-fin interaction, which is assumed to be zero for this purpose since it is much smaller than the other two and not currently computable in KSP. Table 29 defines the other variables used in Equation 7.3.

Table 29: Damping Torque Equations Symbol Definitions

Symbol	Definition
N	Number of fins
$C_{d,fin}$	Drag coefficient of fins
$C_{d,f}$	Skin friction drag coefficient of rocket cylinder
Z_{fin}	Fin geometry constant (m^4)
ρ	Atmospheric density of air (kg/m^3)
R	Radius of rocket (m)
A_{cyl}	Surface area of rocket cylinder (m^2)
ω	Angular velocity (rad/s)
v_d	Vertical speed (m/s)

As the real rocket is spinning on the FRAME, and the simulated rocket is flying in KSP, ROSMOD continuously calculated the damping torque that a real rocket would experience and applies that torque to the motor. The flow of information between the FRAME, ROSMOD, and KSP is shown in Figure 160.

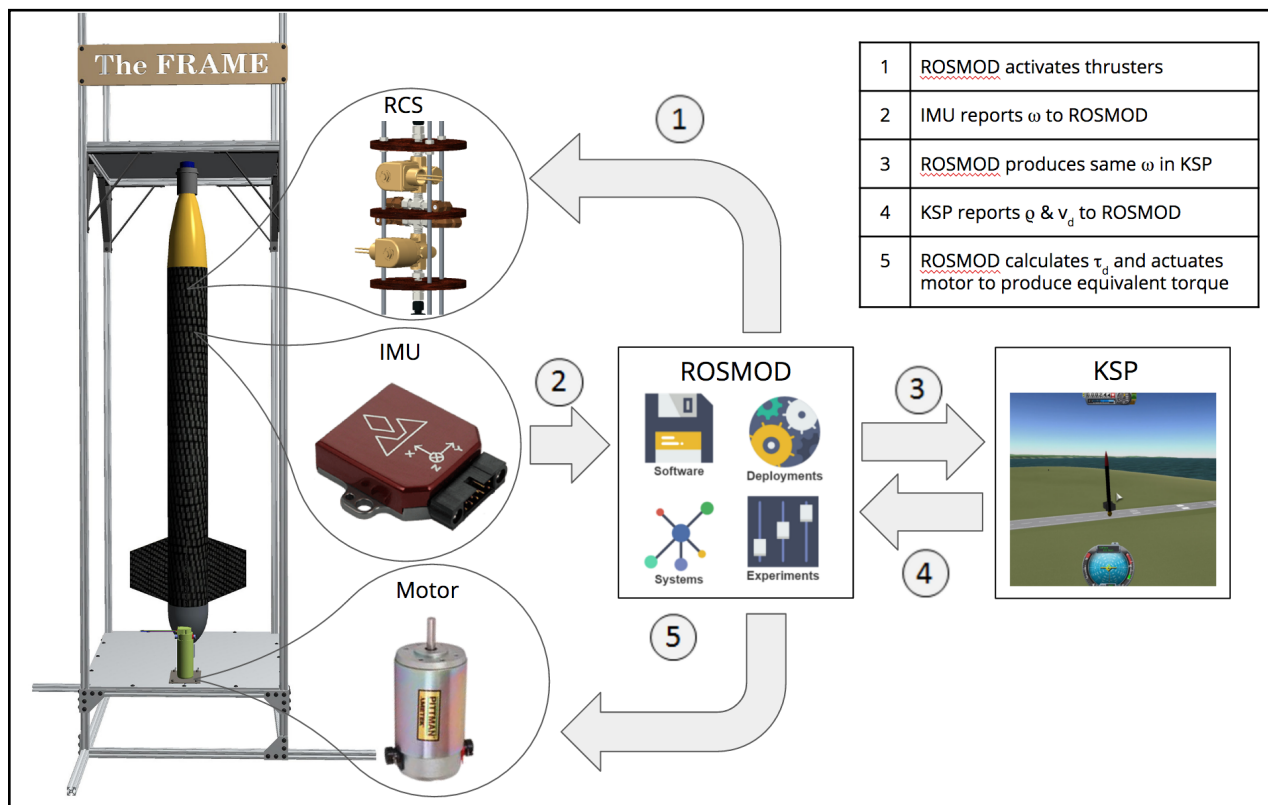


Figure 160: Information Flow Between FRAME, ROSMOD, and KSP during Ground-based Testing

The following list outlines what each of the numbers in Figure 160 represent after the simulated rocket is launched in KSP and reaches MECO.

1. ROSMOD activates thrusters
2. IMU reports ω to ROSMOD
3. ROSMOD produces same ω on KSP rocket
4. KSP reports ρ & v_d to ROSMOD
5. ROSMOD calculates damping torque and actuates motor to produce the equivalent torque

The four inputs in Equation 7.3 that are changing during the course of the flight are ω , ρ , v_d , and C_f . Rotational speed, ω , is obtained from the IMU aboard the real rocket on the FRAME. Atmospheric density, ρ and vertical speed, v_d are outputted by KSP. The skin friction drag coefficient of the cylinder, C_f , is calculated by Equation 7.4.

$$C_f = \frac{0.455}{[\log_{10}(Re)]^{2.58}}, 2 \times 10^5 < Re < 10^7 \quad (7.4)$$

As Equation 7.4 show, C_f is only dependent on Reynold's Number, which is a function of air density, flow speed, air viscosity, and characteristic length, all of which can be calculated in real time from KSP, so KSP can also be configured to output this number. The rest of the inputs remain constant and can just be plugged into ROSMOD to remember. Thus, ROSMOD can know in real time all variables needed to calculate the damping torque that should be produced by the motor, which is does so at 10 Hz. It is then programmed to supply the correct current to the motor to produce the necessary torque.

7.1.4.8 Testing

Overview Thus far, a number of tests have been successfully conducted on the FRAME, which has aided in design improvements of the payload as well as the FRAME itself. The tests have verified the payload's ability to perform its fundamental function, but have also validated the FRAME as a means of testing the payload. The following list shows the tests either already performed or planned to be performed as the roll control algorithm continues to be developed.

1. Open Loop Thruster Test
2. Subscale Integration
3. Flight Environment Comparison Test
4. Preliminary Roll Control Algorithm Development Testing
5. Fullscale Integration Test
6. Roll Control Algorithm Refinement with Atmospheric Damping
7. Roll Control Algorithm Robustness Test with Disturbance Input Torques

Open Loop Thruster Test

Objective

- Open solenoid to activate thrusters while mounted on the FRAME
- Validate thrusters' ability to rotate subscale flight vehicle

Success Criteria

- Solenoids open to actuate thrusters
- Thrusters fire with enough thrust to rotate subscale flight vehicle

Variables

- Angular Position
- Angular Velocity

Methodology

- Activate solenoid externally via 9V battery
- Use the FRAME to constrain the flight vehicle in a vertical orientation and allow for frictionless rotation
- Monitor variables visually

Results The open loop thruster test of the subscale payload was successful, as the solenoids were able to activate the thrusters. Furthermore, the thrust produced by the thruster couple was sufficient to cause the flight vehicle to rotate about its main axis.

Subscale Integration Test

Objective

- Use payload electronics to activate solenoid and pulse thrusters to cause vehicle to rotate

Success Criteria

- Payload electronics successfully activates thrusters to cause rotation
- IMU successfully records variables for analysis

Variables

- Angular Position
- Angular Velocity
- Angular Acceleration

Methodology

- Activate solenoid using onboard payload electronics
- Use the FRAME to constrain the flight vehicle in a vertical orientation and allow for frictionless rotation
- Monitor variables using onboard IMU and payload electronics

Results The subscale integration test was a success, as the payload electronics were able to activate the solenoid, which actuated the thruster couple and caused the subscale flight vehicle to rotate. Furthermore, the data obtained from the onboard IMU was compared to the dynamic model of the subscale flight vehicle. Figure 161 shows the dynamic model and IMU data plotted against one another. While the two data sets agree for the most part, a slight discrepancy occurs as the flight vehicle comes to a rest at around 15 seconds. The more rapid deceleration experienced by the physical frame test is likely due to the friction within the top support that is not accounted for in the dynamic model. Other than this minor detail, the two data sets largely agree, which validates the dynamic model.

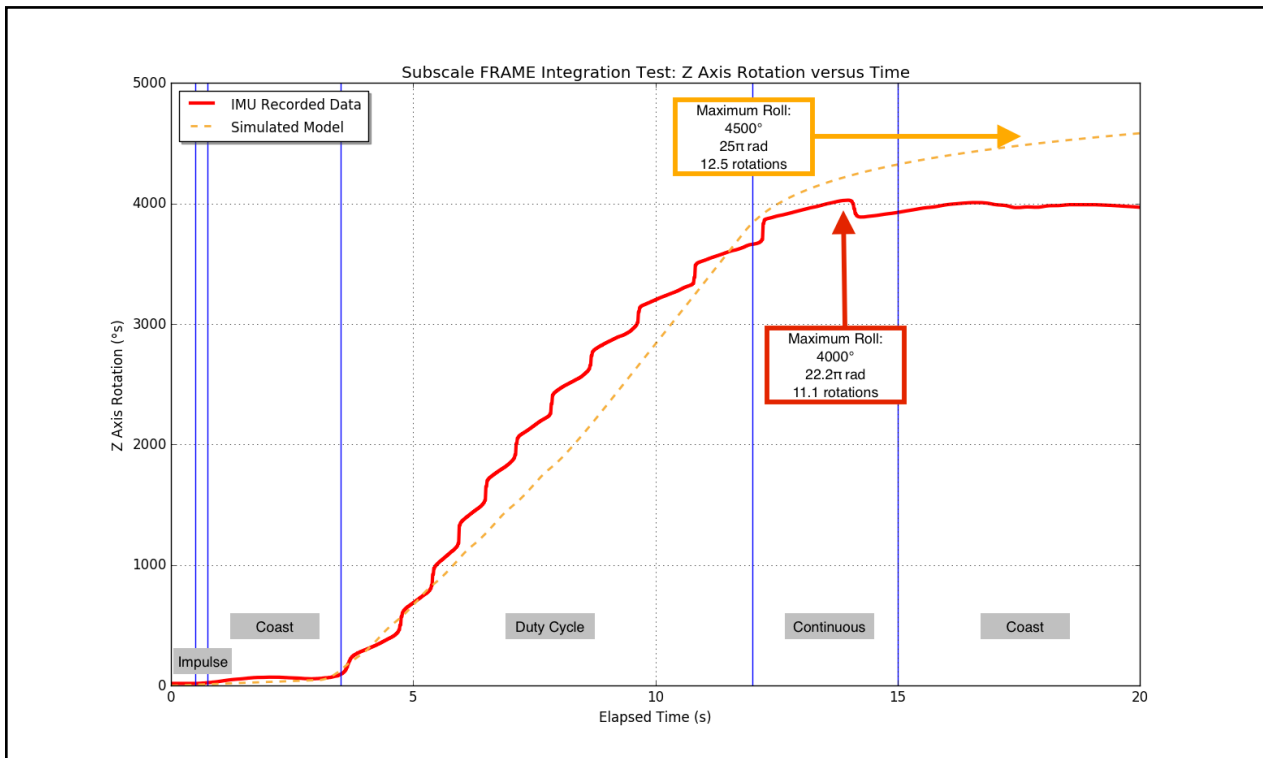


Figure 161: Dynamic Model and IMU Data Comparison

Flight Environment Comparison Test

Objective

- Compare behavior of rocket in flight compared to mounted on The FRAME
- Use payload electronics to operate solenoid and actuate thrusters in identical scheme as subscale flight

Success Criteria

- Payload electronics successfully actuates thrusters to cause rotation
- IMU successfully records variables for analysis

Variables

- Angular Position
- Angular Velocity
- Angular Acceleration

Methodology

- Compare data to subscale flight data to contrast test conditions of the FRAME and flight
- Operate solenoid using onboard payload electronics to actuate thrusters in identical scheme as subscale flight
- Use the FRAME to constrain the flight vehicle in a vertical orientation and allow for frictionless rotation
- Monitor variables using onboard IMU and payload electronics

Results The flight environment comparison test was a success, as it illustrated the differences between the test conditions of the FRAME and the flight environment. Figure 162 shows the angular position data gathered from the onboard IMU for each test. Clearly, the subscale flight vehicle performed many more rotations on the FRAME compared to the subscale launch. This is due to the lack of aerodynamic forces present on the FRAME. While this discrepancy is greater than anticipated, it validates the inclusion of a motor as part of the FRAME. Additionally, it has allowed the team to explore the phenomena of pressure drag and jet-fin interaction. Overall, this test represents an important step in the evolution of the FRAME, as it illustrated the need for real-time aerodynamic force modeling and transmission. Furthermore, this test highlighted the need for modifications to the payload design, as more thrust is needed to overcome the aerodynamic rotational damping.

Fullscale Integration Test

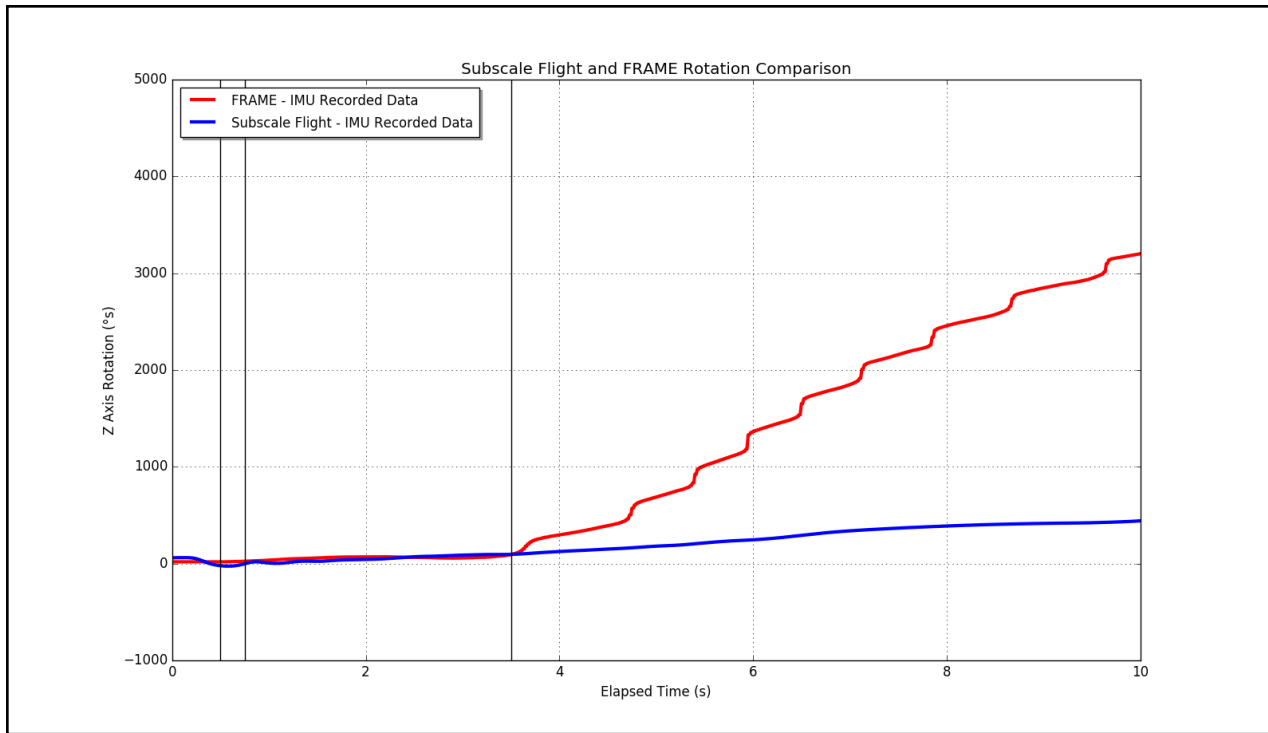


Figure 162: Subscale Flight and FRAME Angular Position Comparison

Objective

- Use payload electronics to operate solenoids to actuate thrusters and cause vehicle to rotate 4π radians
- Maintain angular position using both forward and reverse thruster couples after 4π radians of initial rotation
- Monitor current angular position with onboard IMU

Success Criteria

- Payload electronics successfully activates thrusters to cause 4π radians of rotation
- Flight vehicle maintains angular position after initial rotation
- IMU successfully records variables for analysis

Variables

- Angular Position
- Angular Velocity
- Angular Acceleration

Methodology

- Activate solenoids using onboard payload electronics
- Control system angular position with Bang Bang control
- Use the FRAME to constrain the flight vehicle in a vertical orientation and allow for frictionless rotation
- Monitor variables using onboard IMU and payload electronics

Results The Fullscale Integration test was a success, as the payload was able to cause the flight vehicle to rotate 4π radians and then maintain its angular position. As can be seen in Figure 163, the payload was able to induce 720 degrees of rotation and then oscillate about its final position. This severe oscillation is due to the Bang Bang control scheme used and the lack of atmospheric damping during this test. Functionally, the control scheme has a 5 degree window on either side of the desired position where the control scheme will consider the vehicle to be at the desired position. Once the vehicle's angular momentum carries it outside of that window, the appropriate thruster couple is actuated to return the vehicle to its desired position. The overshoot present was expected and is not of concern, as the considerable atmospheric damping present during flight quickly damps out any oscillation. Overall, this test demonstrated the ability of the thruster system to induce rotation in the fullscale launch vehicle, and the electronic' ability to sense and control the solenoids to appropriately accomplish the desired angular maneuvers.

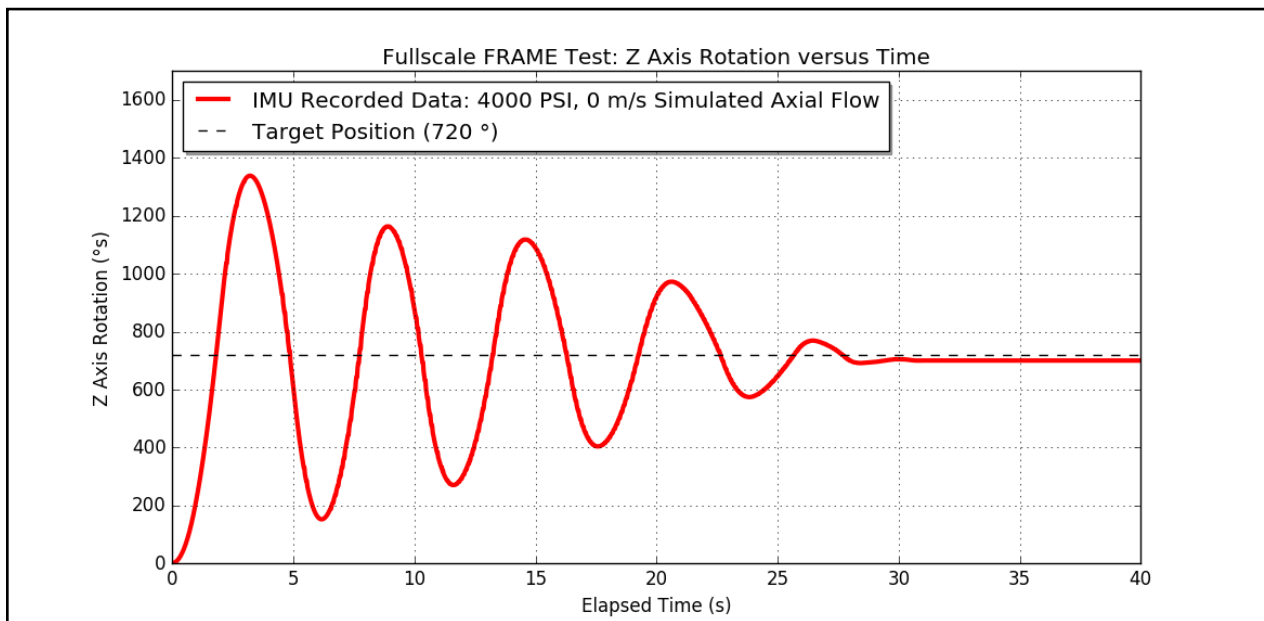


Figure 163: Fullscale Integration FRAME Test

Roll Control Algorithm Refinement with Atmospheric Damping

Objective

- Refine roll control algorithms so that precise roll control is possible with atmospheric damping
- Develop roll control algorithms so that at least 4π radians of roll can be accomplished in eight seconds with rotational damping
- Use payload electronics to operate solenoids and activate thrusters and cause vehicle to rotate
- Develop an understanding of how axial velocity and air tank pressure affect ability to complete experiment

Success Criteria

- Roll control algorithm is able to overcome atmospheric damping to execute desired rotation within eight seconds
- Payload electronics successfully activates thrusters to cause desired rotation within eight seconds
- IMU successfully records variables for analysis
- Develop relationships between axial velocity and experiment time

Variables

- Angular Position
- Angular Velocity
- Angular Acceleration

Methodology

- Test a variety of axial flow conditions that reflect the range that will be experienced during fullscale flight, varying from 0 to 250m/s
- Use DC motor to input atmospheric damping torques to the rocket based on axial velocity
- Activate solenoids using onboard payload electronics
- Use the FRAME to constrain the flight vehicle in a vertical orientation and allow for frictionless rotation
- Monitor variables using onboard IMU and payload electronics

Results The roll control algorithm refinement with atmospheric damping test was a success, as the payload was able to induce 2 full rotations and then maintain its final position in a variety of damping scenarios. Figure 164 shows the variation of angular position with time for different axial flow velocities. It is clear that with greater axial flow, the flight vehicle experiences a longer rise time to 4π radians, but also experiences significantly more oscillation about its final position. This is expected, and is due to the Bang Bang control scheme used to control the flight vehicle. A Bang Bang control scheme was chosen precisely due to the presence of rotational damping from axial flow, and this test clearly validates that choice. In general, this test demonstrates the readiness of the payload for flight conditions, and confirms that Bang Bang control is an effective choice.

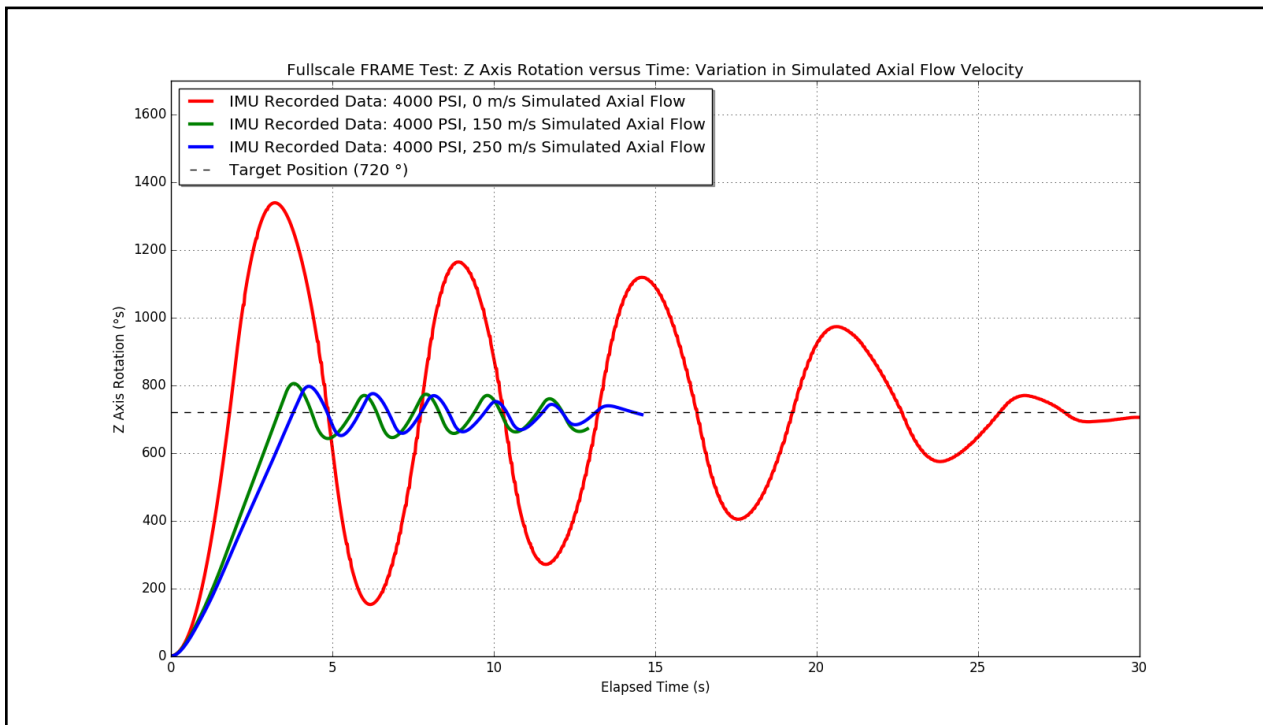


Figure 164: Fullscale Angular Position vs Time for Various Axial Velocities

Roll Control Test with Varying Tank Pressure

Objective

- Observe effect of air tank pressure on payload's ability to induce 4π radians of rotation
- Perform tests at identical axial flow velocities in order to isolate tank pressure as independent variable

Success Criteria

- Roll control algorithm is able to overcome atmospheric damping to execute desired rotation within eight seconds

- Payload electronics successfully activates thrusters to cause desired rotation within eight seconds
- IMU successfully records variables for analysis
- Develop relationships between air tank pressure and experiment time

Variables

- Angular Position
- Angular Velocity
- Angular Acceleration

Methodology

- Define constant axial velocity
- Use DC motor to input atmospheric damping torques to the rocket based on axial velocity
- Activate solenoids using onboard payload electronics
- Use the FRAME to constrain the flight vehicle in a vertical orientation and allow for frictionless rotation
- Monitor variables using onboard IMU and payload electronics

Results The roll control test with varying tank pressure test was a success, as the payload was able to induce 2 full rotations and then maintain its final position for a variety of air tank pressures. Figure 165 shows the variation of angular position with time for different air tank pressures. From this graph, it is clear that tank pressure has a negligible effect on the payload's ability to complete the payload experiment in a limited timeframe. This was expected, as the regulator located downstream of the air tank manages the compressed air to the same pressure. Nevertheless, this test was needed to confirm that as the air tank is depleted throughout the flight, it will be equally effective at completing the experiment.

Roll Control Algorithm Robustness Test with Disturbance Input Torques

Objective

- Improve robustness of roll control algorithms so that precise roll control is possible in a variety of conditions
- Develop roll control algorithms so that at least 4π roll can be accomplished in eight seconds
- Use payload electronics to operate solenoids and activate thrusters and cause vehicle to rotate

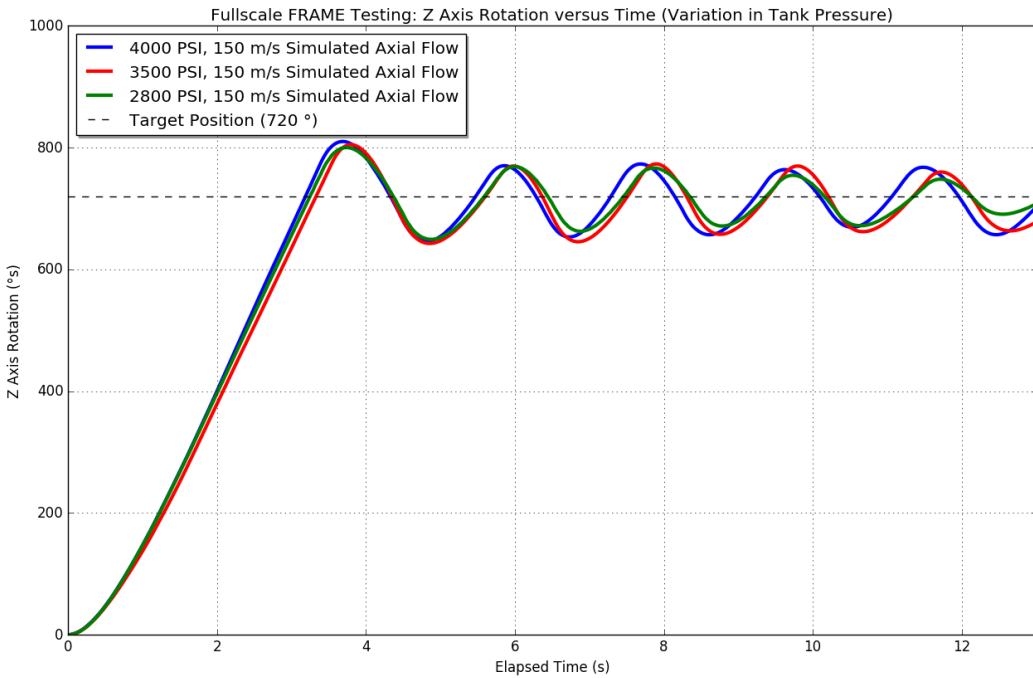


Figure 165: Fullscale Angular Position vs Time for Various Air Tank Pressures

Success Criteria

- Roll control algorithm is able to overcome disturbances to execute desired rotation within eight seconds
- Payload electronics successfully activates thrusters to cause desired rotation within eight seconds
- IMU successfully records variables for analysis

Variables

- Angular Position
- Angular Velocity
- Angular Acceleration

Methodology

- Use DC motor to input random disturbance torques to the rocket
- Activate solenoid using onboard payload electronics

- Use the FRAME to constrain the flight vehicle in a vertical orientation and allow for frictionless rotation
- Monitor variables using onboard IMU and payload electronics

Results This test has yet to be completed.

7.1.4.9 Conclusions

When considering the tests conducted thus far alongside the careful design choices made, it becomes clear that the FRAME offers a viable platform for testing the payload. Both the subscale and fullscale payloads have been tested and verified to function properly in an environment with damping due to axial flow. Looking forward, the robustness of the fullscale roll control algorithm will be tested using torque disturbances to emulate the affect of side winds and other potential disturbances present during flight. This will provide opportunity for refinement of the roll control algorithms up until Student Launch, and ultimately provide the team with ample opportunity to perfect the roll control payload. Overall, successful tests on the FRAME have thus far validated the design of both the payload design and the FRAME itself. Looking forward, future tests will allow for robust roll control algorithms to be developed in a realistic flight environment.

7.1.5 Recovery System Testing

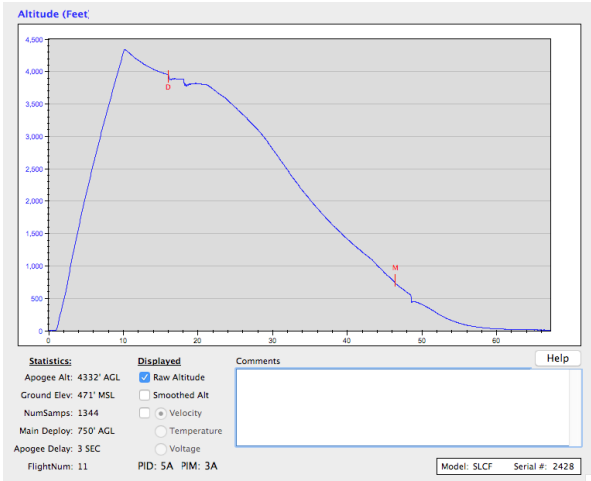
A complete test of the deployment system on the rocket is carried out before each launch. The test consists of two different aspects: testing the deployment charges / rocket separation, and testing the altimeters.

7.1.5.1 Altimeter Testing

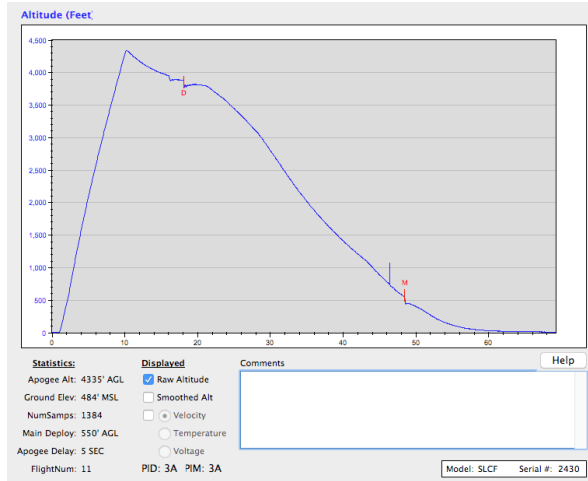
The main and backup PerfectFlite StratoLoggerCF altimeters were tested for accuracy and ignition performance in a pressurization chamber. The VADL created a modular, testable avionics bay simulator containing the flight altimeters, individual power sources, and individual arming switches. The altimeters in test were set to simulate proper flight conditions: the main altimeter with an apogee drogue deployment delay of 1s and main chute deployment at 750' AGL, and the backup altimeter with a 2s apogee drogue deployment delay and main chute deployment at 550' AGL. The pressurization chamber was set to simulate flight to roughly 5000' AGL and then the subsequent descent. This altitude AGL was chosen to be well within the usage restrictions of the altimeters, but also to assure that the altimeters can fire at altitudes at and above the desired Student Launch apogee. In the event that the rocket breaches the target apogee, the VADL team wanted to assure that the altimeters would still function properly in order to recover the launch vehicle safely and reliably. Results of the experimentation are shown below.

It is important to note that the apogee delay for launch day will be 1s for the main altimeter and 2s for the backup.

The altitudes sensed by the altimeters were off by 3 feet; however, apogee was detected by both altimeters simultaneously at 10s after launch. Despite the discrepancy in altitude, both altimeters sensed the apogee event at the same time. This assures the team that the main and backup



(a) Main Altimeter Testing



(b) Backup Altimeter Testing

altimeter drogue deployment charges will fire with a 1s offset- as desired for redundancy purposes. This is purposeful in order to limit both the force on the shear pins holding the foreword section and nosecone together, as well as the pressure fluctuations sensed by the altimeters due to close-range blast-charge ignitions. Although the StratoLoggerCF is designed to sense pressure fluctuations due to blast charges, the team chose to implement a time offset to limit the possible effect of simultaneous ignitions. Subsequently, it is easy to see that the main and backup altimeters fired their respective main deployment charges at 750' AGL and 550' AGL, respectively. This is proper operation and reflects the settings as designated by the VADL. This means that both altimeters are in good working order, and act consistently.



Figure 167: Deployment Testing

The second phase of testing is ground-based deployment/separation event testing to assure that the electric matches, altimeter firing mechanisms, and drogue and main parachute deployment charges meet safety and operational standards.

To test the deployments, the launch vehicle is assembled in the horizontal position using mass simulators for the payload components. During assembly, carefully calculated and measured 4F Black Powder charges are carefully placed in the designated blast locations. The avionics bay is secured in the forward section of the vehicle, as it would be for a true launch. The edges of the

bay are sealed with putty to protect the internal instrumentation from forces experienced during the black powder ignition. Parachutes are packed and placed in their correct positions.

An ignition mechanism is connected to a custom electrical relay control mechanism that allows for remote, manual ignition. The area is cleared for obstructions and personnel as verified by Safety Mentor, Robin Midgett, and Student Safety Officer, Paul Register. Subsequently, the drogue blast charges are fired manually. Next, the main blast charges are fired manually. After verifying both separation events, the Safety Officers assure there is no live black powder in the launch vehicle that could cause a safety hazard. Once this is verified, the test of the rocket separation is complete and equipment is transported back to the laboratory for manual inspection for damage.

7.1.6 Carbon Fiber Reinforced Blue Tube testing

To ensure the carbon fiber reinforced Blue Tube is an appropriate material, two compression tests were performed. The first tested the solid carbon fiber reinforced Blue Tube. The failure load of this airframe was 10,880 lbs force, which correlates to a stress of 6468 psi. Its stress-strain diagram is shown in Figure 168.

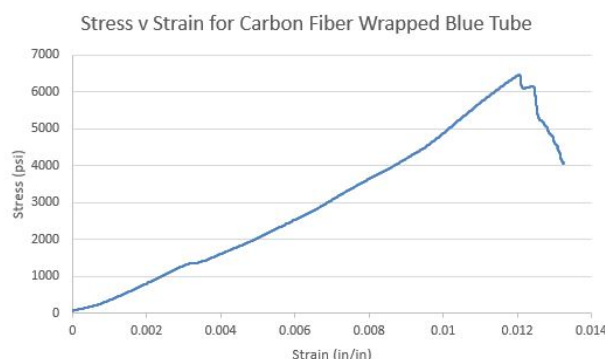


Figure 168: Stress-Strain Diagram for Solid Bodytube

The next crush test took into account airframes with holes in them. Holes will be drilled into the launch vehicle airframe for a variety of reasons, such as exhaust holes to prevent over-pressurization in the payload section, or access holes in the avionics section. An airframe was therefore tested to characterize the strength of the carbon fiber reinforced Blue Tube containing stress concentrations caused by the holes. As expected, the airframe failed along the lines of the holes. This is shown in Figure 169.



Figure 169: Failure Points for Bodytube with Stress Concentrations

The failure point of this tube is 9,790 lbs force, which correlates to a stress of 5827 psi. The stress-strain diagram is shown in Figure 170.

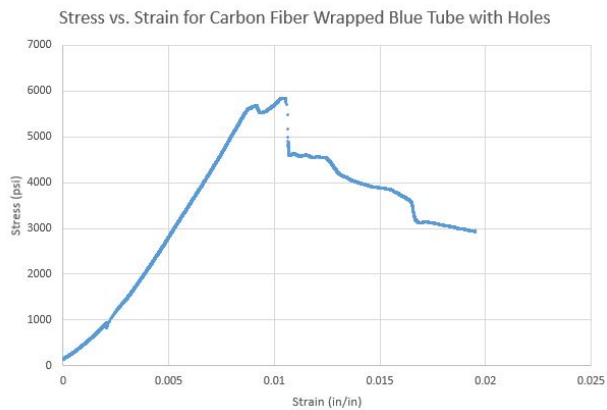


Figure 170: Stress-Strain Diagram for Bodytube with Holes

This test proved that holes in the airframe somewhat decrease the minimum failure load. In order to prove that the carbon fiber wrapped Blue Tube can stand up to inertial effects of rocket acceleration, a worst case scenario was analyzed. The acceleration of the rocket is greatest at takeoff. If the takeoff acceleration was 18g's, healthily above the predicted 15g's, and the isolated tail section instantaneously hit the rest of the rocket body, there would be an inertial force of 334 lbf. This is well below the experimental deformation value of 9,790 lbf. The airframe will withstand all inertial forces during takeoff and the duration of the launch, thereby making the carbon fiber wrapped Blue Tube an appropriate material choice for the airframe.

7.2 Requirements Compliance

7.2.1 NASA Handbook Requirements

To ensure a safe and successful flight as well as a rigorous design and experimental procedure for the VADL payload, the requirements of the NASA USLI competition must be satisfied. These requirements are separated into five system categories representing the entirety of the 2016-2017 USLI competition:

1. Vehicle Requirements
2. Recovery System Requirements
3. Experiment Requirements
4. Safety Requirements
5. General Requirements

Assigned to each requirement is one of (or a combination of) four methods of verification standard to systems engineering, in order of increasing time-consumption/expense:

- **Inspection:** The least expensive of verification methods, *inspection* is the verification of the requirement using the five senses. No exercising of the system is required; a simple observation can prove that the requirement is met.
- **Analysis:** By using simulations, calculations, models, or similarity, the requirement is verified by *analysis*. Often times it predicts the failure point of the system. Typical uses of *analysis* are CFD, structural analysis, rocket simulation, and mathematical calculations for shear pins, fin geometry, kinetic energy, center of mass, power draw, etc.
- **Test:** *Testing* is using a predefined series of inputs to ensure that the output will verify the requirement. It involves the testing of a particular subsystem as opposed to the full system. Common uses are deployment testing, hydrostatic testing, altimeter testing, tracking device testing, etc.
- **Demonstration:** The most expensive of verification methods, a *demonstration* is verification through the intended use of the system. In our case, *demonstration* involves a full flight test of the launch vehicle in subscale, fullscale, or competition flights.

The requirements, respective verification methods, and a description of the verification plan can be seen in the [NASA Handbook Requirements](#) Table. Also included is a status update on the verification method, and a link to the relevant portion of our document.

Table 30: NASA Handbook Requirements

Requirement	Verif. Method	Description of Verification Plan	Status	Document Section
1. Vehicle Requirements				
1.1. The vehicle shall deliver the science or engineering payload to an apogee altitude of 5,280 feet above ground level (AGL).	Analysis and Demonstration	The apogee altitude will be analyzed by simulation and demonstrated during fullscale test and competition flights using the altimeters.	In Progress -Motor thrust and mass predictions, when fed into simulation, predict an altitude around 4400 ft. AGL.	Mission Performance Predictions
1.2. The vehicle shall carry one commercially available, barometric altimeter for recording the official altitude used in determining the altitude award winner. Teams will receive the maximum number of altitude points (5,280) if the official scoring altimeter reads a value of exactly 5280 feet AGL. The team will lose one point for every foot above or below the required altitude. The altitude score will be equivalent to the percentage of altitude points remaining after and deductions.	Inspection	Inspection will verify that altimeters are onboard.	Complete -Dual StratoLoggerCF altimeters are included in avionics bay.	Recovery Subsystem
1.2.1. The official scoring altimeter shall report the official competition altitude via a series of beeps to be checked after the competition flight.	Demonstration	Competition flight demonstration will verify the official competition altitude. Full scale and subscale launches will test this capability.	In Progress - subscale and fullscale launches have verified the functionality of this system. Final verification will come from competition flight.	Recovery Subsystem
1.2.2. Teams may have additional altimeters to control vehicle electronics and payload experiment(s).	Inspection	Inspection will verify the presence of a redundant altimeter.	Complete -Dual StratoLoggerCF altimeters are included in avionics bay.	Recovery Subsystem
1.2.3. At the LRR, a NASA official will mark the altimeter that will be used for the official scoring.	Inspection	The official scoring altimeter will be inspected by a NASA official on launch day.	In Progress - Verification will come on competition day. Subscale and fullscale launches have verified the functionality of this system.	Recovery Subsystem
1.2.4. At the launch field, a NASA official will obtain the altitude by listening to the audible beeps reported by the official competition, marked altimeter.	Inspection	An inspection of the audible beeps will verify the altitude reported by the marked altimeter.	In Progress - Verification will come on competition day. Subscale and fullscale launches have verified the functionality of this system.	Recovery Subsystem

NASA Handbook Requirements

Requirement	Verif. Method	Description of Verification Plan	Status	Document Section
1.2.5. At the launch field, to aid in determination of the vehicles apogee, all audible electronics, except for the official altitude-determining altimeter shall be capable of being turned off.	Inspection	An inspection of the audible electronics will verify they are turned off.	In Progress -Verification will come on competition day. Subscale and fullscale launch has verified that all audible electronics are capable of being turned off from outside the rocket.	Recovery Subsystem
1.2.6. The following circumstances will warrant a score of zero for the altitude portion of the competition:	Demonstration	Final competition flight demonstration will ensure that none of the circumstances are met.	Incomplete - Verification will come on competition day.	Recovery Subsystem
1.2.6.1. The official, marked altimeter is damaged and/or does not report altitude via a series of beeps after the teams competition flight.	Demonstration			
1.2.6.2. The team does not report to the NASA official designated to record the altitude with their official, marked altimeter on the day of the launch.	Demonstration			
1.2.6.3. The altimeter reports an apogee altitude over 5,600 feet AGL.	Demonstration			
1.2.6.4. The rocket is not flown at the competition launch site.	Demonstration			
1.3. All recovery electronics shall be powered by commercially available batteries.	Test	A preflight test of the avionics subsystem will be performed to verify its functionality with commercially available batteries.	Complete - Two redundant 9V Li-Ion batteries are used to power the altimeters	Recovery Subsystem
1.4. The launch vehicle shall be designed to be recoverable and reusable. Reusable is defined as being able to launch again on the same day without repairs or modifications.	Analysis and Demonstration	Simulation analysis and subscale/fullscale flight demonstrations will verify the recoverability and reusability of the launch vehicle.	Complete - Fullscale flight has verified the recoverability and reusability of the launch vehicle.	Fullscale Flight Results
1.5. The launch vehicle shall have a maximum of four (4) independent sections. An independent section is defined as a section that is either tethered to the main vehicle or is recovered separately from the main vehicle using its own parachute.	Inspection	An inspection of the design plans for the fullscale flight vehicle shows three independent sections.	Complete - The fullscale launch vehicle has three independent sections	Vehicle Criteria

NASA Handbook Requirements

Requirement	Verif. Method	Description of Verification Plan	Status	Document Section
1.6. The launch vehicle shall be limited to a single stage.	Inspection	An inspection of the design plans for the fullscale flight vehicle shows a single stage.	Complete - The fullscale launch vehicle uses a single stage Loki L1400.	Vehicle Criteria
1.7. The launch vehicle shall be capable of being prepared for flight at the launch site within 4 hours, from the time the Federal Aviation Administration flight waiver opens.	Demonstration	Fullscale flight demonstration will verify the ability of the flight vehicle to be prepared within 4 hours.	Complete - The fullscale launch vehicle is able to be assembled within 2 hours.	Launch Operations Procedures
1.8. The launch vehicle shall be capable of remaining in launch-ready configuration at the pad for a minimum of 1 hour without losing the functionality of any critical on-board component.	Analysis and Test	An analysis and subsequent test of the power draw of the electronic subsystems will verify the ability of the launch vehicle to remain in launch ready configuration for a minimum of one hour.	Complete - a power draw analysis and test have proven the capability of the system to remain armed for over an hour.	Payload Electronics
1.9. The launch vehicle shall be capable of being launched by a standard 12 volt direct current firing system. The firing system will be provided by the NASA-designated Range Services Provider.	Demonstration	The firing system used at the subscale flight demonstration and fullscale flight demonstration will verify the capability of being launched by a standard 12V DC firing system.	Complete - Fullscale flight verified the capability of launch by standard 12V firing system.	Fullscale Flight Results
1.10. The launch vehicle shall require no external circuitry or special ground support equipment to initiate launch (other than what is provided by Range Services).	Inspection and Demonstration	An inspection of the design plans and demonstration during subscale and fullscale flights will verify that no external circuitry will be required to initiate flight.	Complete - no external circuitry is required to initiate launch.	Launch Operations Procedures
1.11. The launch vehicle shall use a commercially available solid motor propulsion system using ammonium perchlorate composite propellant (APCP) which is approved and certified by the National Association of Rocketry (NAR), Tripoli Rocketry Association (TRA), and/or the Canadian Association of Rocketry (CAR).	Inspection	An inspection of the design plans shows the planned motor meets the required specs.	Complete - The fullscale launch vehicle uses a single stage Loki L1400.	Vehicle Criteria
1.11.1. Final motor choices must be made by the Critical Design Review (CDR).	Inspection			

NASA Handbook Requirements

Requirement	Verif. Method	Description of Verification Plan	Status	Document Section
1.11.2. Any motor changes after CDR must be approved by the NASA Range Safety Officer (RSO), and will only be approved if the change is for the sole purpose of increasing the safety margin.	Inspection			
1.12. Pressure vessels on the vehicle shall be approved by the RSO and shall meet the following criteria:	Inspection and Test	An analysis of the safety factor for components seeing pressure and a hydrostatic test of the custom subsystems under pressure will verify the 4:1 safety factor.	Complete - a full pressure and safety factor diagram for all components can be found in the appendix.	Air Delivery System Safety
1.12.1. The minimum factor of safety (Burst or Ultimate pressure versus Max Expected Operating Pressure) shall be 4:1 with supporting design documentation included in all milestone reviews.	Inspection and Test			
1.12.2. The low-cycle fatigue life shall be a minimum of 4:1.	Inspection and Test			
1.12.3. Each pressure vessel shall include a solenoid pressure relief valve that sees the full pressure of the tank.	Inspection and Test			
1.12.4. Full pedigree of the tank shall be described, including the application for which the tank was designed, and the history of the tank, including the number of pressure cycles put on the tank, by whom, and when.	Inspection	An inspection of the log being kept for the tank will verify the full pedigree of the tank.	Complete - A detailed log is kept next to the filling station and is available upon request.	Payload-/Control Failure Modes
1.13. The total impulse provided by a Middle and/or High School launch vehicle shall not exceed 5,120 Newton-seconds (L-class).				
1.14. The launch vehicle shall have a minimum static stability margin of 2.0 at the point of rail exit.	Inspection and Demonstration	An analysis (simulation) of the static stability margin (SSM) will be performed to ensure the minimum SSM. This SSM will be verified on the fullscale launch vehicle.	Complete - The SSM at rail exit is 2.94.	Launch Stability
1.15. The launch vehicle shall accelerate to a minimum velocity of 52 fps at rail exit.	Analysis and Demonstration	An analysis (simulation) and fullscale flight demonstration will verify the minimum velocity at rail exit.	Complete - The rail exit velocity is 84.7 fps.	Launch Stability

NASA Handbook Requirements

Requirement	Verif. Method	Description of Verification Plan	Status	Document Section
1.16. All teams shall successfully launch and recover a subscale model of their rocket prior to CDR.	Demonstration	The subscale flight demonstration of launch and recovery will be performed prior to CDR submission.	Complete - The subscale flight test was performed in December of 2016.	Milestone Review Flysheet
1.16.1. The subscale model should resemble and perform as similarly as possible to the fullscale model, however, the fullscale shall not be used as the subscale model.	Analysis	An analysis of the differences between subscale and fullscale will verify their similarities and differences.	Complete - The subscale flight model used the majority of the same construction techniques and flew a unidirectional roll control payload.	Flight Test Validation
1.16.2. The subscale model shall carry an altimeter capable of reporting the models apogee altitude.	Inspection	A pre-flight inspection of the subscale model will verify that a capable altimeter is onboard.	Complete - The subscale launch vehicle flew to 1393 feet and uses the same Stratologger altimeters as the fullscale.	Recovery Subsystem
1.17. All teams shall successfully launch and recover their fullscale rocket prior to FRR in its final flight configuration. The rocket flown at FRR must be the same rocket to be flown on launch day. The purpose of the fullscale demonstration flight is to demonstrate the launch vehicles stability, structural integrity, recovery systems, and the teams ability to prepare the launch vehicle for flight. A successful flight is defined as a launch in which all hardware is functioning properly (i.e. drogue chute at apogee, main chute at a lower altitude, functioning tracking devices, etc.). The following criteria must be met during the full scale demonstration flight:	Inspection and Demonstration	An inspection of the rocket at competition demonstration will verify it is the same rocket recovered from fullscale demonstration.	Complete - The fullscale launch vehicle with the full mass and payload configuration was flown in February 2017 and will be flown again at the competition.	Fullscale Flight Results
1.17.1. The vehicle and recovery system shall have functioned as designed.	Analysis and Demonstration	Proceeding the fullscale flight demonstration, an analysis will verify the functionality of the vehicle and recovery system.	Complete - Fullscale flight had successful launch and recovery.	Fullscale Flight Results
1.17.2. The payload does not have to be flown during the fullscale test flight. The following requirements still apply:	Analysis and Demonstration	Proceeding the fullscale flight demonstration, an analysis will verify the functionality of the vehicle and recovery system.	Complete - Fullscale flight had successful launch and recovery.	Fullscale Flight Results

NASA Handbook Requirements

Requirement	Verif. Method	Description of Verification Plan	Status	Document Section
1.17.2.1. If the payload is not flown, mass simulators shall be used to simulate the payload mass.	Analysis	In the case that the payload is not flown, an analysis of estimated payload mass will verify the payload mass is simulated onboard.	Complete - the full mass of the payload was flown at fullscale flight.	FULLSCALE Flight Results
1.17.2.1.1. The mass simulators shall be located in the same approximate location on the rocket as the missing payload mass.	Inspection	An inspection of the mass simulators will show their location is the same as the missing payload.	Complete - the full mass of the payload was flown at fullscale flight.	FULLSCALE Flight Results
1.17.3. If the payload changes the external surfaces of the rocket (such as with camera housings or external probes) or manages the total energy of the vehicle, those systems shall be active during the fullscale demonstration flight.	Demonstration	Any external surfaces will be demonstrated in the fullscale flight.	Complete - the holes for thruster outlet were flown at fullscale flight.	FULLSCALE Flight Results
1.17.4. The fullscale motor does not have to be flown during the fullscale test flight. However, it is recommended that the fullscale motor be used to demonstrate full flight readiness and altitude verification. If the fullscale motor is not flown during the fullscale flight, it is desired that the motor simulate, as closely as possible, the predicted maximum velocity and maximum acceleration of the launch day flight.	Analysis and Demonstration	In the case that a different motor from that which is flown at competition is flown in the fullscale test flight, an analysis of the max velocity and acceleration from the demonstration will verify the similarity between the flights.	Complete - The same motor flown at fullscale demonstration is the one that will be flown at the competition.	FULLSCALE Flight Results
1.17.5. The vehicle shall be flown in its fully ballasted configuration during the fullscale test flight. Fully ballasted refers to the same amount of ballast that will be flown during the launch day flight.	Analysis and Demonstration	An analysis of the amount of ballast flown during fullscale flight demonstration will be used to verify the same amount of ballast will be flown at competition flight.	Complete - No ballast was flown during the fullscale flight.	FULLSCALE Flight Results
1.17.6. After successfully completing the fullscale demonstration flight, the launch vehicle or any of its components shall not be modified without the concurrence of the NASA Range Safety Officer (RSO).	Inspection	An inspection of the congruency between fullscale and competition flight vehicles will verify that any modifications were made with the concurrence of the RSO.	In Progress - Any changes made to the launch vehicle will be verified with the RSO.	

NASA Handbook Requirements

Requirement	Verif. Method	Description of Verification Plan	Status	Document Section
1.17.7. Full scale flights must be completed by the start of FRRs (March 6th, 2017). If the Student Launch office determines that a re-flight is necessary, than an extension to March 24th, 2017 will be granted. This extension is only valid for re-flights; not first time flights.	Inspection and Demonstration	An inspection of the FRR will verify the completeness of the full scale flight demonstration. In the case that a reflight is required, an inspection will verify that the re-flight demonstration will take place before March 24th.	Complete - A successful fullscale launch was performed in February 2017.	FULLSCALE FLIGHT RESULTS
1.18. Any structural protuberance on the rocket shall be located aft of the burnout center of gravity.	Analysis	An analysis of the center of gravity (CG) will verify that any structural protuberances are located aft the CG.	Complete - the fullscale launch vehicle has no structural protuberances.	VEHICLE CRITERIA
1.19. Vehicle Prohibitions	Inspection	An inspection of the rocket design will verify that the condition is not met.	Complete - the fullscale rocket does not break any of the prohibitions mentioned.	VEHICLE CRITERIA
1.19.1. The launch vehicle shall not utilize forward canards.	Inspection			
1.19.2. The launch vehicle shall not utilize forward firing motors.	Inspection			
1.19.3. The launch vehicle shall not utilize motors that expel titanium sponges (Sparky, Skidmark, MetalStorm, etc.)	Inspection			
1.19.4. The launch vehicle shall not utilize hybrid motors.	Inspection			
1.19.5. The launch vehicle shall not utilize a cluster of motors.	Inspection			
1.19.6. The launch vehicle shall not utilize friction fitting for motors.	Inspection			
1.19.7. The launch vehicle shall not exceed Mach 1 at any point during flight.	Inspection			
1.19.8. Vehicle ballast shall not exceed 10% of the total weight of the rocket.	Inspection			

2. Recovery System Requirements

NASA Handbook Requirements

Requirement	Verif. Method	Description of Verification Plan	Status	Document Section
2.1. The launch vehicle shall stage the deployment of its recovery devices, where a drogue parachute is deployed at apogee and a main parachute is deployed at a much lower altitude. Tumble recovery or streamer recovery from apogee to main parachute deployment is also permissible, provided that kinetic energy during drogue-stage descent is reasonable, as deemed by the Range Safety Officer.	Analysis and Demonstration	The deployment events are controlled by the redundant altimeters. An analysis using simulation and demonstration of the deployment events during fullscale testing will verify their efficacy.	Complete - Fullscale rocket was successfully recovered using dual deployment	Recovery Subsystem
2.2. Each team must perform a successful ground ejection test for both the drogue and main parachutes. This must be done prior to the initial subscale and full scale launches.	Test	A test of the deployment subsystem will verify its functionality prior to subscale and fullscale launch.	Complete - A successful deployment test was performed prior to fullscale flight.	Recovery System Testing
2.3. At landing, each independent sections of the launch vehicle shall have a maximum kinetic energy of 75 ft-lbf.	Analysis and Demonstration	An analysis (simulation) to predict the maximum kinetic energy and results from the fullscale demonstration launch will verify the maximum kinetic energy is less than 75 ft-lbf.	Complete - analysis (simulation) and analysis of the fullscale flight show a max landing energy of 49.6 ft-lbs.	Landing Kinetic Energy
2.4. The recovery system electrical circuits shall be completely independent of any payload electrical circuits.	Inspection	An inspection of the design plan verifies the avionics to be completely independent of the payload electronics. The avionics are separated from the payload electronics by bulkheads and surrounding coupler tube.	Complete - the fullscale and payload electronics are in completely different sections with separate power sources.	Recovery Subsystem Payload Electronics
2.5. The recovery system shall contain redundant, commercially available altimeters. The term "altimeters" includes both simple altimeters and more sophisticated flight computers.	Inspection and Demonstration	An inspection of the design plan verifies the presence of two PerfectFlite StratoLoggerCF altimeters, each altimeter will control the firing of independent ejection charges for both the drogue and main parachute. The altimeters will be demonstrated in the subscale and fullscale launches.	Complete - Dual StratoLoggerCF altimeters are included in avionics bay.	Recovery Subsystem

NASA Handbook Requirements

Requirement	Verif. Method	Description of Verification Plan	Status	Document Section
2.6. Motor ejection is not a permissible form of primary or secondary deployment.	Inspection and Demonstration	An inspection of the design plan verifies the presence of two PerfectFlite StratoLoggerCF altimeters, each altimeter will control the firing of independent ejection charges for both the drogue and main parachute. The altimeters will be demonstrated in the subscale and fullscale launches.	Complete - Dual StratoLoggerCF altimeters are included in avionics bay.	Recovery Subsystem
2.7. Each altimeter shall be armed by a dedicated arming switch that is accessible from the exterior of the rocket airframe when the rocket is in the launch configuration on the launch pad.	Inspection and Test	An inspection of the fullscale rocket verifies the presence of a dedicated arming switch accessible on the launch pad. Two independent screw-based switches, accessible from the exterior of the vehicle, are used to engage the pair of redundant altimeters. This will be tested in the laboratory and on the launch pad.	Complete - the altimeters are capable from being armed from outside the rocket.	Recovery Subsystem
2.8. Each altimeter shall have a dedicated power supply.	Inspection and Test	An inspection of the design plan verifies the presence of a redundant altimeter in addition to the scored altimeter. Laboratory and on-pad testing will verify the functionality of the independent, tested 9V batteries that will be wired to the arming switches.	Complete - the altimeters are powered by separate 9V Li-Ion batteries.	Recovery Subsystem
2.9. Each arming switch shall be capable of being locked in the ON position for launch.	Inspection and Test	An inspection of the screw-based switches show they are capable of being locked in the ON position. Laboratory and on-pad testing will verify this functionality.	Complete - arming switches in the avionics bay are capable of being locked down.	Recovery Subsystem
2.10. Removable shear pins shall be used for both the main parachute compartment and the drogue parachute compartment.	Analysis and Demonstration	The number and size of shear pins will be verified through mathematical analysis and demonstrated in subscale and fullscale flights.	Complete - 4-40 shear pins are used to connect the tail and nose sections to the avionics section.	Vehicle Criteria

NASA Handbook Requirements

Requirement	Verif. Method	Description of Verification Plan	Status	Document Section
2.11. An electronic tracking device shall be installed in the launch vehicle and shall transmit the position of the tethered vehicle or any independent section to a ground receiver.	Test	Small radio transmitters that communicate with a base-station receiver track the location of the launch vehicle. The system's functionality will be tested on the ground and in subscale and fullscale flights. In the case that independent sections are added to the design plans, each section will have its own tracking device.	In Progress - Final verification will come with competition flight. A radio transmitter was flown and its function verified at fullscale test flight.	Rocket-Locating Transmitters
2.11.1. Any rocket section, or payload component, which lands untethered to the launch vehicle, shall also carry an active electronic tracking device.	Test			
2.11.2. The electronic tracking device shall be fully functional during the official flight on launch day.	Test			
2.12. The recovery system electronics shall not be adversely affected by any other on-board electronic devices during flight (from launch until landing).	Inspection and Demonstration	An inspection of the recovery system electronics plans show they will be housed in an electrically shielded bay to prevent interference from transmitting devices. The recovery system will be demonstrated in subscale and fullscale flights in the presence of transmitting tracking devices to ensure unaffected functionality.	Complete - The fullscale avionics bay is completed separate and shielded from all other operating electronics.	Recovery Subsystem Payload Electronics Rocket-Locating Transmitters
2.12.1. The recovery system altimeters shall be physically located in a separate compartment within the vehicle from any other radio frequency transmitting device and/or magnetic wave producing device.	Inspection and Demonstration			
2.12.2. The recovery system electronics shall be shielded from all onboard transmitting devices, to avoid inadvertent excitation of the recovery system electronics.	Inspection and Demonstration			

NASA Handbook Requirements

Requirement	Verif. Method	Description of Verification Plan	Status	Document Section
2.12.3. The recovery system electronics shall be shielded from all onboard devices which may generate magnetic waves (such as generators, solenoid valves, and Tesla coils) to avoid inadvertent excitation of the recovery system.	Inspection and Demonstration			
2.12.4. The recovery system electronics shall be shielded from any other onboard devices which may adversely affect the proper operation of the recovery system electronics.	Inspection and Demonstration			
3. Experiment Requirements				
3.1.1. Each team shall choose one design experiment option from the following list.				
3.1.2. Additional experiments (limit of 1) are encouraged, and may be flown, but they will not contribute to scoring.		The design plan does not include an additional payload experiment.		
3.1.3. If the team chooses to fly additional experiments, they shall provide the appropriate documentation in all design reports so experiments may be reviewed for flight safety.				
3.3. Roll induction and counter roll				
3.3.1. Teams shall design a system capable of controlling launch vehicle roll post motor burnout.	Analysis and Test	A computational analysis of the thrusters and ground-based testing will verify their ability to control vehicle roll post motor burnout. The payload's control ability will also be verified through fullscale flight.	In Progress - the groundbased testing facility (FRAME) with incorporated damping, as well as extensive MATLAB simulations, have proved the ability of the roll control payload to complete the experiment. Final verification will come from a fullscale reflight or competition flight.	Payload Criteria The FRAME Mission Performance Predictions

NASA Handbook Requirements

Requirement	Verif. Method	Description of Verification Plan	Status	Document Section
3.3.1.1. The systems shall first induce at least two rotations around the roll axis of the launch vehicle.	Analysis and Test	Cold-gas thrusters, tangential to the rocket body, will be actively controlled to induce rolling. A simulation analysis, ground-based testing, and fullscale flight will verify the ability of the payload to induce at least two rotations and halt all rolling motion.	In Progress - the groundbased testing facility (FRAME) with incorporated damping, as well as extensive MATLAB simulations, have proved the ability of the roll control payload to complete the experiment. Final verification will come from a fullscale reflight or competition flight.	
3.3.1.2. After the system has induced two rotations, it must induce a counter rolling moment to halt all rolling motion for the remainder of launch vehicle ascent.	Analysis and Test	Cold-gas thrusters, tangential to the rocket body, will be actively controlled to induce rolling. A simulation analysis, ground-based testing, and fullscale flight will verify the ability of the payload to induce at least two rotations and halt all rolling motion.	In Progress - the design features two sets of thruster couples and a robust control system to dynamically monitor and induce roll in both directions. Final verification will come from a fullscale reflight or competition flight.	Payload Mission Requirements Overview Payload Electronics
3.3.1.3. Teams shall provide proof of controlled roll and successful counter roll.	Analysis and Test	Cold-gas thrusters, tangential to the rocket body, will be actively controlled to induce rolling. A simulation analysis, ground-based testing, and fullscale flight will verify the ability of the payload to induce at least two rotations and halt all rolling motion.	In Progress - data from the onboard IMU will be used to prove the actuation and completion of the roll experiment. Final verification will come from competition flight.	Payload Criteria Payload Electronics
3.3.2. Teams shall not intentionally design a launch vehicle with a fixed geometry that can create a passive roll effect.	Analysis and Test	Cold-gas thrusters, tangential to the rocket body, will be actively controlled to induce rolling. A simulation analysis, ground-based testing, and fullscale flight will verify the ability of the payload to induce at least two rotations and halt all rolling motion.	Complete - the vehicle was not intentionally designed to produce a passive roll.	Vehicle Criteria

NASA Handbook Requirements

Requirement	Verif. Method	Description of Verification Plan	Status	Document Section
3.3.3. Teams shall only use mechanical devices for rolling procedures.	Analysis and Test	Cold-gas thrusters, tangential to the rocket body, will be actively controlled to induce rolling. A simulation analysis, ground-based testing, and fullscale flight will verify the ability of the payload to induce at least two rotations and halt all rolling motion.	Complete - cold gas thrusters have been fabricated and integrated to produce a mechanically actuated roll.	Design and Construction Payload Electronics
4. Safety Requirements				
4.1. Each team shall use a launch and safety checklist. The final checklists shall be included in the FRR report and used during the Launch Readiness Review (LRR) and any launch day operations.	Inspection	The PDR includes a preliminary checklist. An inspection of the FRR will verify the presence of the final checklist to be used during LRR and launch day operations.	Complete - a full checklist of operations for launch day operations has been compiled.	Launch Operations Procedures
4.2. Each team must identify a student safety officer who shall be responsible for all items in section 4.3.	Inspection	An inspection of the proposal verifies the designation of a student safety officer.	Complete - Paul R. is the student safety officer.	Safety Officer/LEUP Holder
4.3. The role and responsibilities of each safety officer shall include, but not limited to:	Inspection	An inspection of the design reports verifies the presence of current safety documentation. The Student Safety Officer will oversee the overall safety and launch procedures of the team and will work to fulfill the safety requirements.	In Progress - safety is an ongoing process that should never be assumed to be completed.	
4.3.1. Monitor team activities with an emphasis on Safety during:	Inspection			
4.3.1.1. Design of vehicle and launcher	Inspection		Complete - all of these activities were performed under supervision and instruction from team safety officers.	Project Management
4.3.1.2. Construction of vehicle and launcher	Inspection		Complete - all of these activities were performed under supervision and instruction from team safety officers.	Personnel Hazard Analysis
4.3.1.3. Assembly of vehicle and launcher	Inspection		Complete - all of these activities were performed under supervision and instruction from team safety officers.	Launch Operations Procedures

NASA Handbook Requirements

Requirement	Verif. Method	Description of Verification Plan	Status	Document Section
4.3.1.4. Ground testing of vehicle and launcher	Inspection		In Progress - Safety officers have and will continue to supervise ground based testing procedures.	Personnel Hazard Analysis
4.3.1.5. Sub-scale launch test(s)	Inspection		Complete - all of these activities were performed under supervision and instruction from team safety officers.	Launch Operations Procedures
4.3.1.6. Fullscale launch test(s)	Inspection		In Progress - Safety officers have and will continue to supervise launch test procedures.	
4.3.1.7. Launch day	Inspection		Incomplete - Verification will come on competition day.	
4.3.1.8. Recovery activities	Inspection		In Progress - Safety officers have and will continue to supervise all recovery activities including the disarming of blast charges.	
4.3.1.9. Educational Engagement Activities	Inspection		In Progress - The student safety officer is sure to emphasize safety at outreach events, especially with live demonstrations such as bottle rockets and FRAME actuation.	Safety
4.3.2. Implement procedures developed by the team for construction, assembly, launch, and recovery activities	Inspection		In Progress - the student safety officer will continue to monitor these processes through the fullscale competition flight.	Launch Operations Procedures
4.3.3. Manage and maintain current revisions of the teams hazard analyses, failure modes analyses, procedures, and MSDS/chemical inventory data	Inspection		In Progress - safety is an ongoing process that should never be assumed to be completed.	Hazard Analysis
4.3.4. Assist in the writing and development of the teams hazard analyses, failure modes analyses, and procedures.	Inspection		In Progress - safety is an ongoing process that should never be assumed to be completed.	Hazard Analysis

NASA Handbook Requirements

Requirement	Verif. Method	Description of Verification Plan	Status	Document Section
<p>4.4. Each team shall identify a "mentor." A mentor is defined as an adult who is included as a team member, who will be supporting the team (or multiple teams) throughout the project year, and may or may not be affiliated with the school, institution, or organization. The mentor shall maintain a current certification, and be in good standing, through the National Association of Rocketry (NAR) or Tripoli Rocketry Association (TRA) for the motor impulse of the launch vehicle, and the rocketeer shall have flown and successfully recovered (using electronic, staged recovery) a minimum of 2 flights in this or a higher impulse class, prior to PDR. The mentor is designated as the individual owner of the rocket for liability purposes and must travel with the team to launch week. One travel stipend will be provided per mentor regardless of the number of teams he or she supports. The stipend will only be provided if the team passes FRR and the team and mentor attends launch week in April.</p>	Inspection	<p>A self-imposed inspection shows that the necessary requirements are met by our designated mentor.</p>	Complete - Our rocketry mentor is Robin Midgett, NAR certified	Safety Officer/LEUP Holder
<p>4.5. During test flights, teams shall abide by the rules and guidance of the local rocketry clubs RSO. The allowance of certain vehicle configurations and/or payloads at the NASA Student Launch Initiative does not give explicit or implicit authority for teams to fly those certain vehicle configurations and/or payloads at other club launches. Teams should communicate their intentions to the local clubs President or Prefect and RSO before attending any NAR or TRA launch.</p>	Inspection	<p>A self-imposed inspection will verify that the rules and guidance provided by our RSO, including the NAR high power rocket safety code, and our ability to launch our particular payload, will be followed.</p>	Complete - we have followed all regulations in place by our RSO for test flights.	Launch Operations Procedures

NASA Handbook Requirements

Requirement	Verif. Method	Description of Verification Plan	Status	Document Section
4.6. Teams shall abide by all rules set forth by the FAA.	Inspection	A self-imposed inspection will verify that the FAA regulations, included in the safety binder of the VADL and our design reports, will be abided by.	Complete - all test flights follow the rules imposed by the FAA.	Launch Operations Procedures
5. General Requirements				
5.1. Students on the team shall do 100% of the project, including design, construction, written reports, presentations, and flight preparation with the exception of assembling the motors and handling black powder or any variant of ejection charges, or preparing and installing electric matches (to be done by the teams mentor).	Inspection	A self-conducted inspection will verify that only students on the team work on the project, with the exception of operations handled by the team's mentor.	In Progress	
5.2. The team shall provide and maintain a project plan to include, but not limited to the following items: project milestones, budget and community support, checklists, personnel assigned, educational engagement events, and risks and mitigations.	Inspection	An inspection of our operations shows the Vanderbilt Student Launch meets weekly to discuss these aspects of the competition. Our design reports include budgeting, project milestones, checklists, personnel specialties, and risks and mitigations in our design reports, while educational engagement events are submitted using the proper form.	Complete - a full timeline of operations is maintained throughout the year to help manage our project plan.	Project Plan
5.3. Foreign National (FN) team members shall be identified by the Preliminary Design Review (PDR) and may or may not have access to certain activities during launch week due to security restrictions. In addition, FNs may be separated from their team during these activities.	Inspection	Our team does not involve any FN participants.	Complete - Our team does not contain FN members.	
5.4. The team shall identify all team members attending launch week activities by the Critical Design Review (CDR). Team members shall include:	Inspection	A self-conducted inspection of team members, mentors, and educators will identify all team members attending launch week.	Complete - the team has identified all team members attending launch week activities.	Project Title and School Name
5.4.1. Students actively engaged in the project throughout the entire year.	Inspection			
5.4.2. One mentor (see requirement 4.4).	Inspection			
5.4.3. No more than two adult educators.	Inspection			

NASA Handbook Requirements

Requirement	Verif. Method	Description of Verification Plan	Status	Document Section
5.5. The team shall engage a minimum of 200 participants in educational, hands-on science, technology, engineering, and mathematics (STEM) activities, as defined in the Educational Engagement Activity Report, by FRR. An educational engagement activity report shall be completed and submitted within two weeks after completion of an event. A sample of the educational engagement activity report can be found on page 28 of the handbook.	Inspection	An inspection of our Educational Engagement Activity Reports and final summary will show our engagement meets the required specifications.	Complete - our educational outreach reports and events go far beyond the minimum required by the competition.	Timeline of Operations
5.6. The team shall develop and host a Web site for project documentation.	Inspection	An inspection of the team's website, https://www.vanderbilt.edu/usli/ will verify our development and presence of documentation throughout the competition cycle.	In Progress- All reports will continue to be posted on the team website. Final verification will come with PLAR.	Project Title and School Name
5.7. Teams shall post, and make available for download, the required deliverables to the team Web site by the due dates specified in the project timeline.	Inspection	An inspection of our website after each due date will show that deliverables are posted before the required due dates.	In Progress - All deadlines will continue to be met. Final verification will come with PLAR.	Timeline of Operations
5.8. All deliverables must be in PDF format.	Inspection	An inspection of our deliverables shows they are all in .pdf format.	In Progress - future deliverables will continue to be in pdf format. Final verification will come with PLAR.	Project Title and School Name
5.9. In every report, teams shall provide a table of contents including major sections and their respective sub-sections.	Inspection	An inspection of our design reports show they all include a table of contents with sections and subsections.	Complete - all reports contain a table of contents with links to all sections and subsections.	
5.10. In every report, the team shall include the page number at the bottom of the page.	Inspection	An inspection of our design reports will verify that page numbers are included.	In Progress - reports will continue to have page numbers at the bottom of each page. Final verification will come with PLAR.	Project Title and School Name

NASA Handbook Requirements

Requirement	Verif. Method	Description of Verification Plan	Status	Document Section
5.11. The team shall provide any computer equipment necessary to perform a video teleconference with the review board. This includes, but not limited to, a computer system, video camera, speaker telephone, and a broadband Internet connection. If possible, the team shall refrain from use of cellular phones as a means of speakerphone capability.	Inspection	An inspection shows that VADL provides the necessary equipment perform a video teleconference.	Complete - the team provides all equipment needed to perform these activities.	Project Title and School Name
5.12. All teams will be required to use the launch pads provided by Student Launchs launch service provider. No custom pads will be permitted on the launch field. Launch services will have 8 ft. 1010 rails, and 8 and 12 ft. 1515 rails available for use.	Demonstration	The launch vehicle will be designed to use the launch pads provided by the service provider at the competition demonstration flight.	Complete - our launch vehicle is designed to use a 12ft. 1515 rail.	Launch Pad, Launch Rail, and Ignition System
5.13. Teams must implement the Architectural and Transportation Barriers Compliance Board Electronic and Information Technology (EIT) Accessibility Standards (36 CFR Part 1194) Subpart B-Technical Standards (http://www.section508.gov): 1194.21 Software applications and operating systems.1194.22 Web-based intranet and Internet information and applications.	Inspection	An self-conducted inspection of our operations will prove that we will follow the proper standards outlined in 5.13.	Complete - The team meets all of the standards required by section 508	Project Title and School Name

7.2.2 Team Derived Requirements

Deriving team-specific requirements outside the boundaries of the competition is an essential step to ensure program success. The VADL has derived requirements for our launch vehicle and operations in five categories:

1. Thruster System Requirements
2. Control System Requirements
3. Ground Based Test Facility Requirements
4. Vehicle and Recovery Requirements
5. Safety Requirements

Since CDR, "Vehicle Requirements" has been updated to include Recovery, and requirements 5.9-5.16 have been added. A few thruster system requirements have been modified as the definition of the experiment has developed. Any changed requirements have been denoted with an asterisk.

Assigned to each requirement is a method of verification (the same four methods defined in [NASA Handbook Requirements](#)) and thorough verification plan. The team derived requirements can be found in the tables below:

The requirements, respective verification methods, a description of the verification plan, and the current verification status can be seen in the [Team Derived Requirements Table](#) below. Also included is a link to the relevant portion of our document.

Table 31: Team Derived Requirements

Requirement	Verif. Method	Description of Verification Plan	Status	Document Section
1. Thruster System Requirements				
1.1 System shall deliver a minimum of 2.12 N per thruster.	Analysis and Test	Our isentropic gas dynamic analysis will verify the ideal thrust from our nozzle geometry. The thruster stand shall be used to test the real thrust received given both continuous and pulsed conditions of the solenoid actuation.	Complete - Cold gas thrusters produce 6N of thrust each.	Thruster Testing
1.2 Solenoid should actuate in under 30 ms.	Inspection	Manufacturers should be contacted to verify all specifications before purchase. An inspection of the accompanying spec sheets will verify the actuation time.	Complete - The Parker solenoid valve selected has an actuation time of 30ms.	Design and Construction
1.3 Orifice of all pressurized components upstream of the nozzle shall have 2X the area of the nozzle .	Inspection	An inspection of all component dimensions prior to purchase will verify their flow area.	Complete - All components upstream of the nozzle have an area at least 2x that of the nozzle throat.	Design and Construction
1.4 Nozzles should be mounted on an inner bulkhead in such a manner as to maximize moment arm.	Analysis	A CAD-based analysis of our mounts and fittings will verify that the moment arm approaches the bulkhead diameter of 5.35".	Complete - the maximum moment arm has been achieved by carefully selecting fittings and validating fitment in CAD.	Design and Construction
1.5 Nozzle will have machinable geometry: standard diameter throat and exit, no smaller than 1.5 mm based on machining tool availability.	Analysis	The isentropic gas dynamic analysis shall be run recursively to verify standard nozzle dimensions.	Complete - the nozzles have been custom machined using bits purchased from online suppliers.	Design and Construction

Team Derived Requirements

Requirement	Verif. Method	Description of Verification Plan	Status	Document Section
1.6 System should provide an upstream pressure of 350 psi to the nozzle during solenoid actuation.*	Test	The analog and digital pressure sensors present on the thruster test stand will be used to verify the upstream pressure during solenoid actuation.	Complete - The CP Regulator selected since CDR allows us to mitigate the effects of regulator droop to achieve the upstream pressure we need.	Thruster Testing
1.7 Thrust produced should be within 25% of the calculated ideal thrust even with the effects of regulator droop.*	Test	The thruster test stand will verify the accuracy of our custom-machined thrusters.	Complete - while we reach very near the design thrust with one nozzle, regulator droop brings us within 25% of the calculated design thrust with two nozzles.	Thruster Testing
1.8 Payload will be rigidly supported as to not shift within rocket body during flight.	Inspection	Inspection will ensure team uses three threaded rods and fixed bulkheads to constrain the movement of the payload skeleton within the rocket body before the top body tube is assembled.	Complete - the combination of steel and aluminum rods, bulkheads, and a compressed coupler tube with shear pins allows the payload skeleton to be rigidly supported - even without the nosecone and payload airframe.	Design and Construction Vehicle Criteria
1.9 The system shall be modular to enable troubleshooting and interchangeability.	Inspection	The skeleton payload system will be designed with sliding bulkheads and Yor-Lok compression fittings to allow ease of assembly and modification of thruster system for simple troubleshooting.	Complete - the threaded rod design allows easy assembly and disassembly of all the components.	Design and Construction
1.10 The payload skeleton must minimize unnecessary mass.*	Analysis	A CAD-based analysis of the payload skeleton will be used, along with real masses, to minimize the weight of non-structural elements like bulkheads.	Complete - the non load-bearing bulkheads have been redesigned for the final rocket to minimize mass.	Payload Assembly and Rocket Integration
2. Control System Requirements				
2.1 The roll simulated in KSP should be consistent within 10% of the data obtained from the IMU.	Analysis and Test	The KSP analysis and the ground-based test facility shall be used to verify the synching of KSP and physical IMU output.	In Progress - while KSP works statically, the Wi-Fi image for Beaglebone needs to be written for full integration.	The FRAME
2.2 The control system shall activate the first thruster pair within 2 seconds of MECO.	Demonstration	Data from the subscale and fullscale demonstration will verify the actuation time delay.	Complete - Fullscale flight analysis shows successful detection of MECO.	Fullscale Flight Results

Team Derived Requirements

Requirement	Verif. Method	Description of Verification Plan	Status	Document Section
2.3 The IMU shall define a zero-angular-velocity target upon completion of two full rotations.	Test	The ground-based test facility shall be used to verify that the rocket will return to original orientation.	Complete - FRAME testing shows the validity of the control system's logic	The FRAME
2.4 The control system shall determine the response necessary to complete the roll.	Test	The ground-based test facility will verify the ability of the control system to predict an underdamped or overdamped response in accordance with the input.	Complete - FRAME testing and fullscale launch validate the control system's efficacy.	The FRAME Control Schemes Fullscale Flight Results
2.5 The control system should keep rocket at fixed rotational orientation from time roll stops until apogee.	Test	The ground-based test facility shall be used along with pre-competition launch data to verify the post-roll angular position control capabilities.	The ground-based test facility shall be used along with pre-competition launch data to verify the post-roll angular position control capabilities.	The FRAME Control Schemes
2.6 The control system shall be robust enough to respond to atmospheric disturbances	Test and Demonstration	The motor input on the ground based test facility will simulate atmospheric disturbances and be correlated to data collected from subscale and fullscale demonstrations.	Complete - FRAME testing with induced wind loading from a leaf blower shows its ability to respond to atmospheric disturbances.	The FRAME Control Schemes
2.7 The Hotbox shall use ROSMOD and BeagleBone Black to help the team build familiarity with the payload electronic hardware and software	Inspection	An inspection of our hotbox assembly will show the use of ROSMOD and BBB and their relation to our launch vehicle.	Complete - the Hotbox was built with ROSMOD and BBB to allow the controls team to gain experience.	Hotbox with Airframe Curing Inside
3. Payload Electronics Requirements				
3.1 All electronics, except for solenoids, must fit within the upper coupler tube section, and allow for safe assembly with no damage to any team member or the rocket itself.	Analysis and Demonstration	Use of CAD software will ensure all components integrate in the space provided.	Complete - the payload electronics sled fits well within the confines of the Blue Tube coupler of the payload skeleton.	Payload Electronics
3.2 The payload must be powered by rechargeable batteries, chargeable from outside the coupler tube section.	Demonstration	Integrate charging port, and extend leads outside top bulkheads for each battery	Complete - a charging circuit has been integrated, allowing the batteries to be charged without full disassembly.	Auxiliary Circuit Board
3.3 The payload must be able to remain armed on the launchpad for at least 3 hours.	Analysis	Calculate normal use-case battery life for both testing and launch environments, then compare to battery capacity	Complete - The Li-Ion batteries on board have been verified to last at least four hours in the armed state.	Power Supply

Team Derived Requirements

Requirement	Verif. Method	Description of Verification Plan	Status	Document Section
3.4 The payload must be armable from the exterior of the airframe while on the launch rail.	Test and Demonstration	Install and integrated screw switch, assemble airframe and drill access holes	Complete - the fullscale vehicle incorporates a screw switch to arm the payload electronics.	Auxiliary Circuit Board
3.5 No electrical components will experience levels of voltage or current for which they are not rated.	Analysis	Check ratings on components before finalizing design, simulate circuit, addition of flyback diode	Complete - the final board has been designed and fully tested to ensure no components experience unrated loads	Payload Electronics
3.6 Solenoid valve leads will be connected to a flyback diode to prevent current spikes.	Test	Operate solenoids using a flyback diode, verifying continuity of power to BeagleBone	Complete - a flyback diode has been incorporated on the final board design.	Solenoid Valves
3.7 The payload computer will have wireless communication capabilities.	Test and Demonstration	Connect to BeagleBone Wireless while payload is both inside and outside of the airframe.	In Progress - the Wi-Fi image for Beaglebone needs to be written for full wireless integration.	Beagle-Bone Black Wireless Single Board Computer
4. Ground Based Test Facility Requirements				
4.1 Test stand should simulate torque on the rocket to simulate in-flight wind disturbances.	Test	The ground-based test facility shall be equipped with a motor with enough torque to simulate the resistive response of wind effects.	Complete - damped flow tests on the FRAME validate the ability of the rocket to return to original orientation, even with simulated wind disturbances.	The FRAME
4.2 Yaw, pitch, and roll data will be collected by the IMU and plotted in real-time via ROSMOD.	Test	Ground-based test facility shall be used to verify the data delivery and graphic representation.	Complete - ROSMOD has demonstrated the capability to write yaw, pitch, and roll data from the IMU.	The FRAME
4.3 Test facility will be able to transmit the peak torque output of the motor via the fin gripper system.	Test	This load-bearing capability of the fin gripper system will be verified by the first test.	Complete - while full output torque of the motor is rarely used, the system has shown its ability to transfer the load to the rocket.	The FRAME
4.4 Test facility shall have a motor capable of inducing torques equal to or greater than that of the thrusters system.	Test	The motor capability will be analyzed by comparing experimental data of the rocket rotation in the test facility with the thruster actuation to data with motor actuation but without thruster actuation.	Complete - the FRAME has a motor with the capability to out torque the thrusters, providing test disturbances for the launch vehicle to respond to.	The FRAME

Team Derived Requirements

Requirement	Verif. Method	Description of Verification Plan	Status	Document Section
4.5 Test facility should be able to operate at angular velocities up to 240 RPM.	Analysis and Test	An analysis of the motor specs and mass properties of the rocket will be verified by fullscale rocket experiments on the test facility.	Complete - the FRAME has been bolted to the wall to mitigate vibrations at high angular velocities	The FRAME
4.6 Test facility axial constraint system shall be able to support rocket during dynamic loading from thruster fire at maximum thrust.		Analysis using free body diagram of stand while thrusters are being fired will be verified by preliminary tests.	Complete - The retainment system for the launch vehicle has been proven to contain the rocket during thruster firing.	
4.7 KSP visualization shall use hardware-in-the-loop simulation to visualize the rocket's current angular position during flight.	Test	This visualization will be refined and verified during experimentation after fullscale rocket integration onto the test facility.	In Progress - while KSP works statically, the Wi-Fi image for Beaglebone needs to be written for full integration.	The FRAME
5. Vehicle and Recovery Requirements				
5.1 Carbon fiber wrapped Blue Tube will offer twice the strength of standalone Blue Tube.	Test	Compression testing will be conducted for both materials to compare yield strength values.	Complete - compression testing of the carbon fiber Blue Tube shows to be over 2x stronger than regular Blue Tube.	Carbon Fiber Reinforced Blue Tube testing
5.2 The launch vehicle should weigh less than 40 lbs. before takeoff.	Inspection	The weights of all components will be summed to verify total vehicle weight is less than 40 lbs.	Complete - the final mass of the vehicle is 34 lbs.	Vehicle Criteria
5.3 The launch vehicle should be capable of being prepared at launch site within 2 hours.		This will be verified and demonstrated at launch site.	Complete - the fullscale test launch verified the ability to assemble the launch vehicle in less than two hours.	
5.4 The tail section shall be capable of withstanding temperatures of over 200F due to recirculation of hot air during initial launch phase.	Analysis and Test	An analysis of material properties and testing Hotbox will ensure capability of withstanding hot temperatures.	Complete - the carbon fiber boat tail can take temperatures well above the 200F requirement.	Design & Construction of Launch Vehicle
5.5 Average drag coefficient of entire rocket in upwards orientation should be known to the nearest 0.01 before launch.	Analysis	Computational fluid dynamic (CFD) analysis will be performed on a CAD version of the rocket to compute drag.	Complete - CFD simulations and analysis of inflight testing have validated the accuracy of the CFD	Computational Modeling Fullscale Flight Results

Team Derived Requirements

Requirement	Verif. Method	Description of Verification Plan	Status	Document Section
5.6 Center of pressure of launch shall be known to nearest 1" before launch.	Analysis	Mathematical pressure analysis and CFD will be performed to calculate and verify the placement of the COP.	Complete - CFD has been validated with Rocksim simulations within 1"	Computational Modeling Mission Performance Predictions
5.7 The descent speed of the rocket after the drogue parachute is released should be greater than 60 ft./s to minimize drift.	Analysis and Demonstration	A simulation analysis and the onboard sensors will monitor speed during flight demonstration and verify the descent speed after release of the drogue parachute.	Complete - the descent speed under drogue was 75ft/s, predicted by simulation and validated by fullscale launch.	Mission Performance Predictions Fullscale Flight Results
5.8 The lengths of parachute cord will be sized such that no two independent sections will be able to hit each other during deployment.	Analysis and Demonstration	Inspection and mathematical analysis considering lengths of rocket airframe sections will be performed.	Complete - the shock cords have been cut to a size so as not to let any sections of the rocket interfere with each other.	Milestone Review Flysheet
5.9 The launch vehicle shall be capable of being transported in sections and assembled on the launch site.*	Analysis	An analysis of the vehicle's CAD shows its ability to be split into three sections.	Complete - the vehicle can easily be split into three sections for transport.	Design & Construction of Launch Vehicle
5.10 Putty shall be used to seal any holes where pressure from black powder blasts may be present.*	Inspection	Putty shall be incorporated into the launch checklist.	Complete - the launch checklist shows putty as an essential step for successful launch.	Launch Operations Procedures
5.11 The launch vehicle must minimize unnecessary mass.*	Analysis	Any non-load bearing parts should be analyzed to see where mass can be reduced.	Complete - a size reduction to bulkheads in the payload and components of the avionics skeleton have led to a more optimized, lightweight design.	Payload Assembly and Rocket Integration Design and Construction
5.12 The launch vehicle shall cover all parachutes with a fire retardant blanket to mitigate the risk of parachute burning during deployment events.*	Inspection	A fire retardant blanket will be added to the launch checklist.	Complete - the presence of fire-retardant blanket installation on the launch checklist ensures that no parachutes will be damaged during deployment.	Launch Operations Procedures

Team Derived Requirements

Requirement	Verif. Method	Description of Verification Plan	Status	Document Section
5.13 The launch vehicle shall incorporate an anti-zipper design.*	Inspection	A fireball anti-zipper device will be added to the shock cords.	Complete - the presence of a fireball anti-zipper device as an essential step to installing the parachutes ensures that the shock cords will not tear out through the airframe.	Launch Operations Procedures
5.14 Sharp objects within the avionics section, like weld nuts and threaded rods, shall be covered to mitigate the risk of parachute tearing.*		The launch checklist shall incorporate the taping of sharp objects that pose a risk to parachutes.	Complete - the launch checklist shows protecting the parachutes from tearing using tape to be an essential step for successful launch.	
5.15 Properly sized vent holes must be drilled in the avionics bay to allow accurate pressure readings by the altimeters.*	Analysis	The literature for the avionics shall be used to verify that the holes drilled for venting are large enough.	Complete - properly sized holes have been drilled in the avionics bay to allow for venting to the altimeters.	Launch Operations Procedures
5.16 4-40 Nylon shear pins shall be used and secured with electrical tape prior to launch.*	Inspection	The launch checklist shall incorporate the taping of shear pins.	Complete - shear pin taping as an essential part of launch operations ensures they will not come out under vibrational loading.	Launch Operations Procedures

6. Safety Requirements

Note: see Safety for the complete list of team derived safety requirements

6.1 All VADL members involved in fabrication shall wear latex or vinyl gloves when handling chemicals, allergens, or carbon fiber layup.	Inspection	A self-imposed inspection by our student safety officer will verify our use of proper equipment during operations.	In Progress - the student safety officer will continue to ensure latex gloves are worn while handling caustic materials.	Safety Data Sheets
6.2 All personnel present at machining operations will wear eye protection.		Students involved in machining will sign an agreement to always wear proper equipment.	Complete - all students who machine have signed an agreement verifying that they understand proper shop safety.	Personnel Hazard Analysis
6.3 All personnel will wear close-toed shoes in the lab.		A self-imposed inspection by our students will verify our use of proper equipment during operations.	In progress - all students will continue to check each other to ensure that closed toed shoes are being worn in the shop.	Personnel Hazard Analysis

Team Derived Requirements

Requirement	Verif. Method	Description of Verification Plan	Status	Document Section
6.4 At least two team members will be present for hazardous operations such as machining and carbon fiber layup.	Inspection	Students will sign a safety agreement to always work with a partner.	Complete - students have signed an agreement stating they understand the importance of working with a partner during hazardous operations.	Personnel Hazard Analysis
6.5 All team members operating or present around heavy machinery will wear hearing protection.	Inspection	A self-imposed inspection by our student safety officer will verify our use of proper equipment during operations.	In progress - students are sure to continue wearing hearing protection during loud operations.	Safety
6.6 Internal cavities in the launch vehicle shall be kept at atmospheric pressure.	Inspection	Inspection of the launch vehicle design will show proper venting throughout the payload bay to the atmosphere.	Complete - venting holes have been drilled to ensure that pressure does not build up.	Design and Construction
6.7 Black powder charges will be isolated from all components excluding parachutes.	Inspection	Launch vehicle will be inspected to ensure black powder charges are not in contact with any other components.	Complete - the avionics bay design ensures that blast charges only directly impact the parachutes.	Recovery System Failure Modes
6.9 When particulates are released during cutting operations, an air filter shall be used.	Inspection	A self-imposed inspection will verify our use of the air filter during cutting operations.	In Progress - the air filter will continue to be used for all cutting operations where particulates are released.	Personnel Hazard Analysis
6.10 The hotbox shall have a control algorithm to prevent reaching excess temperatures.	Analysis and Test	An analysis and test of the control algorithm used on the hotbox will verify its ability to prevent excess temperatures.	Complete - the control system for the Hotbox specifies a temperature limit that the box will not exceed.	See PDR for Hotbox Control Scheme
6.11 The hotbox shall be wired according to electric code to reduce the risk of fire.	Inspection	An inspection of the wiring plan for the hotbox will show its compliance with electric codes.	Complete - the hotbox was wired to fit all relevant electric codes to reduce the risk of fire.	Personnel Hazard Analysis
6.12 The hotbox will have a protective box over the control panel that prevents exposure to high voltage.	Inspection	An inspection of the design plan for the hotbox will show the use of a protective box.	Complete - the hotbox features a high voltage protective box to prevent shock.	Personnel Hazard Analysis
6.13 The solenoids selected will be normally closed to prevent venting in the case of power loss.	Inspection	An inspection of the solenoid spec sheet will verify it is normally closed in the case of power loss to the system.	Complete - the solenoid features a pilot-operated normally closed valve.	Air Delivery System Safety

Team Derived Requirements

Requirement	Verif. Method	Description of Verification Plan	Status	Document Section
6.14 Heating elements in the hotbox will be deactivated if the BeagleBone is deactivated	Inspection	An inspection of the schematic for the hotbox will show its ability to turn off heating elements if the BeagleBone is deactivated.	Complete - the wiring for the hotbox features a design that relies on control system power to maintain heating element power.	See PDR for Hotbox Control Scheme
6.15 All components exposed to heat in the Hotbox shall be rated to above 200F.	Inspection	An inspection of the manufacturer spec sheet for hotbox components will show their rating to be above the required amount.	Complete - the hotbox components are all rated well above 200 F, the maximum expected temperature to be used.	See PDR for Hotbox Component Details
6.16 The chosen air tank shall contain burst discs to prevent excess pressure from flooding the thruster system.	Inspection	An inspection of the regulator used on the air tank will show the presence of properly rated burst disks.	Complete - the air tank features a 1.8kpsi burst disc.	Air Delivery System Safety
6.17 Payload electronics will not present an electrical hazard by way of fire, heat, or ground fault.	Inspection and Test	Wires will be routed to prevent shorts, and components will be cooled appropriately.	Complete - components that generate considerable heat utilize a heat sink, while all wires are shielded.	Payload Electronics

7.3 Budgeting and Timeline

7.3.1 Budget

VADL receives funding from multiple sources, including NASA, Boeing, and Vanderbilt University. These funding sources and amount are listed in the Table 32.

Table 32: Funding Source

Funding Source	Amount
Boeing	2750
NASA	5000
Vanderbilt	12250
Total	20000

Table 33 shows the categorized purchases to this point in the project.

Table 33: 2016-2017 Categorized Purchases

Company	Item	Part cost	Quantity	Total Cost	Order cost	Category
Sparkfun	Resistor Kit - 1/4 W	\$7.95	1	\$7.95		Electronics
Sparkfun	LED- Assorted 20 pack	\$2.95	1	\$2.95		Electronics
Sparkfun	Discrete Semiconductor Kit	\$8.95	1	\$8.95		Electronics
Sparkfun	Solid State Relay- 40A	\$9.95	1	\$9.95		Electronics
Sparkfun	Screw Terminals 3.5mm Pitch	\$0.95	10	\$9.50		Electronics
Sparkfun	Molex Jumper 2 Wire Assembly	\$0.95	20	\$19.00		Electronics
Sparkfun	DC Barrel Jack Adapter- Breadboard Compatible	\$0.95	5	\$4.75		Electronics
SparkFun	Triple Axis Accelerometer and Gyro Breakout - MPU-6050	\$39.95	1	\$39.95		Electronics
SparkFun	SparkFun OpenLog	\$14.95	1	\$14.95		Electronics
SparkFun	P-Channel MOSFET 60V 27A	\$0.95	1	\$0.95		Electronics
SparkFun	Arduino ProtoShield - Bare PCB	\$4.95	1	\$4.95		Electronics
SparkFun	Arduino Stackable Header Kit	\$1.50	1	\$1.50		Electronics
Sparkfun	Shipping	\$21.96	1	\$37.30	\$162.65	Electronics

2016-2017 Categorized Purchases

Company	Item	Part cost	Quantity	Total Cost	Order cost	Category
Sparkfun	Sparkfun Electronics	\$15.15	1	\$15.15	\$15.15	Electronics
Amazon	Wick	\$5.95	1	\$5.95	\$355.18	Electronics
Amazon	Soldering Paste	\$17.95	1	\$17.95		Electronics
Amazon	Soldering Station	\$250.52	1	\$250.52		Electronics
Amazon	16 GB MicroSD cards	\$7.11	5	\$35.55		Electronics
Amazon	AC Fan (Heavy Duty Aluminum)	\$18.99	2	\$37.98		Electronics
Amazon	Shipping	\$7.23	1	\$7.23		Electronics
Amazon	Digital Multimeter	\$17.99	1	\$17.99	\$17.99	Electronics
Amazon	Drone Connectors	\$2.99	4	\$11.96	\$11.96	Electronics
Adafruit	Element 12 BeagleBone Black	\$55.00	5	\$275.00	\$433.24	Electronics
Adafruit	Stacking Header Set for Beagle Bone Capes	\$4.95	5	\$24.75		Electronics
Adafruit	Half-size Breadboard	\$5.00	5	\$25.00		Electronics
Adafruit	Thermistors	\$4.00	4	\$16.00		Electronics
Adafruit	Miniature Wifi (802.1b/g/n) Module	\$11.95	3	\$35.85		Electronics
Adafruit	SMT/SMD 0805 Resistor and Capacitor Book	\$39.96	1	\$39.96		Electronics
Adafruit	Shipping	\$16.68	1	\$16.68	\$433.24	Electronics
Adafruit	5V 2.4A Switching Power Supply	\$7.95	2	\$15.90	\$91.52	Electronics
Adafruit	Adafruit Proto Cape Kit for Beagle Bone Black	\$9.95	5	\$49.75		Electronics
Adafruit	5V 2A Switching Power Supply	\$7.95	2	\$15.90		Electronics
Adafruit	Shipping	\$9.97	1	\$9.97		Electronics
Southern Fluid Power	Solenoid Coil	\$75.07	2	\$150.14	\$378.54	Rocket Fab
Southern Fluid Power	Valve Body	\$114.20	2	\$228.40		Rocket Fab
Loftis Steel & Alu-minum	1/4" Alum Plate 6061-T6	\$68.36	2	\$136.72		FRAME

2016-2017 Categorized Purchases

Company	Item	Part cost	Quantity	Total Cost	Order cost	Category
Loftis Steel & Aluminum	1/4" Alum Plate 6061-T6 Saw Cut	\$46.00	1	\$46.00	\$182.72	FRAME
Loftis Steel & Aluminum	Water jet cutting of carbon fiber material for sub-scale fins	\$100.00	1	\$100.00	\$100.00	FRAME
Loftis Steel & Aluminum	Custom Cutting	\$250.00	1	\$250.00	\$250.00	FRAME
McMaster Carr	1" Aluminum T-Slotted Framing Extrusion - 2 ft	\$8.35	8	\$66.80		FRAME
McMaster Carr	1" Aluminum T-Slotted Framing Extrusion - 3 ft	\$11.53	4	\$46.12		FRAME
McMaster Carr	1" Aluminum T-Slotted Framing Extrusion - 8 ft	\$26.38	4	\$105.52		FRAME
McMaster Carr	90 Plate for Aluminum T-Slotted Framing Extrusion	\$8.47	24	\$203.28		FRAME
McMaster Carr	Pack of 4 Steel End-Feed Fastener for 1" Aluminum T-Slotted Framing Extrusion	\$2.30	35	\$80.50		FRAME
McMaster Carr	Brace for 1" Aluminum T-Slotted Framing Extrusion	\$5.51	6	\$33.06		FRAME
McMaster Carr	Thrust Bearing	\$5.11	2	\$10.22		FRAME
McMaster Carr	Radial Bearings	\$5.59	4	\$22.36		FRAME
McMaster Carr	3 ft Carbon Steel 3/8" Diameter Rod	\$8.25	1	\$8.25		FRAME
McMaster Carr	1/8" Diameter 1/2" long alloy steel dowel (pack of 100)	\$10.01	1	\$10.01		FRAME
McMaster Carr	1/4" 20, 1" Long Socket Head Cap Screws pack of 50	\$7.84	1	\$7.84		FRAME

2016-2017 Categorized Purchases

Company	Item	Part cost	Quantity	Total Cost	Order cost	Category
McMaster Carr	Large Diameter Radial Bearing	\$11.89	2	\$23.78	\$617.74	FRAME
McMaster Carr	Multipurpose 6061 Aluminum with Certification Rod, 1' Long	\$12.92	2	\$25.84		Rocket Fab
McMaster Carr	High-Speed Steel Metric Size Chucking Reamer 1.5mm Dia	\$16.27	2	\$32.54		Rocket Fab
McMaster Carr	Carbide Chamfer End Mill Four Flute	\$29.56	2	\$59.12		Rocket Fab
McMaster Carr	1/4" 316 Stainless Steel Yor-Lok Tube Fitting Through-Wall	\$23.32	2	\$46.64		Rocket Fab
McMaster Carr	1/4" 316 Stainless Steel Yor-Lok Tube Fitting Tee	\$34.98	2	\$69.96		Rocket Fab
McMaster Carr	1/4" 316 Stainless Steel Yor-Lok Tube Fitting Elbow	\$19.55	4	\$78.20		Rocket Fab
McMaster Carr	Smooth-Bore Seamless Stainless Steel Tubing 1 ft	\$7.83	3	\$23.49		Rocket Fab
McMaster Carr	1/4", 12L14 Carbon Steel Tight-Tol. Rod 1 ft	\$2.17	3	\$6.51		Rocket Fab
McMaster Carr	Power Strip (15' cord, 4 outlets)	\$31.17	1	\$31.17		Rocket Fab
McMaster Carr	GFIC Outlet (Duplex)	\$20.00	3	\$60.00		Rocket Fab
McMaster Carr	Power Cord Whips (NEMA)	\$11.82	2	\$23.64		Rocket Fab
McMaster Carr	Ceramic Lightbulb Sockets (4.5" dia)	\$3.68	6	\$22.08		Rocket Fab
McMaster Carr	Flex Connectors	\$1.11	20	\$22.20		Rocket Fab
McMaster Carr	Electrical Boxes (4")	\$1.96	6	\$11.76	\$513.15	Rocket Fab
McMaster Carr	1/4"-20, 1" Long stainless bolt	\$5.24	1	\$5.24		Misc

2016-2017 Categorized Purchases

Company	Item	Part cost	Quantity	Total Cost	Order cost	Category
McMaster Carr	1/4"-20, 3" Long stainless bolt	\$8.99	1	\$8.99	\$70.17	Misc
McMaster Carr	1/2"-13, 3.5" Long stainless partial threaded bolt	\$1.97	9	\$17.73		Misc
McMaster Carr	1/4" Stainless washer	\$8.25	1	\$8.25		Misc
McMaster Carr	1/4"Lock washers	\$5.12	1	\$5.12		Misc
McMaster Carr	1/2" Stainless washers	\$9.71	1	\$9.71		Misc
McMaster Carr	1/4"-20 Stainless nuts	\$4.21	1	\$4.21		Misc
McMaster Carr	1/2"-13 Stainless nuts	\$5.10	1	\$5.10		Misc
McMaster Carr	1/2"-13 Stainlesslock nuts	\$5.82	1	\$5.82		Misc
McMaster Carr	Yor Lok to 1/4" NPT Female Adapter	\$14.11	1	\$14.11		Rocket Fab
McMaster Carr	Reducing 1/8" to 1/4" NPT Elbow	\$8.38	1	\$8.38		Rocket Fab
McMaster Carr	Stainless Steel Cable Tie	\$11.44	1	\$11.44		Rocket Fab
McMaster Carr	BrassSnap-TiteH-ShapeHose Coupling	\$12.37	1	\$12.37		Rocket Fab
McMaster Carr	Grade 8 Steel Fully Threaded Rod	\$3.60	3	\$10.80		Rocket Fab
McMaster Carr	Extreme-StrengthSteel Hex Nut (50 pk)	\$11.46	1	\$11.46		Rocket Fab
McMaster Carr	Aligning Weld Nut (20 pk)	\$15.81	1	\$15.81		Rocket Fab
McMaster Carr	Snap-in Nut	\$9.09	1	\$9.09		Rocket Fab
McMaster Carr	Galvanized Steel U-Bolt 1/4"20 Thread	\$0.97	3	\$2.91		Rocket Fab
McMaster Carr	Sleeves for 1/4" Tube OD Stainless Steel Yor Lok	\$3.53	5	\$17.65		Rocket Fab

2016-2017 Categorized Purchases

Company	Item	Part cost	Quantity	Total Cost	Order cost	Category
McMaster Carr	Nut for 1/4" Tube OD Steel Yor Lok	\$0.87	5	\$4.35		Rocket Fab
McMaster Carr	High Strength Stainless Steel Sheet (6" x 6")	\$16.41	1	\$16.41		Rocket Fab
McMaster Carr	Large Clamping U-Bolt	\$6.42	1	\$6.42		Rocket Fab
McMaster Carr	0.055" bit	\$2.29	3	\$6.87		Rocket Fab
McMaster Carr	Compact Extreme-Pressure Steel Thrd Fitting 1/4 Pipe Size, Female X Male X Female Tee	\$6.02	1	\$6.02		Rocket Fab
McMaster Carr	Compact Extreme-Pressure Steel Thrd Fitting 1/4" Male X 1/8" Fem Pipe Size, Hex Head Bushing	\$1.60	3	\$4.80		Rocket Fab
McMaster Carr	Liquid-Filled Gauge Plastic Case, 2-1/2" Dial, 1/4 Bottom, 1000 PSI	\$19.72	1	\$19.72		Rocket Fab
McMaster Carr	Rubber Edge Trim 1/16" Inside Width, 1/4" Inside Height, 10 ft. Length	\$8.80	1	\$8.80		Rocket Fab
McMaster Carr	Grade 8 Steel Fully Threaded Rod 1/4"-20 Thread, 2 ft Long	\$6.93	5	\$34.65		Rocket Fab
McMaster Carr	Pan Head Drilling Screw for Metal 410 SS, 6-20 Thread, Packs of 100	\$5.40	2	\$10.80		Rocket Fab
McMaster Carr	Indoor Steel Enclosure with Knockouts Hinged Cover	\$24.38	1	\$24.38		Rocket Fab
McMaster Carr	Smooth-Bore Seamless 304 SS Tubing 1/4" OD, 0.028" Wall Thickness, 3 ft. Long	\$13.53	3	\$40.59		Rocket Fab

2016-2017 Categorized Purchases

Company	Item	Part cost	Quantity	Total Cost	Order cost	Category
McMaster Carr	Clamping U-Bolt Znc-Pltd STL, 5/16"-18 Thrd Sz, 2" ID	\$1.84	3	\$5.52		Rocket Fab
McMaster Carr	Steel Yor-Lok Tube Fitting Straight Adapter for 1/4" Tube OD X 1/4 NPT Male	\$4.86	4	\$19.44		Rocket Fab
McMaster Carr	Steel Yor-Lok Tube Fitting Straight Adapter for 1/4" Tube OD X 1/8 NPT Male	\$4.61	2	\$9.22		Rocket Fab
McMaster Carr	Compact Extreme-Pressure Steel Pipe Fitting Tee Connector, 1/4 NPTF Female	\$6.13	1	\$6.13		Rocket Fab
McMaster Carr	Compact Extreme-Pressure Steel Pipe Fitting Right-Angle Tee Adapter, 1/4 NPTF Female X Male	\$6.38	1	\$6.38		Rocket Fab
McMaster Carr	Medium-Strength Steel Thin Hex Nut Grade 5, Zinc-Plated, 5/16"-18 Thread Size, Packs of 100	\$5.53	1	\$5.53		Rocket Fab
McMaster Carr	General Purpose 1074/1075 Spring Steel Sheet .050" Thick, 8" X 24"	\$36.04	1	\$36.04		Rocket Fab
McMaster Carr	Compact Extreme-Pressure Steel Pipe Fitting 90 Degree Elbow Adapter, 1/4 NPTF Female X Male	\$4.14	2	\$8.28		Rocket Fab
McMaster Carr	Compact Extreme-Pressure Steel Pipe Fitting Straight Connector, 1/4 NPTF Male	\$1.29	4	\$5.16	\$142.29	Rocket Fab

2016-2017 Categorized Purchases

Company	Item	Part cost	Quantity	Total Cost	Order cost	Category
McMaster Carr	Timing Belt Pulley XL Series, 4.564" OD	\$49.87	1	\$49.87		FRAME
McMaster Carr	XL Series Lightweight Timing Belt Pulley 1.75" OD	\$8.20	1	\$8.20		FRAME
McMaster Carr	XL Series Timing Belt, Trade NO. 290XL025	\$5.55	1	\$5.55		FRAME
McMaster Carr	XL Series Timing Belt, Trade NO. 250XL025	\$5.01	1	\$5.01		FRAME
McMaster Carr	Black-Oxide Steel U-Bolt W/Mounting Plate,	\$1.73	1	\$1.73		FRAME
McMaster Carr	18-8 Stainless Steel Hex Nut Black-Oxide, 5/16"-18 Thread Size,	\$5.89	1	\$5.89		FRAME
McMaster Carr	T0-220 Heat Sink	\$0.25	10	\$2.50		Electronics
McMaster Carr	4 pin Connector PCB (Female)	\$1.13	15	\$16.95		Electronics
McMaster Carr	4 pin Connector PCB (Male)	\$1.05	5	\$5.25		Electronics
McMaster Carr	18-8 SS Hex Drive Rounded Head Screw 1/4"-20 Thread Size,	\$7.06	1	\$7.06		Electronics
McMaster Carr	Extreme-Strength Steel Hex Nut Grade 9	\$11.46	1	\$11.46		Electronics
McMaster Carr	Button/Coin Cell Battery Alkaline, Size LR44	\$1.44	1	\$1.44		Electronics
McMaster Carr	Button/Coin Cell Battery Lithium, Size CR2032	\$1.92	2	\$3.84		Electronics
McMaster Carr	TiCN-Coated Carbide End Mill Two Flute	\$14.17	2	\$28.34		Electronics
McMaster Carr	J-B Weld Adhesive 8265-S, 2 Ounce Tube	\$6.17	1	\$6.17		Electronics

2016-2017 Categorized Purchases

Company	Item	Part cost	Quantity	Total Cost	Order cost	Category
McMaster Carr	Sanding Sheet for Alum, Soft Metal, & Nonmetal Waterproof, 600 Grit,	\$16.82	1	\$16.82		Electronics
McMaster Carr	Sanding Sheet for Alum, Soft Metal, & Nonmetal Waterproof, 1000 Grit,	\$15.87	1	\$15.87		Electronics
McMaster Carr	Plastic Syringe with Taper Tip, 4.7 oz Capacity	\$12.50	1	\$12.50		Electronics
McMaster Carr	Grade 8 Steel Washer Black Ultra-Corrosion-Rst,	\$7.47	1	\$7.47	\$110.97	Electronics
McMaster Carr	18-8 SS Hex Drive Rounded Head Screw 1/4"-20 Thread Size, 3/4" Long, Packs of 50	\$7.06	1	\$7.06		Electronics
McMaster Carr	Extreme-Strength Steel Hex Nut Grade 9, Cadmium Ylw-Chromate Pltd, 1/4"-20 Thrd Sz, Packs of 50	\$11.46	1	\$11.46		Electronics
McMaster Carr	Button/Coin Cell Battery Alkaline, Size LR44	\$1.44	1	\$1.44		Electronics
McMaster Carr	Button/Coin Cell Battery Lithium, Size CR2032	\$1.92	2	\$3.84		Electronics
McMaster Carr	TiCN-Coated Carbide End Mill Two Flute, 1/8" Mill Dia, 1/8" Shank Dia	\$14.17	2	\$28.34		Electronics
McMaster Carr	J-B Weld Adhesive 8265-S, 2 Ounce Tube	\$6.17	1	\$6.17		Electronics

2016-2017 Categorized Purchases

Company	Item	Part cost	Quantity	Total Cost	Order cost	Category
McMaster Carr	Sanding Sheet for Alum, Soft Metal, & Nonmetal Waterproof, 600 Grit, 4-1/2" X 11", Packs of 25	\$16.82	1	\$16.82	\$112.00	Electronics
McMaster Carr	Sanding Sheet for Alum, Soft Metal, & Nonmetal Waterproof, 1000 Grit, 4-1/2" X 11", Packs of 25	\$15.87	1	\$15.87		Electronics
McMaster Carr	PVC Tubing for Chemicals, 1/4" ID, 3/8" OD, 25 ft. Length	\$8.50	1	\$8.50		Electronics
McMaster Carr	Plastic Syringe with Taper Tip, 4.7 oz Capacity	\$12.50	1	\$12.50		Electronics
McMaster Carr	Nut for 1/4" Tube OD Type 316 Stainless Steel Yor-Lok Tube Fitting	\$2.42	10	\$24.20	\$72.24	Electronics
McMaster Carr	Front & Back Sleeve for 1/4" Tube OD Type 316 Stainless Steel Yor-Lok Tube Fitting	\$3.53	10	\$35.30		Electronics
McMaster Carr	Steel Yor-Lok Tube Fitting Straight Adapter for 1/4" Tube OD X 1/8 NPT Female	\$6.37	2	\$12.74		Electronics
McMaster Carr	SideMount External Retaining Ring (E-Style) Stainless Steel	\$4.45	1	\$4.45	\$41.21	Tools
McMaster Carr	Chipbreaking Cutoff Blade for Steel, Alum, Brass	\$12.96	1	\$12.96		Tools
McMaster Carr	Swivel Leveling Mount	\$5.95	4	\$23.80		Tools
MSC Industrial Supply Co	Carbide Tapered End Mill	\$63.14	2	\$126.28		Electronics

2016-2017 Categorized Purchases

Company	Item	Part cost	Quantity	Total Cost	Order cost	Category
MSC Industrial Supply Co	3/16" Chamfer End Mill, 60 degree	\$59.40	1	\$59.40	\$185.68	Electronics
Mouser	Inrush Current Limiter (NTC Thermistor)	\$2.49	3	\$7.47	\$32.52	Electronics
Mouser	DC Fan	\$9.35	1	\$9.35		Electronics
Mouser	100uF Capacitor	\$0.55	5	\$2.75		Electronics
Mouser	10uF Capacitor	\$0.48	5	\$2.40		Electronics
Mouser	0.1uF Capacitor	\$0.10	5	\$0.50		Electronics
Mouser	5V Regulator	\$1.49	5	\$7.45		Electronics
Mouser	NPN Transistor	\$0.13	20	\$2.60		Electronics
Newegg	SSR/Heatsink Assembly	\$18.78	1	\$18.78	\$18.78	Electronics
Newegg	Digital Thermistor	\$26.04	1	\$26.04	\$26.04	Rocket Fab
Newark	High Current Terminal Block	\$5.90	5	\$29.50	\$29.50	Electronics
Lowes	2 x 4 x 8 Laboratory Supplies	\$2.64	8	\$21.12	\$181.17	Rocket Fab
Lowes	Top Choice 1/2-in Common Birch/Blondewood Plywood	\$34.27	4	\$137.08		Rocket Fab
Lowes	The Hillman Group 100-Count Wood Screws	\$14.99	1	\$14.99		Rocket Fab
Lowes	3M 1.88-in W x 150-ft L HVAC Tape Model #3381	\$7.98	1	\$7.98	\$181.17	Rocket Fab
Digikey	Fans	\$9.36	3	\$28.08	\$28.08	Rocket Fab
Digikey	12V 36W AC/DC External Wall Mount Adapter Fixed Blade Input	\$20.27	1	\$20.27	\$20.27	Electronics
Digikey	TO-220 Heat sink	\$0.21	10	\$2.10	\$32.55	Electronics
Digikey	4 pin Connector PCB (Female)	\$1.23	5	\$6.15		Electronics
Digikey	4 pin Connector PCB (Male)	\$1.05	10	\$10.50		Electronics
Digikey	Shottkey Diode	\$1.38	10	\$13.80		Electronics

2016-2017 Categorized Purchases

Company	Item	Part cost	Quantity	Total Cost	Order cost	Category
Digikey	IC OPAMP INSTR 800KHZ 8DIP	\$15.44	5	\$77.20	\$192.44	Rocket Fab
Digikey	IC OPAMP GP 14KHZ RRO 8DIP	\$0.80	10	\$8.00		Rocket Fab
Digikey	IC REG LDO 5V 1.5A TO2203	\$1.45	10	\$14.46		Rocket Fab
Digikey	IC REG LDO 1.8V 0.5A TO2203	\$1.16	8	\$9.28		Rocket Fab
Digikey	IC OPAMP INSTR 800KHZ RRO 8DIP	\$7.47	3	\$22.41		Rocket Fab
Digikey	RES KIT 10K97.6K 1/4W 480PCS	\$29.95	1	\$29.95		Rocket Fab
Digikey	CAP CER 10000PF 100V NP0 RADIAL	\$3.64	6	\$21.84		Rocket Fab
Digikey	POT 10K OHM 0.15W CARBON LINEAR	\$1.55	3	\$4.65		Rocket Fab
Digikey	POT 1K OHM 0.15W CARBON LINEAR	\$1.55	3	\$4.65		Rocket Fab
Fibre Glast	3K, 2 x 2 Twill Weave Carbon Fiber Fabric, 60" Wide, 5 Yard Roll	\$299.95	1	\$299.95	\$638.45	Rocket Fab
Fibre Glast	System 2000 Epoxy Resin - Gallon (8lbs)	\$104.95	1	\$104.95		Rocket Fab
Fibre Glast	Epoxy Hardener 60 Minute Pot Life - Quart	\$44.95	1	\$44.95		Rocket Fab
Fibre Glast	Gray Sealant Tape - Single Roll	\$10.95	4	\$43.80		Rocket Fab
Fibre Glast	5 yd. Low Temperature Release Film - Perforated, 60" Wide Sheet	\$29.95	1	\$29.95		Rocket Fab
Fibre Glast	5 yd. Low Temperature Release Film - Non-Perforated, 60" Wide Sheet	\$14.95	1	\$14.95		Rocket Fab
Fibre Glast	1" Flash Tape	\$29.95	1	\$29.95		Rocket Fab
Fibre Glast	Shipping	\$69.95	1	\$69.95		Rocket Fab

2016-2017 Categorized Purchases

Company	Item	Part cost	Quantity	Total Cost	Order cost	Category
Fibre Glast	6 lb Polyurethane Mix and Pour Foam	\$34.95	1	\$34.95	\$44.90	Tools
Fibre Glast	Shipping	\$9.95	1	\$9.95		Tools
AMETEK	Brush DC Motor	\$375.67	1	\$375.67	\$403.02	FRAME
AMETEK	Shipping	\$27.35	1	\$27.35		FRAME
A-L Compressed Gases, Inc	Cylinder of compressed air	\$15.00	1	\$15.00	\$15.00	Rocket Fab
Drop Zone Extreme Sports	Air Tank	\$69.95	1	\$69.95	\$89.49	Misc
Drop Zone Extreme Sports	Shipping	\$19.54	1	\$19.54		Misc
All-battery.com	Tenergy TLP-2000 Smart Charger for Li-Ion/LiPo Battery Packs: 3.7V - 14.8V	\$14.99	1	\$14.99	\$25.00	Electronics
All-battery.com	Tenergy Li-Ion 14.8V 2200mAh Rechargeable Battery Pack w/ PCB (4S1P, 32.56Wh, 4A Rate)	\$28.40	3	\$85.20		Electronics
All-battery.com	Shipping	\$14.97	1	\$14.97		Electronics
Featherwieght Altimeters	Screw Switch	\$5.00	3	\$15.00	\$25.00	Electronics
Featherwieght Altimeters	Shipping	\$10.00	1	\$10.00		Electronics
Technical Training Aids	Black Build Material	\$130.00	3	\$390.00		Tools

2016-2017 Categorized Purchases

Company	Item	Part cost	Quantity	Total Cost	Order cost	Category
Technical Training Aids	Shipping	\$11.70	1	\$11.70	\$401.70	Tools
Enterprise	Vans	\$170.38	2	\$340.76	\$340.76	Travel
McMaster Carr	SpringLoaded Ball Fastener	\$1.12	40	\$44.80	\$48.17	FRAME
McMaster Carr	1/4" Stainless Steel Washer 100pk	\$3.37	1	\$3.37		FRAME
RiteAid	Soft Drinks & Water	\$16.27	1	\$16.27	\$16.27	Travel
Chris's Rocket Supplies	L1400 Loki White	\$165.00	4	\$660.00		Misc
Chris's Rocket Supplies	54-2800 Motor	\$165.00	1	\$165.00		Misc
Chris's Rocket Supplies	Fireware Electric Match	\$0.85	160	\$136.00	\$961.00	Misc
A-L Compressed Gases, Inc	Compressed Air	\$7.87	1	\$7.87	\$7.87	Misc
IR-G	Hydraulic Hose Assembly	\$40.73	1	\$40.73	\$40.73	Rocket Fab
Digikey	Diode	\$0.69	10	\$6.90	\$34.02	Electronics
Digikey	LED- Assorted 20 pack	\$0.05	30	\$1.62		Electronics
Digikey	N Channel MOSFET	\$1.12	10	\$11.20		Electronics
Digikey	5V Regulator	\$1.51	5	\$7.55		Electronics
Digikey	Splice Connector	\$0.27	25	\$6.75		Electronics
Mouser	4 GB Beagleboard	\$68.75	1	\$68.75	\$80.79	Electronics
Mouser	Right Angle USB Adapter	\$6.02	2	\$12.04		Electronics
Missile Works	6-32 Screw Switch	\$2.95	4	\$11.80	\$24.80	Electronics
Missile Works	Screw Switch Cover Guide	\$1.50	4	\$6.00		Electronics
Missile Works	Shipping	\$7.00	1	\$7.00		Electronics
Amazon	Electronics components	\$20.69	1	\$20.69	\$20.69	Electronics

2016-2017 Categorized Purchases

Company	Item	Part cost	Quantity	Total Cost	Order cost	Category
Advanced Circuits	Custom Circuit	\$33.00	2	\$66.00	\$86.74	Electronics
Advanced Circuits	Shipping	\$20.74	1	\$20.74		Electronics
B&H	Sony Action Cam Mini	\$179.00	1	\$179.00	\$278.00	Misc
B&H	Panasonic Wearable action cam	\$99.00	1	\$99.00		Misc
Apogee Rockets	5.5IN BLUE TUBE	\$56.95	2	\$113.90	\$147.85	Rocket Fab
Apogee Rockets	54MM BLUE TUBE	\$23.95	1	\$23.95		Rocket Fab
Apogee Rockets	LARGE AIRFOILED RAIL BUTTONS (FITS 1.5" RAIL - 1515)	\$10.00	1	\$10.00		Rocket Fab
FiberGlast	Stretchlon200 Bagging Film - 5 yd Roll - 60" Wide Sheet	\$19.95	1	\$19.95	\$64.90	Rocket Fab
FiberGlast	Epoxy Hardener 120 Minute Pot Life - Quart	\$44.95	1	\$44.95		Rocket Fab
Aeropack	Retainer Assembly, 54mm	\$29.00	4	\$116.00	\$116.00	Rocket Fab
McMaster	Hex Drive Rounded Head Screw Black-Oxide Alloy Steel, 5-40 Thread Size, 1/2" Long, Pack of 50	\$7.85	1	\$7.85	\$6.44	Rocket Fab
McMaster	Aligning Weld Nut Zinc-Plated Steel with Aluminum Retainer, 1/4"-20 Thread Size, Pack of 10	\$11.10	1	\$11.10		Rocket Fab
McMaster	Hex Drive Rounded Head Screw Black-Oxide Alloy Steel, 1/4"-20 Thread Size, 9/16" Long, pack of 10	\$6.44	1	\$6.44		Rocket Fab

2016-2017 Categorized Purchases

Company	Item	Part cost	Quantity	Total Cost	Order cost	Category
McMaster	Black-OxideSteelU-Bolt with MountingPlate,5/16"-18ThreadSize,3"ID	\$1.73	2	\$3.46	\$34.67	Rocket Fab
McMaster	Galvanized Steel U-Bolt 1/4"-20 Thread Size, 2" ID	\$0.97	6	\$5.82		Rocket Fab
Amazon	Dremel 4300-5/40 High Performance Rotary Tool Kit with Universal 3-Jaw Chuck, 5 Attachments and 40 Accessories	\$119.99	1	\$119.99	\$119.99	Rocket Fab
Tacoma Screw	#4-40 x 1/4" Pan Head Slotted Machine Screws Nylon, Coarse, 100/PKG	\$6.78	1	\$6.78	\$6.78	Rocket Fab
Sparkfun	Audio Jack 3.5 mm	\$1.50	2	\$3.00	\$26.11	Electronics
Sparkfun	Non-Invasive Current Sensor	\$9.95	1	\$9.95		Electronics
Sparkfun	Shipping	\$13.16	1	\$13.16		Electronics
McMaster	Double Spring Tab Fastener	\$1.40	40	\$56.00	\$56.00	FRAME
Local Gas Station	Gas for Outreach Event	\$184.79	1	\$184.79	\$184.79	Outreach
Local Gas Station	Gas for Outreach Event	\$62.45	1	\$62.45	\$62.45	Outreach
Local Gas Station	Gas for Outreach Event	\$150.12	1	\$150.12	\$150.12	Outreach

2016-2017 Categorized Purchases

Company	Item	Part cost	Quantity	Total Cost	Order cost	Category
Loftis Steel & Alu-minum	Water-cut Carbon fiber fins	\$100.00	1	\$100.00	\$100.00	Rocket Fab
McMaster	High-StrengthSteel Hex Nut	\$3.22	1	\$3.22		Rocket Fab
McMaster	Nut for 1/4"Tube OD SteelYor-LokTube Fitting	\$0.87	10	\$8.70		Rocket Fab
McMaster	Sleeve for 1/4"Tube OD SteelYor-LokTube Fitting	\$3.53	10	\$35.30	\$47.22	Rocket Fab
McMaster	Ball Bearing Dbl Shielded	\$12.38	1	\$12.38	\$12.38	FRAME
Avnet	Encoder Replacement Piece	\$20.81	1	\$20.81		Electronics
Avnet	Shipping	\$18.31	1	\$18.31	\$39.12	Electronics
Amazon	USB Connectors	\$9.99	1	\$9.99	\$9.99	Electronics
McMaster	Oil-Resistant Buna-N Multipurpose O-Ring 1/16 Fractional Width, Dash Number 010, Packs of 100	\$2.11	1	\$2.11		Tools
McMaster	13 Piece Hex L-Key Set	\$7.60	1	\$7.60		Tools
McMaster	STL End-Feed Fastener for 1-1/2" Single/3" Quad Aluminum T-Slotted Framing Extrusion, Packs of 4	\$2.71	2	\$5.42		Tools
McMaster	Oil-Resistant Buna-N Rubber Strip 6" X 36", 1/8" Thk, 50A Duro	\$13.14	1	\$13.14		Tools
McMaster	Multipurpose 6061 Aluminum Rod 7/8" Diameter, 2' Long	\$11.97	1	\$11.97	\$47.84	Tools
Amazon	Electop USB Male to Female	\$5.89	1	\$5.89	\$5.89	Electronics

2016-2017 Categorized Purchases

Company	Item	Part cost	Quantity	Total Cost	Order cost	Category
McMaster	Steel Eyebolt with Shoulder	\$13.43	2	\$26.86	\$26.86	Rocket Fab
Southern Fluid Power	Stainless Steel Valve	\$187.54	2	\$375.08	\$375.08	Rocket Fab
McMaster	Type 316 Stainless Steel Yor-Lock Tube Fitting	\$23.32	1	\$23.32		Misc
McMaster	Type 316 Stainless Steel Yor-Lock Tube Fitting Inline Tee	\$34.98	2	\$69.96		Misc
McMaster	Type 316 Stainless Steel Yor-Lock Tube 90 Degree Elbow	\$19.55	4	\$78.20		Misc
McMaster	Smooth Bore Seamless SS Fitting	\$13.53	1	\$13.53		Misc
McMaster	Front & Type 316 SS Back Sleeve	\$4.67	10	\$46.70		Misc
McMaster	High Strength Stainless Steel Sheet	\$16.41	1	\$16.41	\$248.12	Misc
Drop Zone Extreme Sports	NinjaPaintball Pro V2 Rotational Regulator	\$69.95	1	\$69.95		Misc
Drop Zone Extreme Sports	NinjaPaintball Universal Fill Adapter Black	\$14.95	1	\$14.95		Misc
Drop Zone Extreme Sports	EmpireBasicsCarbon Fiber HPA Tank	\$139.95	1	\$139.95	\$224.85	Misc
All-battery.com	Tenergy LiIon 14.8V 2200mAh Rechargeable Battery Pack	\$56.80	2	\$113.60	\$71.44	Misc
All-battery.com	Shipping	\$14.64	1	\$14.64	128.24	Misc

VADL organizes all orders through the budget officer and one mentor to ensure that all items are ordered promptly and the budget remain accurate and up to date. As discussed in 2.3, the budget has been modified according to the spending trends throughout fullscale launch. Figure 171

shows the new breakdown of this year's budget by category.

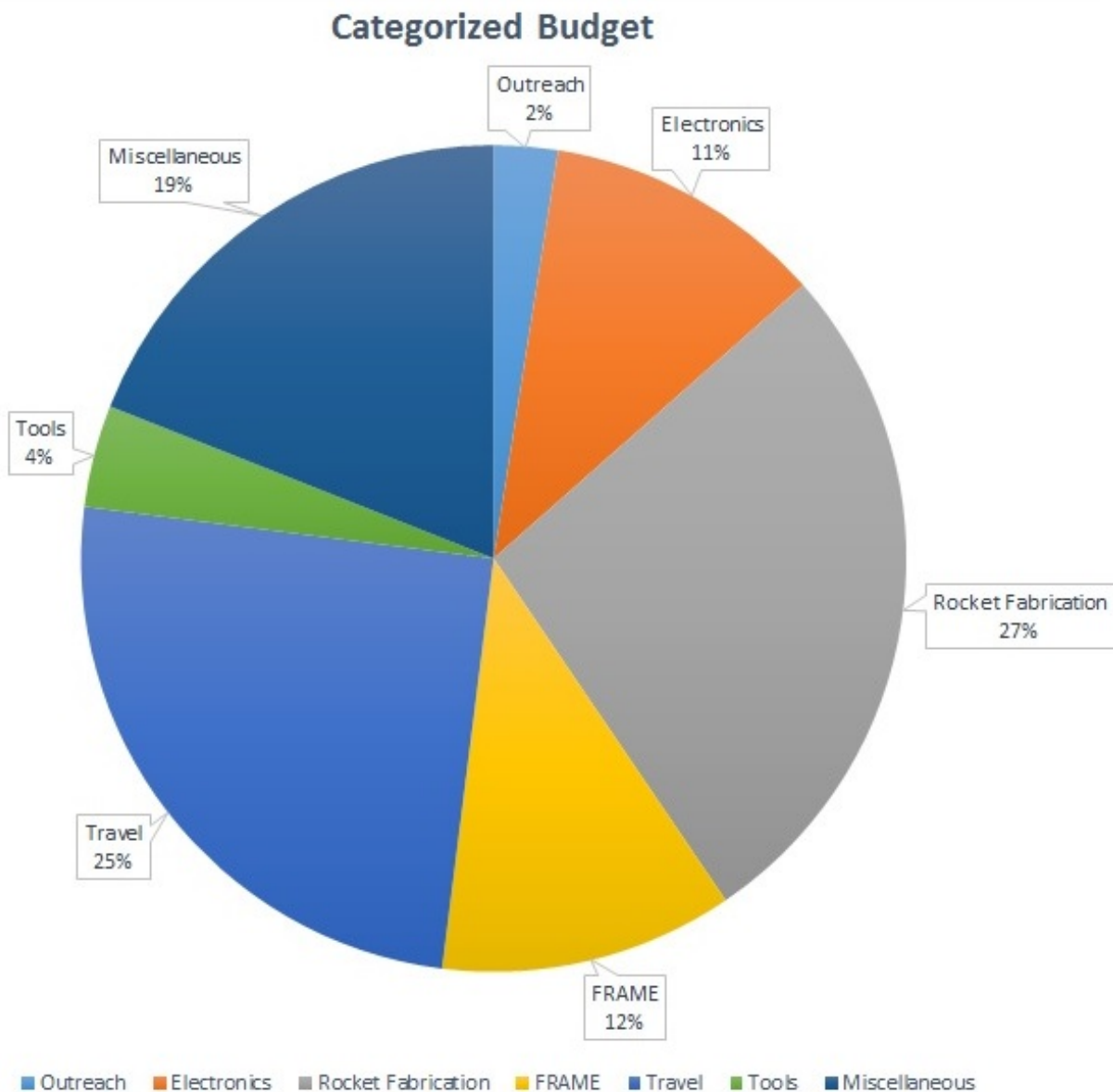


Figure 171: Budget by Category

The largest items in the budget are travel and housing for the competition launch, rocket fabrication, and miscellaneous expenses that may come up during the year. Examples of miscellaneous spending include launchpad materials, a new air filtration unit for the lab, and air tanks. The large allocation for miscellaneous expenses also mediates the risk of unexpected events that may require large purchases. So far, about \$2200 has been spent on electronics, \$5000 on rocket fabrication supplies, \$2300 on the FRAME, \$360 on travel, \$520 on tools, and \$2200 on miscellaneous purchases. Figure 172 shows the team's current status.

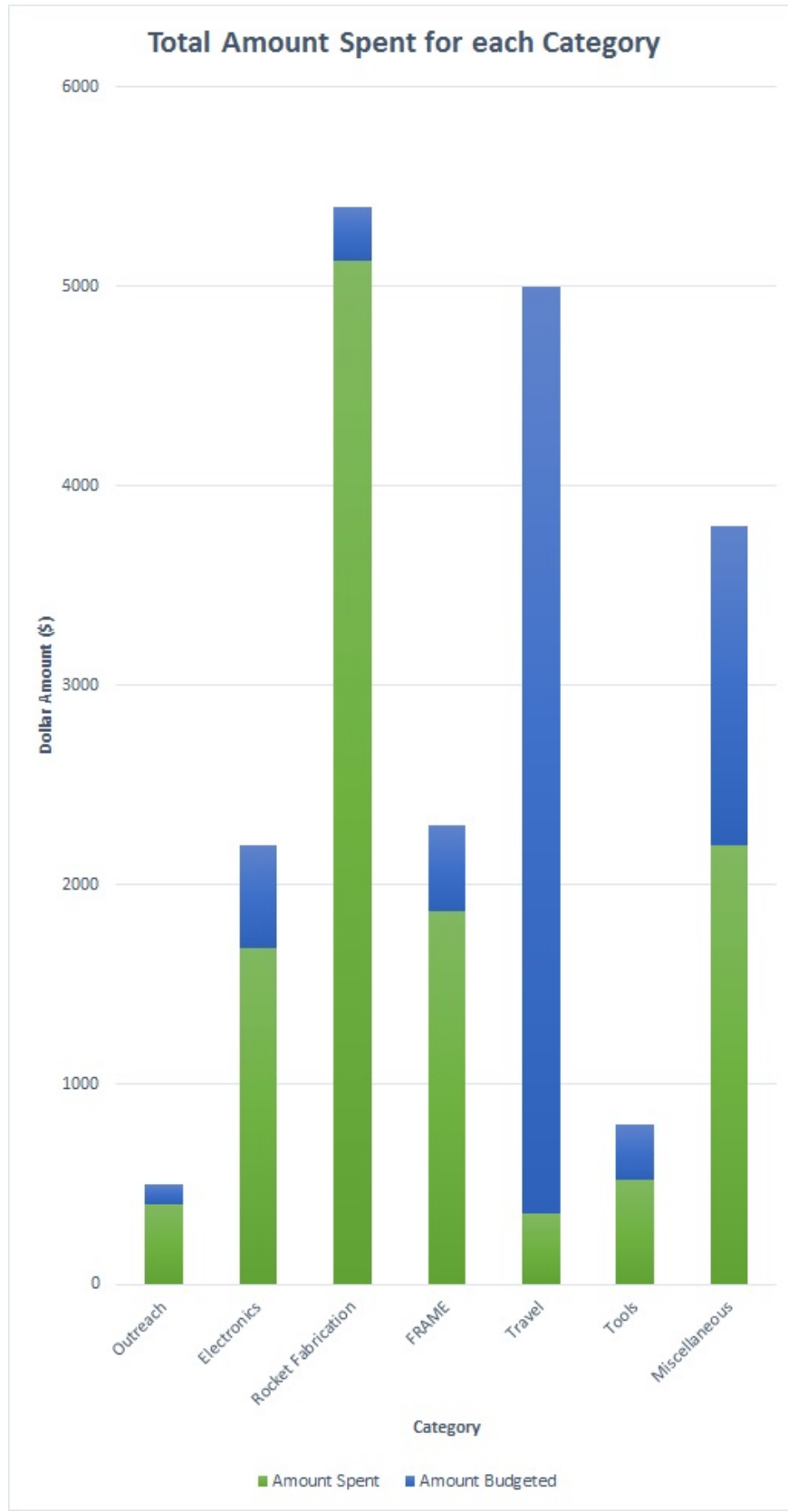
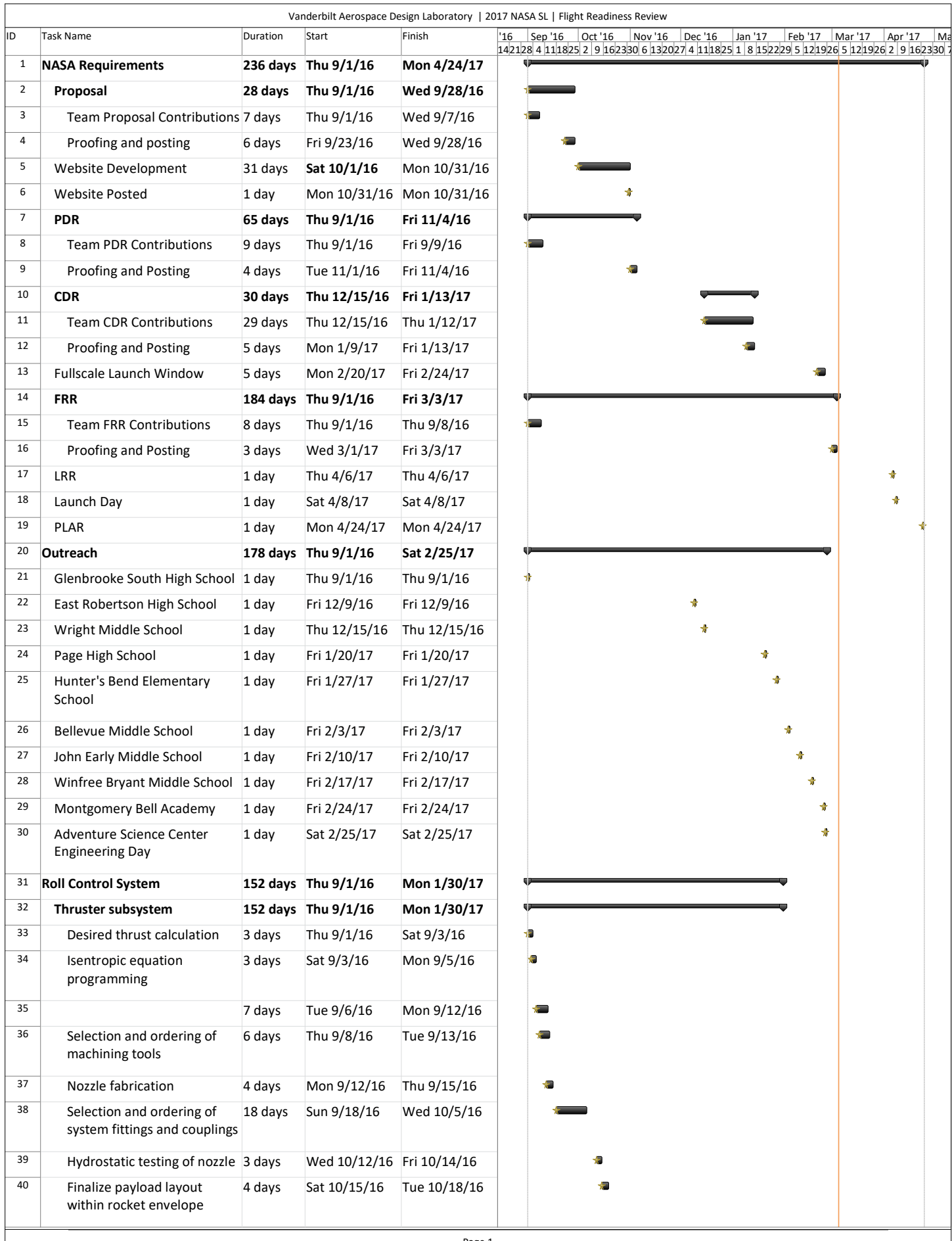


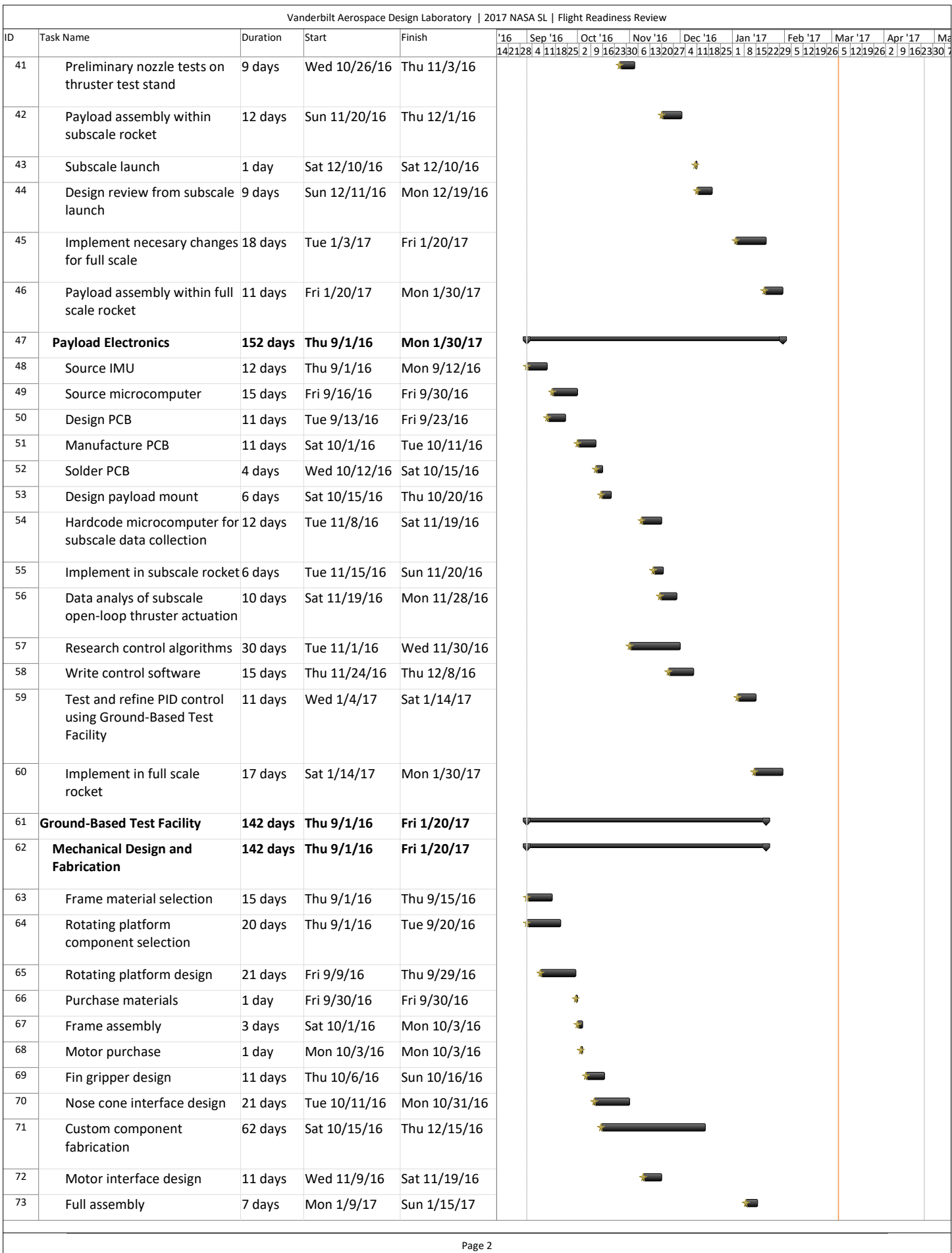
Figure 172: Budget and Present Expenditures

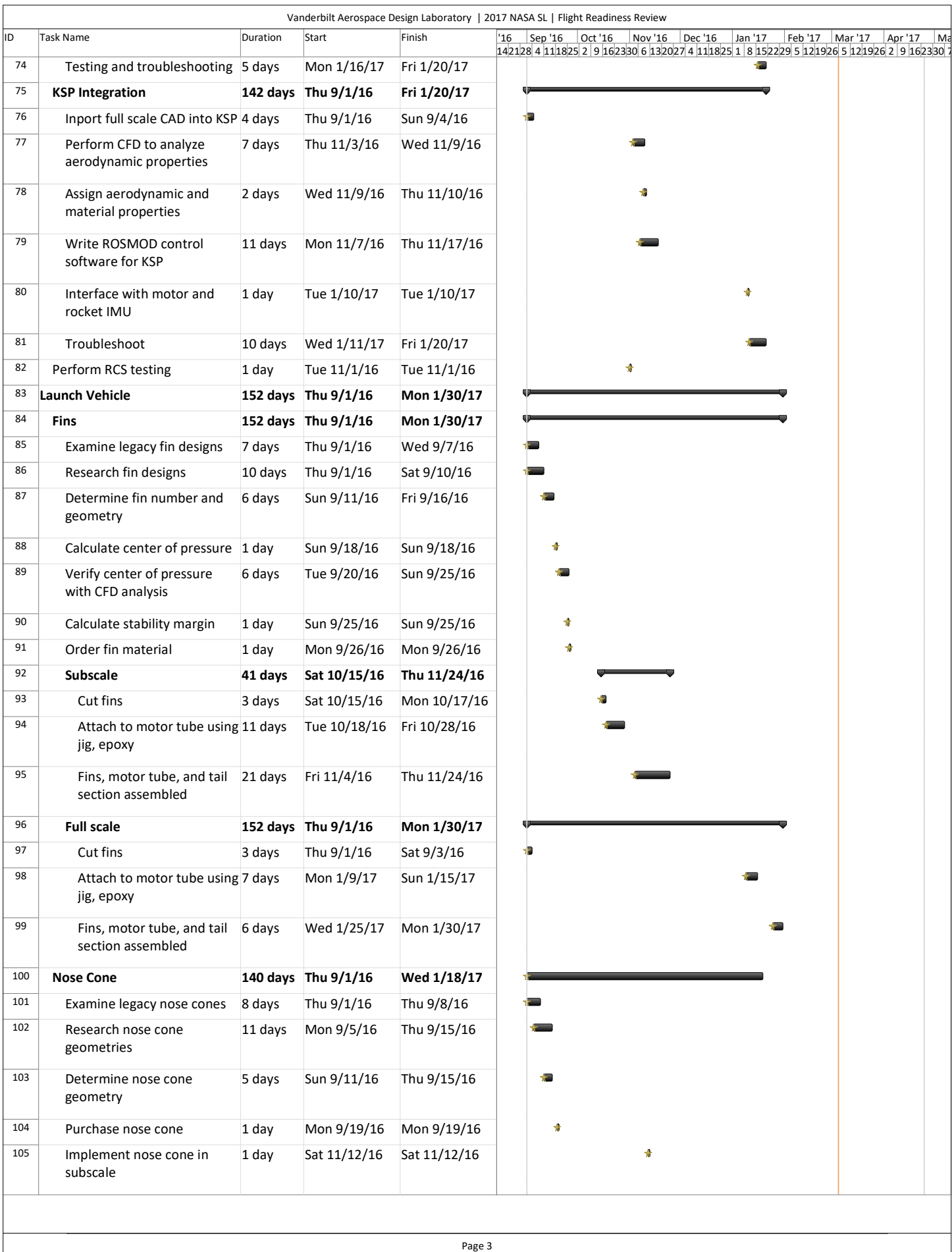
The team tries to be as materially efficient as possible and always considers cost in the decision making process. The budget officer will continue to create budget projections and monitor the team's spending as the project timeline closes.

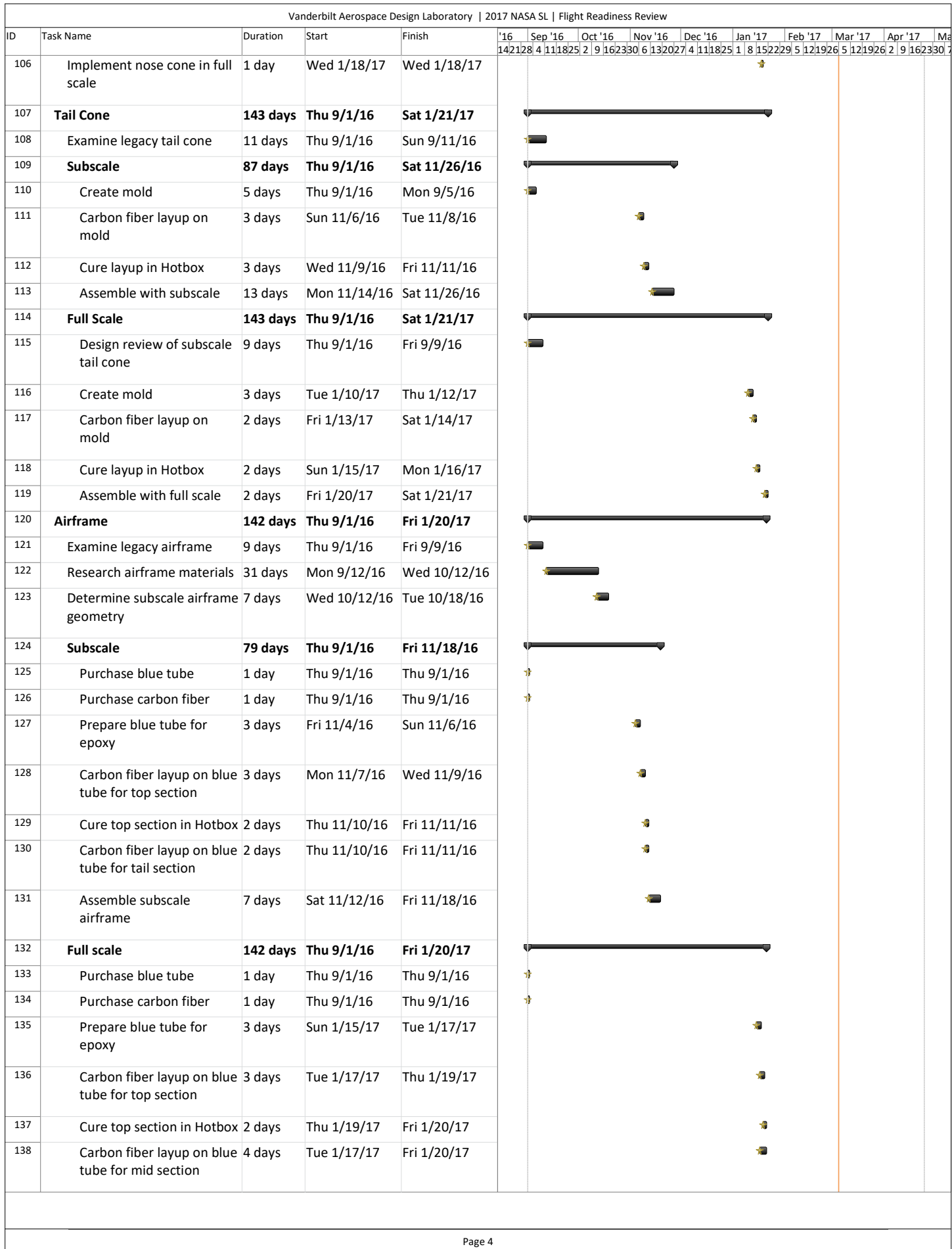
7.3.2 Timeline of Operations

A Gantt Chart was used to illustrate the team's timeline. The Gantt chart has been converted from GanttProject.biz to Microsoft Project, allowing better formatting and visualization of critical paths and free slack. In addition, various dates have been refined throughout the fullscale fabrication process.









ID	Task Name	Duration	Start	Finish	'16	Sep '16	Oct '16	Nov '16	Dec '16	Jan '17	Feb '17	Mar '17	Apr '17	May '17												
139	Cure mid section in Hotbox	2 days	Thu 1/19/17	Fri 1/20/17	14	2128	4	111825	2	9	162330	6	132027	4	111825	1	8	152229	5	121926	5	121926	2	9	162330	2
140	Carbon fiber layup on blue tube for tail section	3 days	Mon 1/16/17	Wed 1/18/17																						
141	Cure tail section in Hotbox	2 days	Wed 1/18/17	Thu 1/19/17																						
142	Hotbox	64 days	Thu 9/1/16	Thu 11/3/16																						
143	Design structure	10 days	Thu 9/1/16	Sat 9/10/16																						
144	Order structural components	1 day	Wed 10/5/16	Wed 10/5/16																						
145	Fabricate structure	7 days	Wed 10/12/16	Tue 10/18/16																						
146	PCB design	6 days	Fri 10/14/16	Wed 10/19/16																						
147	Order PCB components	1 day	Wed 10/19/16	Wed 10/19/16																						
148	PCB fabrication	6 days	Thu 10/20/16	Tue 10/25/16																						
149	PCB soldering	3 days	Tue 10/25/16	Thu 10/27/16																						
150	High power wiring	2 days	Thu 10/27/16	Fri 10/28/16																						
151	Electronics assembly	2 days	Fri 10/28/16	Sat 10/29/16																						
152	Write control software	7 days	Tue 10/25/16	Mon 10/31/16																						
153	Test control software	3 days	Tue 11/1/16	Thu 11/3/16																						
154	Avionics	106 days	Thu 9/1/16	Thu 12/15/16																						
155	Examine legacy avionics bay	8 days	Thu 9/1/16	Thu 9/8/16																						
156	Research new components	8 days	Sun 10/9/16	Sun 10/16/16																						
157	Prucure altimeters and arming switches	8 days	Mon 10/17/16	Mon 10/24/16																						
158	Construct bay	9 days	Wed 11/2/16	Thu 11/10/16																						
159	Deployment Tests	3 days	Fri 11/11/16	Sun 11/13/16																						
160	Subscale Launch	1 day	Sat 12/10/16	Sat 12/10/16																						
161	Altimeter data collection and analysis	5 days	Sun 12/11/16	Thu 12/15/16																						
162	Modifications to bay	11 days	Thu 9/1/16	Sun 9/11/16																						
163	Recovery Systems	220 days	Thu 9/1/16	Sat 4/8/17																						
164	Examine Legacy Recovery Systems	27 days	Thu 9/1/16	Tue 9/27/16																						
165	Design recovery systems	6 days	Thu 10/20/16	Tue 10/25/16																						
166	Purcahse parachutes	1 day	Wed 10/26/16	Wed 10/26/16																						
167	Test chamber fits	8 days	Thu 10/27/16	Thu 11/3/16																						
168	Deployment tests	3 days	Thu 11/10/16	Sat 11/12/16																						
169	Recover subscale rocket	1 day	Sat 12/10/16	Sat 12/10/16																						
170	Validate design and landing energies	4 days	Sun 12/11/16	Wed 12/14/16																						
171	Confirm selections with full scale mass	3 days	Sat 1/7/17	Mon 1/9/17																						
172	Recover full scale rocket	1 day	Tue 2/14/17	Tue 2/14/17																						
173	Recover competition vehicle	1 day	Sat 4/8/17	Sat 4/8/17																						

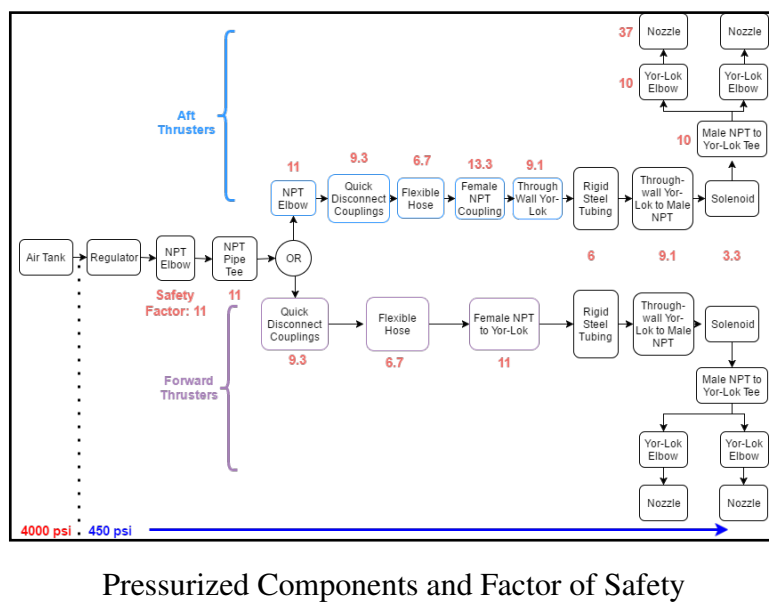
Appendix

A Air Delivery System Safety

A.1 System Overview

The purpose of the air delivery system is to provide 450 psi air to the thruster nozzles, thus providing thrust for the roll control experiment. To do this the system uses the following components:

1. 4500 Psi Ninja Air Tank (ASTM certified regulator, DOT certified tank)
2. NPT pipe fittings
3. Quick disconnect fittings
4. Yor-Lok tube fittings
5. Steel tubing
6. Hydraulic hose
7. Parker solenoid valve



Pressurized Components and Factor of Safety

Parker Solenoid Valve The solenoid valve is designed to remain closed in normal operation when it is not being energized. The maximum differential pressure for the valve is 1500 psi. Above this pressure, the valve will not be able to open, since the closing force imposed by the upstream pressure will exceed the force that the solenoid coil can produce. This operating pressure is not the same as the valve burst pressure. According to the Parker General Purpose Solenoid Valve catalog, valve burst pressure is typically five times the maximum operating pressure. Thus, the burst pressure of this valve is approximately 7500 psi.

Parker			
	Part Number	Operating Pressure	Orifice Size
2 Way Direct Acting	71215SN1GF00	700	1/16"
	71215SN2GF00	700	1/16"
	71216SN2BL00	2500	1/32"
2 Way Pilot Operated	73216BN2MT00	1500	1/4"
Hydraulic	A126LB13001	3000	3/32"

Parker Solenoid Valves

ASCO			
	Part Number	Operating Pressure	Orifice Size
General Service	8262H214	2200	3/64"
	8262H185	500	1/8"
	8262H185	500	1/8"
High Pressure	8223G025	500	5/16"

ASCO Solenoid Valves

Thruster Nozzles The thruster nozzles are the only custom fabricated part in the pressurized system. They were machined from steel bar stock and have demonstrated a factor of safety of over six in hydrostat tests, and analytical calculations predict a factor of safety of 37 for burst pressure.

Burst Discs The pressure regulator incorporates two burst discs into its design, which protect both the upstream and downstream sides of the regulator. The downstream side, which connects to the air delivery system, bursts at 1800 psi and vents excess pressure to the atmosphere. Burst discs are considered one of the most reliable pressure relief mechanisms available and are used widely across industry.

A.2 Solenoid Valve Selection

The solenoid valve was selected based on the requirements of the cold gas thruster system. The valve must meet a 4X factor of safety for burst pressure. The valve orifice, which is the smallest restriction in the valve, must be sufficiently large compared to the total nozzle throat area in order to prevent choking or excessive pressure loss in the valve. Choking in the valve will prevent choking in the throats of the two thruster nozzles and will result in a subsonic exit velocity from the nozzle, dropping thrust to a small fraction of the original thrust value. Finally, the solenoid coil must operate on DC power in order to be incorporated into the launch vehicle.

Valve Selection Criteria:

- Orifice at least 50% larger than nozzle throat area (at least 1/8")
- DC operated
- ≥ 1800 psi burst pressure for a 4X factor of safety

Several valve manufacturers were considered in the search for a solenoid valve to meet these specifications. The design team spent considerable time reviewing the entire catalogs of two major valve manufacturers, Parker Hannifan and ASCO, and the valves most closely matching the desired specifications are shown below.

As seen in the tables above, there are no commercially available solenoid valves that maintain an adequate orifice size and a 4x factor of safety on operating pressure. The selected valve is a Parker

pilot operated solenoid valve with a rated operating pressure of 1500 Psi. As mentioned previously, this is not the valve burst pressure, which is approximately 7500 Psi.

A.3 External Effects of the System

In the event that the burst discs rupture for any reason, a primary concern is a pressure rise in the payload section that could result in faulty altimeter readings or even rupture of the rocket body. For this reason, pressure relief holes (1/4") were placed concentrically around the burst discs to allow for venting of excess pressure. Additionally, the large holes that allow the thruster exhaust to escape the rocket body will serve as additional venting ports. In order to isolate the altimeters from any transient pressure rise that may result from a venting burst disc or firing of the thrusters, putty is used to seal off the altimeters from the payload section.

For more information on the cold gas thruster system and the associated components, see Section 4.